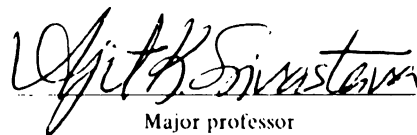This is to certify that the

thesis entitled
"A Rheological Model Of Apple Flesh Failure During
The Magness-Taylor Puncture Test"

presented by

Sanghyup Jeong

has been accepted towards fulfillment
of the requirements for

___M.S._____degree in _Agricultural_ Engineering

Major professor

Date _5-19-97_

PLACE IN RETURN BOX
to remove this checkout from your record.
**TO AVOID FINES** return on or before date due.

| DATE DUE | DATE DUE | DATE DUE |
|----------|----------|----------|
| DEC 1 0 7 2001 | | |
| | | |
| | | |
| | | |
| | | |

1/98  c:/CIRC/DateDue.p65-p.14

A RHEOLOGICAL MODEL OF APPLE FLESH FAILURE DURING THE
MAGNESS-TAYLOR PUNCTURE TEST

By

Sanghyup Jeong

A THESIS

Submitted to
Michigan State University
in partial fulfillment of the requirements
for the degree of

MASTER OF SCIENCE

Department of Agricultural Engineering

1997

**ABSTRACT**

**A RHEOLOGICAL MODEL OF APPLE FLESH FAILURE DURING THE
MAGNESS-TAYLOR PUNCTURE TEST**

By

Sanghyup Jeong


In an attempt to assess firmness, rheological behavior of apple flesh was studied by developing a laminated cell layer model which can be used to emulate Magness-Taylor puncture test.

Each layer of the model consisted of a compressive and a shear-tensile element. Compressive component consisted of a Maxwell model with a fracture element. The shear-tensile component consisted of an elastic element. The annular pumping effect was also included in model. Layers were connected in series and each shear-tensile component was grounded. Simulation was performed on this model with element parameters and the postulated deformation sequence. The model depicted fairly well the Magness-Taylor test results both quantitatively as well as qualitatively.

Nondestructive techniques using Hertz contact stress theory and acoustic impulse technique (Armstrong, 1990) were used for estimating model parameters. These methods were fairly accurate in predicting the model parameters. Also, a strong correlation with the Magness-Taylor firmness reading was found.

# ACKNOWLEDGMENTS

# TABLE OF CONTENTS

## LIST OF FIGURES

**Chapter 1**

**INTRODUCTION**

**1.1 Justification**

Fresh market apples are sorted by color, size, weight and firmness. Apples classed by their physical properties and texture are processed for the various apple products. The texture of apples is an important quality attribute. Apple firmness is an indicator of textural qualities. Bourne (1982) defined firmness as a texture characteristic during mastication that displays moderate resistance to breaking. The Magness-Taylor pressure test developed in 1925 to measure firmness, has been accepted as an industry standard. The Magness-Taylor pressure test consists of forcing a cylindrical metal tip into the apple flesh without skin and measuring the maximum force. The penetration depth is about 8 mm (5/16 in) and the diameter of the tip is approximately 11 mm (7/16 in) or 8 mm (5/16 in). The plunger tip is round and the penetration depth is marked on the plunger.

The destructive nature of the Magness-Taylor pressure test results in fruit loss which contributes to economic loss for the apple industry. The firmness assessment is based on sampling. Export markets require a better quality assessment of the product. A non-destructive technique that can make it possible to test individual fruit would be beneficial. The Magness-Taylor method relies on only one indicator to describe the textural quality of the apple, the maximum force to masticate apple flesh. Other parameters such as elastic modulus also contribute to texture.

1

An in-depth understanding of the Magness-Taylor test would be very helpful in developing a nondestructive technique assessing fruit firmness to meet the needs of high quality produce.

**1.2 Objectives**

The objectives of the research were

1. to develop a rheological model of apple flesh and to examine the capability of the model for predicting the Magness-Taylor puncture test result.

2. to evaluate the potential of a rubber spherical indentor as a means of estimating the compression and shear failure stresses of apple flesh.

3. to investigate the capability of the spherical indentor as a non-destructive technique to measure apple firmness.

**Chapter 2**

**REVIEW OF LITERATURE**

**2.1 Rheological Models Representing the Textural Characteristics of Food Materials**

Much effort have been devoted to developing rheological models to describe complex texture qualities of food materials. New rheological elements have been suggested along with a combination of the conventional rheological elements *e.g.* spring and dashpot. These models have been subjected to different types of loading conditions and their responses have been compared to the experimental results. Maxwell and Kelvin models which are the classical models in rheology have already been studied and evaluated under compression, extension, creep, and relaxation tests. Maxwell and Kelvin models are composed of a spring and a dashpot in a serial and in a parallel pattern, respectively.

Peleg (1976) proposed a model system which was basically a parallel array of generalized Maxwell body. He added two fracture elements which were suggested by Drake (1971) to the model. The general elements of this model had an elastic stage and a Maxwellian stage when the model worked as a Maxwell model until fracture. The number of each stage and the parameters of the elements determine the pattern of rheological behavior of a given material. This model can describe various rheological behavior qualitatively.

Chen and Rosenberg (1977) suggested a nonlinear viscoelastic model which consisted

of Maxwell and Kelvin models containing an yield element. The model exhibited Maxwellian behavior and then it showed the behavior of a four element Burgers model which was a serial combination of a Maxwell and a Kelvin model after the yield element was activated. He indicated that the model was able to represent the behavior of American cheese by adjusting model parameters.

Dickinson and Goulding (1980) tested various types of cheese and found that the model suggested by Chen and Rosenberg (1977) could be used to fit individual compression curve but the model was unable to predict general load deformation behavior.

Johnson and *et al.* (1981) modified the model suggested by Peleg (1976) by incorporation of a contact and a fracture element. In this study the contact and the fracture element were functions of time and temperature to describe the rheological behavior of raw and cooked fish meat. They demonstrated that the model worked well to describe the rheological behavior qualitatively.

McLaughlin (1987) had a different approach to develop a model describing apple tissue failure phenomenon. Yield stress data for 800 cylindrical samples was studied. Statistical test failed to reject (p=0.85) the hypothesis that the data followed a three parameter Weibull distribution. This statistical model was suggested as an adequate probability model for predicting the failure stress of apple flesh.

During the past decade most of the efforts were concentrated on any developing property measurement techniques rather than developing a model having any physical meaning.

## 2.2 Rheological Considerations of Apple

Much research has been conducted about the phenomenological and morphological characteristics of the failure of fruits. Mechanical and structural characteristics of fruits were observed and discussed. An understanding the nature of failure will help develop appropriate models having physical meaning.

Peleg and *et al.* (1976) studied compressive failure patterns of several juicy fruits. Compression tests were performed to the cylindrical samples by using an Instron Universal Testing Machine. Fruits showed their characteristic failure patterns. Effect of the juiciness and dimension of the sample were studied. In this research it was found that structural characteristics, liquid content, and geometry of the sample affect the force-deformation relationship.

Mohsenin (1977) studied the failure of food materials from the point view of solid mechanics. Working with apple tissues he found that the shear resistance was a result of the cementing agent (pectic substance) in the middle lamella holding together the cells in the parenchyma tissue. He also studied the potential usage of the Hertz contact stress theory to find failure parameters from the force-deformation relationship.

Pitt (1982) considered two different types of failure, cell wall rupture and cell debonding. Sample was considered as the sum of a large number of cell layers normal to the direction of the applied force. In case of constant rate strain due to the rupture of the weakest cell of a layer, neighboring cells had higher stress level than before. If the stress is higher than cell strength then failure occurs and this process propagates through the layers of the sample. Due to this fractured transverse plane enzymatic browning occurred

in that cross section. This catastrophic failure was observed in the fresh apple tissue.

Lin and Pitt (1986) reported that turgor pressure and the strain rate affect failure mode of fruit and vegetables and tissue strength.

Khan and Vincent (1990) observed that cells of apple flesh are arranged in radial column and the cell size and shape changes along with the radial direction by using scanning electron microscope, indicating that apple flesh should be considered as an anisotropic material in the radial direction.

Khan and Vincent (1993) observed that if a radial cylindrical apple flesh sample was subjected to a compressive force then it generally fractured by collapse of a single layer of cells at right angle to the direction of force. Tangential sample failed in shear. This phenomenon is due to the anisotropic property of apple parenchyma which was observed by Khan and Vincent (1990).

**Chapter 3**

**THEORY**

**3.1 Modeling Principles and General Assumptions**

To develop a model representing Magness-Taylor puncture test it is necessary to observe and analyze the mastication phenomenon. Basically Magness-Taylor puncture test involves three major factors which are compression, shear-tension and annular pumping effects. These factors will be combined into one system representing the apple flesh after being studied and modeled individually. Throughout this research several simplifying assumptions were made. Even though the actual Magness-Taylor firmness instrument has round tip the radius of curvature is large enough so that the plunger tip was considered as flat. The second assumption was about the cylindrical apple flesh sample. Actually the layer of the sample is curved because of its radial arrangement of cells. However, the curvature was relatively large enough to be treated as flat because the sample diameter was considerably less than that of the whole apple.

**3.2 Modeling Compression Component**

If several ideal conditions of the compression test are satisfied the saw-tooth shaped force deformation relationship as shown in Figure 1 could be obtained. The first ideal condition is to make perfect cylindrical apple flesh sample which means the flat cutting
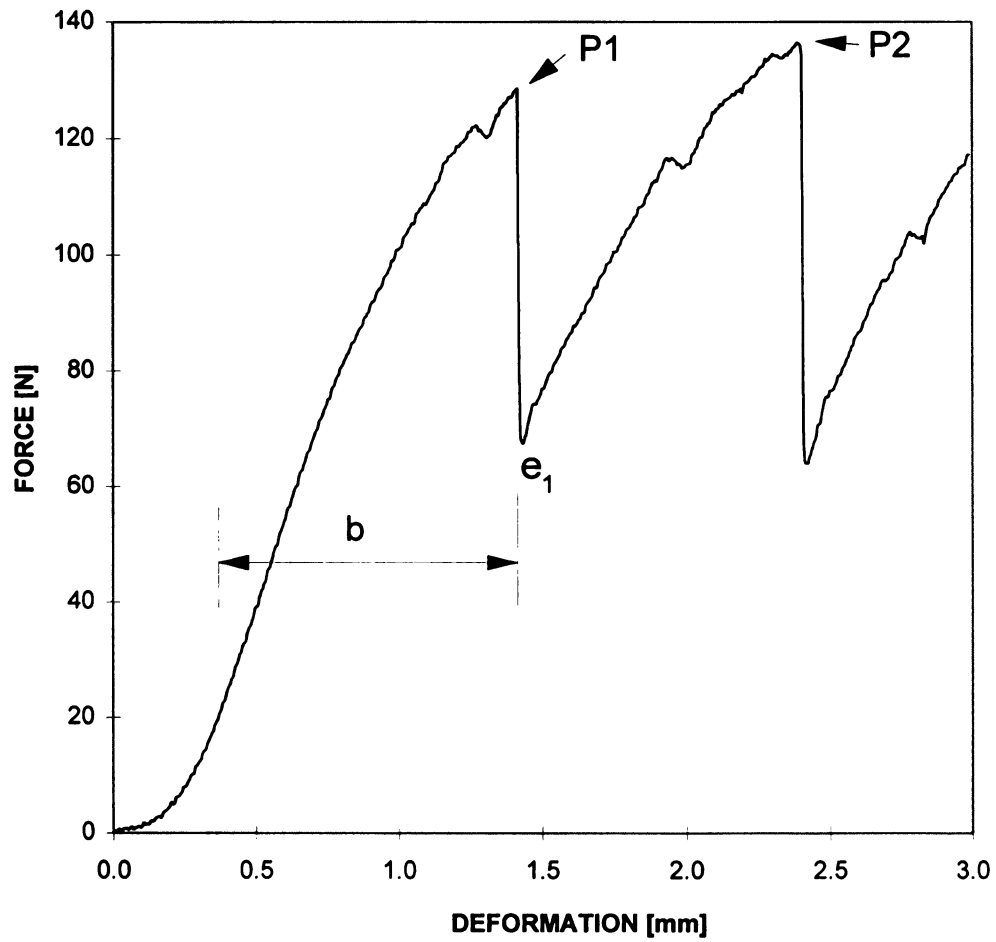
FIGURE 1 - Force-deformation relationship of compression test
for cylindrical apple flesh

surface are normal to the direction of the compressive force. The second ideal condition is lack of friction between cutting surface and the pressing die. The last ideal condition is satisfied if the sample is obtained in the radial direction from the whole apple because of the anisotropic characteristics of apple parenchyma studied by Khan and Vincent (1990). In these ideal conditions sample shows two or three fractures caused by collapse of a single layer of cells at right angles to the force (Figure 1). A simple model representing this phenomenon was developed. This model was the building block of the final model.

The first compression region (b, Figure 1) was represented by a Maxwell model and a fracture element having $\sigma_c$ as its yield stress (Figure 2). The model was used to represent a single layer of cells.

Mathematical expression for the model at constant strain rate is,

$$\sigma = \eta V(1 - e^{-\frac{E}{\eta}t}) \quad , \quad 0 \le \sigma < \sigma_c$$
[1]

where
$\sigma$ = Stress
$\eta$ = Viscosity
$E$ = Elastic modulus
$\sigma_c$ = Critical yielding stress
$t$ = Time
$V$ = Constant strain rate

Based on the research of Khan (1993) a cylindrical apple sample can be considered as a system of stacks of a single cell layer. By connecting the model in a series pattern the system of a cylindrical sample can be depicted physically. The model is shown in Figure 3. If apple flesh is assumed to be an ideal isotropic material in the radial direction $\sigma_c$ would be the same for each layer. However, it is expected that a limited variation would exist from layer to layer in real life. Thus, if the model is subjected to compressive
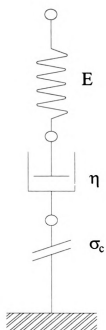
FIGURE 2 - Compression model consisted of a Maxwell and a fracture element
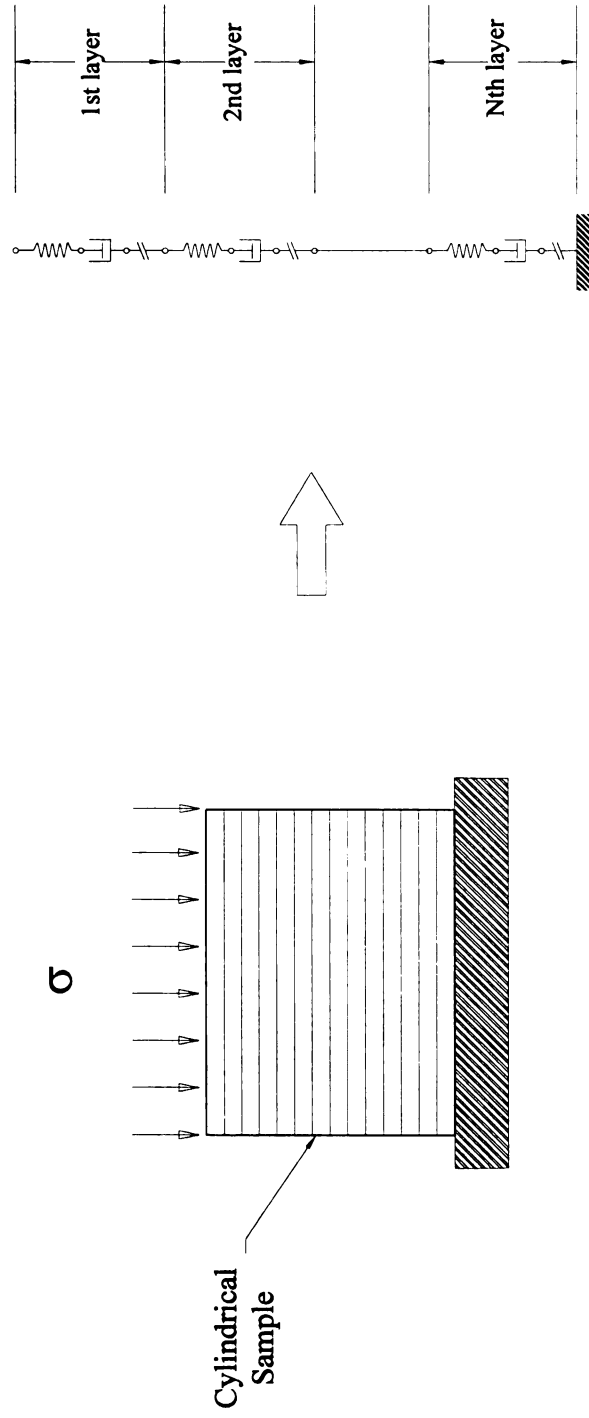
FIGURE 3 - Modeling concept of cylidrical apple flesh sample

force a layer containing the lowest yield stress will collapse first and so on. The fact that the P2 is greater than the P1 in Figure 1 supports the above reasoning.

If the cylindrical apple flesh sample is subjected to a stress σ (Figure 3) the total deformation will be distributed to each cell layer. The layer having the weakest yield stress will collapse first. The cylindrical apple flesh sample which has multi-layer of cells can be represented by stacking the unit compression model (Figure 2). Elasticity and viscosity of each layer were assumed to be the same. However each layer had different critical yield stress.

At time t, the strain and the stress of every layer were equal because the compression model in Figure 3 was a serial system until the stress reached the lowest critical yield stress. The strain of unit layer was equal to the total strain divided by the number of cell layers.

Thus,

$$\sigma_1 = \sigma_2 = \cdots = \sigma_N = \sigma_u = \sigma$$

$$\varepsilon_1 = \varepsilon_2 = \cdots = \varepsilon_N = \varepsilon_u = \frac{\varepsilon}{N}$$

[2]

$$
\begin{aligned}
\text{where} \quad \sigma_u &= \text{Stress of unit layer} \\
\sigma &= \text{Total stress} \\
\varepsilon_u &= \text{Strain of unit layer} \\
\varepsilon &= \text{Total strain} \\
N &= \text{Layer index}
\end{aligned}
$$

If the cylindrical apple flesh sample was considered as a simple combination of a Maxwell model and a fracture element then,

$$\dot{\varepsilon} = \sum_{i=1}^{N} \dot{\varepsilon}_i = N \dot{\varepsilon}_u = V \qquad [3]$$

Eq. [3] can be expressed as follows by using eq. [1]

$$N \frac{\sigma_u}{\eta_u(1-e^{-\frac{E_u}{\eta_u}t})} = \frac{\sigma}{\eta(1-e^{-\frac{E}{\eta}t})}$$  [4]

From eq. [4] the following relationships were obtained.

$$E_u = NE$$
$$\eta_u = N\eta$$  [5]

Therefore the properties of unit layer, $E_u$ and $\eta_u$, can be calculated from eq. [5] if the E and $\eta$ were known. E and $\eta$ can be found from the force deformation relation of the compression test by curve fitting using eq. [1]. These unit parameters will be used in the final allied model.

After the first collapse system is undergoing inequilibrium state for a short period until the system gets to equilibrium state. When the system gets to the equilibrium the total number of layers is reduced by one. Because the transition period is too short, total strain can be assumed to remain unchanged. Thus,

$$\varepsilon_{u,before} = \frac{\sigma}{E}\bigg|_{before} \qquad \varepsilon_{u,after} = \frac{\sigma}{E}\bigg|_{after}$$  [6]

The total strains, before and after collapse of a layer, are assumed to be same due to the short transition. Therefore,

$$N \cdot \varepsilon_{u,before} = (N-1) \cdot \varepsilon_{u,after}$$  [7]

The strain after the fracture is expressed as follows

$$\varepsilon_{u,after} = \frac{\ell - \left\{ (\ell - \ell\varepsilon_{before}) + \frac{(\ell - \ell\varepsilon_{before})}{N-1} \right\}}{\ell} = \frac{N\varepsilon_{before} - 1}{N-1}$$  [8]

where $\ell$ = thickness of a unit layer at time t

By using eq. [6], [7] and [8] the following equation is found

$$\sigma_{after} = \sigma_{before} - \frac{E_{u,before} - \sigma_{before}}{N - 1}$$ [9]

By using eq. [9], $e_l$ in Figure 1 can be predicted. This fact supports that the suggested compression model is reasonable.

## 3.3 Modeling Shear-tensile Component

Figure 4 shows the cross sectional deformation pattern of the apple flesh subjected to compression by a cylindrical plunger. The strain of each layer decreased as the depth increased. In Figure 4, layer shaped like a circular plate in a real situation modeled as a two dimensional elastic element with the presence of a fracture element. A fracture element represents the yield stress of a layer. In this case yielding involves tensile and shear simultaneously. It is difficult to perform an ideal shearing test because of the ductile characteristic of food material and the clearance between the shearing plunger and guiding wall. Thus, the yield stress obtained from shearing test naturally contains tensile and shear contribution. The yield stress from shearing can be used as the critical stress of the fracture element. Also the angle $\alpha$ is important to determine the deformation rate of shear-tensile component. The angle will vary within 0 to 90 degrees as the compression goes on. If the angle is 90 degrees the deformation of shear-tensile component will be the same as the sum of deformation rate of each layer below that shear-tensile component. However, in a real situation the angle is less than 90 degrees and also it changes with time. In this research the angle is assumed constant and the deformation rate of the shear-
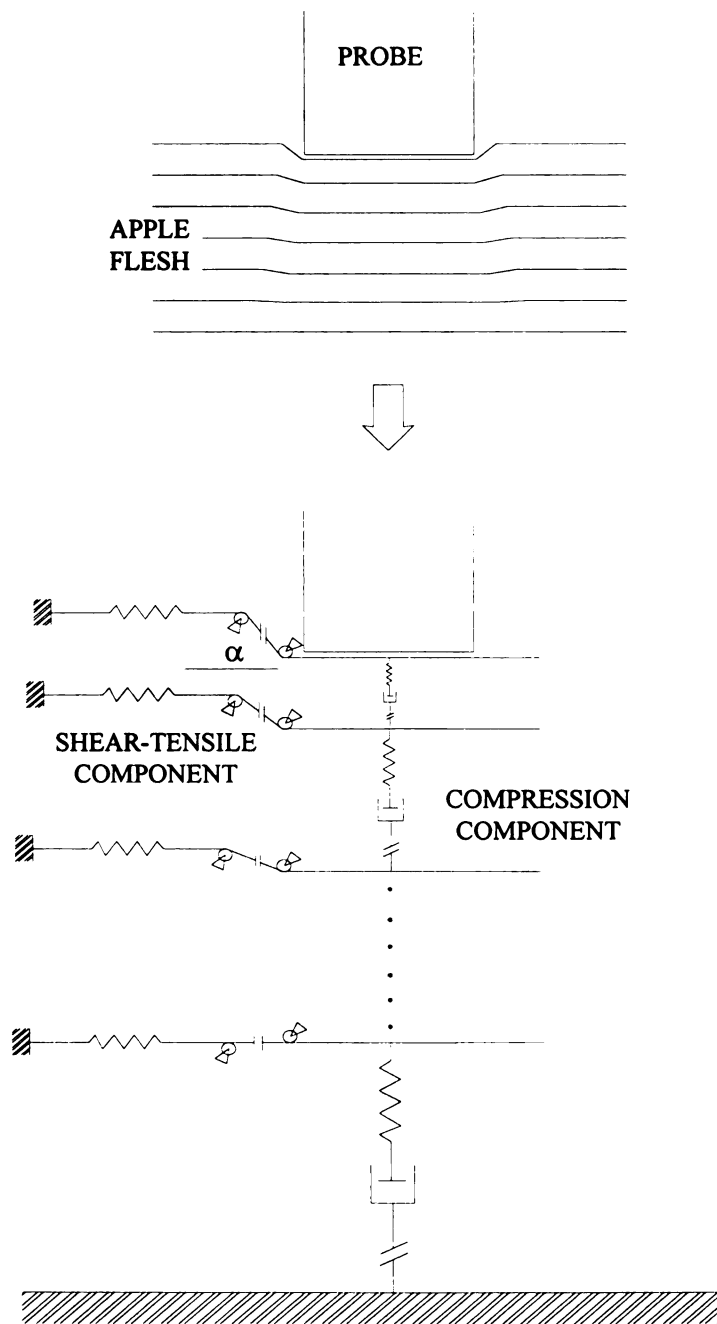
FIGURE 4 - Modeling concept of shear-tensile component

tensile component to the compression component was assumed 0.7.

## 3.4 Modeling Annular Pumping Component

Apple flesh contains about 80% of water by weight. Therefore, the squeezing action of cylindrical probe produces juice. If the speed is high, then the resistance created by juice is significant. The juice is expelled through the clearance in between probe and apple flesh wall in Figure 5. The produced juice is pumped by pressure, $P_o$, and this pressure pushes the apple flesh wall to make clearance, c, in Figure 5.

A mechanical model was devised to imitate the phenomenon as depicted in Figure 6. The model consisted of a piston and a cylinder which represent probe and apple flesh wall respectively. A sliding block and a spring represents apple flesh wall pushed by pressure $P_o$. The cylinder is filled with apple juice entrapped air. As the piston moves forward, pressure, $P_o$, is produced which pushes the fluid through the clearance created by the sliding block moving backward compressing the spring with a force F. Apple juice flows at a high velocity through the clearance.

From the model displaced liquid inside the cylinder discharged through the clearance. The steady flow-mass-conservation relation can be written as

$$\dot{m}_{in} = \dot{m}_{out} \qquad [10]$$

If the juice is assumed as an incompressible liquid, then the inlet and the outlet volume should be the same so that eq. [10] can be replaced with
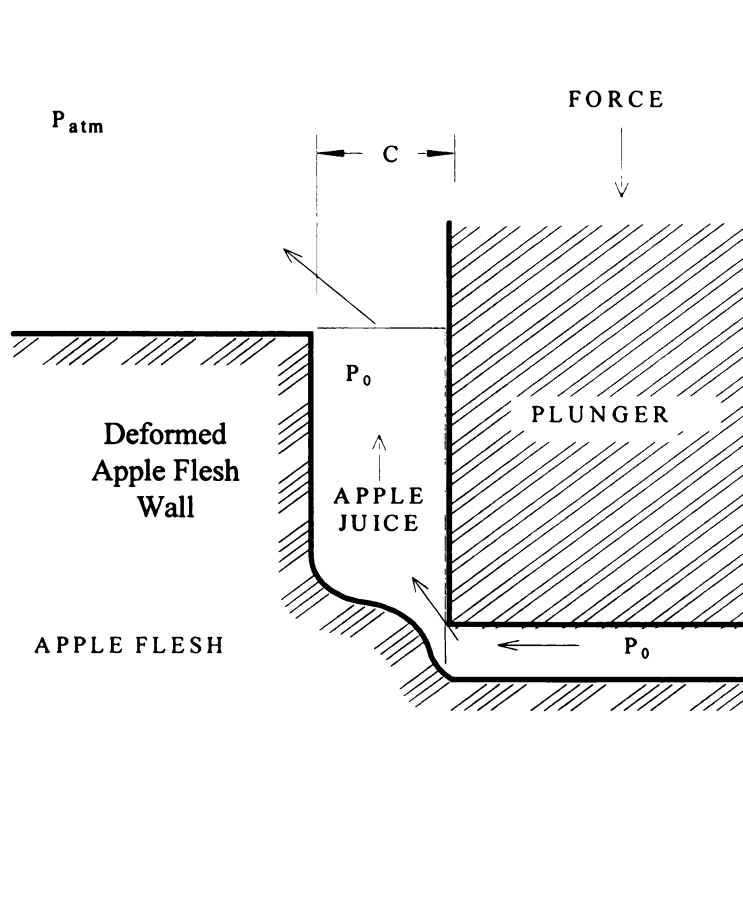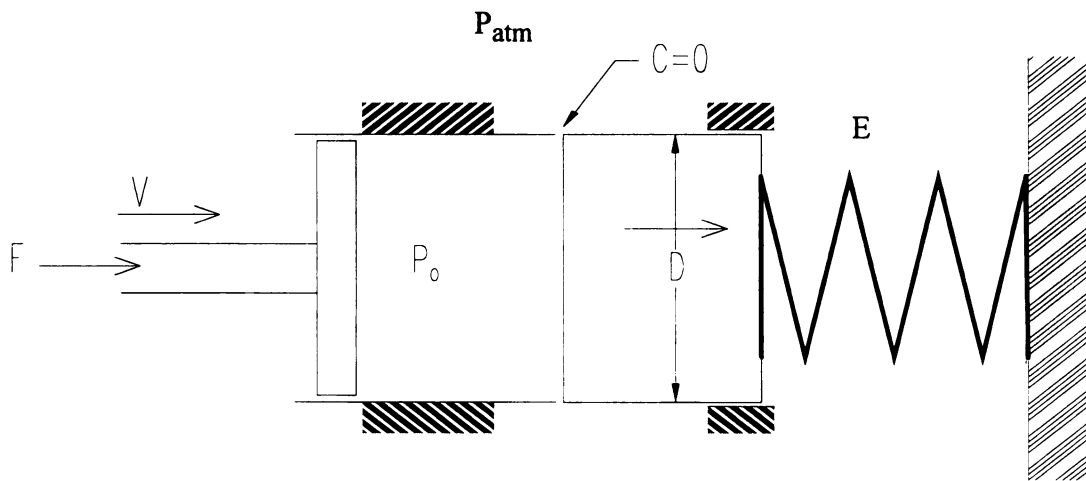
$$\dot{Vol}_{in} = \dot{Vol}_{out} \qquad [11]$$

$P_{atm}$

$\leftarrow C \rightarrow$

FORCE

$P_0$

PLUNGER

Deformed
Apple Flesh
Wall

$\uparrow$

APPLE
JUICE

APPLE FLESH

$\leftarrow P_0$

FIGURE 5 - Annular pumping effect during mastication
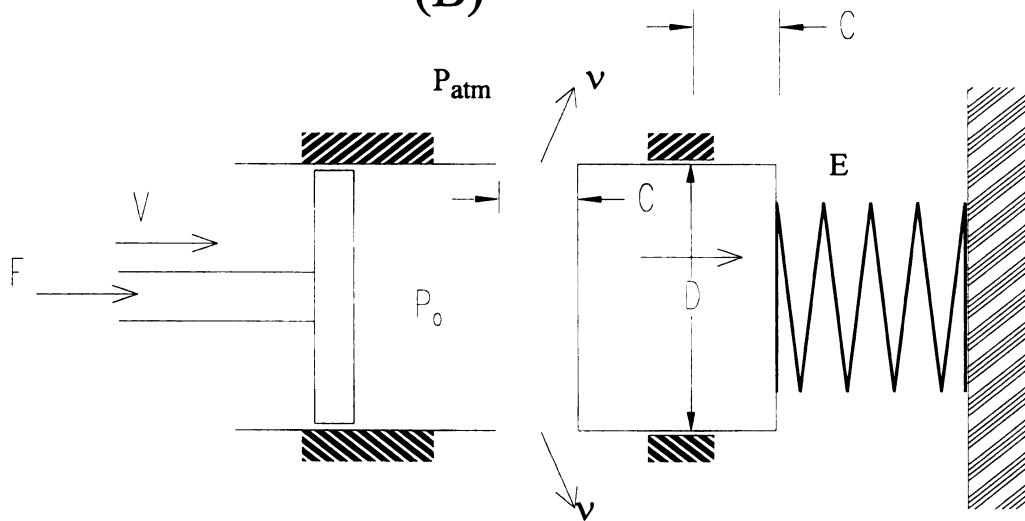
## (A)



## (B)



FIGURE 6 - Model representing annular effect

If the piston moves with a constant velocity, the speed of the juice flowing through the clearance can be calculated as follows.

$$\upsilon = V \frac{A_m}{A_c} = \frac{VD}{4c}$$ [12]

where   $\upsilon$ = Velocity of exiting apple juice
V = Velocity of the moving piston
c = Clearance
$A_m$ = Cross sectional area of the piston
$A_c$ = Area of exit ($= c\pi D$)
D = Diameter of the piston

Bernoulli's equation is used to determine pressure inside the cylinder.

$$P_o(t) - P_a = \frac{1}{2}\rho\upsilon^2$$ [13]

where   $P_o(t)$ = Pressure inside the cylinder
$P_a$ = Atmospheric pressure
$\rho$ = Fluid density inside the cylinder
$\upsilon$ = Exiting speed of the liquid

The pressure or the stress acting on the moving block is,

$$P_0 = \sigma = \varepsilon E = \frac{c}{\ell}E$$ [14]

where $\ell$ is the original length

The clearance, c, can be expressed as following,

$$c = \frac{\ell P_0}{E}$$ [15]

Using eq. [12], [13], and [15] following equation is obtained.

$$P_o(t)^3 - P_a P_o^2 - \frac{\rho}{32}\frac{V^2 D^2 E^2}{} = 0$$ [16]

Eq. [16] can be used to calculate $P_o$.

**3.5 Postulated Deformation Sequence**

In compression test the displacement of a layer is equal to the total displacement divided by the total number of layers because each layer is free to move. Therefore, the displacement of each layer is all the same. For the Magness-Taylor test, however, total displacement cannot be divided equally due to the restraint of each layer. Shear-tensile resistance plays a role of those restraints. Thus, the distribution of the deformation of the entire sample should be considered.

In this study it is assumed that the distribution of deformation of each layer follows the geometric ratio. Therefore, the total displacement is the sum of the deformation of each layer. It is expressed as,

$$D(t) = d_1(t) + d_2(t) + \cdots + d_n(t) \qquad [17]$$

where $D(t)$ = Total deformation at time t
and $d_n(t)$ = Displacement of the n th layer at time t

Because the deformation of each layer follows geometric series, eq. [17] can be represented as follows,

$$\begin{aligned} D(t) &= a_1 t + a_2 t + a_3 t + \cdots + a_n t \\ &= a_1 t + a_1 r t + a_1 r^2 t + \cdots + a_1 r^{n-1} t \end{aligned} \qquad [18]$$

where $a_n$ = Deformation rate of n th layer
$t$ = Time
$r$ = Geometric ratio($0<r<1$)

If $D(t)$ is constant strain rate then eq. [18] is

$$D(t) = Vt = (a_1 + a_1 r + a_1 r^2 + \cdots + a_1 r^{n-1})t \qquad [19]$$

where $V$ = Speed of the cross-head

From eq. [19], $a_1$ is expressed as

$$a_1 = \left(\frac{1-r}{1-r^n}\right)V \tag{20}$$

By using $a_1$ and r the deformation rate of each layer can be determined. In addition, deformation history with time should be considered. Figure 7 shows the deformation sequence based on the mastication phenomenon. The slope of the line OG represents the speed of the cross head. Each layer is assumed to be deformed linearly according to its deformation rate until the deformation gets to $d_c$ which is the critical deformation for the mechanical system failure of a layer. During the period, from $t_1$ to $t_2$, deformation rate of the first layer is increased rapidly due to collapse of mechanical structure until the deformation of the first layer reaches $d_t$ which is the deformation of a layer showing no more compression. At the same period ($t_1$-$t_2$) the other layers experience rapid relaxation and they recover some amount of deformation to compensate the rapid compression of the first layer. The period ($t_1$-$t_2$) can be considered as a non-equilibrium state. However, at time $t_2$ system turns to an equilibrium state. In the practical point of view, time span, $t_1$ and $t_2$, can be neglected because the phenomenon of this period is so rapid.

After $t_2$ the total number of layers is reduced by one because the first layer has already been destroyed. Therefore, the deformation rate of each layer should be determined again.

At $t_3$ the deformation of the second layer reaches $d_c$ and it is deformed to $d_t$ rapidly until the time gets to $t_4$. The other layers get into rapid relaxation.

This discrete pattern of deformation occurs throughout the destruction phenomenon of apple flesh in the ideal condition. However this pattern of deformation is found three to four times in the real life situation.
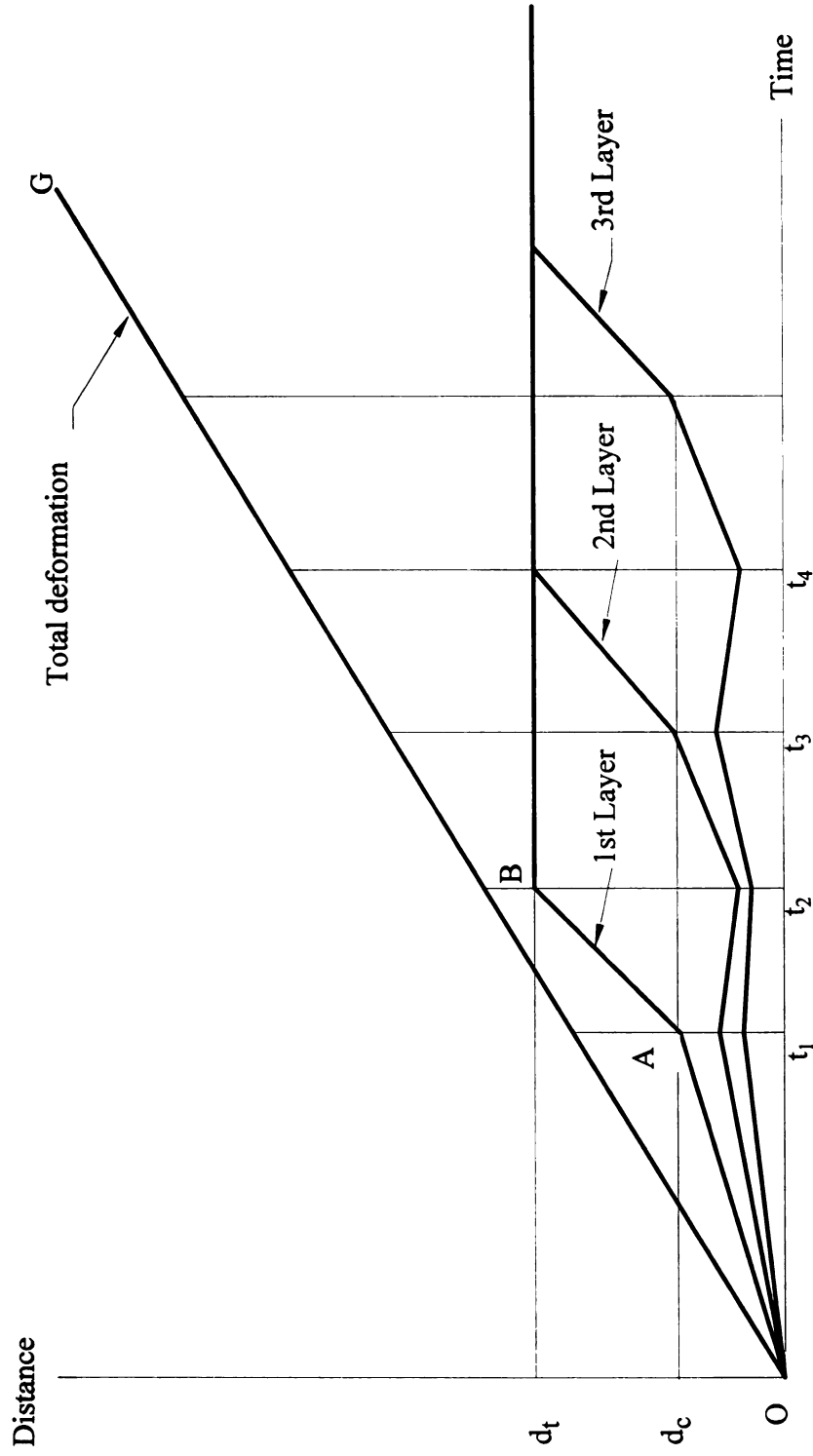
FIGURE 7 - Postulated deformation sequence of Magness-Taylor puncture test

## 3.6 Compression, Shear-tensile and Annular Pumping Component allied Model

Models of each component were combined to generate the combined force

deformation response. Figure 8 shows the allied model composed of the three models. A

in Figure 8 represents the compressive component which consisted of a Maxwell model

and a fracture element. B represents a shear-tensile component and every component is

grounded. C is an annular pumping component. During the early period of compression

flow of juice is not fully developed to produce resistance. S delays the activation timing

of the annular pumping component for a while. Then the postulated deformation

sequence is applied to the allied model to get the force response.

Castigliano's theorem is used to calculate the force response of the system. This is

the simple method for the deflection problems. Castigliano's theorem is that when forces

act on elastic systems subjected to small displacements the displacement corresponding to

any force, collinear with the force, is equal to the partial derivative of the total strain

energy with respect to that force. Using Castigliano's theorem, energy of a system

consisting of non-linear elements is expressed as following.

$$E = \int_0^\delta P \cdot d\delta = \sum_{i=1}^n \int_0^{e_i} F_i \cdot de_i \qquad [21]$$

where      P = Resultant force
            $d\delta$ = Differential total deformation
            $F_i$ = Force of i th element
            $e_i$ = Differential deformation of i th element
            i = Layer index
            n = Total number of layers
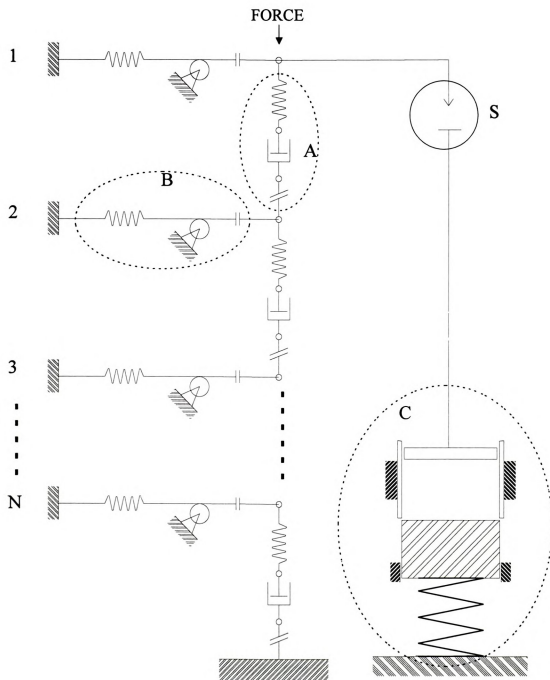            E = Energy

FIGURE 8 - Final model of apple flesh for Magness-Taylor puncture test

Each cell layer is elastic until it gets to failure and the each layer is subjected to very small deflection. Thus the Castigliano's theorem has no problem in the application for this approach. Because the deformation is already known the force response of each layer can be determined. Therefore the strain energy which is the force times of deformation can be calculated for each layer at a certain time

The total strain energy calculated by the theorem is differentiated numerically with total deformation to obtain the resultant force response which is the predicted Magness-Taylor test result.

## 3.7 Parameter Determination Using Rubber "Thumb Test"

Stresses occur at the contact area when two bodies having curved surfaces are pressed together. Hertz contact stress theory has been developed to describe the above situation. Figure 9 shows two spheres contacting each other. By Hertz contact theory the radius of contact area is

$$a = \sqrt[3]{\frac{3F}{8} \cdot \frac{(1 - v_1^2)/E_1 + (1 - v_2^2)/E_2}{1/d_1 + 1/d_2}}$$  [22]

where  $d_1, d_2$  =  Diameters of body 1 and 2
  F  =  Force applied
  $v_1, v_2$  =  Poisson ratio of body 1 and 2
  $E_1, E_2$  =  Modulus of elasticity of body 1 and 2
  a  =  Radius of contact area

The maximum normal stress at the center of the contact area is

$$\sigma_{z, max} = P_{max} = \frac{3F}{2pa^2}$$  [23]

Stresses in direction of x and y can be represented as functions of z.
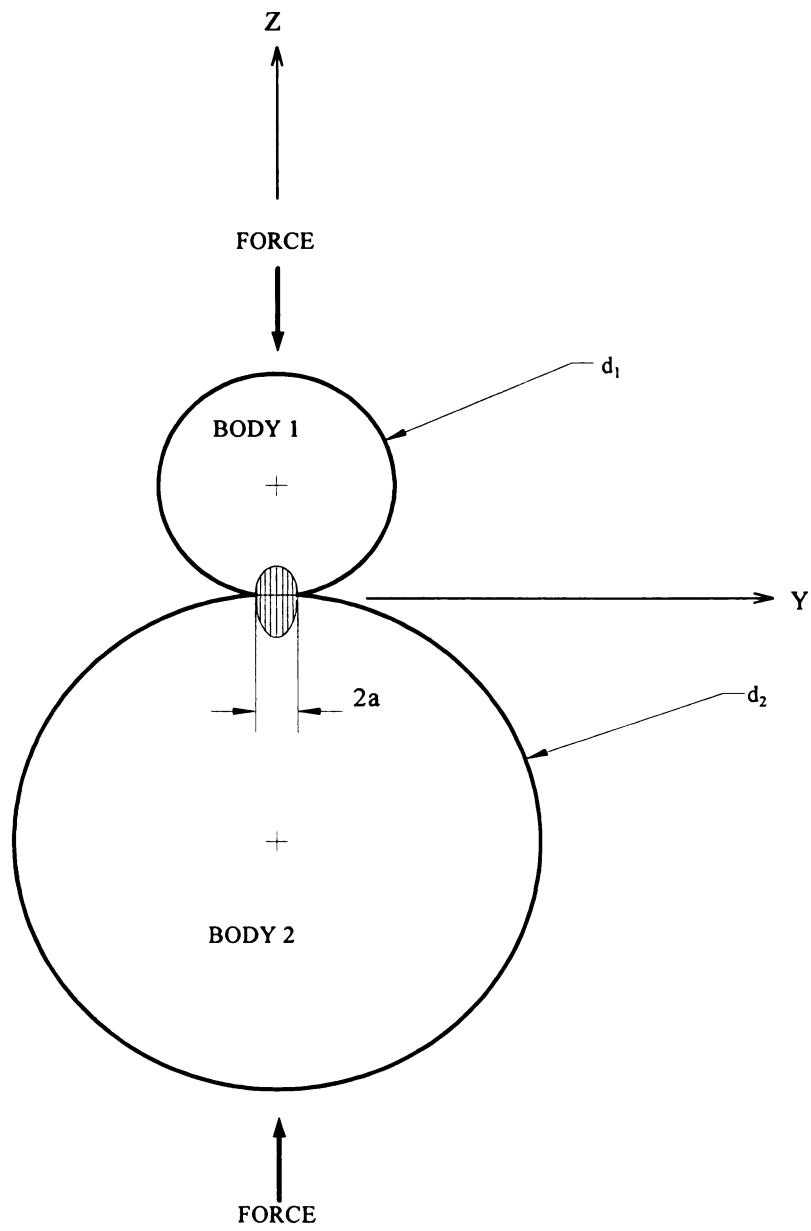
FIGURE 9 - Hertz contact stress of two spheres

$$\sigma_x = \sigma_y = -P_{max}\left[\left(1 - \frac{z}{a}\tan^{-1}\frac{1}{\frac{z}{a}}\right)(1+m) - \frac{1}{2\left(1+\frac{z^2}{a^2}\right)}\right] \qquad [24]$$

$$\sigma_z = \frac{-P_{max}}{1+\frac{z^2}{a^2}} \qquad [25]$$

where $\quad m = \dfrac{3K - E}{6K}$

$\qquad\qquad$ K = Bulk modulus or incompressibility

And the shear stress can be calculated by using $\sigma_x$ and $\sigma_z$ as

$$\tau_{xy} = \frac{\sigma_x - \sigma_z}{2} \qquad [26]$$

where $\quad \tau_{xy}$ = Shear stress

Figure 10 shows the stress change for the distance below the surface *i.e.* along z direction. By using this relationship maximum compressive stress and the shear stress can be calculated. The maximum shear stress is approximately 1/3 of the maximum normal stress.

If body 1 is rubber sphere and the body 2 is apple then by pressing the two objects until the apple goes over the elastic region the yield compressive and shear stress can be predicted.

### 3.7 Parameter Determination Using Acoustic Impulse Technique

Elasticity of a resonating elastic sphere is defined as
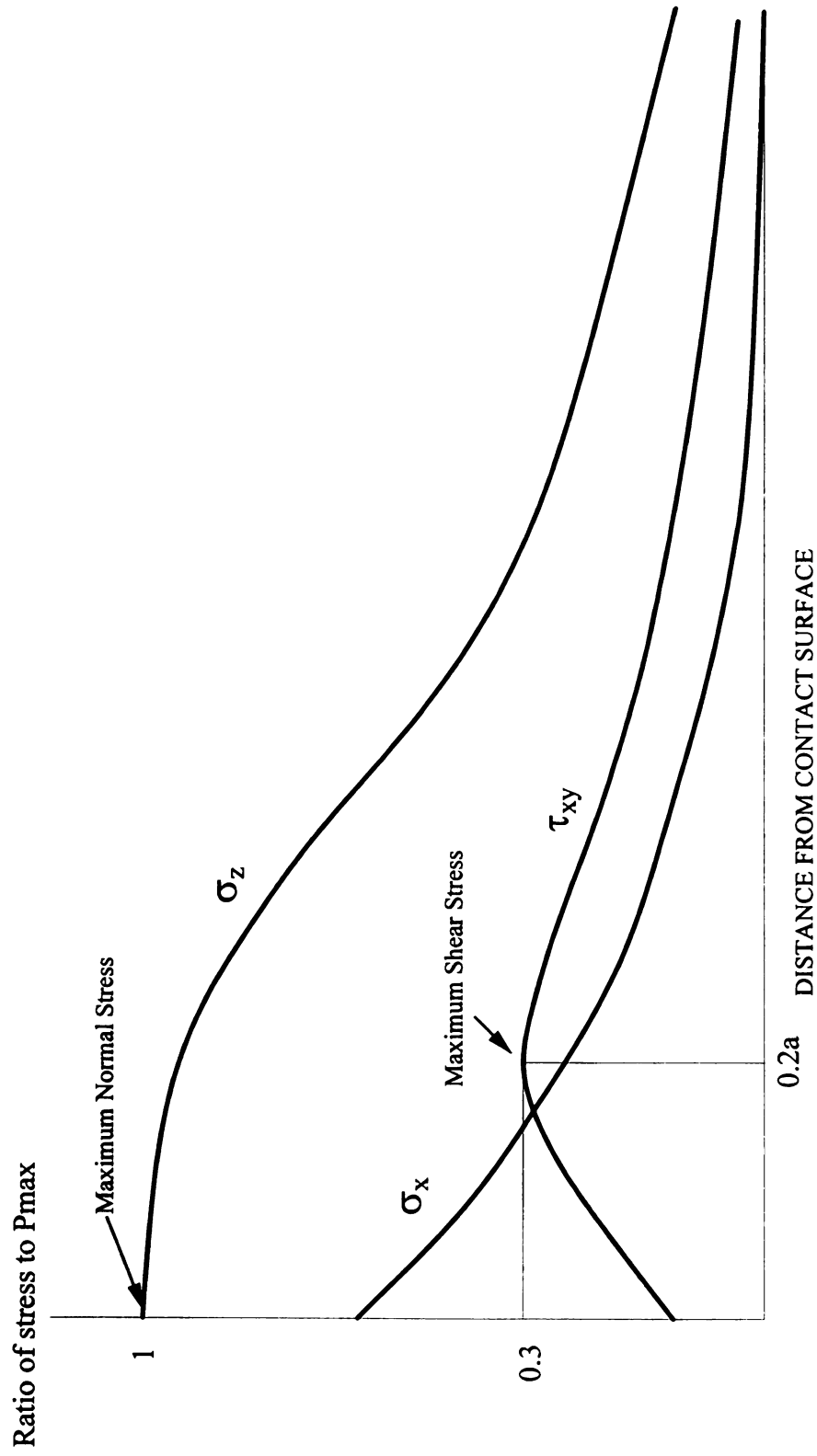
FIGURE 10 - Stress distribution of Hertz contact problem.

$$E = \left[ \frac{\rho^{1/3}(6\pi^2)^{2/3}2(1+\nu)}{\Omega^2} \right] f^2 m^{2/3} \qquad [27]$$

where  $\rho$ = Density
           $\nu$ = Poisson's ratio
           $\Omega$ = Normalized frequency
           $E$ = Modulus of elasticity
           $m$ = Mass
           $f$ = Frequency

The model includes apple mass, apple density, Poisson ratio, and normalized frequency. There are three different kind of vibrating modes. The compressional mode vibrating in the radial direction was assumed as the most predominate resonant frequency by Armstrong (1989).

# Chapter 4

## EXPERIMENTAL METHODS AND PROCEDURES

### 4.1 Methods

### 4.1.1 Compression Test

Cylindrical apple flesh samples 20 mm in diameter and 12 mm in length were prepared for the compression test. Cylindrical specimen was cut from fresh apples by using a borer. The borer was pushed into the direction of center around equator in the radial direction (Figure 11). Then the cylindrical sample was placed on the V-shaped cutting guide (Figure 12) to get the sample having desired length and made ends flat and normal to the direction of compression. A razor blade was used to cut the sample ends.

The sample was placed on platform of the Instron Universal Testing Machine and was pressed with a flat die. The force signal was transmitted to the data acquisition system. Cross-head speed was 0.00423 m/s (10 in/min). Mineral oil was added to both ends of the cylindrical apple flesh specimen to reduce friction between the die and the sample. The sampling rate of the data acquisition system was set to 100 Hz.

Actual force-deformation result was fitted using equation [1] and an optimization program to determine elastic modulus and viscosity of the viscous element in the model. The critical stress, $\sigma_c$, for the fracture element is determined by P1 (Figure 1) divided by the area of die. Elastic modulus, viscosity, and the critical stress will be used as parameters of compression model.
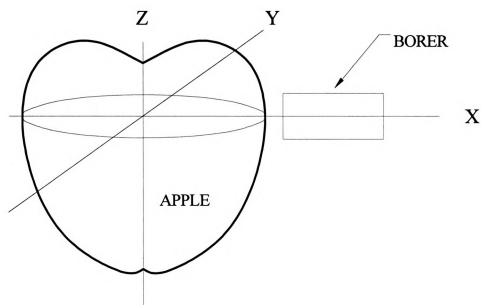
FIGURE 11 - Sampling direction of apple flesh for compression test

RAZOR BLADE
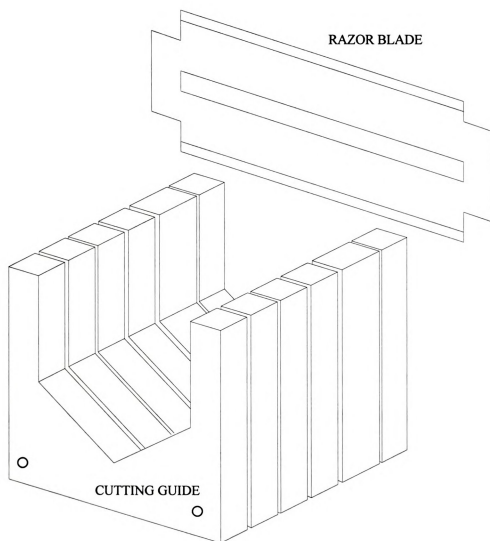
CUTTING GUIDE

FIGURE 12 - Cutting guide for preparing cylindrical apple flesh

### 4.1.2 Shear test

Slices of apple flesh were prepared by using a slicer. A shearing device suggested by

Mohsenin and Goehlich in 1962 to determine shear strength of apple skin was used for

the test (Figure 13). The apparatus was installed on the platform of the Instron Universal

Testing Machine. The shear strength will be used as a critical stress of the fracture

element of shear-tensile model.

Strain rate was 0.00423 m/s (10 in/min). Force signal from the load cell was recorded

by data acquisition system at a sampling rate of 100 Hz.

### 4.1.3 Tensile Test

Slice of apple was obtained from the cheek of whole apple. Tensile specimen was

prepared from the slice of apple flesh (Figure 14). Length, L, and the width, W, were 20

mm and 9 mm, respectively. Thickness of the specimen, t, was measured using calipers.

The specimen was installed on the Instron Universal Testing Machine and tensile force

was applied until it failed. Tensile elasticity was calculated from the stress-strain

relationship. The elasticity will be used as a parameter of shear-tensile model.

### 4.1.4 Magness-Taylor Puncture Test

An apparatus as shown in Figure 15 was used to make the cutting surface of apple

normal to the direction of the force applied. Also this device was used to hold the apple.

The apparatus has cutting blade and guide to remove the skin of apple and to make the

surface flat and even. This device was placed on the platform of the Instron Universal
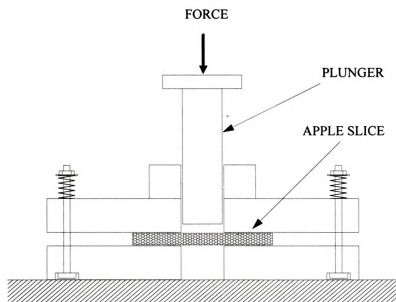
FIGURE 13 - Apparatus for shear test
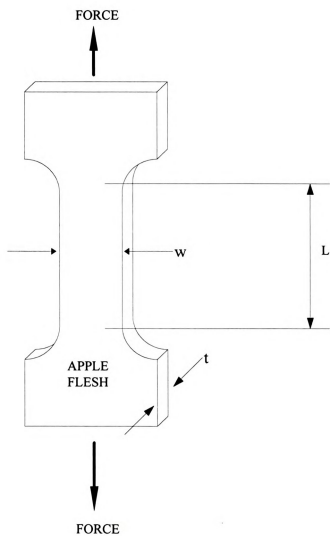
FIGURE 14 - Specimen for tensile test
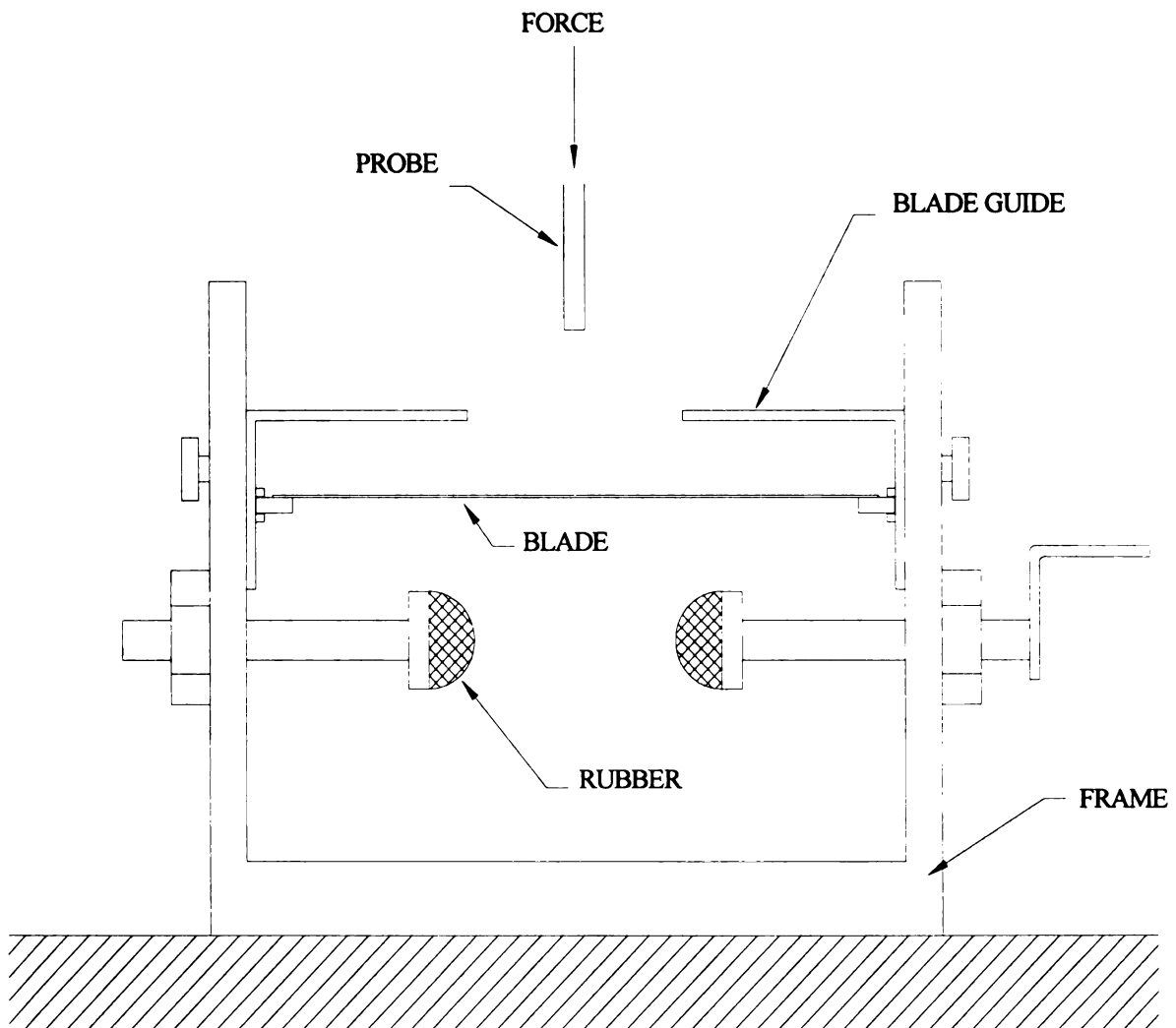
FIGURE 15 - Apple holding apparatus

Testing Machine. A 11.11 mm (7/16 in) diameter probe with flat end was used to push down into apple flesh. Cross-head speed was 0.0042 m/s (10 in/min).

The probe was pushed to a depth of 15 mm. The location for this test was approximately on the equator as the probe was inserted in the radial direction (Figure 16). The probe was lubricated with mineral oil to reduce friction.

### 4.1.5 Nondestructive Tests

Two nondestructive tests were studied in this research. One is rubber thumb test which is developed in this study to predict the critical yield strengths of compression and shear for the apple flesh. The other one is acoustic method which has been already developed and evaluated by Armstrong in 1989. Through acoustic method elasticity of apple flesh was estimated.

### 4.1.5.1 Contact Pressure Measurement using Rubber "Thumb Test"

A rubber indentor was used to measure contact stress using Hertz contact stress theory. The rubber diameter of 26.8 mm diameter had an elastic modulus of 3.2 MPa and a Poisson's ratio of 0.62. The indentor was attached to a steel plunger using adhesive (Figure 17). The pressure between the ball and apple was measured using a paper thin Uniforce pressure sensor. This sensor had a range of 0 to 222 N ( 50 lbf ) and a circular sensing area having 6.35 mm (0.25 in) diameter. The location for this test was on the equator of apple. The radius of curvature of this point was measured in two directions. One is in the direction of equator and the other is in the longitudinal direction. The average value of the two measurements was used as the radius of curvature at that point.
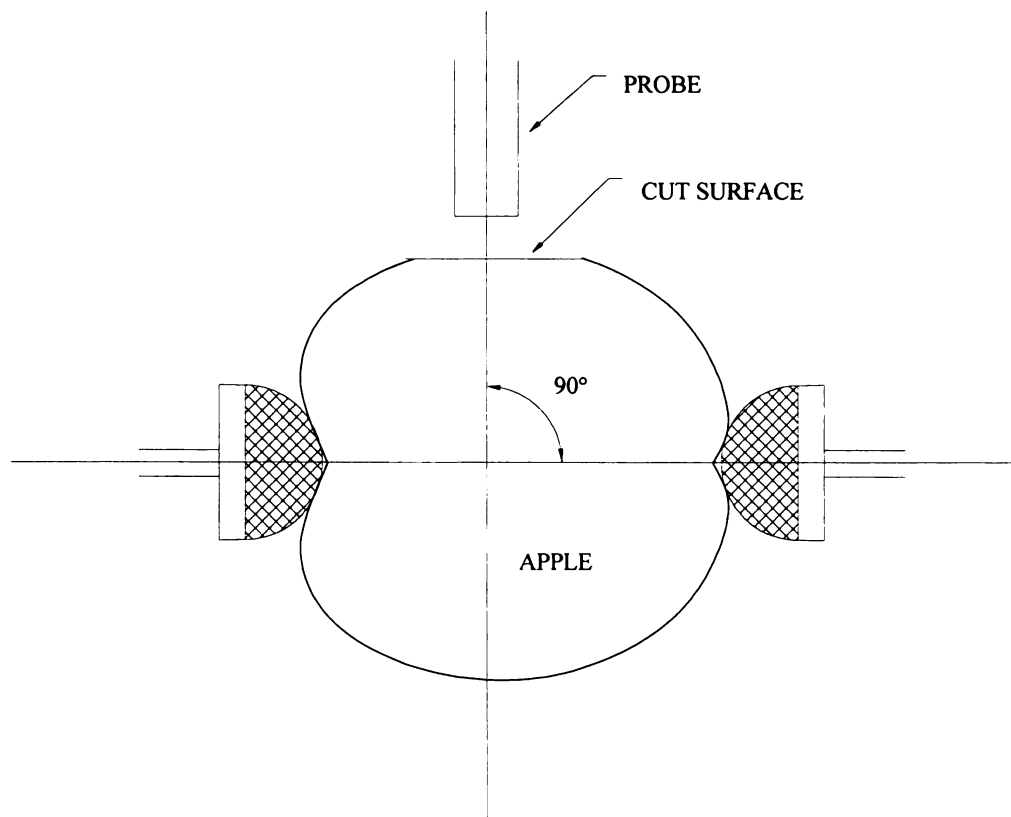
FIGURE 16 - Location of the Magness-Taylor puncture test
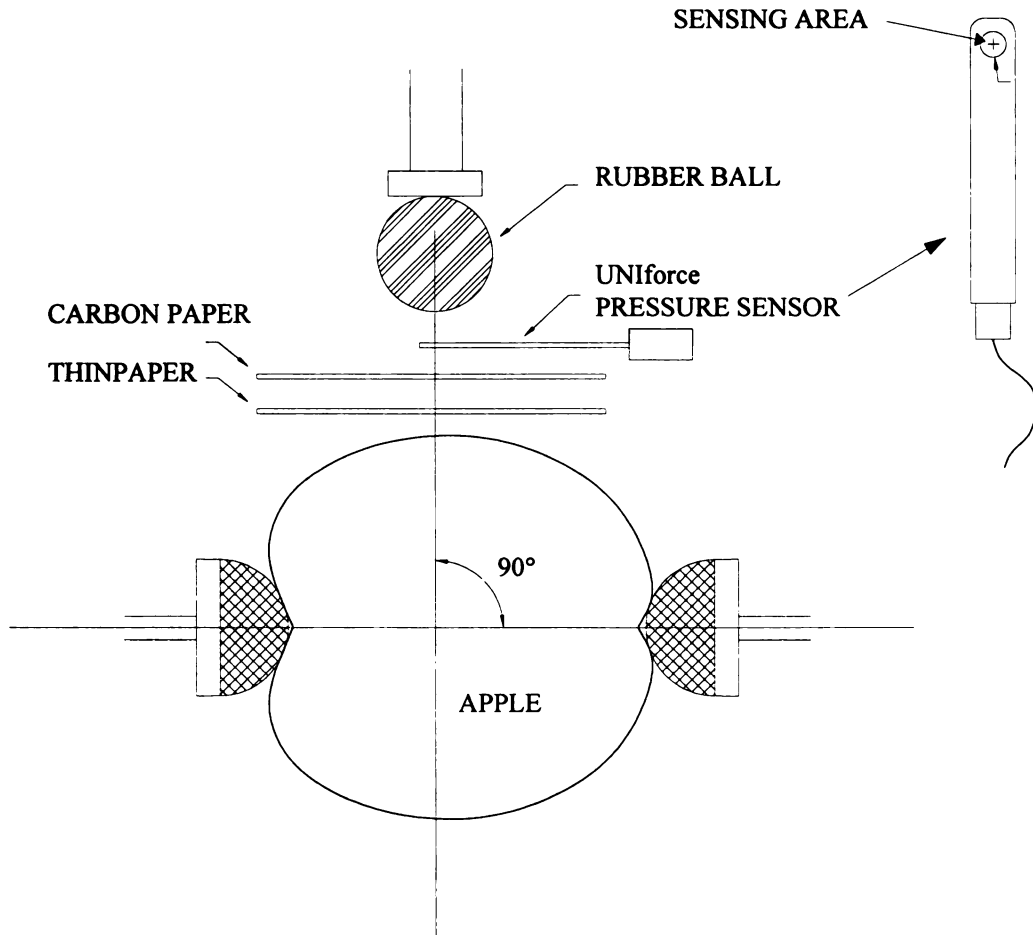
FIGURE 17 - Rubber thumb test

To measure the radii of curvature of convex body, an apparatus composed of a dial indicator and two sharpened rods was used (Figure 18). Radii were calculated as following

$$Radius = \frac{(AC)^2}{8(BD)} + \frac{(BD)}{2}$$ [28]

Apple was held by a fixture as shown in Figure 15. Carbon paper and a sheet of paper were used to get the contact area when the first "give" occurred. The term "give" means a change of force response. The probe, pressure sensor, carbon paper, paper and apple were arranged in the order as shown in Figure 17. The probe speed was 0.0021 m/s (5 in/min). The Instron Universal Testing Machine was manually stopped as quickly as possible when the first failure of tissue was detected by hand. The "give" produced vibration enough to be sensed by hand and it usually accompanied an audible sound.

### 4.1.5.2 Elastic Modulus Measurement using the Acoustic Impulse Response

An apparatus which was designed by Armstrong, *et al*. (1992) was used to determine the elastic modulus of apple. The apparatus was composed of mass measuring sensor, an actuator to swing an impulse hammer, and a microphone to measure the acoustic signal (Figure 19). The device was connected to a data acquisition system and the signal was converted automatically to the elastic modulus.

Every apple was tested using this device before they were tested by any destructive testing methods. Impulse location was approximately at the equator of the apple.

### 4.2 Materials
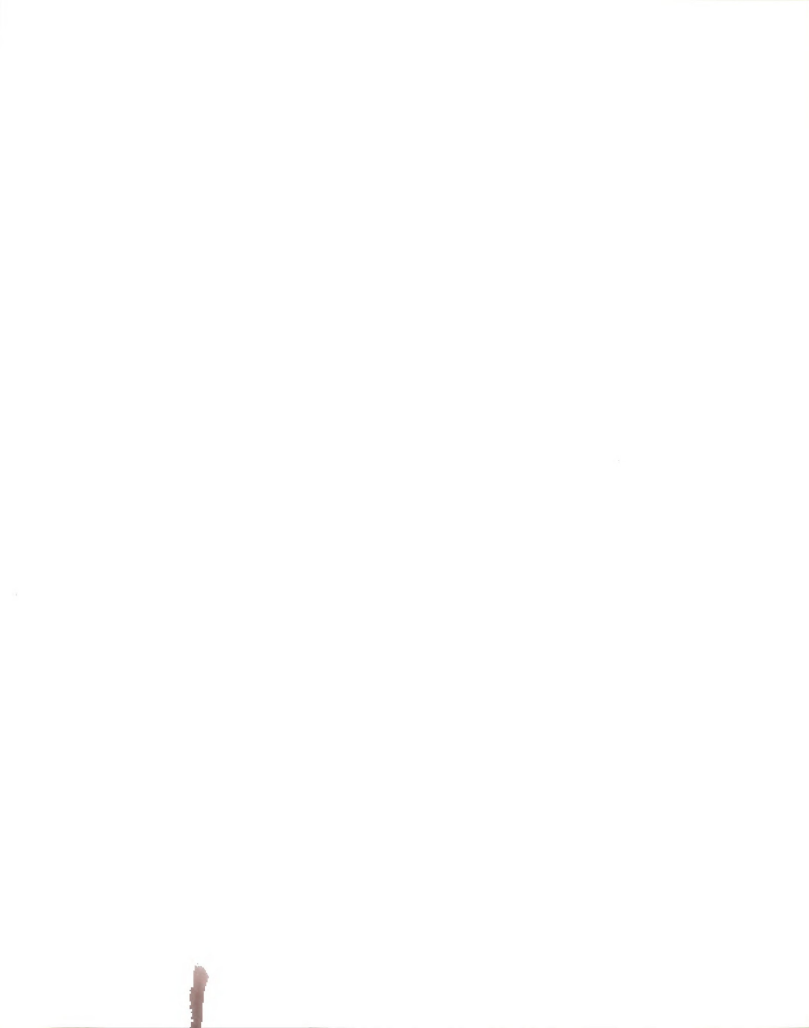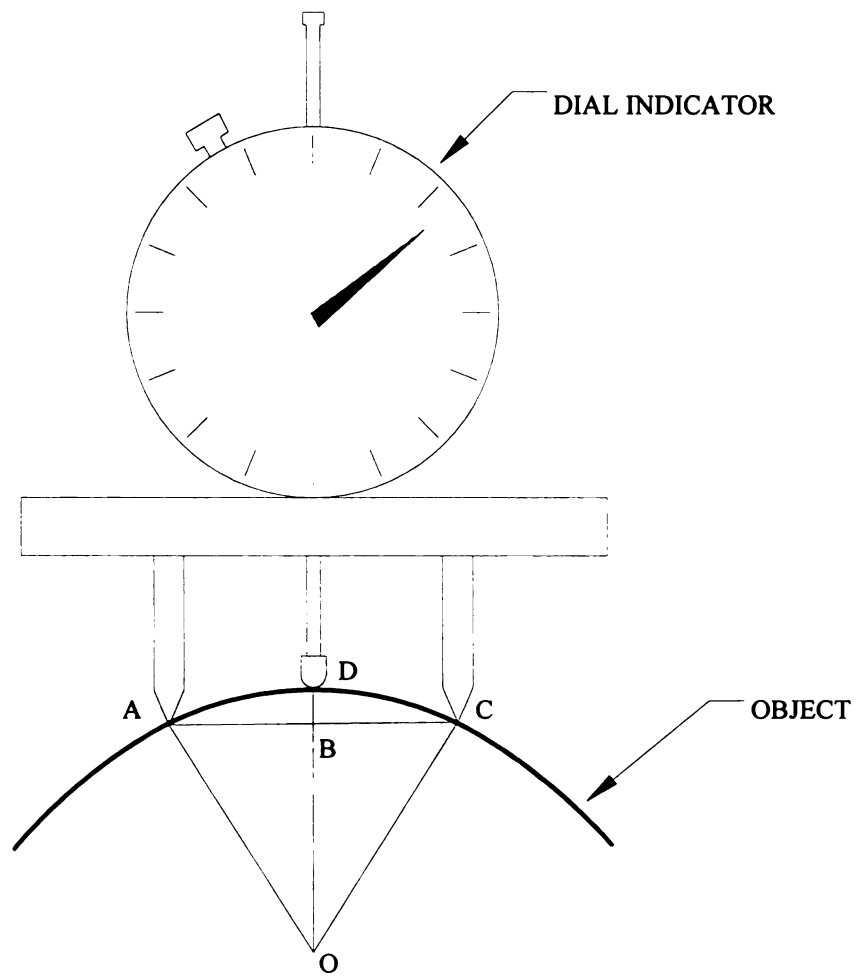
FIGURE 18 - Device for measuring the radius of curvature ( Radius of
Curvature Meter)

SOLENOID

PC

IMPUSE
HAMMER

MASS SCALE

APPLE

MICROPHONE
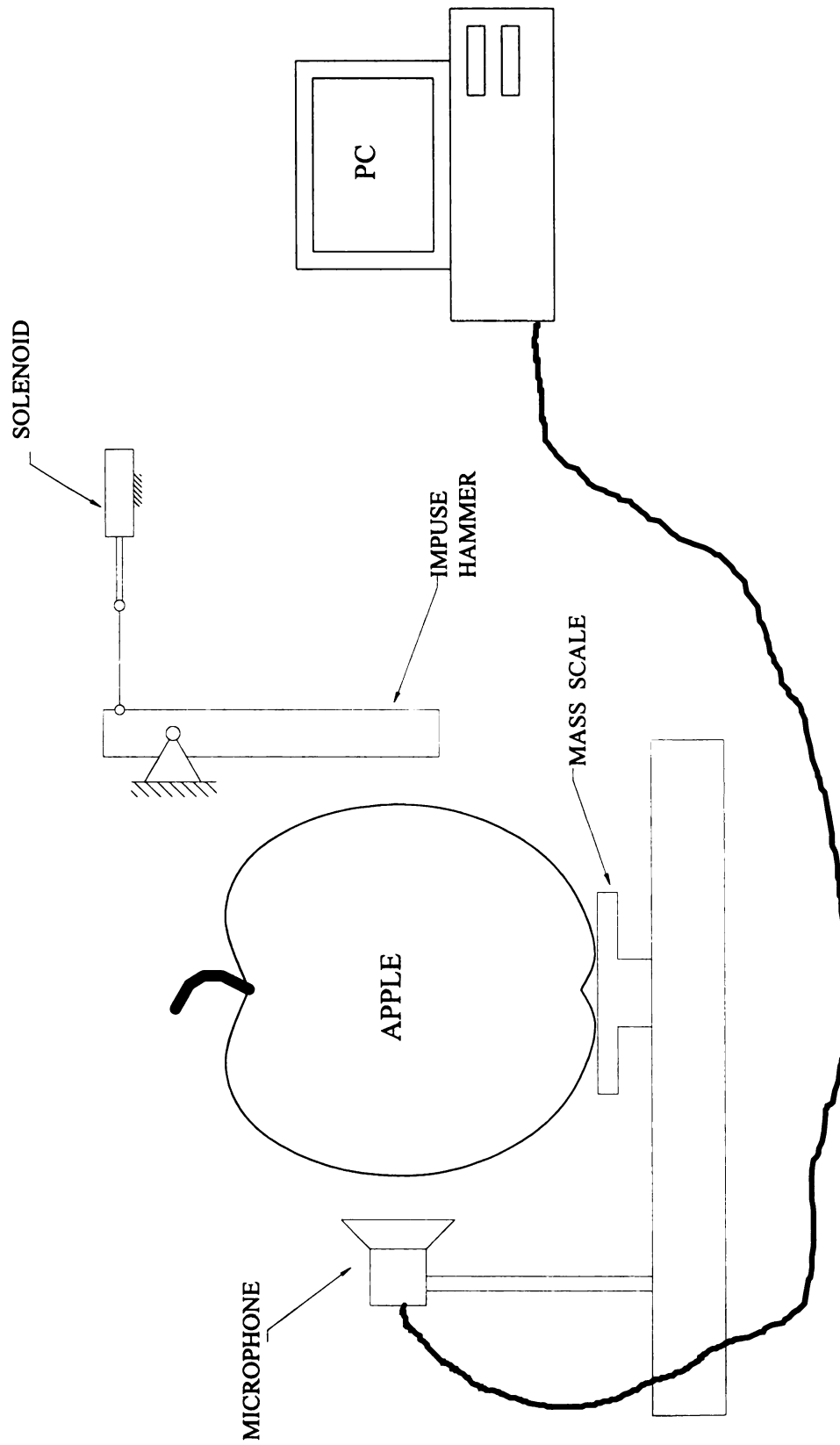
FIGURE 19 - Device for measuring acoustic response of apple.
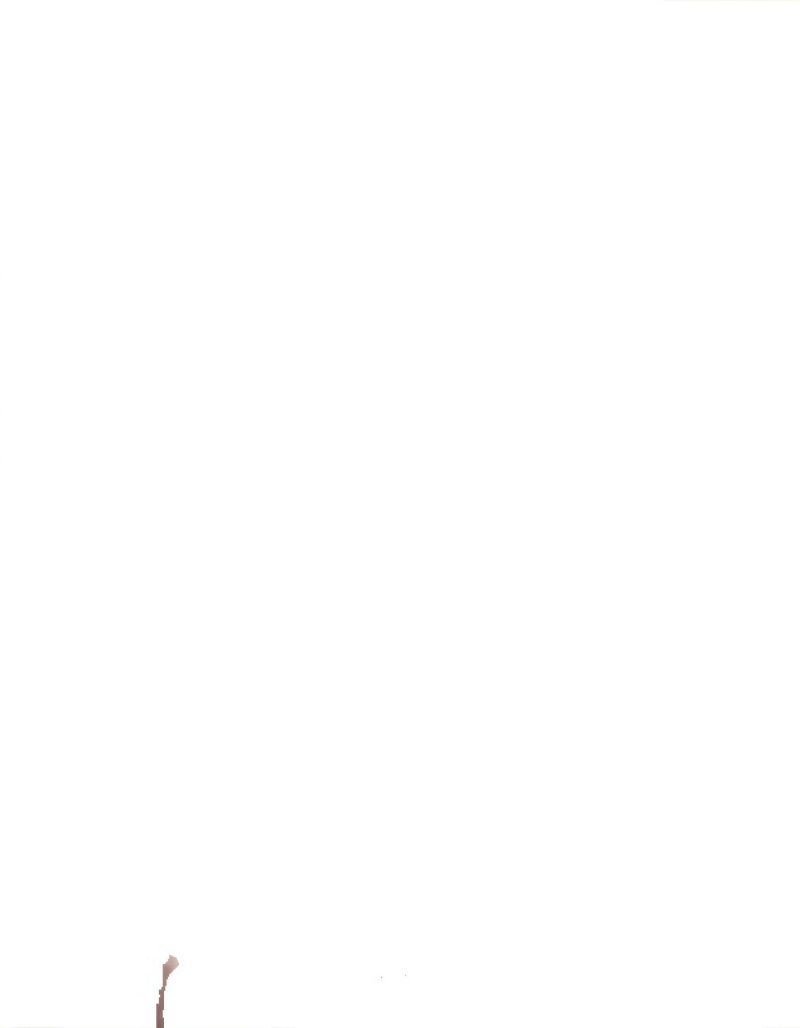
To have wide range of firmness, nine different cultivars were selected. Cultivars were Red Delicious, Red Rome, Fuji, Granny Smith, Golden Delicious, Braeburn, Ida Red, Gala, and Jona Gold. A total of 45 apples were used for the experiment. Apples were purchased from a local supermarket on the day of experiment and they were stored in a refrigerator at 14° C.

Weight measurement, acoustic impulse method, and "rubber thumb" test were performed on each apple prior to the destructive tests. Magness-Taylor puncture test, compression, shear, and tensile test were carried out after non-destructive tests were conducted. Locations for tests were different from test to test .

## 4.3 Computer Simulation of Laminated Cellular Model

A computer program for simulation was written in C language. The major parts of the program were the laminated cellular model, deformation sequence generator, compressive and shear-tensile force calculator, and the Castigliano's theorem. The block diagram of the simulation program structure is in Figure 20.

The model parameters of this simulation come from the compression, shear, and tensile test results. In this simulation 100 layer model represented a thickness, approximately 20 mm of apple flesh sample. Geometric ratio, r, was set to 0.997. The speed of testing tip was 0.00423 m/s (10 in/min) which was the same as that of the experiment. During the infinitesimal time, deformation generator produced deformations for every layer and the force of the components of each layer was calculated based on the deformation information. Force was multiplied by infinitesimal deformation to obtain infinitesimal energy and the energy was summed up throughout the simulation. After 5

45
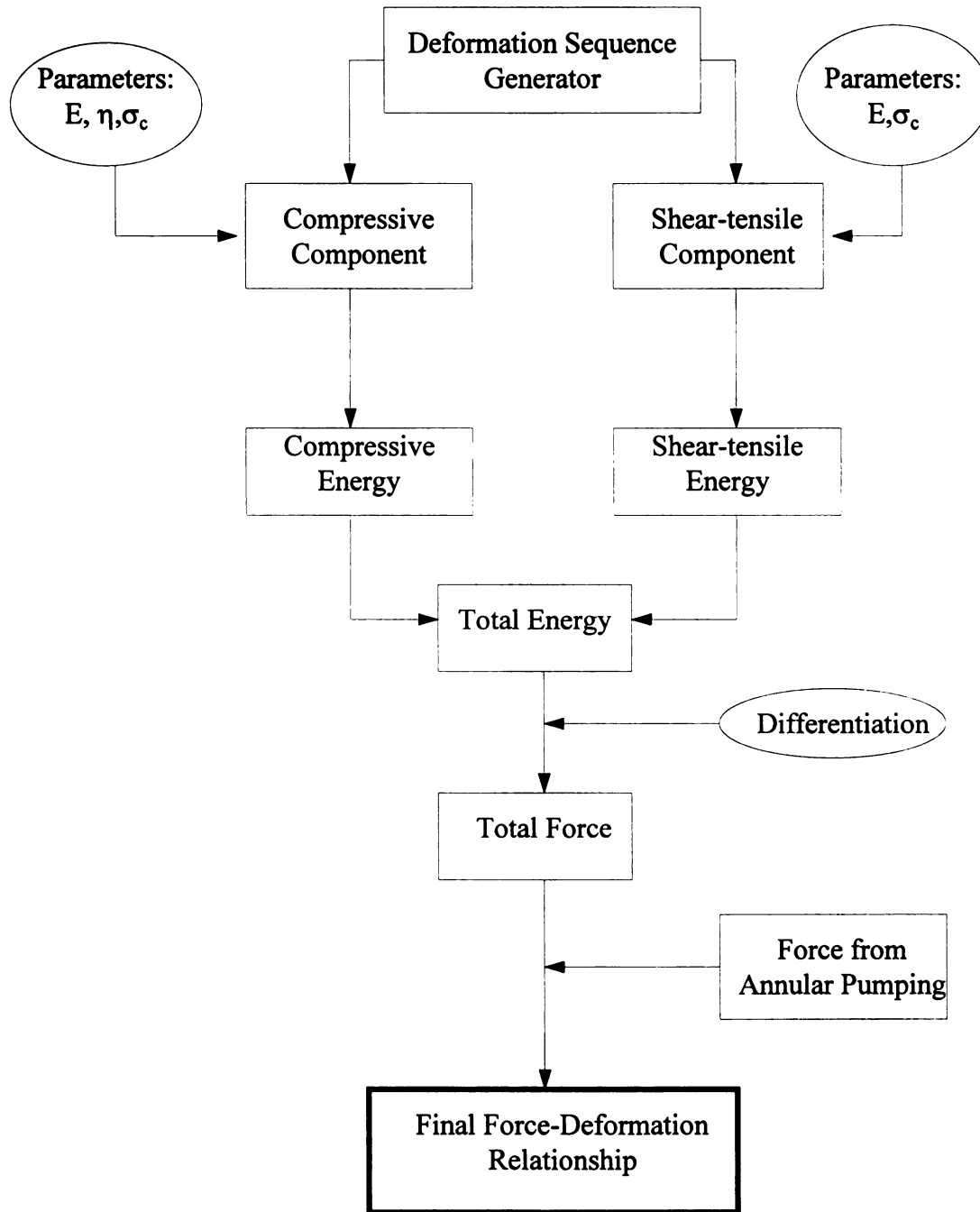


FIGURE 20 - Structure of the simulation program

seconds of simulation, numerical differentiation of energy for the deformation was performed and it produced force-deformation relationship. To the force-deformation result, annular pumping resistance was added gradually after the second peak force.

## Chapter 5

## RESULTS AND DISCUSSION

### 5.1 Results

### 5.1.1 Model Prediction And Magness-Taylor Puncture Test

From the force-deformation relationship of the Magness-Taylor puncture test the first

peak force was determined at a point showing significant drop of force. Figure 21

illustrates the result of the comparison between predicted and measured first peak force of

Magness-Taylor test. The correlation coefficient was 0.76.

The measured second peak force of Magness-Taylor puncture test was compared with

that of model prediction. Figure 22 shows the correlation coefficient of 0.79 which is a

little higher than that of the first peak force shown in Figure 21. In some cases, the

second peak force could not be observed and those cases were not considered.

Even though the first peak forces are same different stiffness indicates different

texture of apple flesh. Figure 23 illustrates that the correlation coefficient was 0.83.

Stiffness constant was defined as the slope of the secant drawn from the origin to the first

peak of the force-deformation curve. Figure 24 is an example of the simulation result.

Magness-Taylor firmness predicted by the model was compared with that measured

by experiment. Figure 25 shows that the correlation coefficient is 0.82.

Even though the juice expelling effect produced constant resistance of 9.67 N which

was calculated by using the eq. [16] it took time until this resistance was fully developed.

$$Y = 1.02\,X + 4.00$$

Correlation Coefficient=0.76
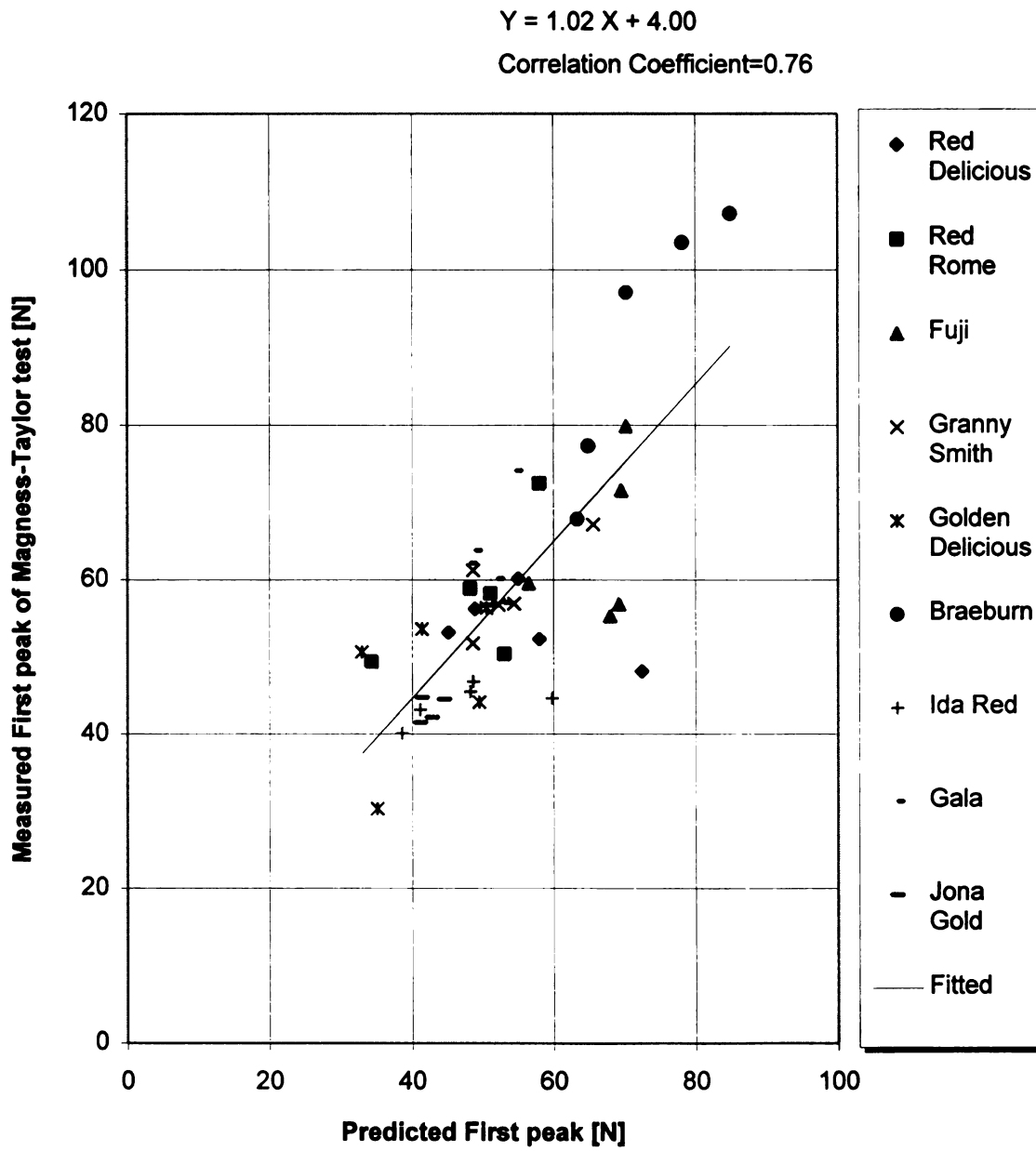
FIGURE 21 - Predicted versus measured first peak force

Y=0.83X+10.67

Correlation Coefficient=0.79
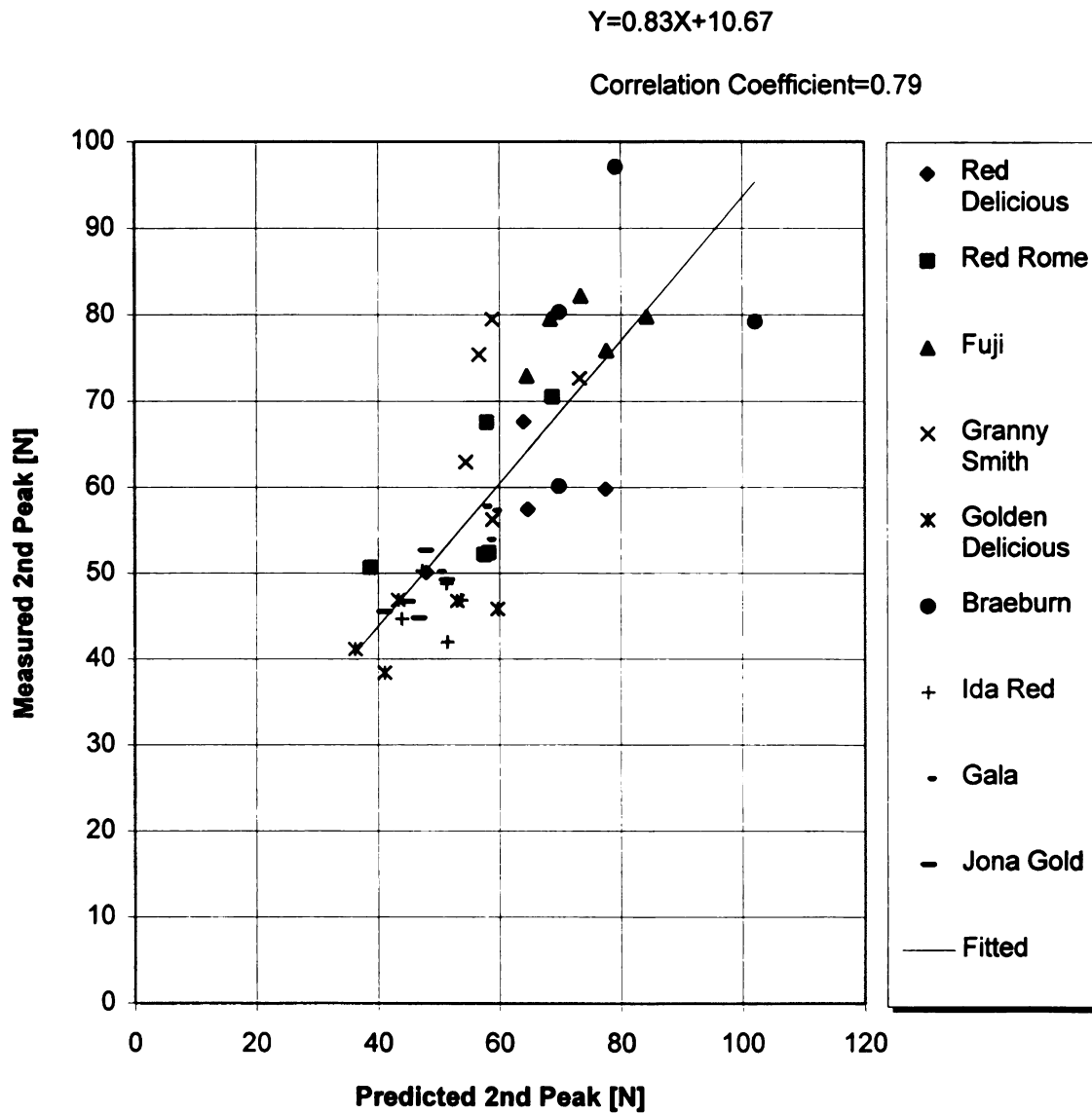


FIGURE 22 - Predicted versus measured second peak force

Y=0.83X+3657

Correlation Coefficient=0.83
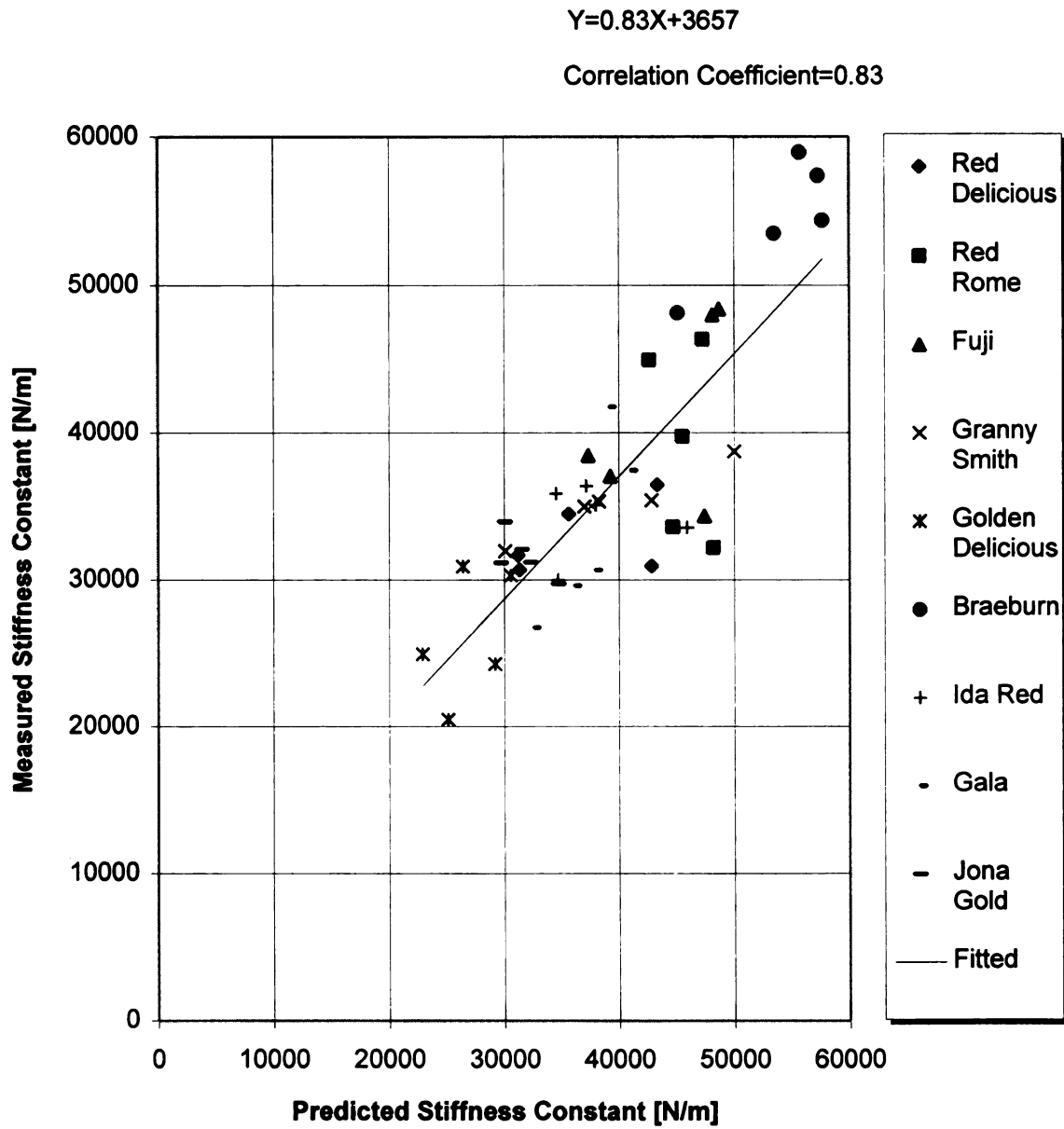


FIGURE 23 - Predicted versus measured stiffness constant
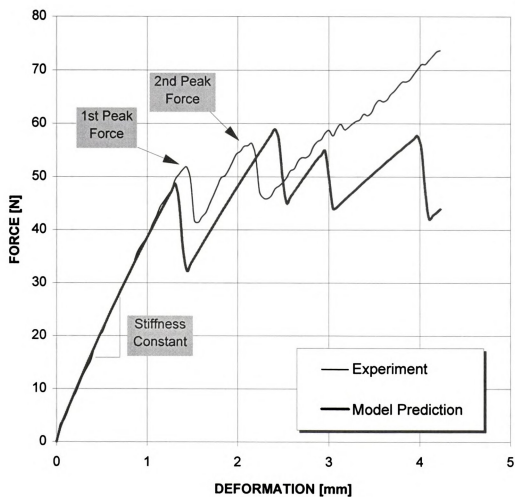
FIGURE 24 - Comparision of model prediction with experiment

Y = 0.7 X + 15.78

Correlation Coefficient=0.82
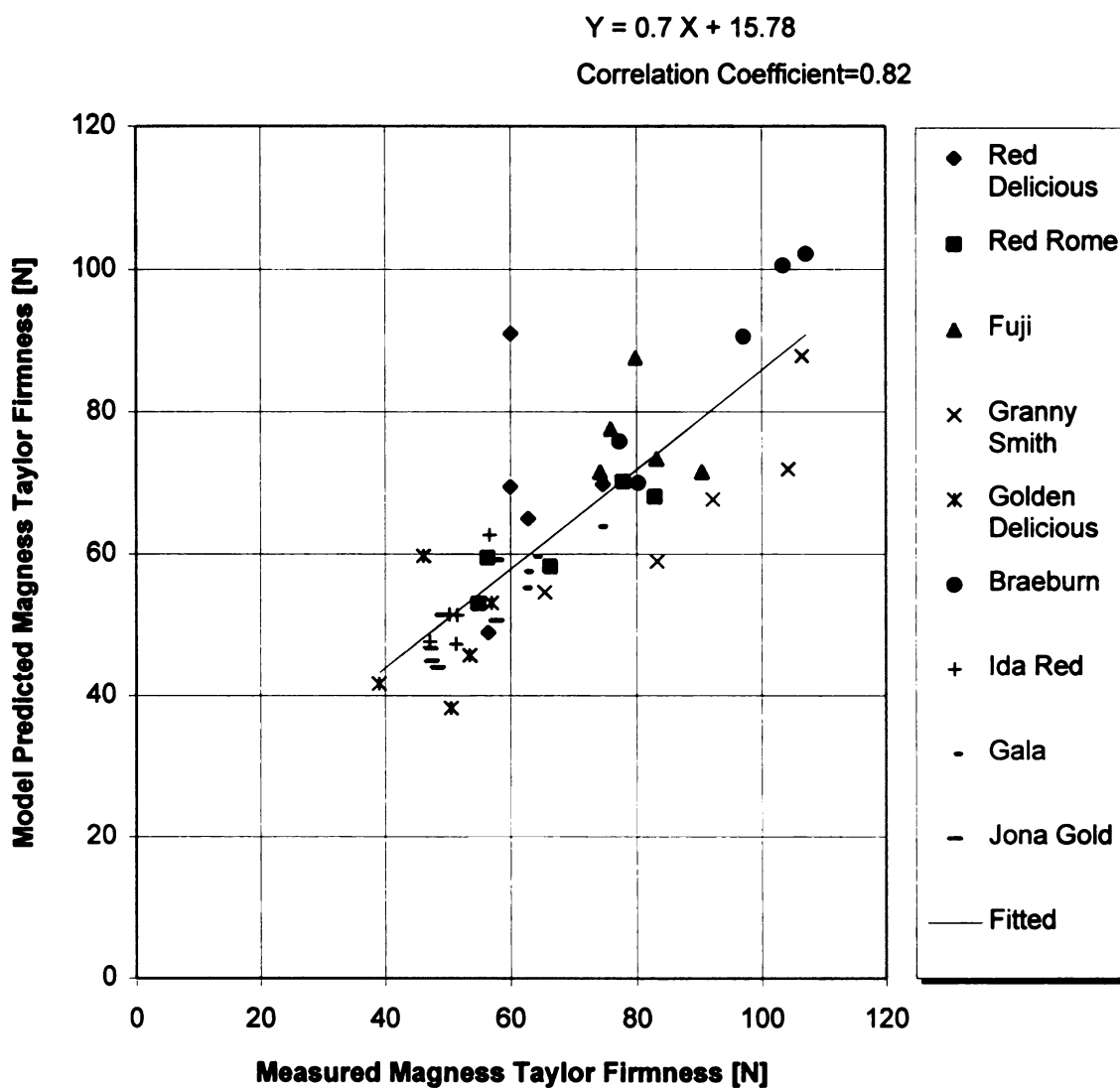


FIGURE 25 - Predicted versus measured Magness Taylor Firmness

The resistance increased linearly after the first peak until it reached a value of 9.67 N and then it was fixed at 9.67 N. Because the viscous element was connected in parallel to the model the resistance was just added to the result.

## 5.1.2 Performance of Rubber "Thumb Test"

The maximum normal stress at the center of the contact area between rubber ball and the apple was calculated by using eq. [23]. Speed of the rubber thumb test was 0.00212 m/s (5 in/min). Figure 26 shows the correlation coefficient of 0.76.

Figure 27 illustrates the correlation coefficient of 0.64 between measured shear failure stress and the predicted maximum shear stress. According to the Hertz contact stress theory the maximum shear stress occurred below the contact surface and it was approximately 1/3 of the maximum normal stress.

Magness-Taylor firmness was compared directly with the failure force which was observed when the contact pressure dropped significantly. In this research this moment of "give" was detected and the testing machine was stopped at that moment. Figure 28 shows a correlation coefficient of 0.9. In rare cases, no significant drop of the pressure was observed due to tissue failure.

The first peak force showed a much higher correlation coefficient of 0.90 with the failure force than that of the Magness-Taylor firmness (Figure 29). The high correlation coefficient implies that the failure force represents the first peak force.

The relationship between the first peak force and the Magness-Taylor firmness was observed in Figure 30. More than a half of the data is almost identical in the range of error.
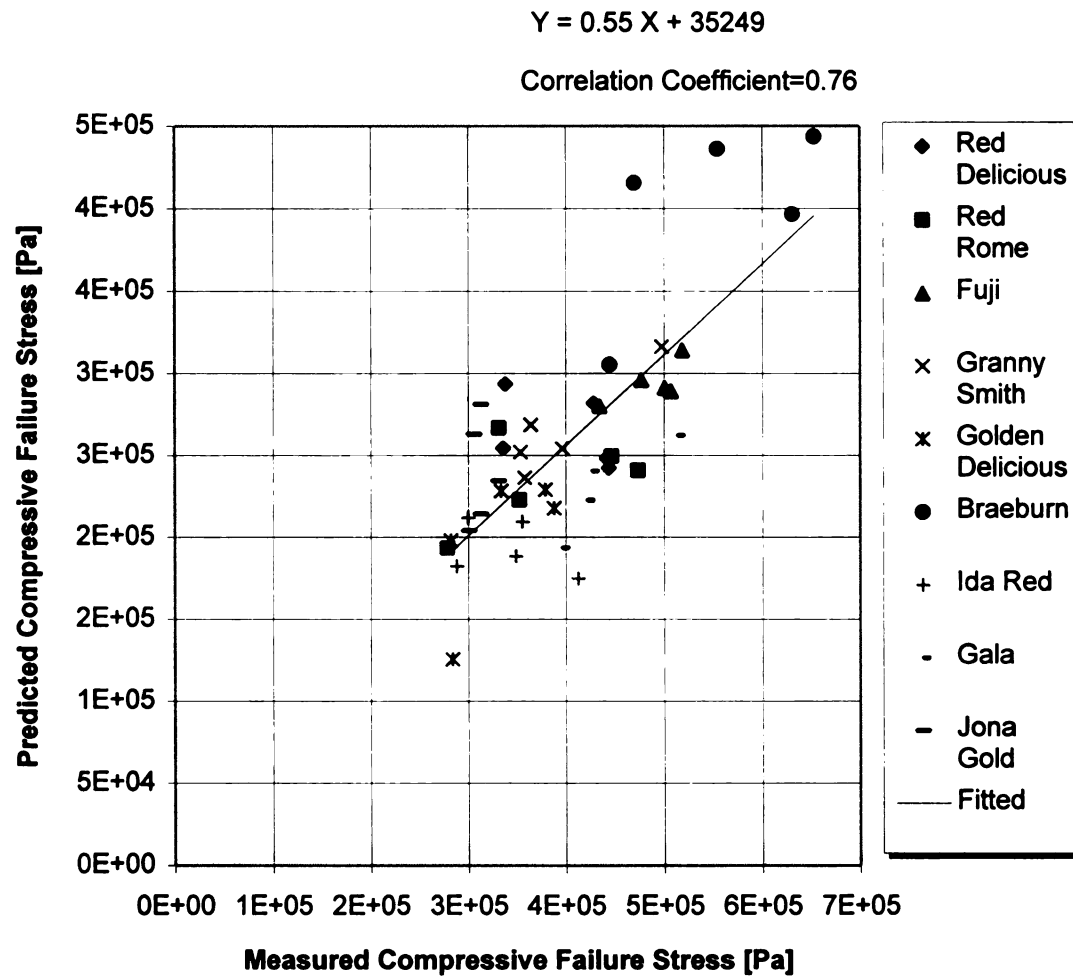
FIGURE 26 - Predicted versus measured compressive failure stress
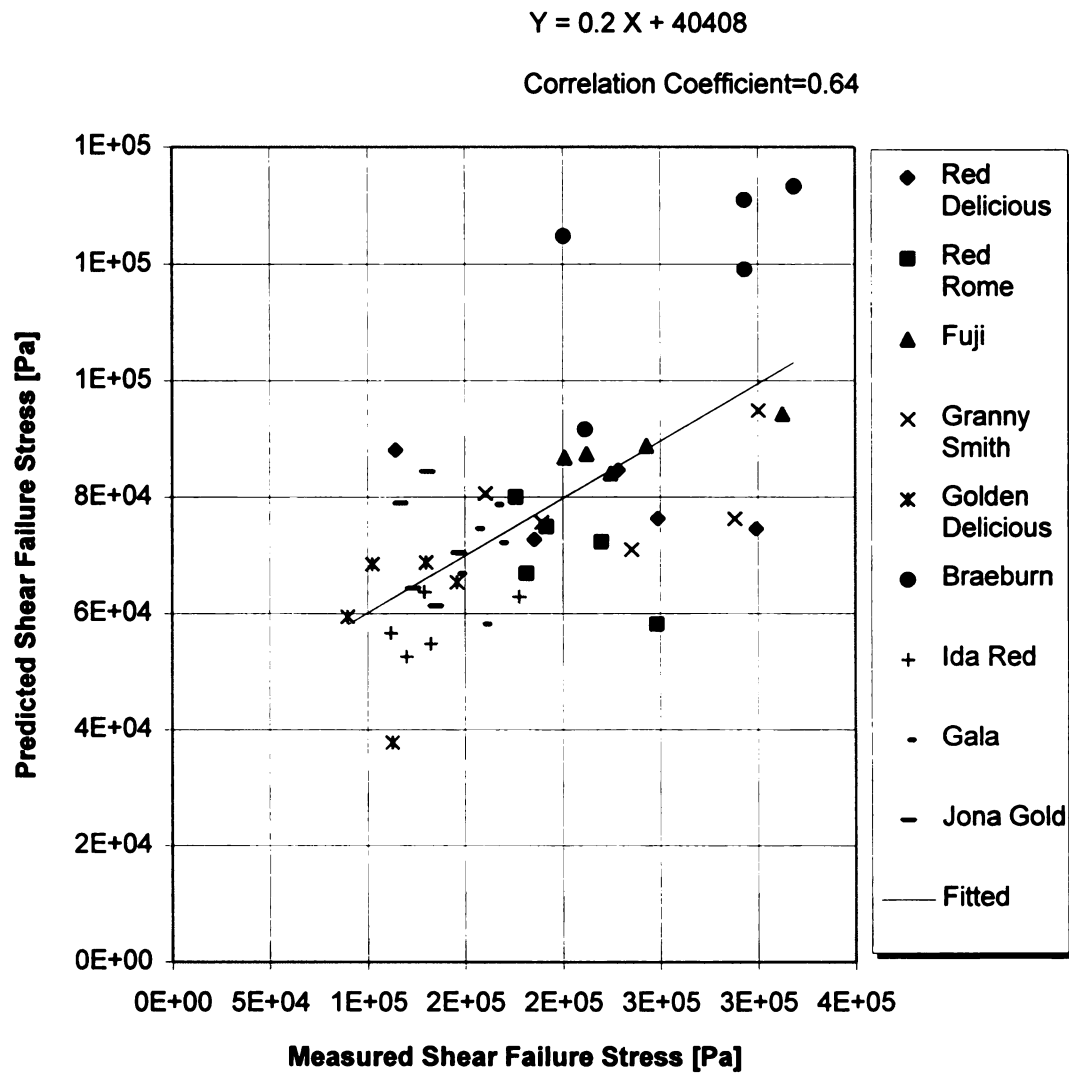
FIGURE 27 - Predicted versus measured shear failure stress
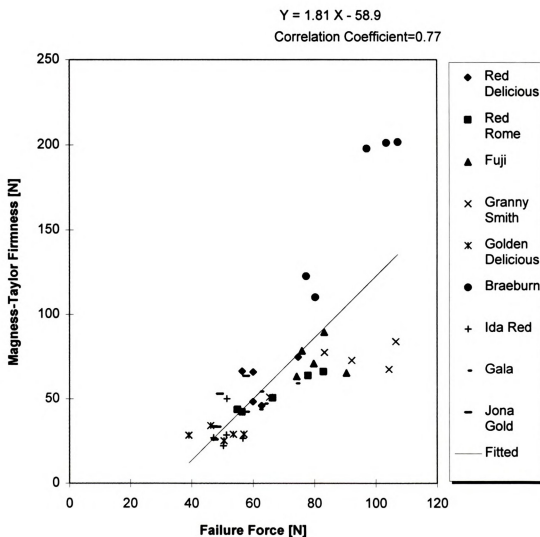
FIGURE 28 - Magness-Taylor firmness versus failure force of rubber thumb test

FIGURE 29- First peak force versus Filure Force
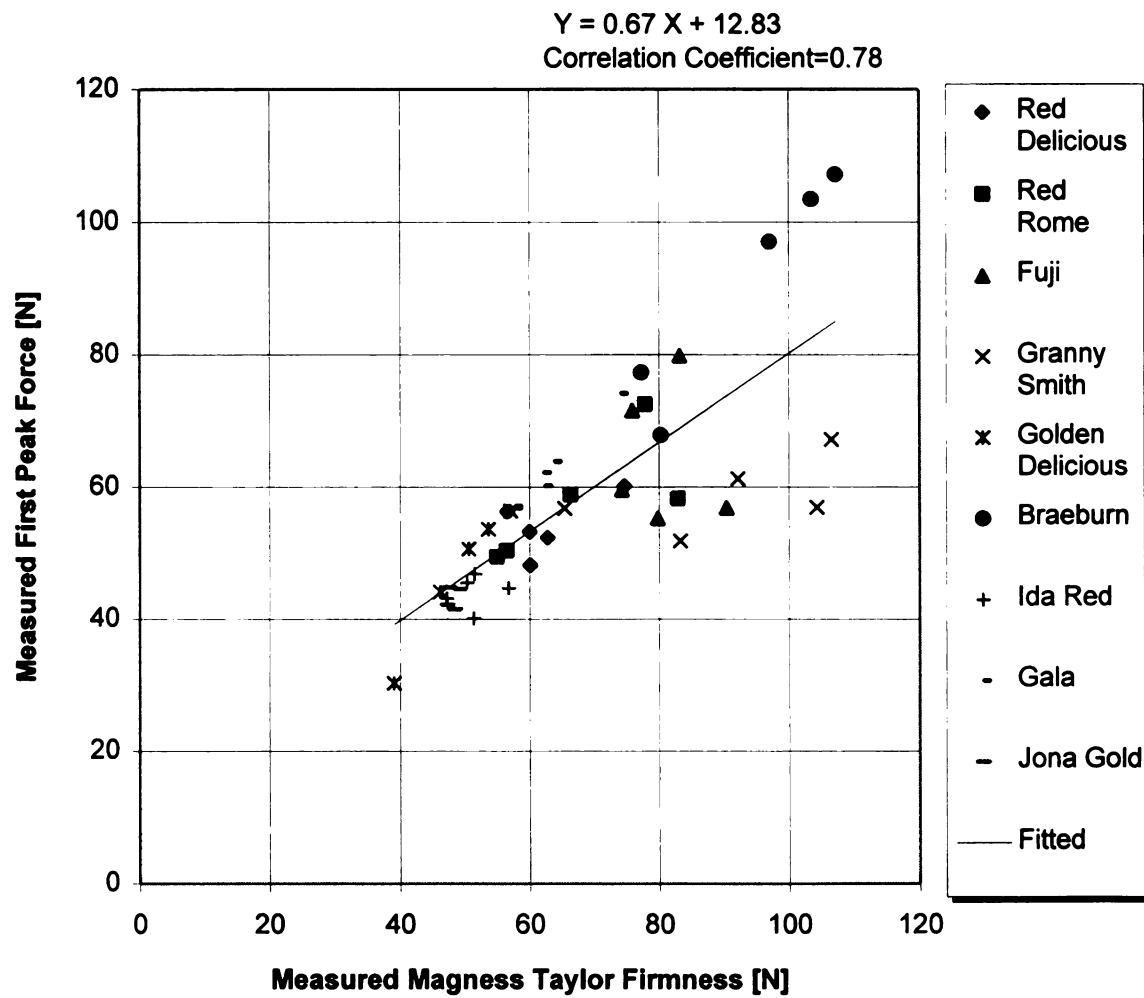
FIGURE 30 - Measured first peak force versus Magness-Taylor Firmness

## 5.1.3 Performance of Acoustic Impulse Technique

Modulus of elasticity of apple tissue was predicted using eq. [27]. In the compression mode, a Poisson's ratio of 0.3 and the density of 800 kg/m$^3$ were assumed for the resonant sphere model. Measured modulus of elasticity was obtained from the compression test of cylindrical apple flesh. From the compression test results initial tangent modulus of elasticity was found. In the compression test cylindrical apple flesh sample was bored in the radial direction which was different from the sampling direction used by Armstrong (1989). Figure 31 illustrates 0.7 as the correlation coefficient between the measured and predicted modulii of elasticity.
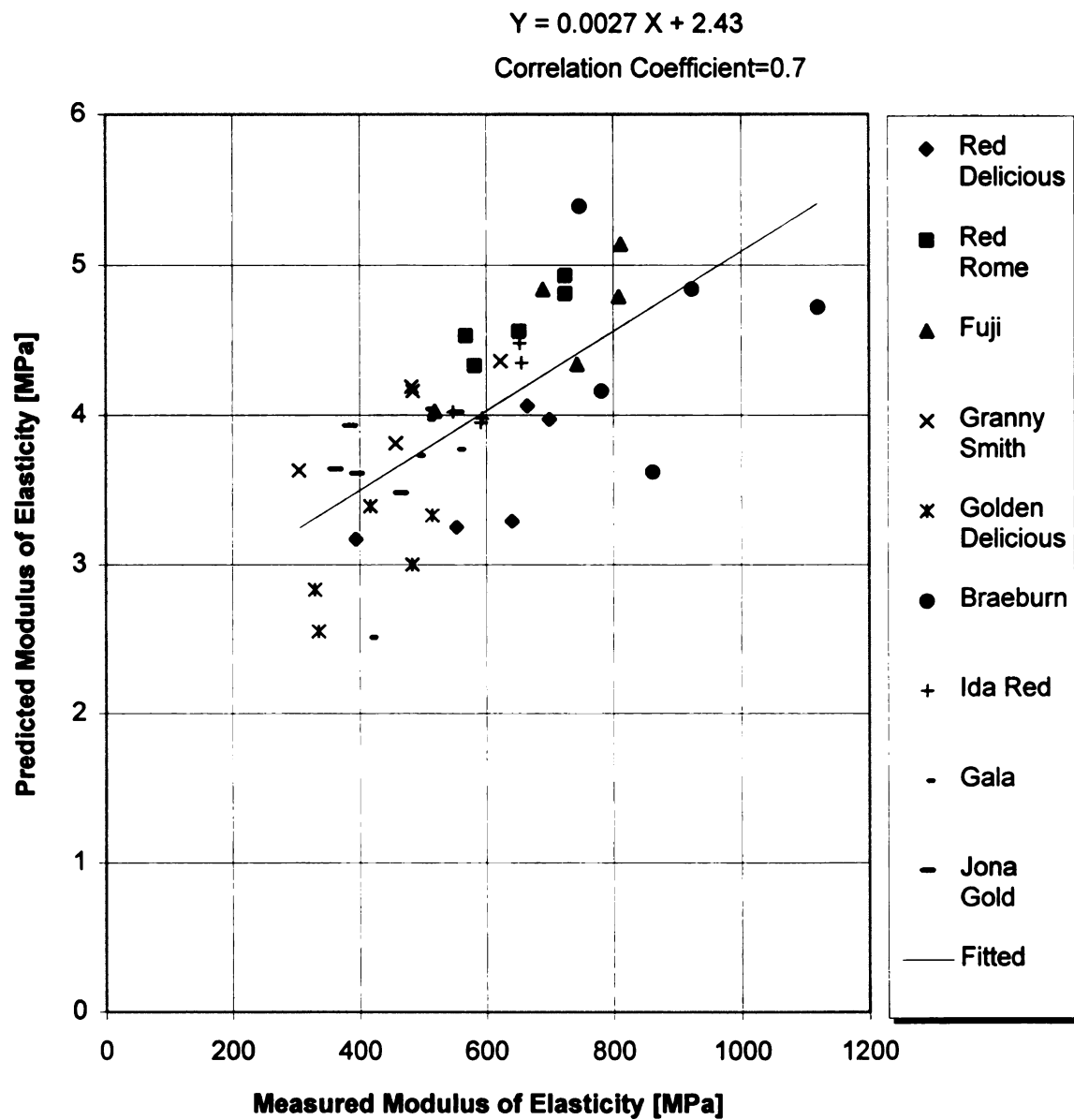
FIGURE 31 - Measured versus predicted modulus of elasticity
by using acoustic impulse

## 5.2 DISCUSSION

### 5.2.1 Quantitative Aspects of The Model Prediction

The laminated cell layer model showed fairly good correlation for the first peak force and the second peak force prediction. The correlation coefficient of the second peak (0.79) was little higher than that of the first peak force (0.76). Thus, the model demonstrated its prediction capability for the first two peak forces. In addition, Figure 23 showed a strong correlation (0.83) in predicting stiffness constant which meant that the model worked not just for the peak forces but also for the first slope of the force-deformation relationship.

After the second peak it was hard to compare because unidentified disorder occurred as the mastication progressed. However, the information about the early period of the mastication period was enough to determine the texture of apple flesh.

In Figure 32, it was found that the percentages of the sample having less than 20% error with its measured values were 51% for the first peak prediction, 78% for the second peak prediction, 73% for the stiffness prediction, and 84% for the Magness-Taylor firmness prediction. From the results explained above the laminated cell layer model was considered as a good means to depict the Magness-Taylor puncture test quantitatively.

### 5.2.2 Qualitative Aspects of The Model Prediction

The characteristics of the force-deformation relationship was a saw-tooth shape which inferred the significant change of force or the catastrophic destruction of material. The model represented well this characteristics of the force-deformation relationship. Figure 23 shows the correlation coefficient of 0.83 for predicting the stiffness which indicates

e:error
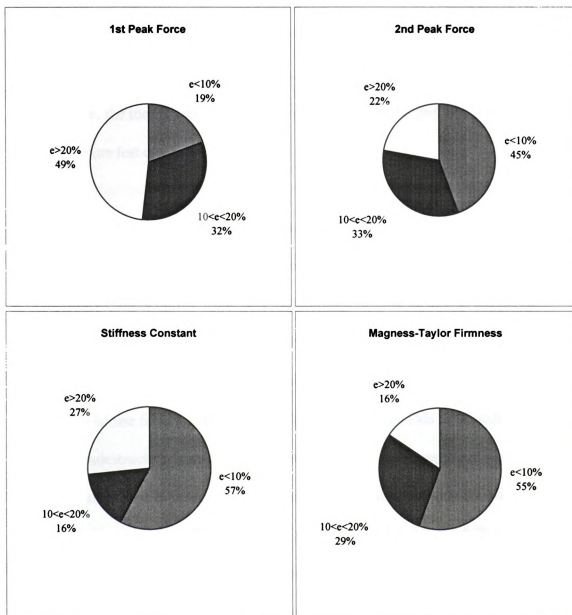


FIGURE 32 - Precision of model prediction

that the model has the capability to describe the different textural quality of two apples having the same first peak force.

Until the second peak the juices expelling effect did not contribute significantly to the total trend of force-deformation relationship because juices were not produced enough to induce resistance and also because the penetration depth was so small.

Therefore, the model was considered to represent the early period of the Magness-Taylor puncture test qualitatively.

### 5.2.3 Evaluation of Nondestructive Method

Rubber thumb test was considered a good method to provide model parameters such as compressive, shear failure stress nondestructively. Figure 26 and 27 support the possibility of the rubber thumb test. In addition, the method could be used to replace Magness-Taylor puncture test. Figure 28 indicates that there was 0.77 of correlation between the failure force and the Magness-Taylor firmness. This new method was not perfectly nondestructive. Actually it made small bruise on the apple surface but it was not significant. If the diameter of rubber ball was minimized up to some point the size of bruise would be negligible. The first peak force was correlated to the failure force to identify what the failure force in fact measured. Figure 29 shows correlation coefficient of 0.9 which means that the rubber thumb test measures the first peak force efficiently rather than the Magness-Taylor firmness.

The contact pressure was also measured using Uniforce pressure sensor and thecorrelations with Magness-Taylor firmness and the failure force were investigated.

Ideally, contact pressure was expected to have good correlation with the failure force but in fact it was not so. The reason for this was the characteristics of the pressure sensor. If the film surface of pressure sensor was bent then it produced undesirable output. In the experiment the contact surface was not flat so that the sensor output interfered with true value. If a proper sensor for this purpose were available then the contact pressure would also be expected to have good correlation with the failure force.

Acoustic impulse technique showed fairly good correlation of predicting the initial modulus of elasticity. This technique was also considered to have the potential for providing model parameters.

# CONCLUSIONS

Considering the results of this research following conclusions are drawn:

1. The laminated cell layer model developed in this research was considered to have reasonable capability for depicting the Magness-Taylor puncture test results quantitatively and also qualitatively. Correlation coefficients for predicting the first peak was 0.76 and for the second peak it was 0.79. Also, the model predicted well the stiffness constant with correlation coefficient of 0.83.

2. Rubber thumb test may be used to estimate model parameters. In this research this method showed 0.76 and 0.64 of correlation for predicting the compressive and shear failure stress, respectively. Moreover, rubber thumb test was found to have strong correlation of 0.9, with Magness-Taylor firmness.

3. Acoustic impulse technique may be used to estimate model parameters. This technique showed correlation coefficient of 0.7 with the measured initial modulus of elasticity.

# SUGGESTIONS FOR FUTURE RESEARCH

For future research the following ideas are suggested:

1.  In preparing the cylindrical sample for compression test it is very critical to ensure that the sample have two flat ends normal to the direction of the compression force. If those ends are not normal to the compression force the shear failure comes first rather than the collapse of the layer. It is also difficult to obtain correct mechanical properties from the compression test if it is not flat.

2.  There are several supplemental constants such as number of layers, geometric ratio, ratio of stress recovery, ratio of increase of contact area and the initial length for calculating the strain of shear-tensile component. Effects of these constants are worthy of future study for better performance of the laminated cell layer model.

3.  Bruise can be minimized by reducing the size of the rubber ball. The effect of size reduction for the performance of the rubber thumb technique can be studied.

4.  As the rubber ball was pressed onto the apple, sudden change of contact pressure occurred which produced audible sound and vibration. By incorporating accelerometer on the surface of apple this vibration can be sensed and testing machine

can be stopped. Thus, it is possible to measure the contact diameter at the moment of flesh failure.

5.   The elasticity and the viscosity obtained by compression test can be studied to find a relationship of these parameters to a textural quality.

**APPENDICES**

**APPENDIX A**

# APPENDIX A

## Table A1 - Magness-Taylor test results

| | 1st Peak Force | | 2nd Peak Force | | Initial Slope | | Magness-Taylor | |
|---|---|---|---|---|---|---|---|---|
| | Obs. | Predic. | Obs. | Predic. | Obs. | Predic. | Obs. | Predic. |
| No. | [N] | [N] | [N] | [N] | [N/m] | [N/m] | [N] | [N] |
| 1 | 56.23 | 48.9 | 50.06 | 47.9 | 31652 | 31209 | 56.49 | 48.88 |
| 2 | 48.12 | 72.5 | 59.80 | 77.5 | 34469 | 35660 | 60.06 | 91.01 |
| 3 | 52.29 | 58.1 | 57.41 | 64.7 | 30906 | 42853 | 62.80 | 64.94 |
| 4 | 53.16 | 45.1 | * | 54.4 | 30655 | 31359 | 59.99 | 69.44 |
| 5 | 60.12 | 55.1 | 67.61 | 64.0 | 36445 | 43365 | 74.70 | 69.78 |
| 6 | 58.24 | 51.1 | 67.56 | 57.9 | 33580 | 44690 | 82.92 | 68.06 |
| 7 | 72.50 | 58.0 | 70.53 | 68.8 | 46324 | 47261 | 77.88 | 70.19 |
| 8 | 50.37 | 53.1 | 52.21 | 57.5 | 32184 | 48218 | 56.41 | 59.49 |
| 9 | 58.85 | 48.2 | 52.41 | 58.2 | 39748 | 45549 | 66.33 | 58.22 |
| 10 | 49.40 | 34.3 | 50.72 | 38.7 | 44921 | 42656 | 54.92 | 53.03 |
| 11 | 55.28 | 68.0 | 79.83 | 84.3 | 48400 | 48697 | 79.83 | 87.60 |
| 12 | 59.56 | 56.5 | 72.96 | 64.5 | 37055 | 39259 | 74.27 | 71.54 |
| 13 | 71.59 | 69.6 | 75.93 | 77.6 | 38467 | 37351 | 75.93 | 77.64 |
| 14 | 56.85 | 69.3 | 79.57 | 68.5 | 48001 | 48132 | 90.47 | 71.56 |
| 15 | 79.89 | 70.3 | 82.25 | 73.4 | 34339 | 47429 | 83.17 | 73.44 |
| 16 | 67.15 | 65.6 | 72.67 | 73.3 | 38721 | 50022 | 106.54 | 87.84 |
| 17 | 51.77 | 48.6 | 56.23 | 58.9 | 34967 | 37026 | 83.28 | 58.91 |
| 18 | 61.22 | 48.6 | 75.40 | 56.7 | 35300 | 38305 | 92.21 | 67.66 |
| 19 | 56.75 | 52.2 | 62.92 | 54.5 | 31940 | 30101 | 65.41 | 54.57 |
| 20 | 56.90 | 54.4 | 79.48 | 58.8 | 35399 | 42868 | 104.30 | 71.92 |
| 21 | 53.59 | 41.4 | 46.90 | 43.3 | 30903 | 26434 | 53.59 | 45.64 |
| 22 | 44.12 | 49.5 | 45.82 | 59.7 | 24255 | 29226 | 46.22 | 59.72 |
| 23 | 56.35 | 50.5 | 46.77 | 53.1 | 30277 | 30607 | 57.01 | 53.08 |
| 24 | 50.60 | 33.0 | 41.14 | 36.2 | 24920 | 22906 | 50.60 | 38.22 |
| 25 | 30.28 | 35.1 | 38.42 | 41.1 | 20454 | 25142 | 39.08 | 41.65 |
| 26 | 77.35 | 65.0 | 60.15 | 69.9 | 48120 | 45126 | 77.35 | 75.83 |
| 27 | 107.21 | 84.9 | 79.25 | 102.1 | 58944 | 55716 | 107.21 | 102.15 |
| 28 | 67.86 | 63.4 | 80.33 | 70.0 | 53474 | 53498 | 80.33 | 69.97 |
| 29 | 103.50 | 78.2 | * | 89.7 | 54374 | 57713 | 103.50 | 100.55 |
| 30 | 97.10 | 70.3 | 97.10 | 79.2 | 57389 | 57289 | 97.10 | 90.58 |
| 31 | 44.64 | 59.8 | 46.87 | 53.7 | 36392 | 37183 | 56.72 | 62.68 |
| 32 | 45.51 | 48.2 | 41.97 | 51.4 | 35866 | 34528 | 50.37 | 51.42 |
| 33 | 43.13 | 41.1 | 44.70 | 43.9 | 29986 | 34706 | 47.20 | 47.58 |
| 34 | 46.81 | 48.6 | 48.78 | 51.3 | 33537 | 45952 | 51.54 | 51.32 |
| 35 | 40.07 | 38.6 | 50.31 | 47.3 | 35085 | 38008 | 51.36 | 47.27 |
| 36 | 63.82 | 48.9 | 50.17 | 50.0 | 29585 | 36127 | 63.82 | 59.65 |
| 37 | 62.18 | 48.3 | * | 55.2 | 26725 | 32570 | 62.18 | 55.15 |
| 38 | 57.06 | 53.0 | 57.32 | 59.1 | 30655 | 37948 | 57.71 | 59.17 |
| 39 | 74.15 | 54.7 | 53.93 | 58.1 | 41736 | 39166 | 74.15 | 63.87 |
| 40 | 60.16 | 52.1 | 57.80 | 57.5 | 37426 | 41032 | 62.39 | 57.52 |
| 41 | 44.52 | 44.6 | 49.25 | 51.4 | 33953 | 30081 | 49.25 | 51.37 |
| 42 | 41.48 | 41.2 | 45.55 | 41.0 | 29715 | 34761 | 48.44 | 43.92 |
| 43 | 44.77 | 41.4 | 46.74 | 44.9 | 32075 | 31555 | 47.53 | 44.87 |
| 44 | 42.17 | 42.8 | 44.80 | 46.7 | 31155 | 29758 | 47.29 | 46.68 |
| 45 | 56.75 | 50.6 | 52.68 | 47.9 | 31198 | 32318 | 57.80 | 50.62 |

\*   unobservable

## Table A2 - Results of compression, shear, and tensile test

| | Compression Test | | | Shear Test | Tensile Test | |
|---|---|---|---|---|---|---|
| | E | η | $\sigma_c$ | $\sigma_c$ | $\sigma_c$ | $E_t$ |
| No. | $\times 10^8$ [Pa] | $\times 10^8$ [Pa s] | [Pa] | [Pa] | [Pa] | [Pa] |
| 1 | 3.94 | 2.65 | 338438 | 114515 | | 2219400 |
| 2 | 6.41 | 1.83 | 441721 | 299244 | | 2893126 |
| 3 | 7.00 | 2.42 | 443736 | 185405 | | 2661103 |
| 4 | 5.53 | 1.61 | 335967 | 248737 | | 2019565 |
| 5 | 6.65 | 2.7 | 428455 | 228580 | | 2603817 |
| 6 | 7.25 | 3.07 | 446245 | 191686 | | 2186119 |
| 7 | 7.25 | 3.22 | 473311 | 219752 | | 2644603 |
| 8 | 6.52 | 2.09 | 352807 | 181504 | | 3603414 |
| 9 | 5.68 | 2.53 | 331709 | 176118 | | 3262707 |
| 10 | 5.82 | 2.61 | 278642 | 248325 | | 2382488 |
| 11 | 8.09 | 2.75 | 518319 | 312775 | | 3038228 |
| 12 | 5.19 | 4.29 | 434385 | 224689 | | 2365463 |
| 13 | 6.90 | 2.09 | 476922 | 242944 | | 2669880 |
| 14 | 8.12 | 2.56 | 506877 | 201034 | | 3140829 |
| 15 | 7.44 | 2.64 | 500491 | 212239 | | 3262553 |
| 16 | 6.23 | 5.17 | 497526 | 300421 | | 3204485 |
| 17 | 4.82 | 2.76 | 353833 | 189325 | | 2495790 |
| 18 | 4.57 | 4.02 | 358053 | 235456 | | 2556493 |
| 19 | 3.05 | 19.3 | 364249 | 160527 | | 2106323 |
| 20 | 4.84 | 6.18 | 396447 | 288385 | | 2878381 |
| 21 | 4.17 | 2.17 | 334104 | 102475 | | 1488604 |
| 22 | 4.83 | 2.21 | 388122 | 145849 | | 1718797 |
| 23 | 5.15 | 2.01 | 379075 | 130190 | | 1910229 |
| 24 | 3.30 | 3.05 | 282443 | 89790 | | 1113635 |
| 25 | 3.36 | 3.01 | 284230 | 112771 | | 1423046 |
| 26 | 8.62 | 1.88 | 444801 | 211617 | | 3227850 |
| 27 | 9.24 | 3.35 | 631107 | 293539 | | 3545828 |
| 28 | 7.48 | 3.31 | 469624 | 200621 | | 3437427 |
| 29 | 11.20 | 3.2 | 653307 | 318823 | | 3034021 |
| 30 | 7.82 | 4.76 | 554547 | 293341 | | 3415703 |
| 31 | 6.56 | 1.46 | 355620 | 177696 | | 3085208 |
| 32 | 5.48 | 2.93 | 412565 | 120155 | | 1748530 |
| 33 | 5.94 | 1.48 | 300310 | 129266 | | 2268548 |
| 34 | 6.53 | 1.67 | 348930 | 111836 | | 3514630 |
| 35 | 5.92 | 1.62 | 288335 | 132484 | | 2438245 |
| 36 | 4.92 | 7.24 | 437958 | 155948 | | 1687081 |
| 37 | 4.17 | 6.04 | 396105 | 159658 | | 1794609 |
| 38 | 5.09 | 4.36 | 421764 | 146990 | | 2176547 |
| 39 | 5.06 | 256 | 513378 | 165813 | | 1578980 |
| 40 | 5.56 | 4.68 | 426326 | 168136 | | 2231997 |
| 41 | 3.62 | 4.42 | 331139 | 146777 | | 1916969 |
| 42 | 4.65 | 2.38 | 306164 | 116952 | | 2252100 |
| 43 | 3.96 | 2.69 | 300994 | 134993 | | 2116101 |
| 44 | 5.53 | 1.44 | 313349 | 123545 | | 1938822 |
| 45 | 3.85 | 2.09 | 313121 | 130808 | | 2625809 |

## Table A3 - Rubber Thumb Test Results

| No. | Failure Force [N] | Failure Pressure [Pa] | Contact Diameter [mm] |
|-----|-----|-----|-----|
| 1 | 66.3 | 513727 | 12 |
| 2 | 65.8 | 513727 | 13 |
| 3 | 46.0 | 405574 | 11 |
| 4 | 48.3 | 459651 | 11 |
| 5 | 74.8 | 567804 | 13 |
| 6 | 66.2 | 513727 | 13 |
| 7 | 63.9 | 540765 | 13 |
| 8 | 42.3 | 405574 | 11 |
| 9 | 50.7 | 486689 | 11 |
| 10 | 43.8 | 405574 | 12 |
| 11 | 71.0 | 999740 | 12 |
| 12 | 63.4 | 896319 | 12 |
| 13 | 78.5 | 965266 | 13 |
| 14 | 65.4 | 965266 | 12 |
| 15 | 89.6 | 965266 | 14 |
| 16 | 83.9 | 999740 | 13 |
| 17 | 77.5 | 1034214 | 14 |
| 18 | 72.7 | 758424 | 14 |
| 19 | 51.0 | 792897 | 11 |
| 20 | 67.4 | 965266 | 13 |
| 21 | 29.0 | 344738 | 9 |
| 22 | 34.2 | 379212 | 10 |
| 23 | 29.1 | 448159 | 9 |
| 24 | 25.2 | 379212 | 9 |
| 25 | 28.4 | 344738 | 12 |
| 26 | 122.7 | 720816 | 16 |
| 27 | 201.8 | 655002 | 18 |
| 28 | 110.3 | 586055 | 13 |
| 29 | 201.3 | 620528 | 17 |
| 30 | 197.9 | 689476 | 17 |
| 31 | 26.6 | 344738 | 9 |
| 32 | 22.2 | 344738 | 9 |
| 33 | 27.0 | 344738 | 9 |
| 34 | 50.0 | 379212 | 13 |
| 35 | 28.6 | 413686 | 10 |
| 36 | 47.2 | 413686 | 11 |
| 37 | 43.8 | 344738 | 12 |
| 38 | 42.3 | 344738 | 11 |
| 39 | 59.3 | 448159 | 12 |
| 40 | 54.3 | 379212 | 12 |
| 41 | 53.0 | 379212 | 12 |
| 42 | 33.4 | 344738 | 9 |
| 43 | 25.9 | 306434 | 9 |
| 44 | 33.6 | 379212 | 10 |
| 45 | 63.5 | 379212 | 12 |

## Table A4 - Elasticity measured by acoustic impulse technique

| | Elasticity |
|---|---|
| | E |
| No. | [MPa] |
| 1 | 3.17 |
| 2 | 3.29 |
| 3 | 3.97 |
| 4 | 3.25 |
| 5 | 4.06 |
| 6 | 4.81 |
| 7 | 4.93 |
| 8 | 4.56 |
| 9 | 4.53 |
| 10 | 4.33 |
| 11 | 4.79 |
| 12 | 4.03 |
| 13 | 4.84 |
| 14 | 5.14 |
| 15 | 4.34 |
| 16 | 4.36 |
| 17 | 4.19 |
| 18 | 3.81 |
| 19 | 3.63 |
| 20 | 4.16 |
| 21 | 3.39 |
| 22 | 3 |
| 23 | 3.33 |
| 24 | 2.83 |
| 25 | 2.55 |
| 26 | 3.62 |
| 27 | 4.84 |
| 28 | 5.39 |
| 29 | 4.72 |
| 30 | 4.16 |
| 31 | 4.35 |
| 32 | 4.02 |
| 33 | 3.98 |
| 34 | 4.48 |
| 35 | 3.95 |
| 36 | 3.73 |
| 37 | 2.51 |
| 38 | 3.97 |
| 39 | 4.04 |
| 40 | 3.77 |
| 41 | 3.64 |
| 42 | 3.48 |
| 43 | 3.61 |
| 44 | 4.02 |
| 45 | 3.93 |

**APPENDIX B**

# APPENDIX B

## Force-Deformation Plots of Magness-Taylor Puncture Test

**General Information:**

1. Material: 5 apples from 9 cultivars (total=45 apples)

2. Explanation of file name: *e.g.* **Y01_02**

       1st character (**Y**): No meaning
       1st two digits (**01**): Sample No.
       2nd two digits (**02**): Testing Code
              *02=Magness-Taylor Test*
              *03=Compression test*
              *04=Shear Test*
              *05=Tensile Test*

3. Numbering:

       01 - 05:  Red Delicious
       06 - 10:  Red Rome
       11 - 15:  Fuji
       16 - 20:  Granny Smith
       21 - 25:  Golden Delicious
       26 - 30:  Braeburn
       31 - 35:  Ida Red
       36 - 40:  Gala
       41 - 45:  Jona Gold

\* The above setups were applied to Magness-Taylor, compression, shear, and tensile test.

\* In compression test, Maxwell model was fitted to the points in between A and B of Figure C1.
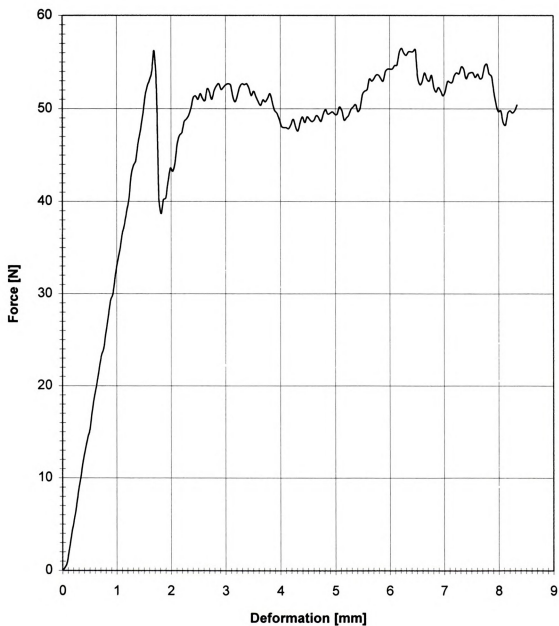
FIGURE B1 - Magness-Taylor puncture test result of  Y01_02
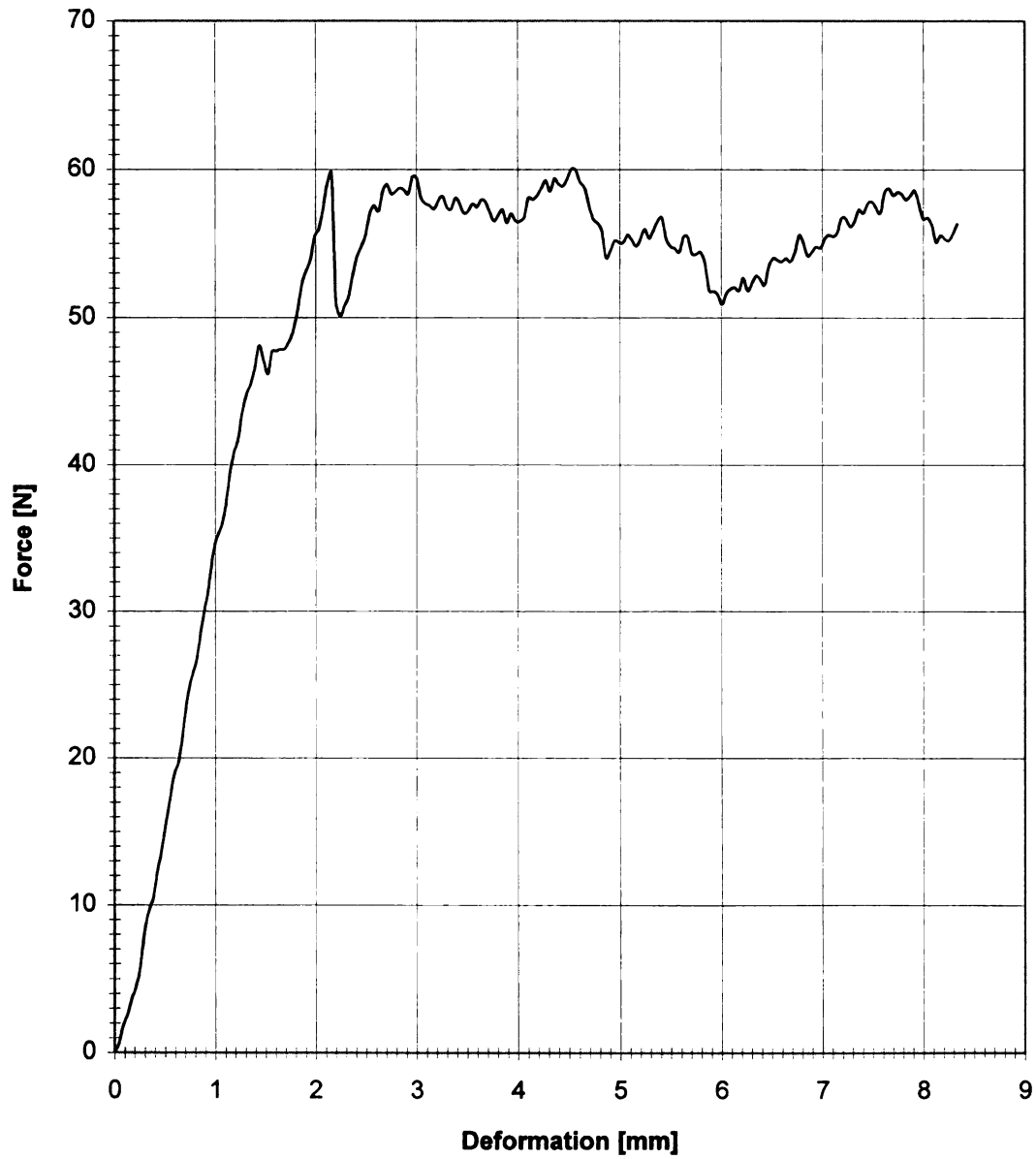
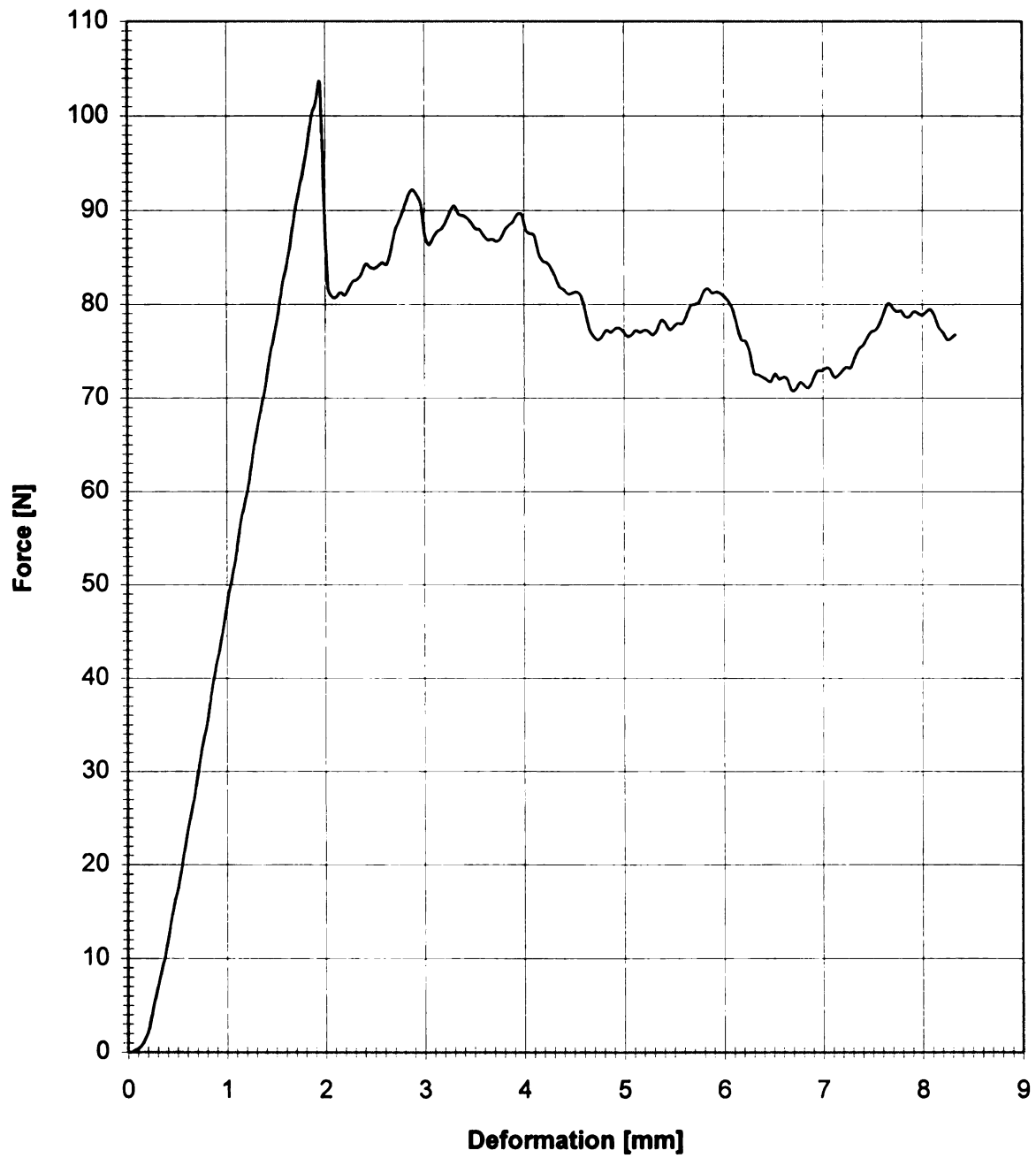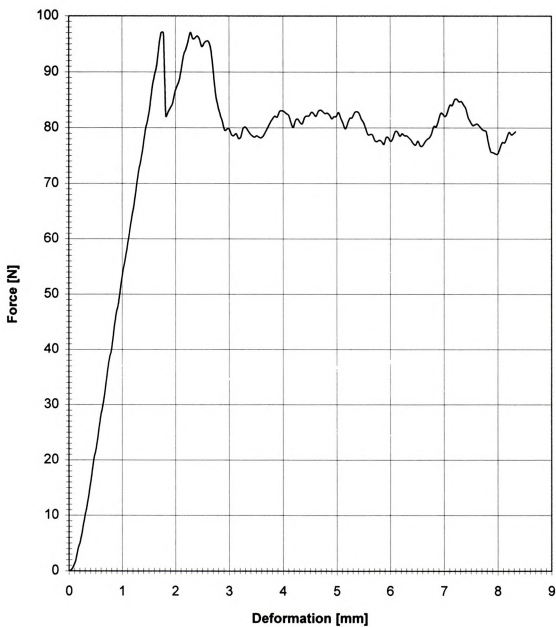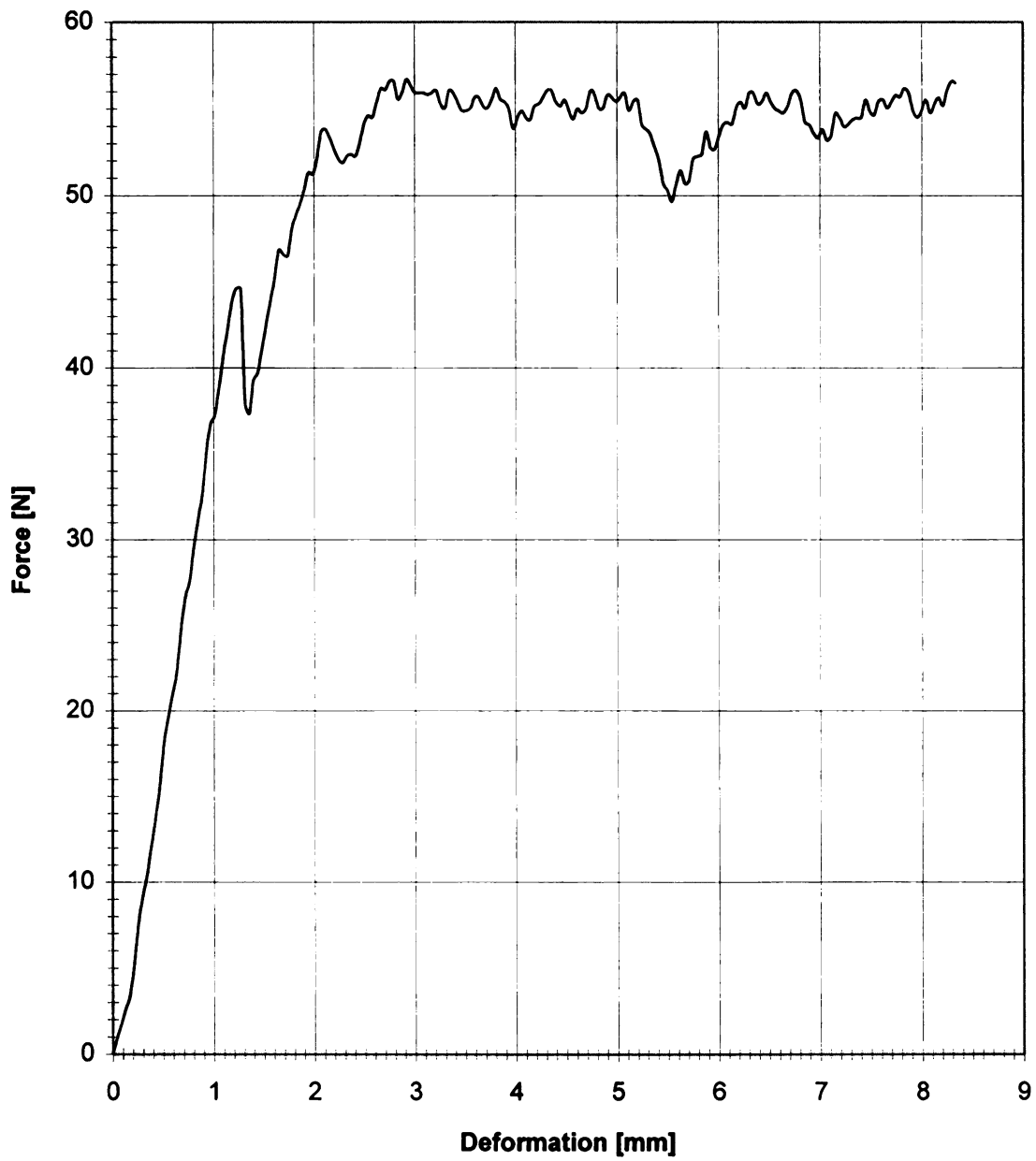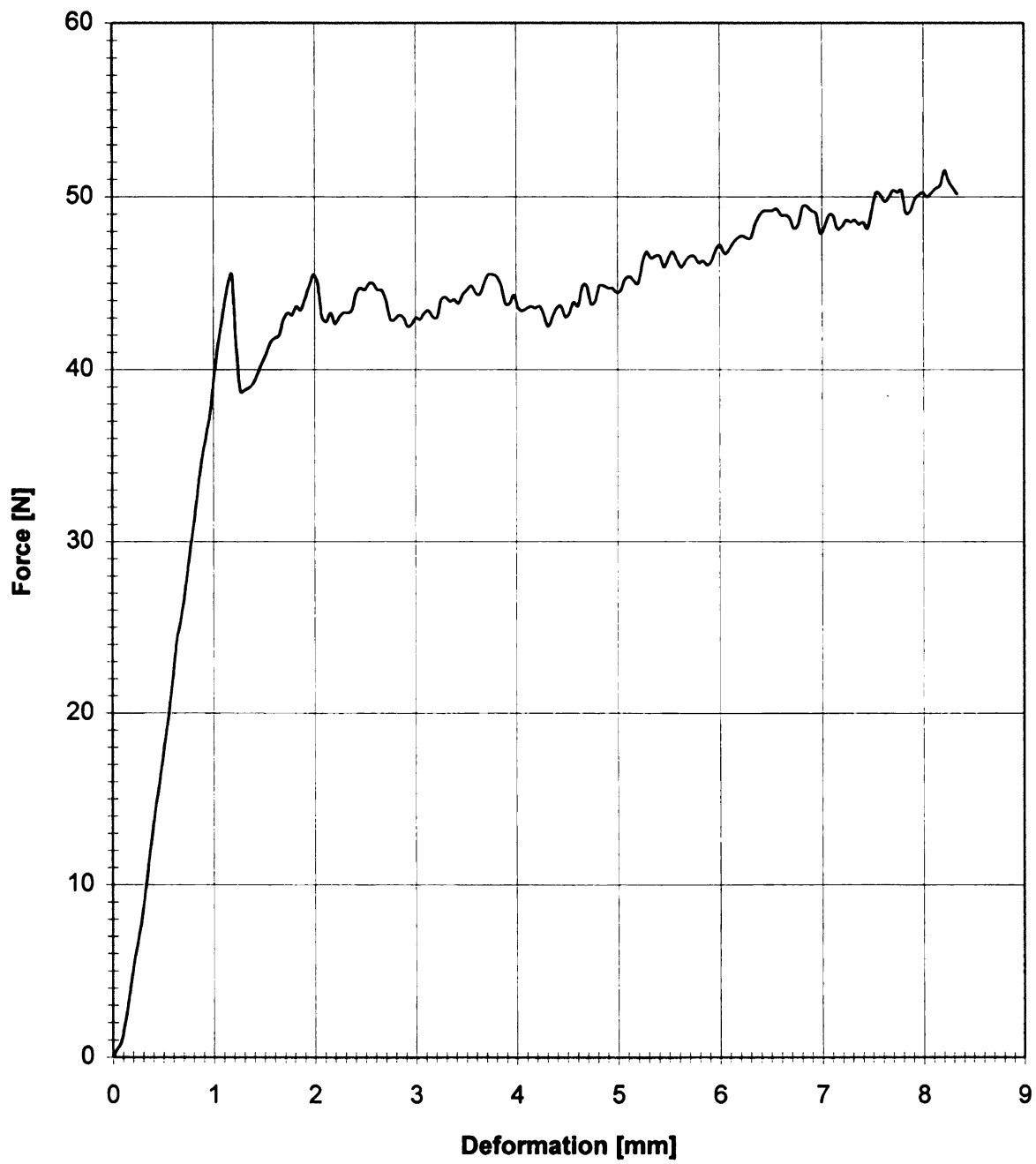FIGURE B2 - Magness-Taylor puncture test result of Y02_02
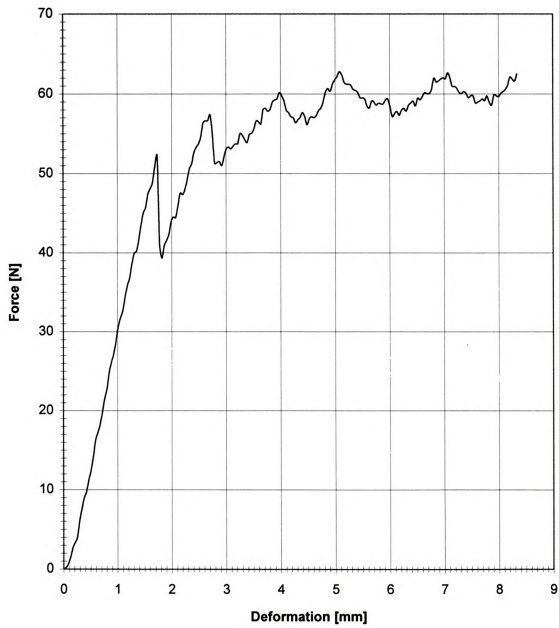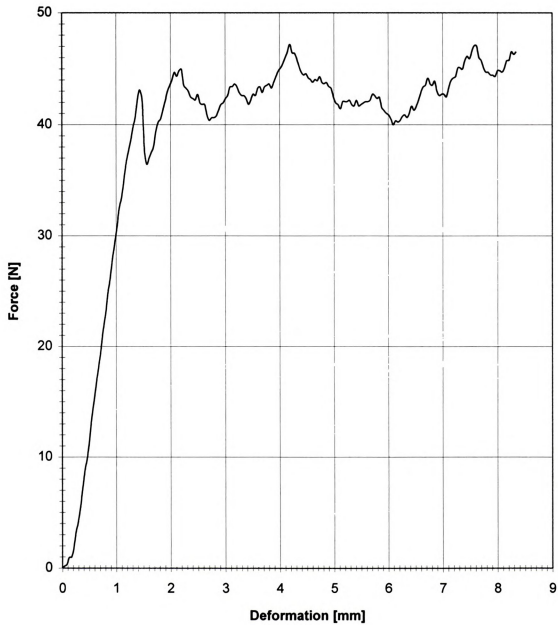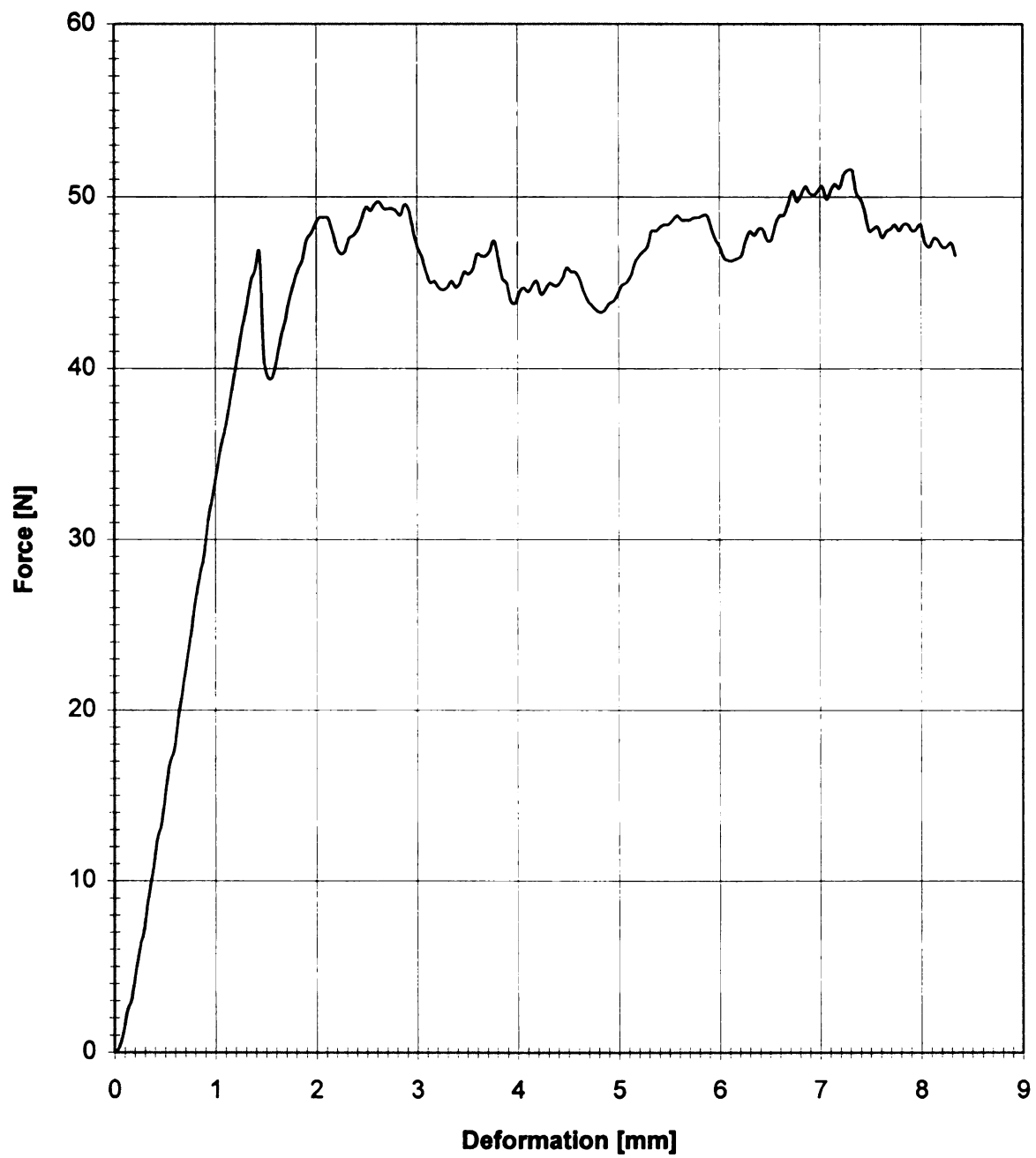
FIGURE B3 - Magness-Taylor puncture test result of Y03_02
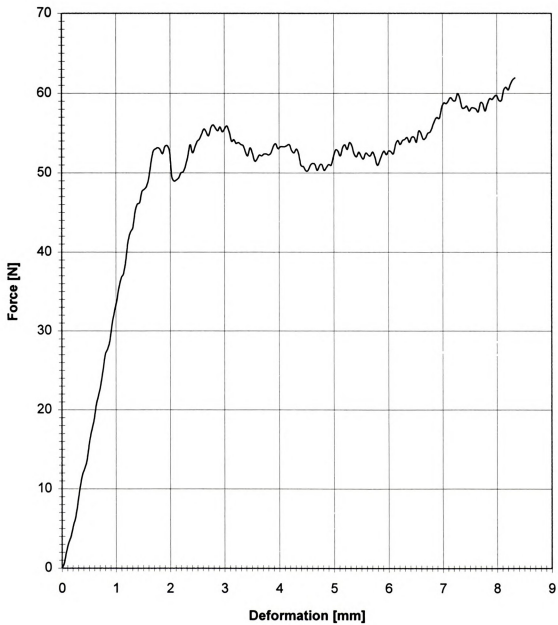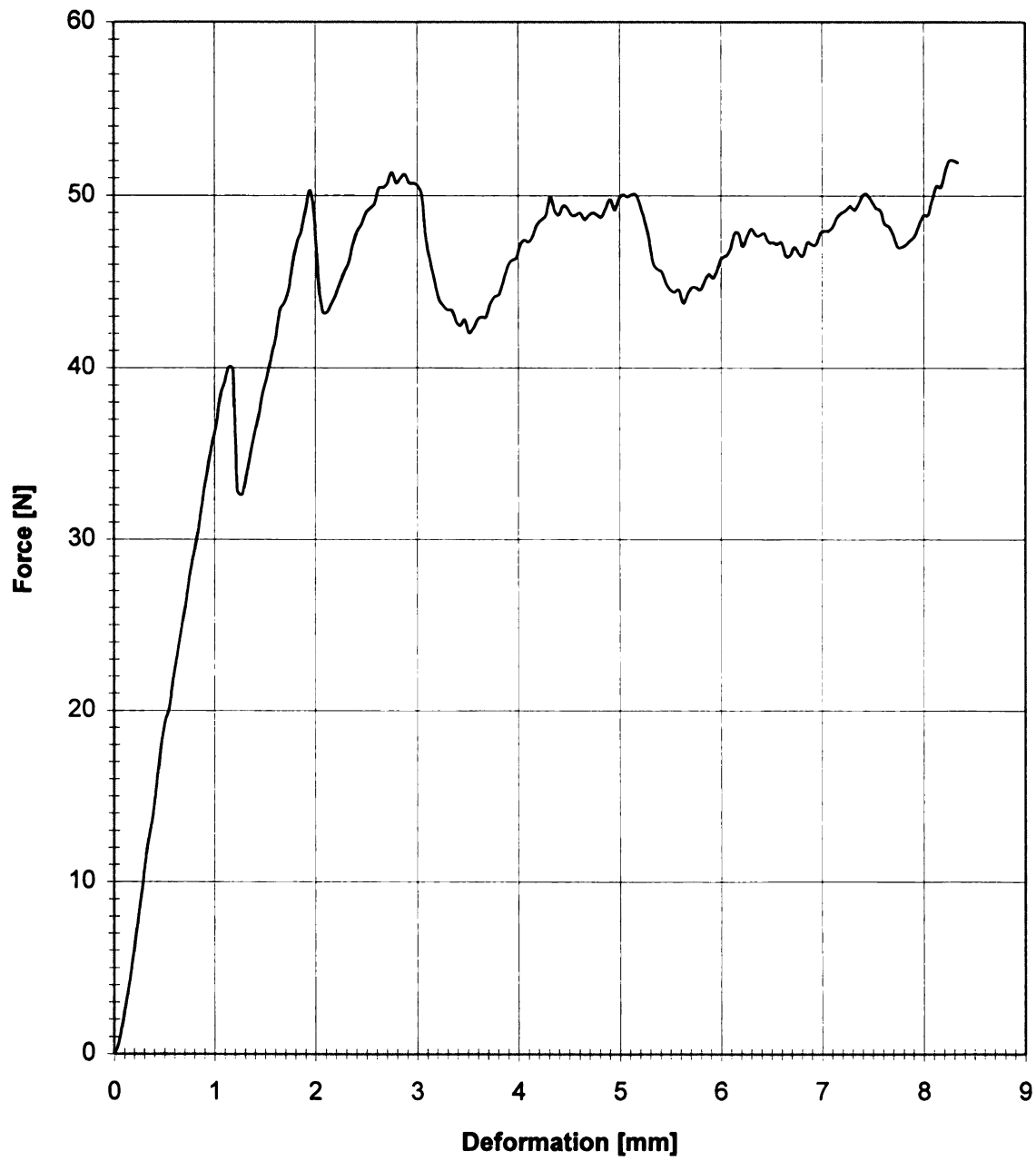
FIGURE B4 - Magness-Taylor puncture test result of Y04_02
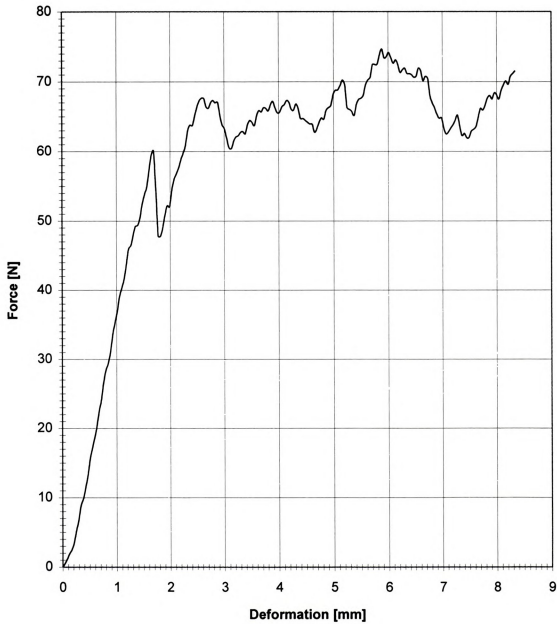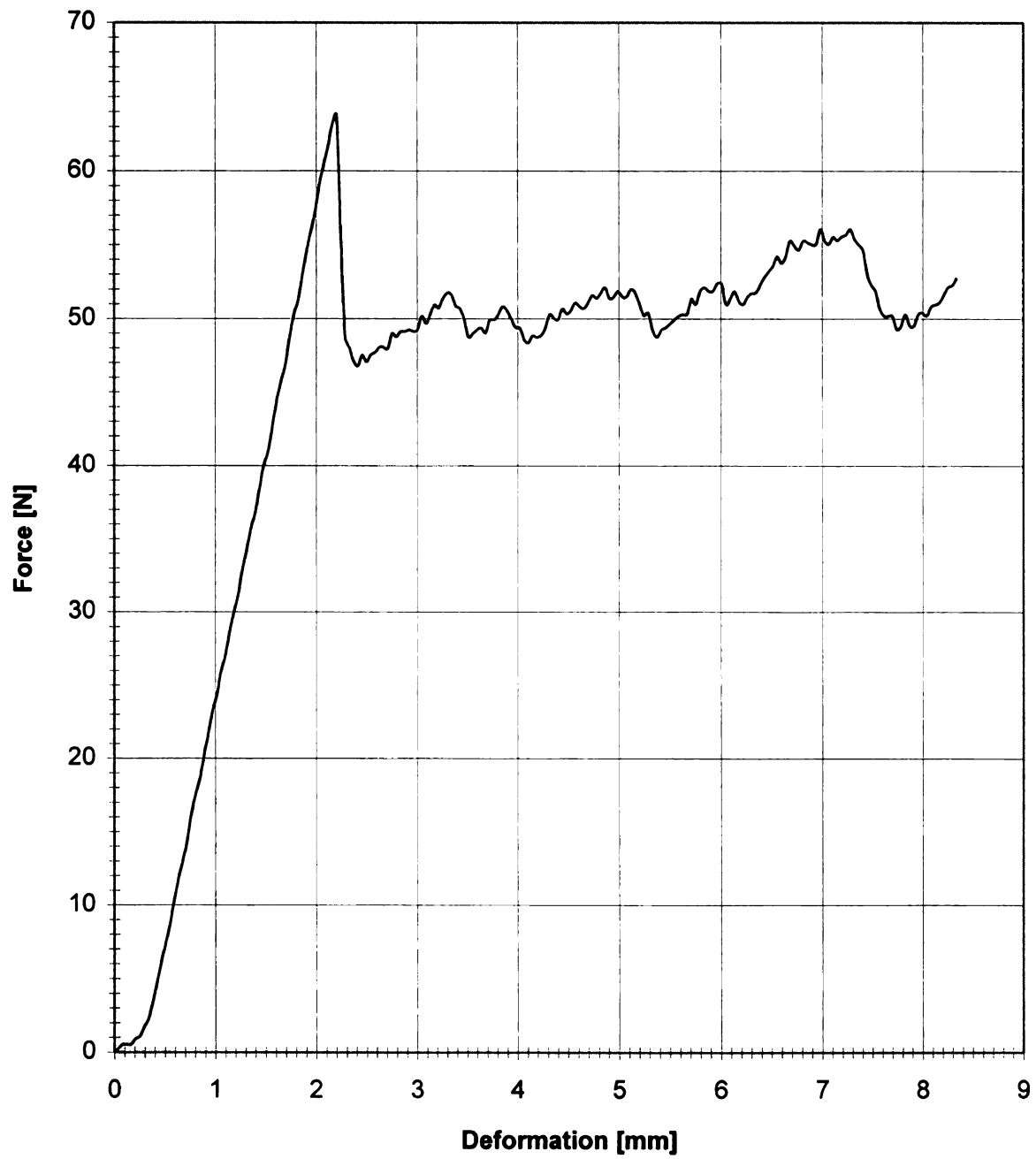
FIGURE B5 - Magness-Taylor puncture test result of Y05_02
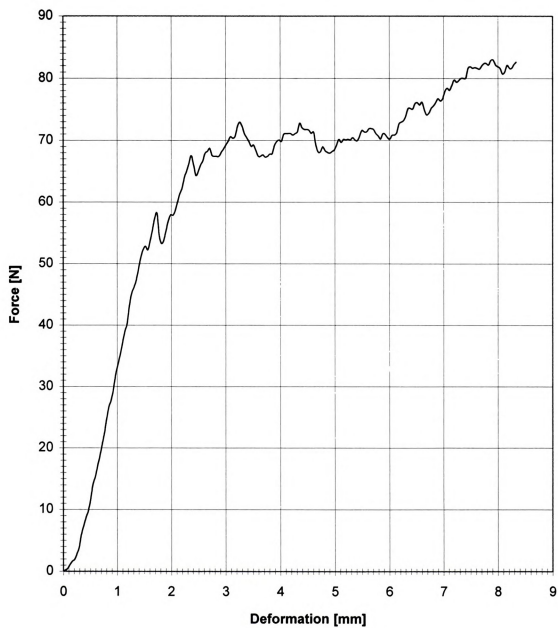
FIGURE B6 - Magness-Taylor puncture test result of Y06_02
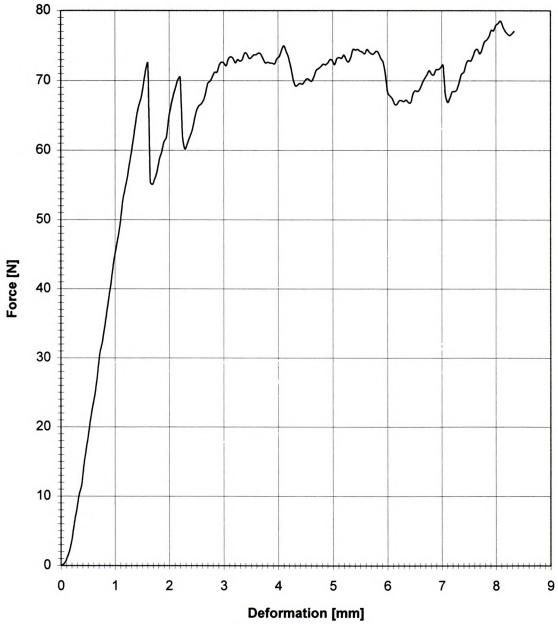
FIGURE B7 - Magness-Taylor puncture test result of Y07_02
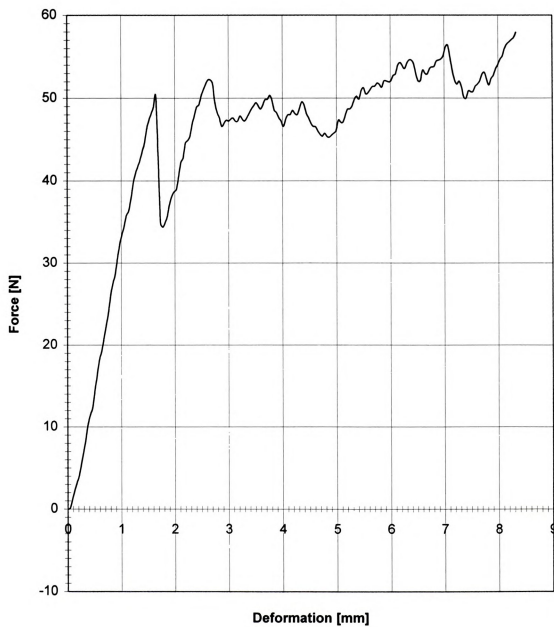
FIGURE B8 - Magness-Taylor puncture test result of Y08_02
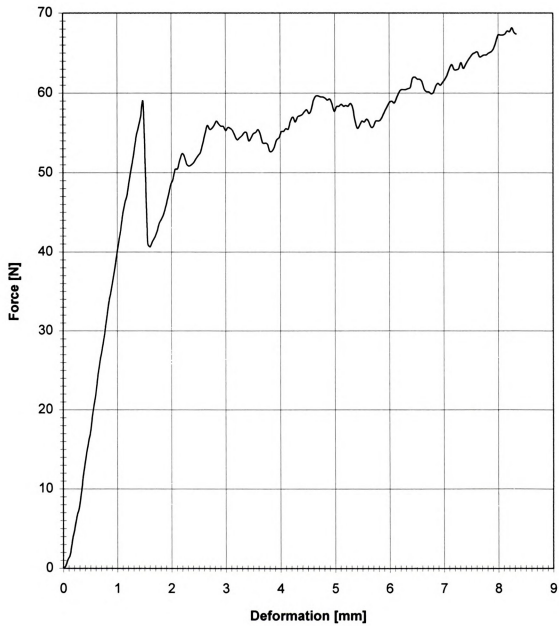
FIGURE B9 - Magness-Taylor puncture test result of Y09_02
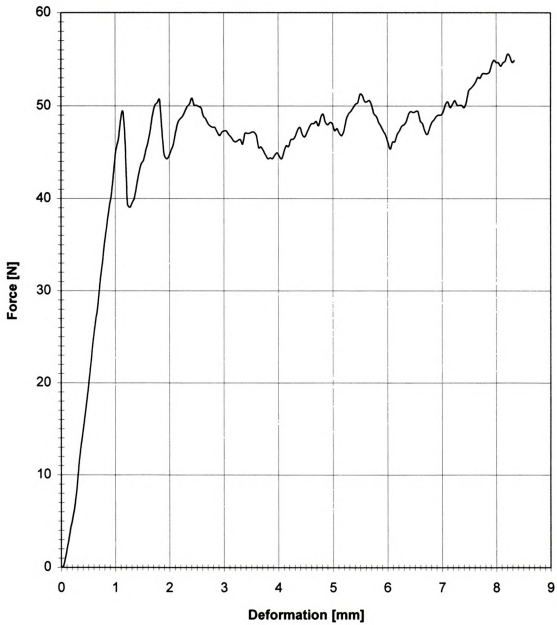
FIGURE B10 - Magness-Taylor puncture test result of Y10_02
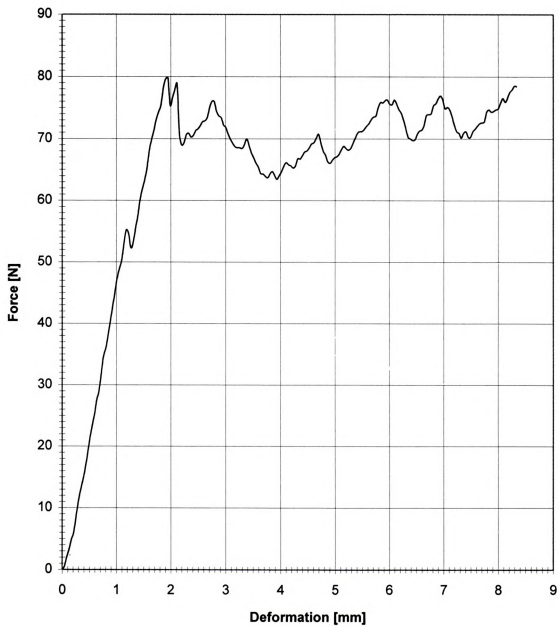
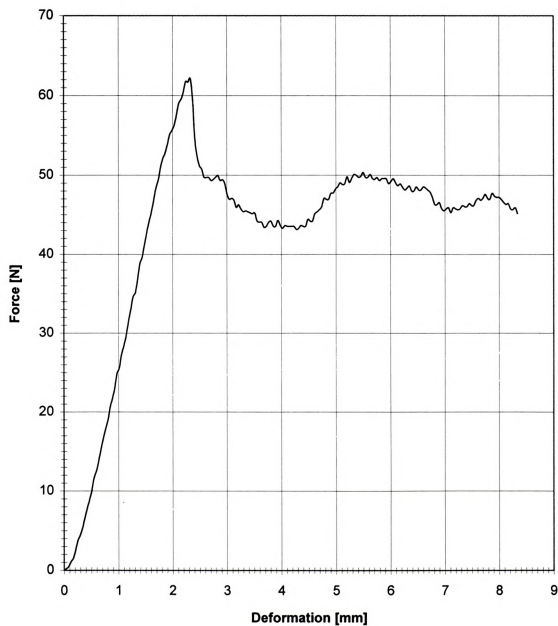FIGURE B11 - Magness-Taylor puncture test result of Y11_02
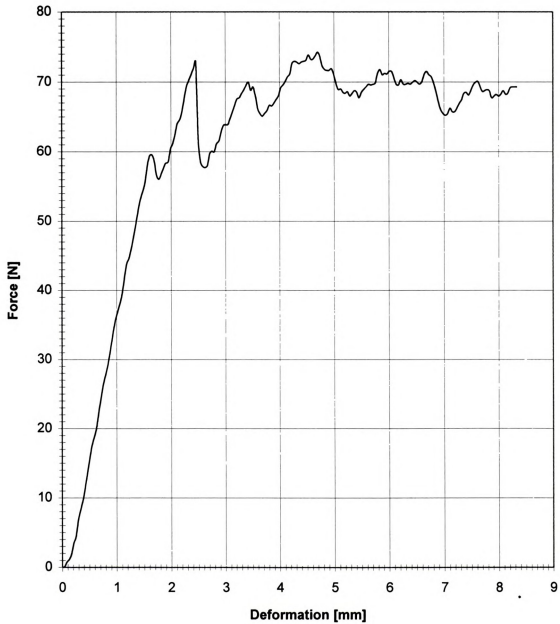
FIGURE B12 - Magness-Taylor puncture test result of Y12_02
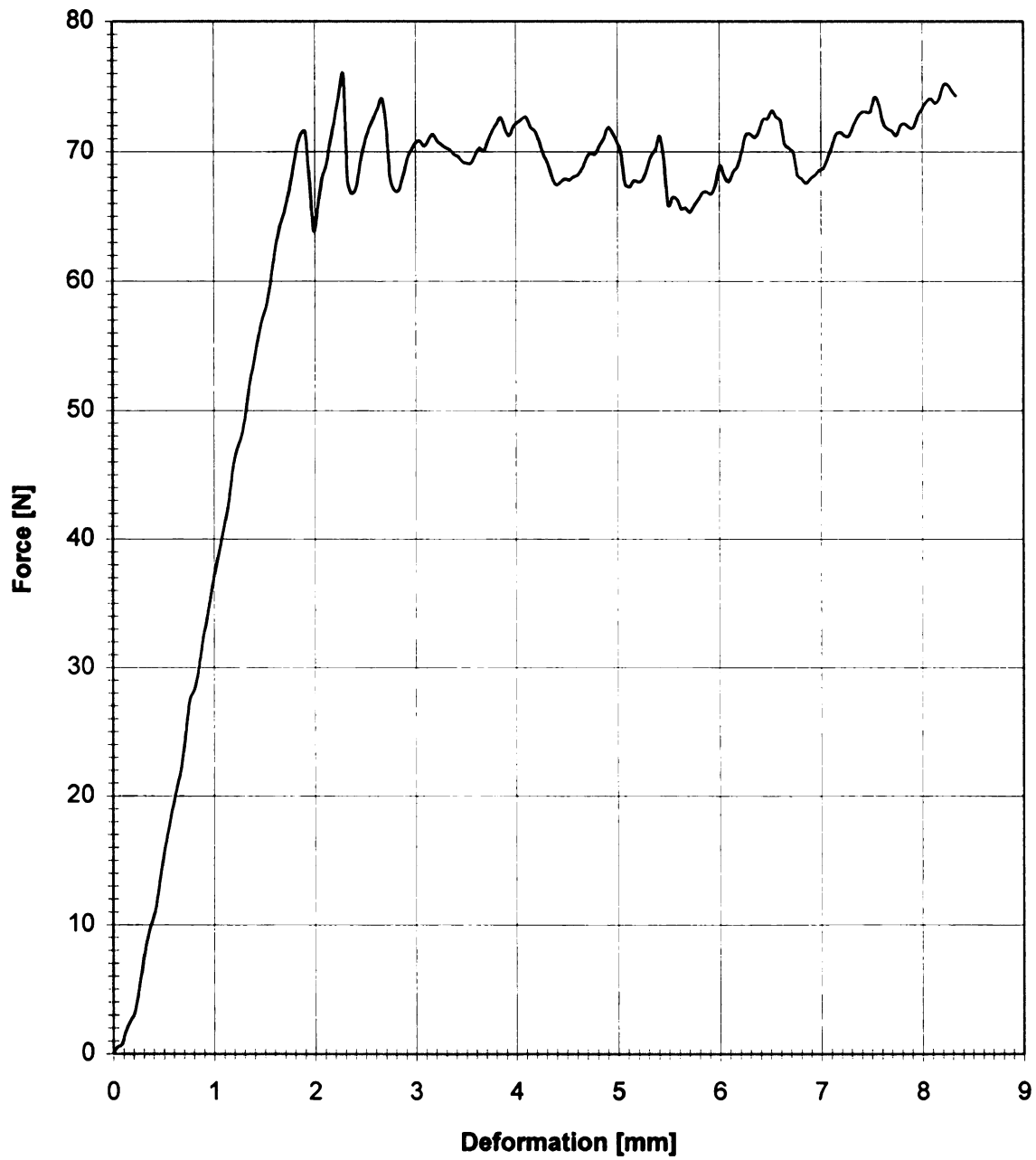
FIGURE B13 - Magness-Taylor puncture test result of Y13_02
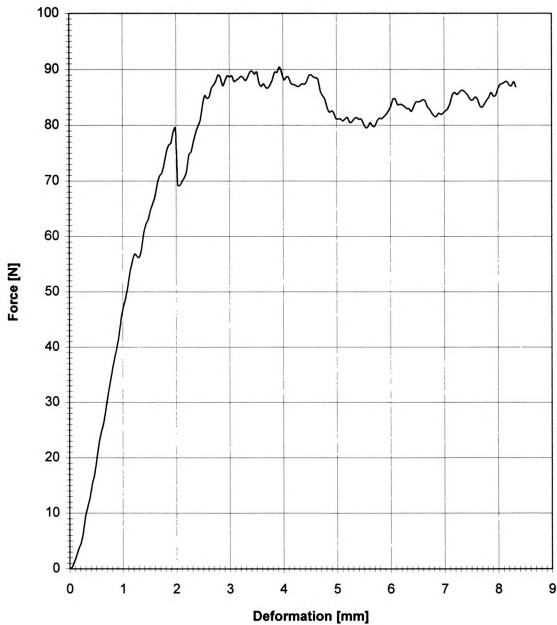
FIGURE B14 - Magness-Taylor puncture test result of Y14_02
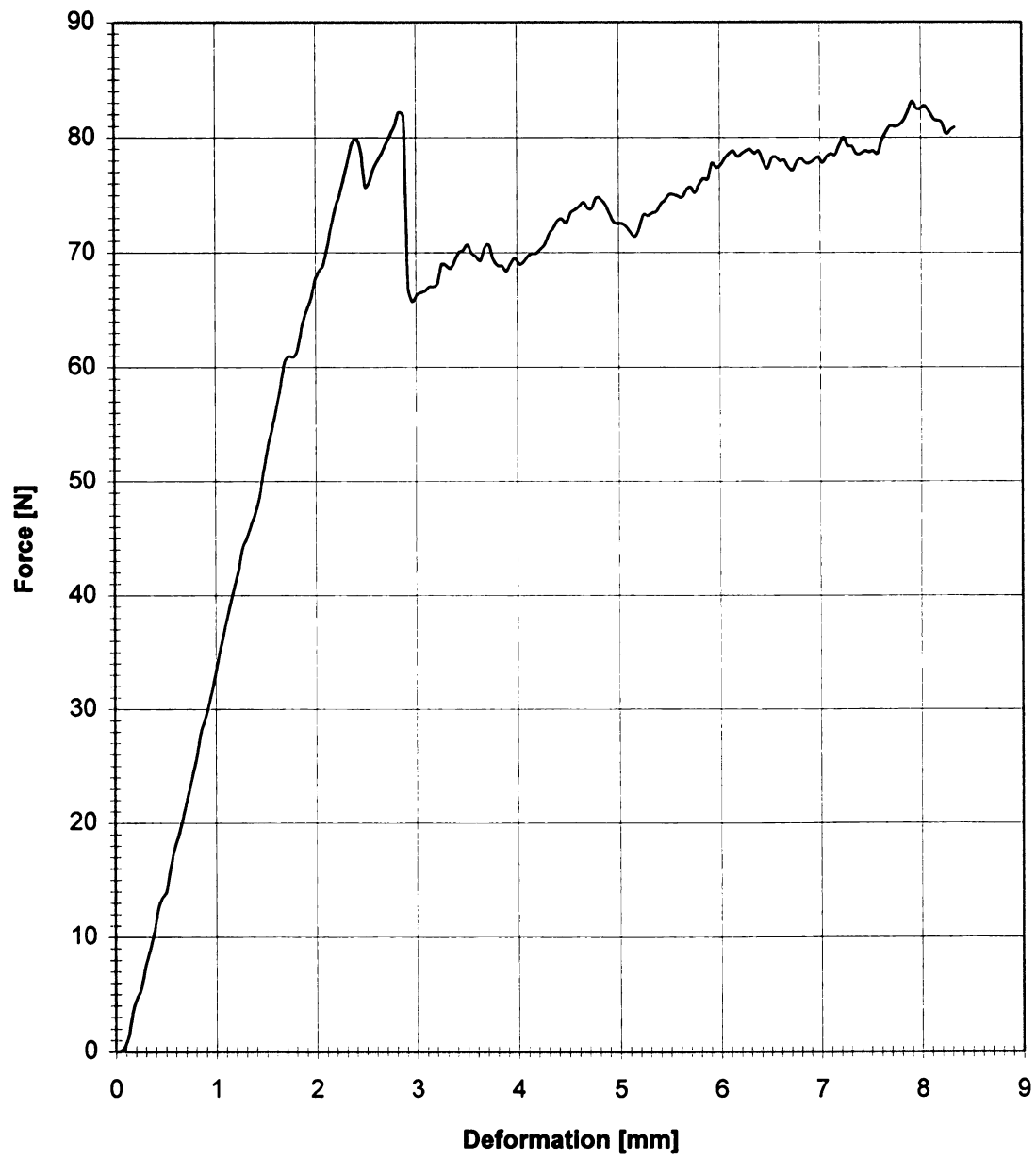
FIGURE B15 - Magness-Taylor puncture test result of Y15_02
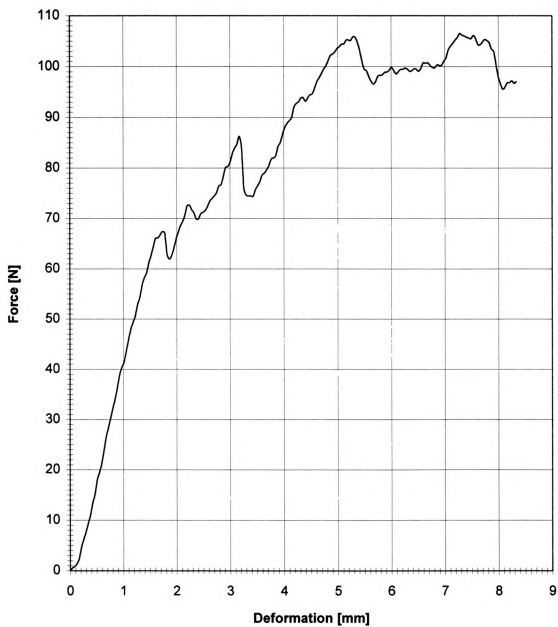
FIGURE B16 - Magness-Taylor puncture test result of  Y16_02
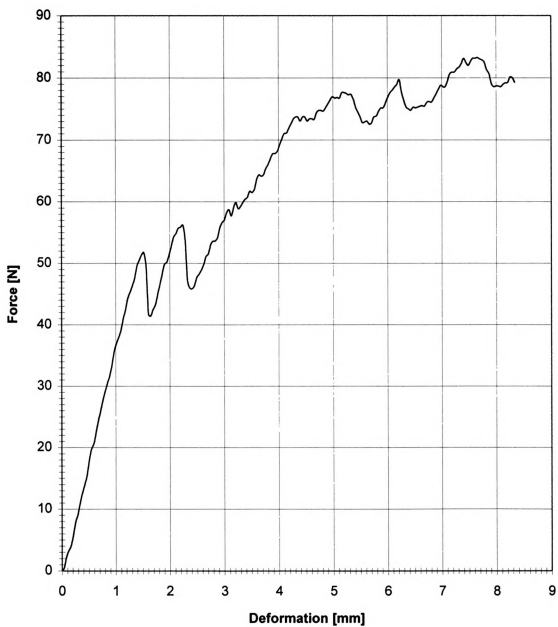
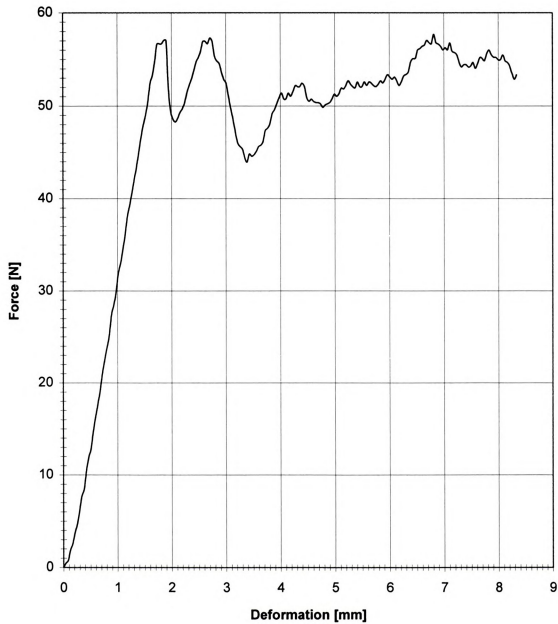FIGURE B17 - Magness-Taylor puncture test result of Y17_02
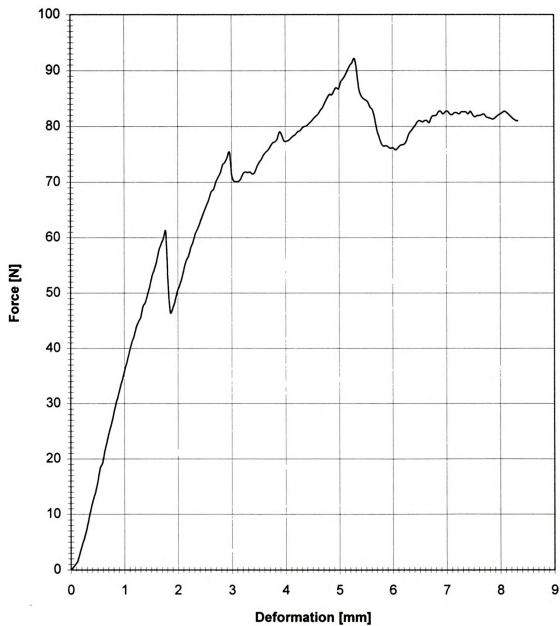
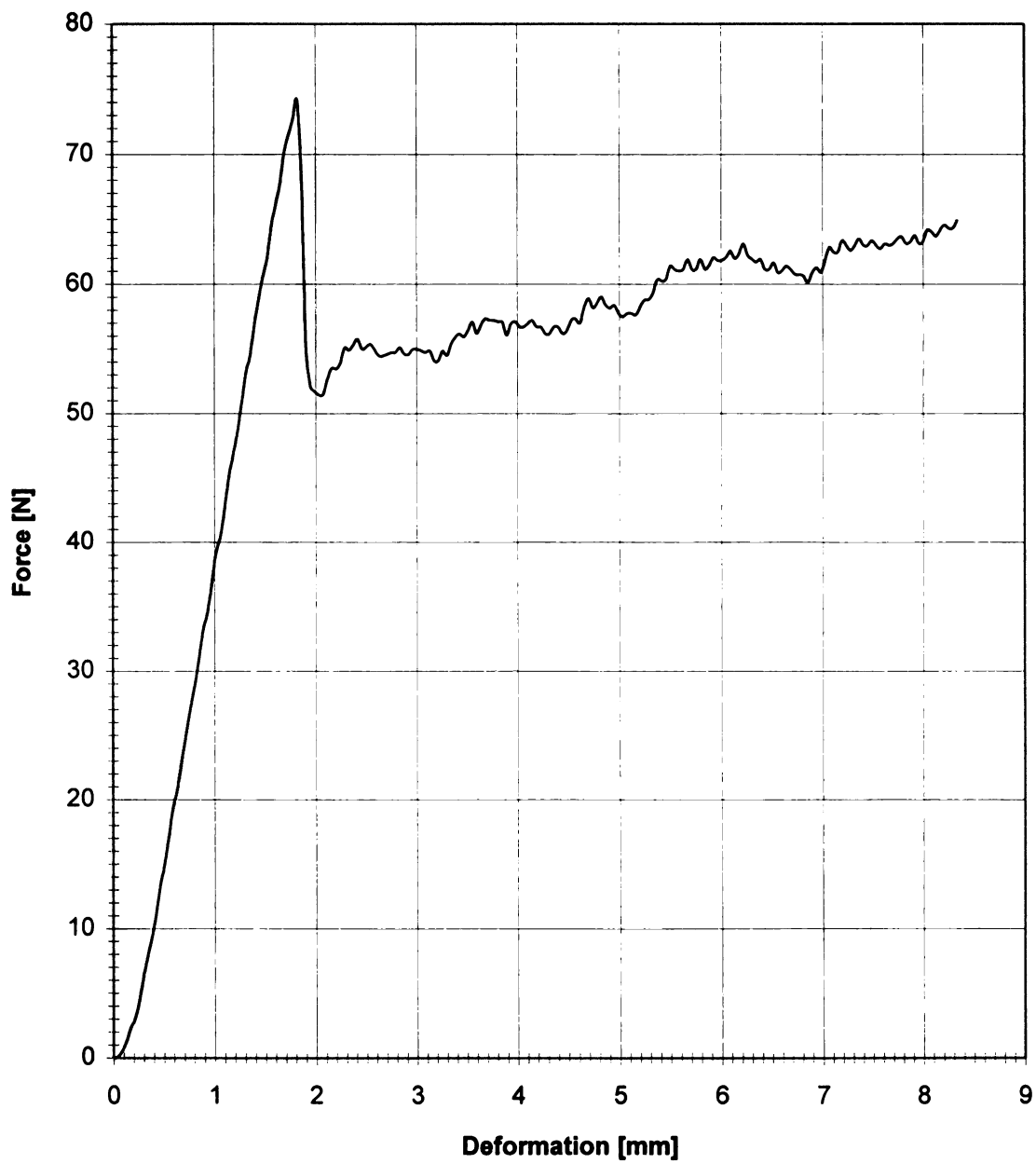FIGURE B18 - Magness-Taylor puncture test result of Y18_02
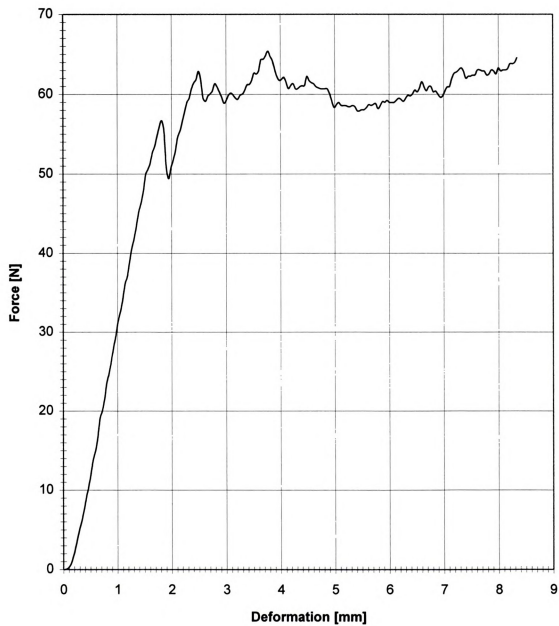
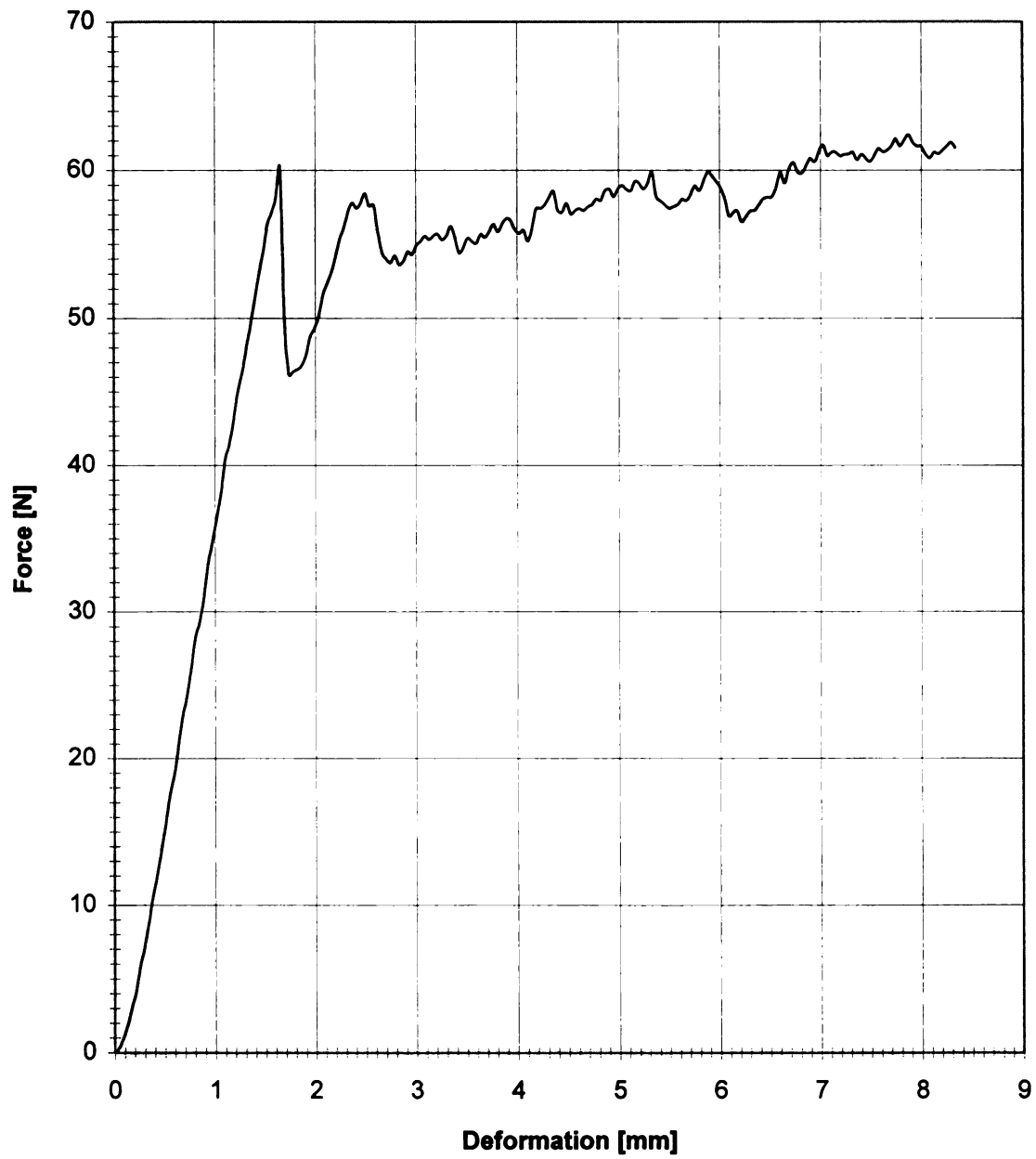FIGURE B19 - Magness-Taylor puncture test result of Y19_02
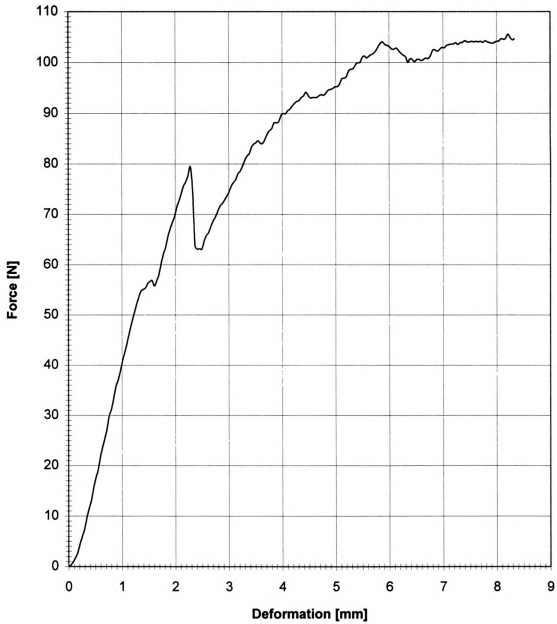
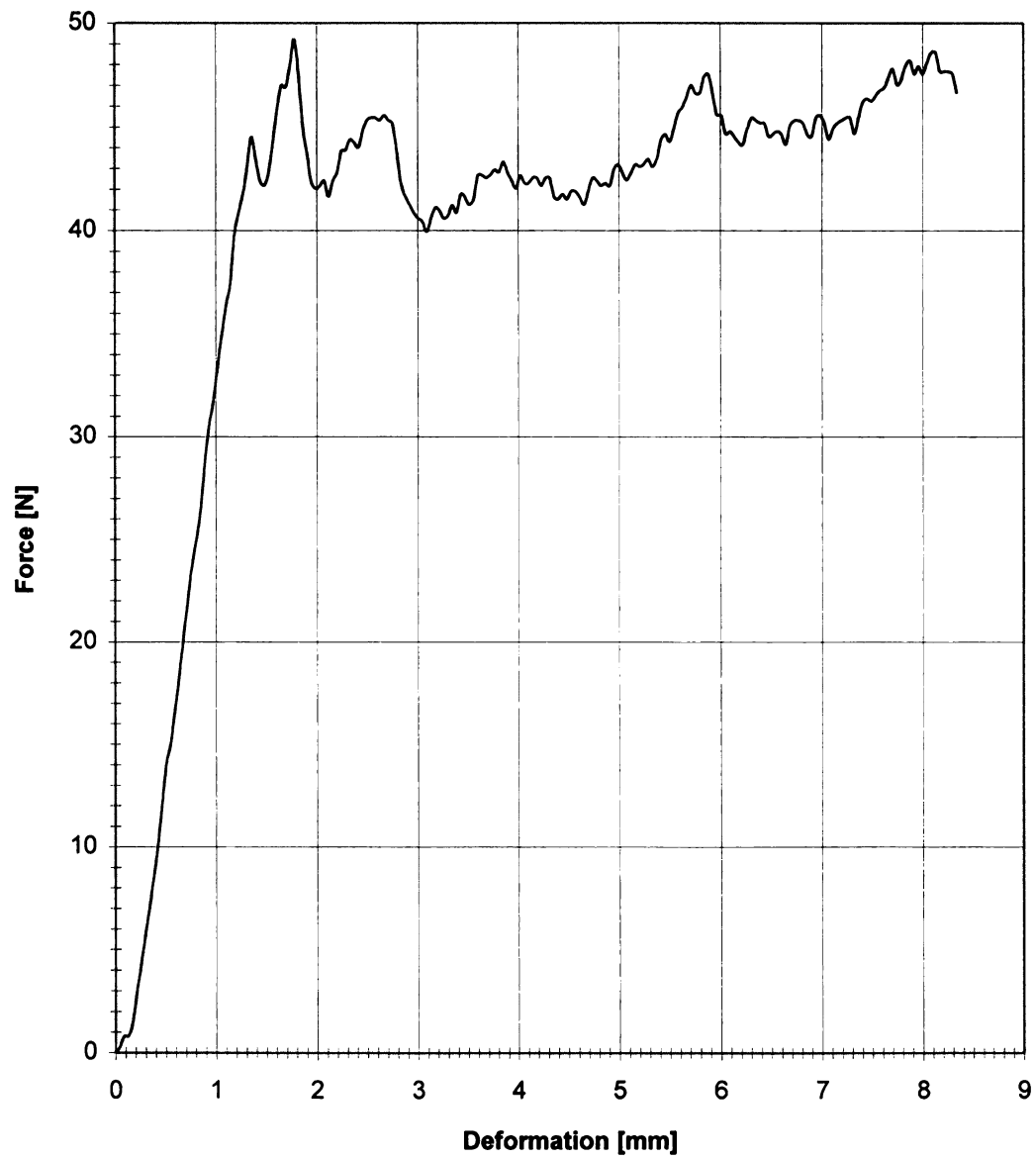FIGURE B20 - Magness-Taylor puncture test result of Y20_02
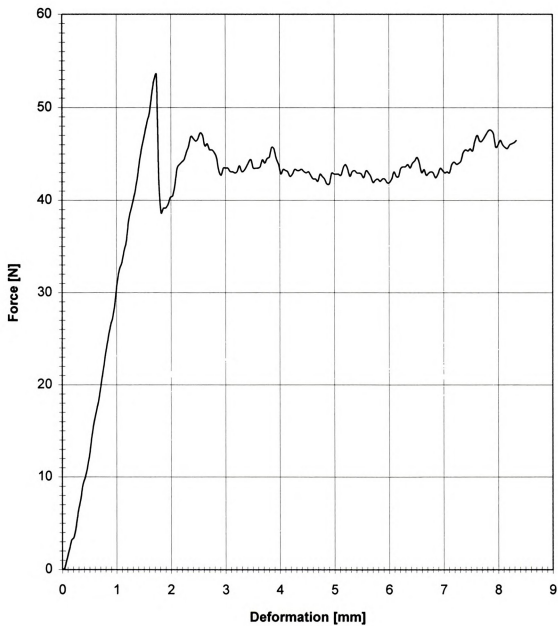
FIGURE B21 - Magness-Taylor puncture test result of Y21_02
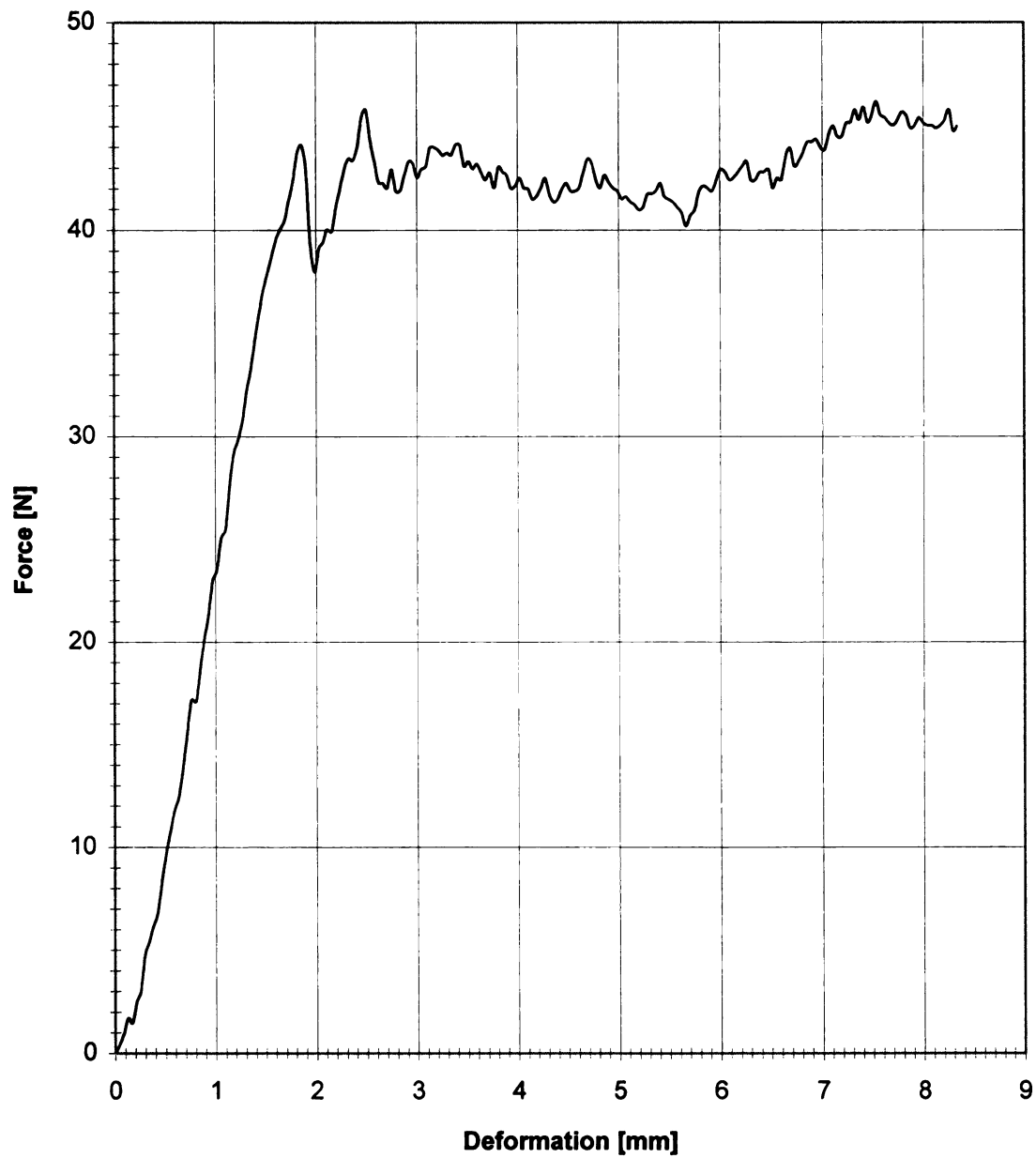
FIGURE B22 - Magness-Taylor puncture test result of Y22_02
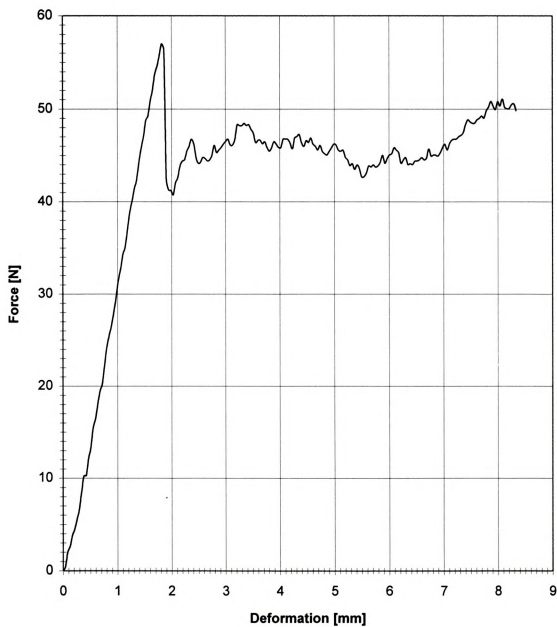
FIGURE B23 - Magness-Taylor puncture test result of Y23_02
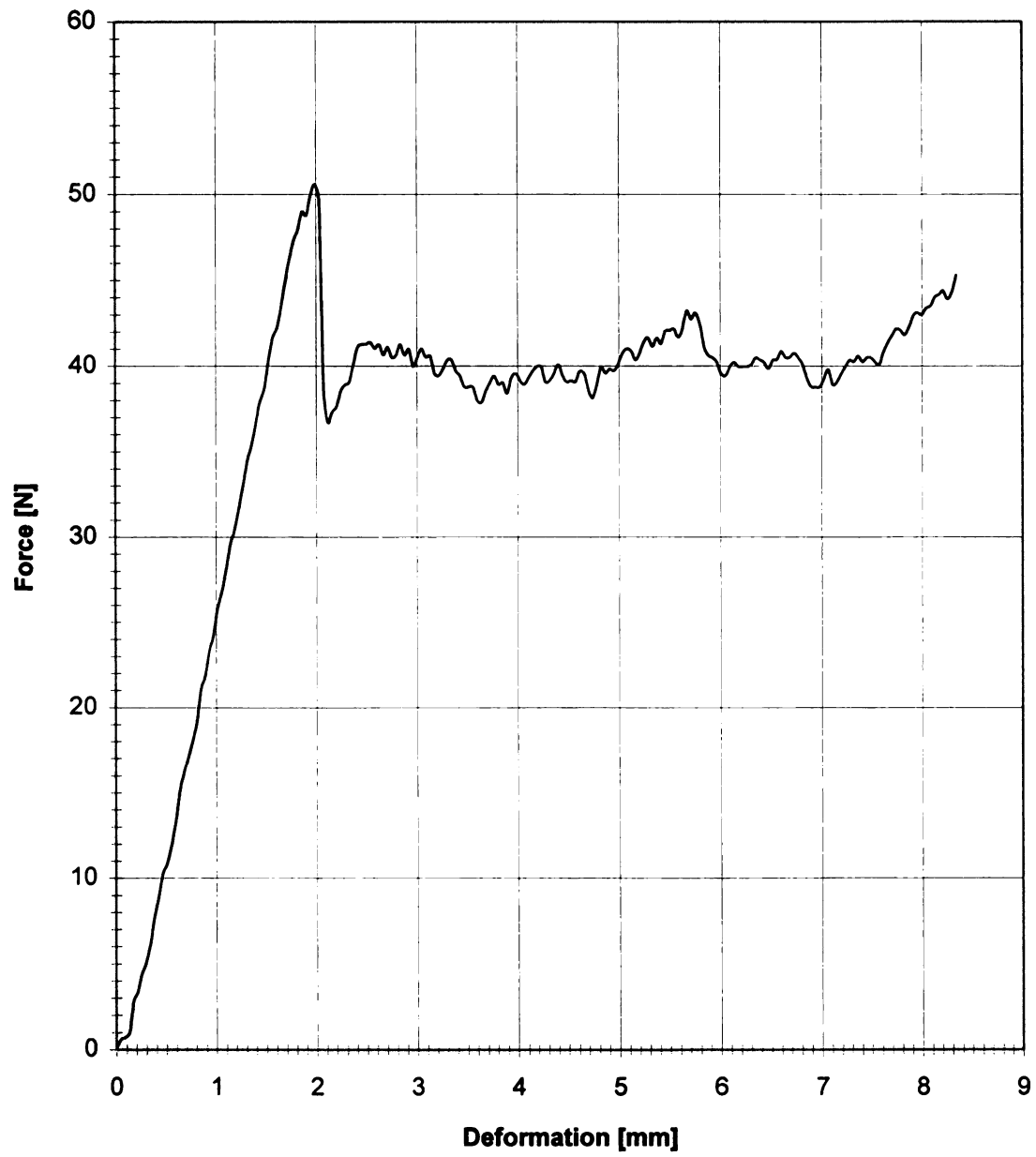
FIGURE B24 - Magness-Taylor puncture test result of Y24_02
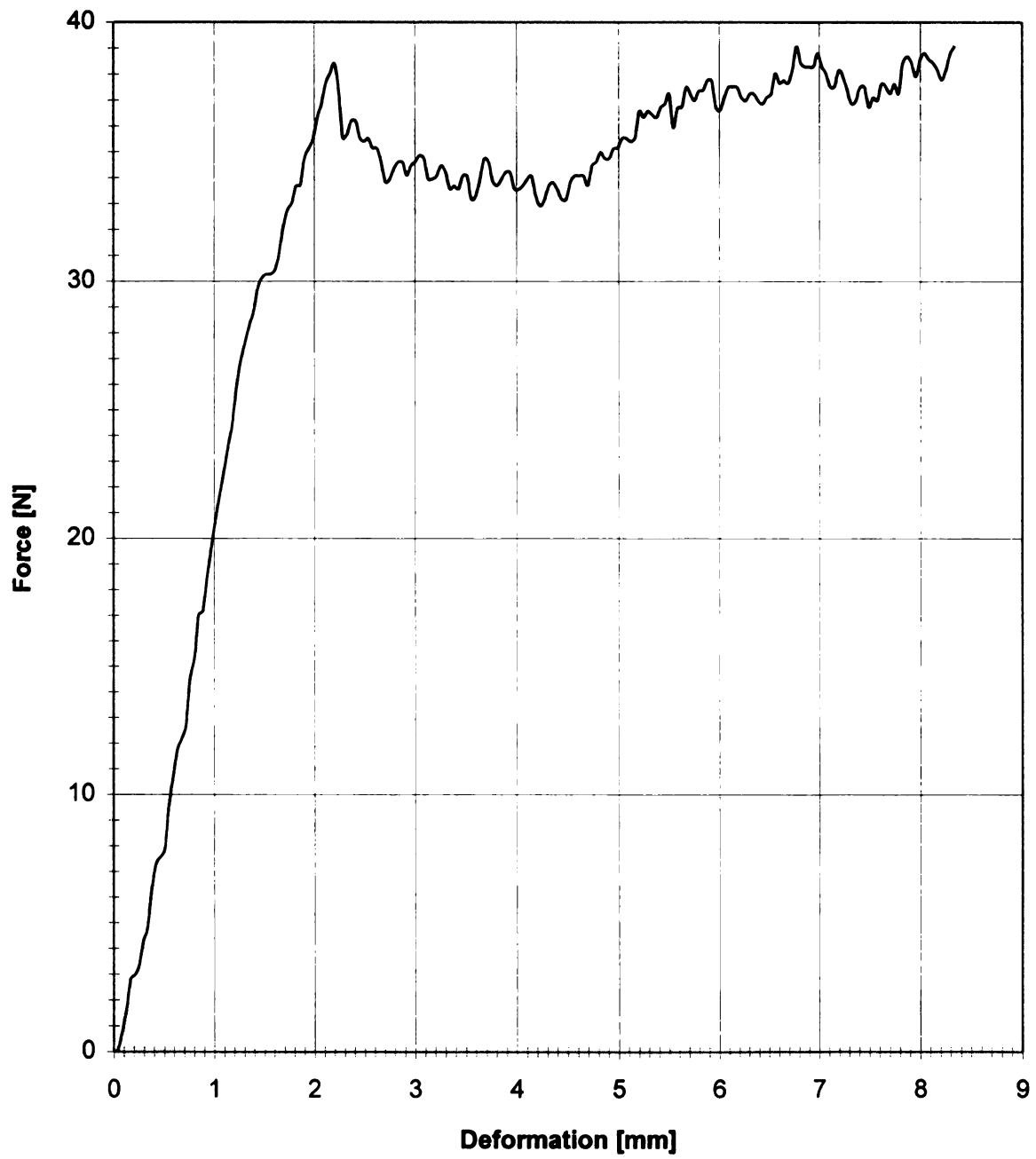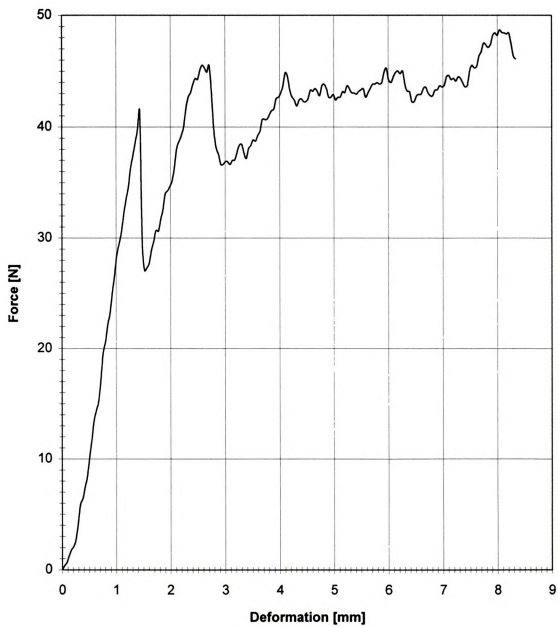
FIGURE B25 - Magness-Taylor puncture test result of Y25_02
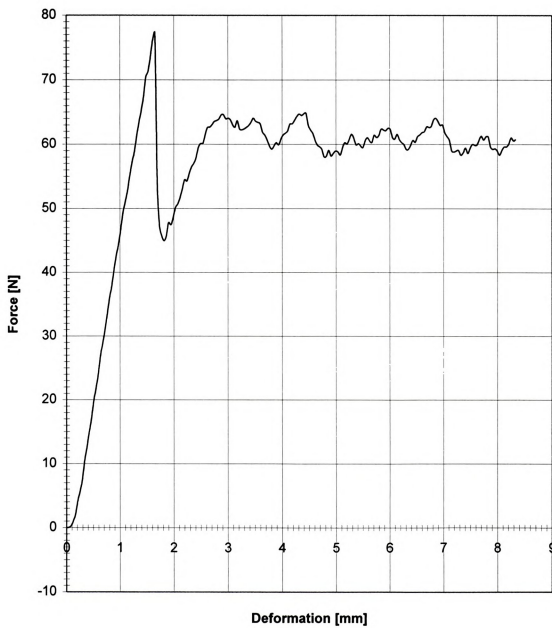
FIGURE B26 - Magness-Taylor puncture test result of Y26_02
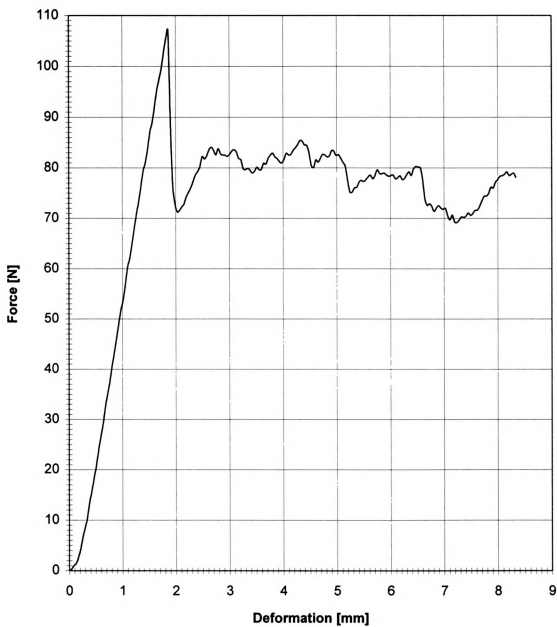
FIGURE B27 - Magness-Taylor puncture test result of  Y27_02
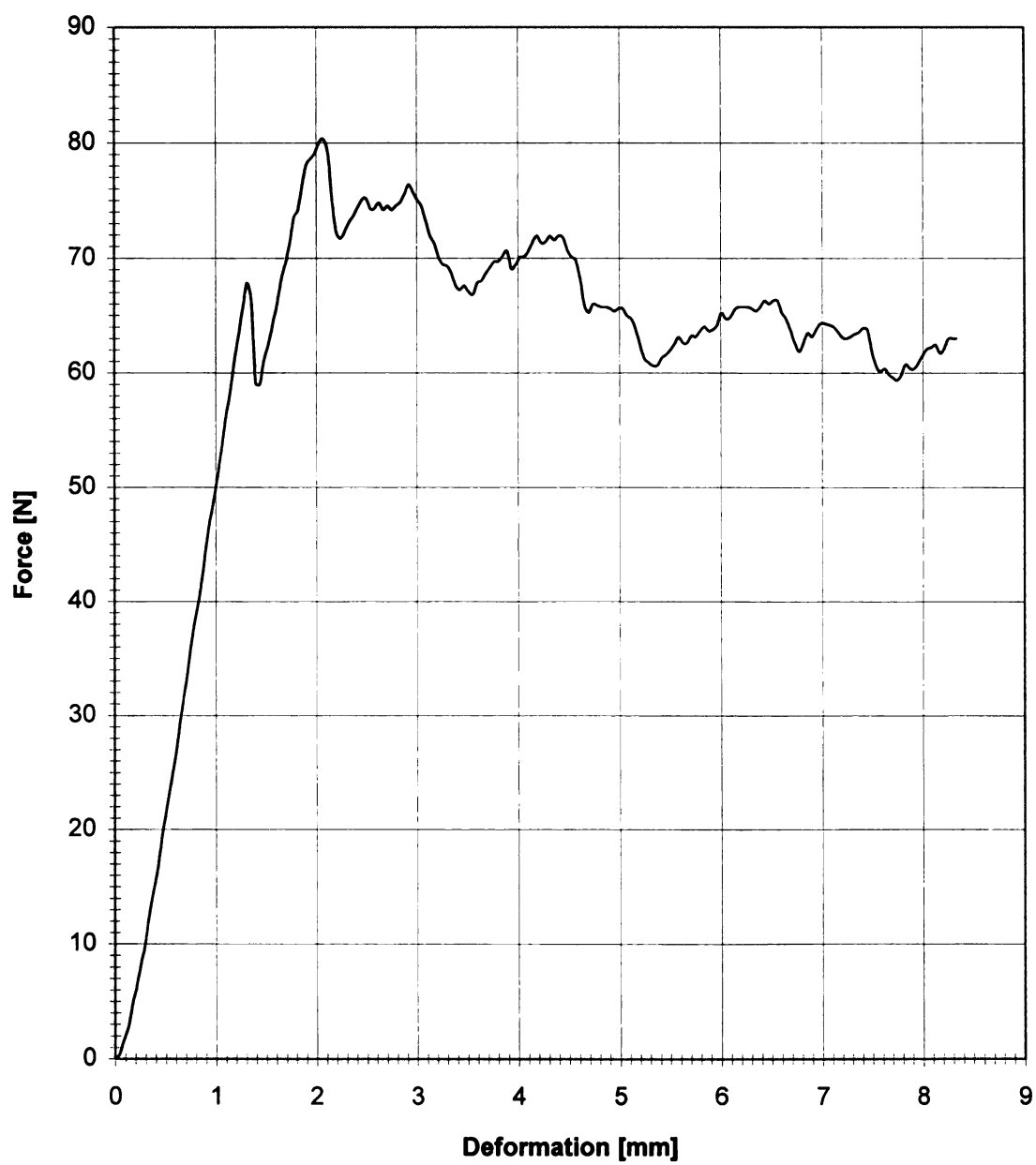
FIGURE B28 - Magness-Taylor puncture test result of Y28_02
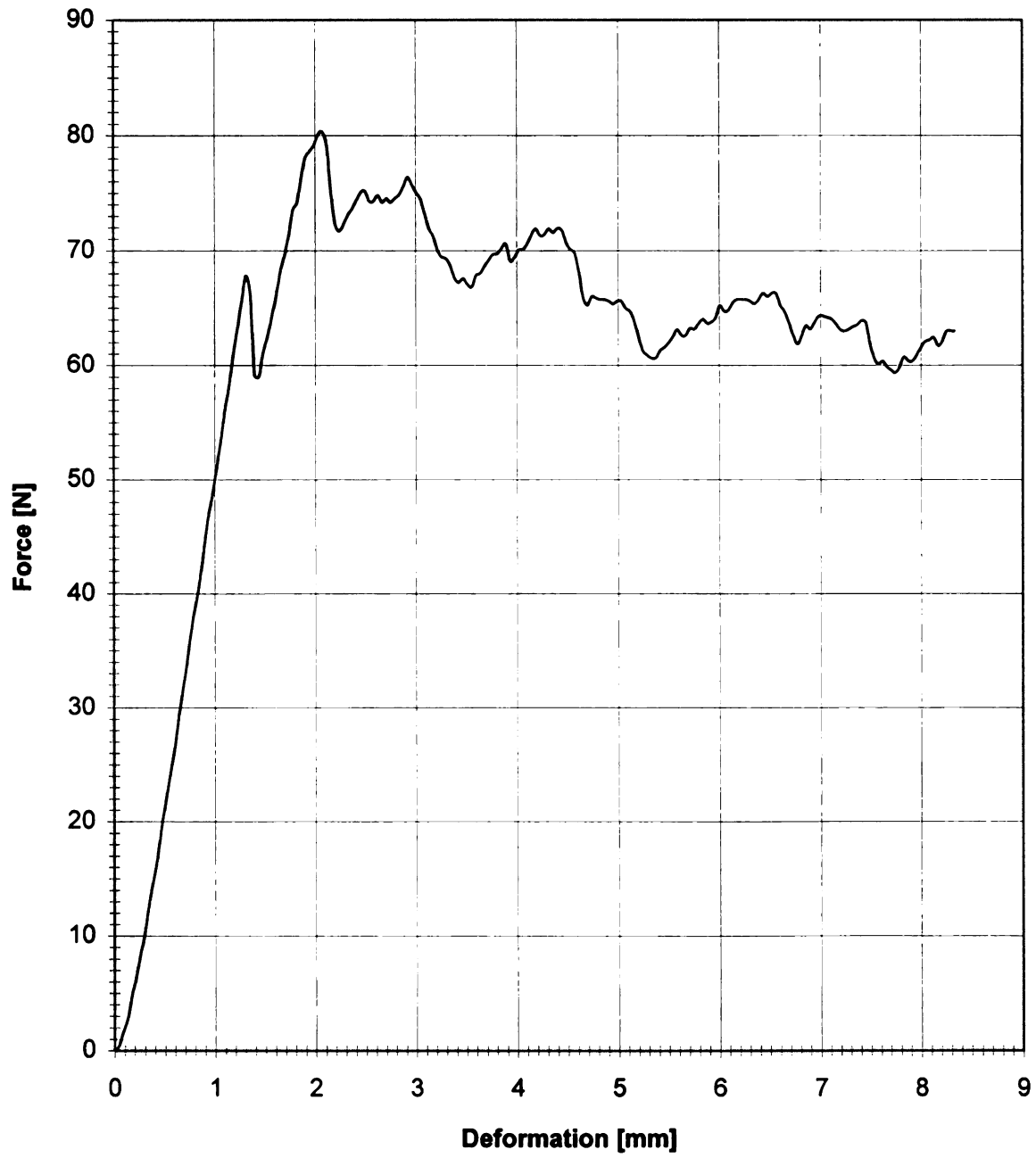
FIGURE B28 - Magness-Taylor puncture test result of Y28_02
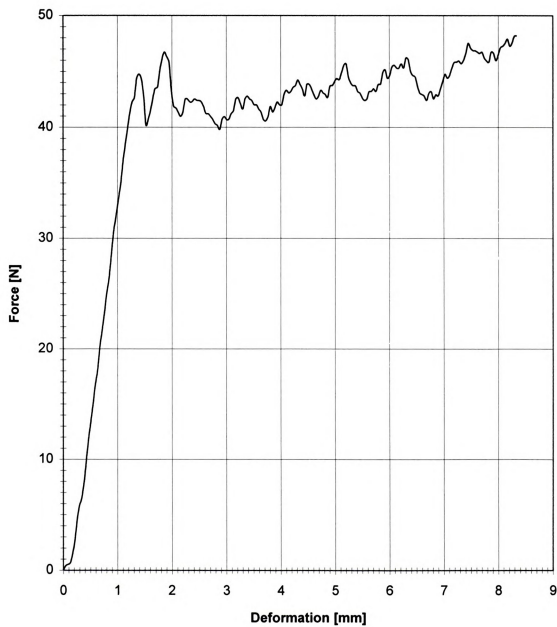
FIGURE B29 - Magness-Taylor puncture test result of Y29_02

FIGURE B30 - Magness-Taylor puncture test result of Y30_02

FIGURE B31 - Magness-Taylor puncture test result of Y31_02

FIGURE B32 - Magness-Taylor puncture test result of Y32_02

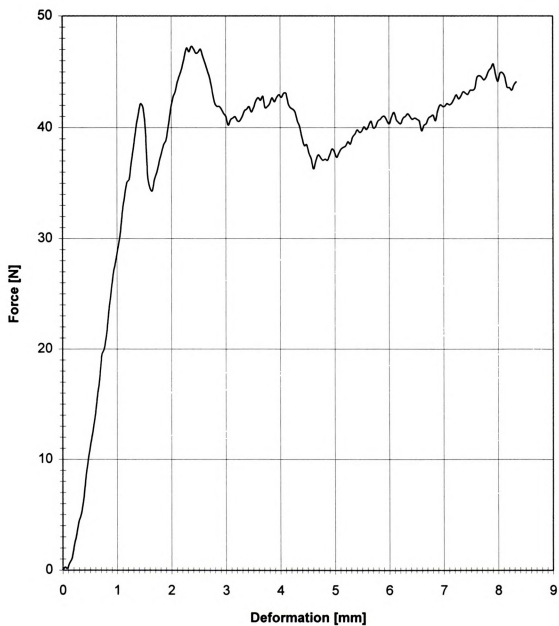FIGURE B33 - Magness-Taylor puncture test result of Y33_02

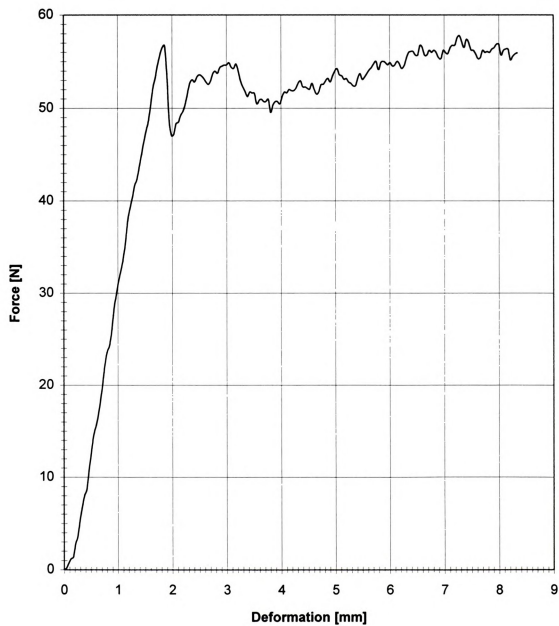FIGURE B34 - Magness-Taylor puncture test result of Y34_02

FIGURE B35 - Magness-Taylor puncture test result of Y35_02

FIGURE B36 - Magness-Taylor puncture test result of Y36_02

FIGURE B37 - Magness-Taylor puncture test result of Y37_02

FIGURE B38 - Magness-Taylor puncture test result of Y38_02

FIGURE B39 - Magness-Taylor puncture test result of Y39_02

FIGURE B40 - Magness-Taylor puncture test result of  Y40_02

FIGURE B41 - Magness-Taylor puncture test result of Y41_02

FIGURE B42 - Magness-Taylor puncture test result of Y42_02

FIGURE B43 - Magness-Taylor puncture test result of Y43_02

FIGURE B44 - Magness-Taylor puncture test result of Y44_02

FIGURE B45 - Magness-Taylor puncture test result of  Y45_02

APPENDIX C

# APPENDIX C

**Force-Deformation Plots of Compression Test and Curve Fitting**

**COMPRESSION TEST   :Maxwell Model**

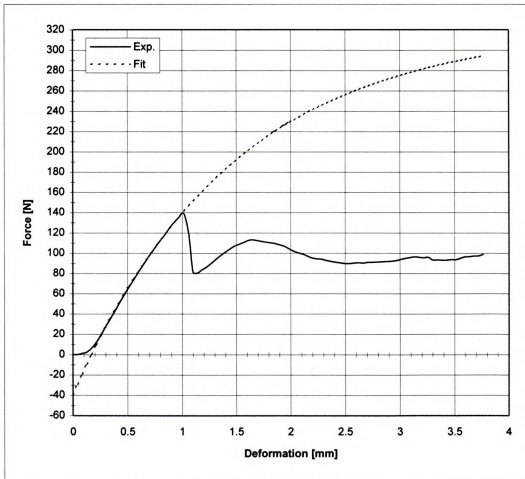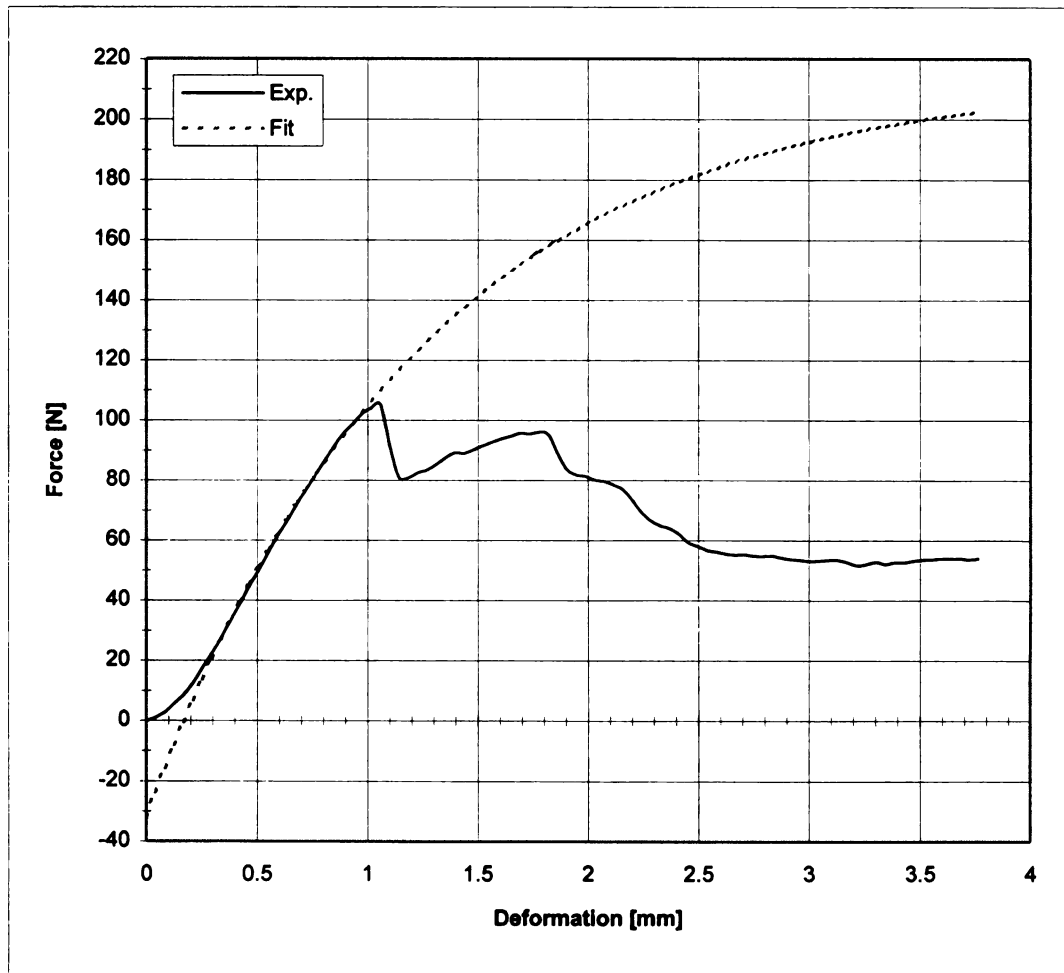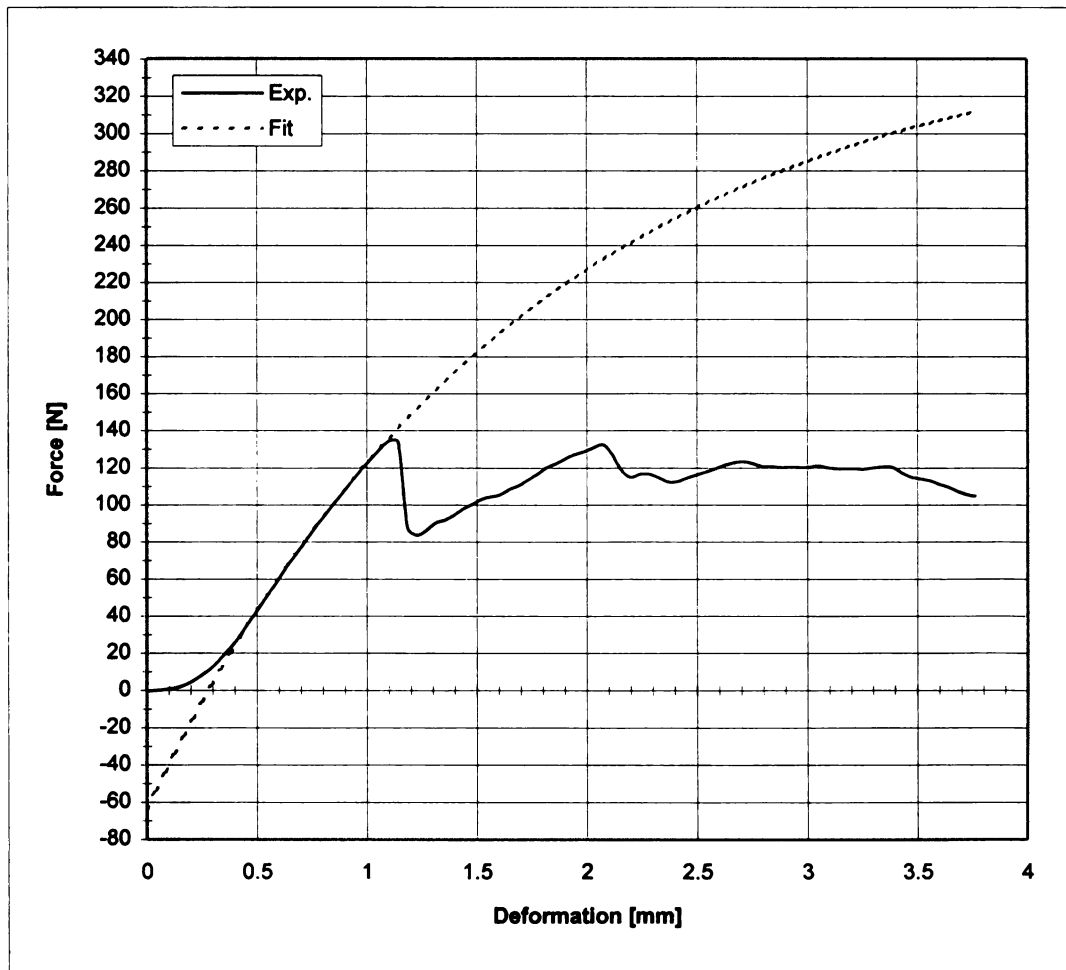| | |
|---|---|
| **Elasticity** | **3.36E+08** [Pa] |
| **Viscosity** | **3.01E+08** [Pa*s] |
| **Yield stress** | **284230** [Pa] |
| | |
| Velocity | 0.00423 [m/s] |
| Contact area | 0.000314 [m^2] |
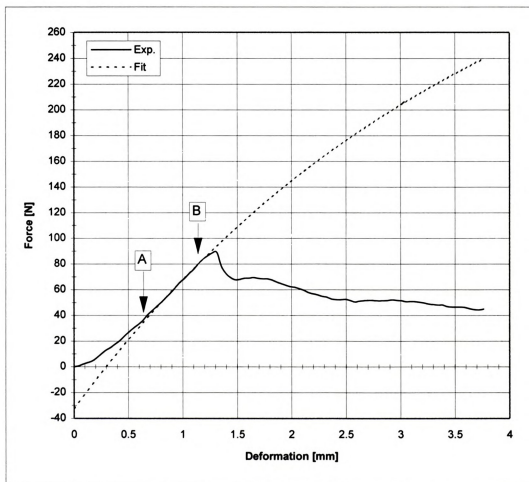


FIGURE C1 - Compression test and curve fit for Y01_03

## COMPRESSION TEST   :Maxwell Model

**Elasticity**        **6.41E+08** [Pa]
**Viscosity**         **1.83E+08** [Pa*s]
**Yield stress**         **441721** [Pa]

Velocity              0.00423 [m/s]
Contact area          0.000314 [m^2]
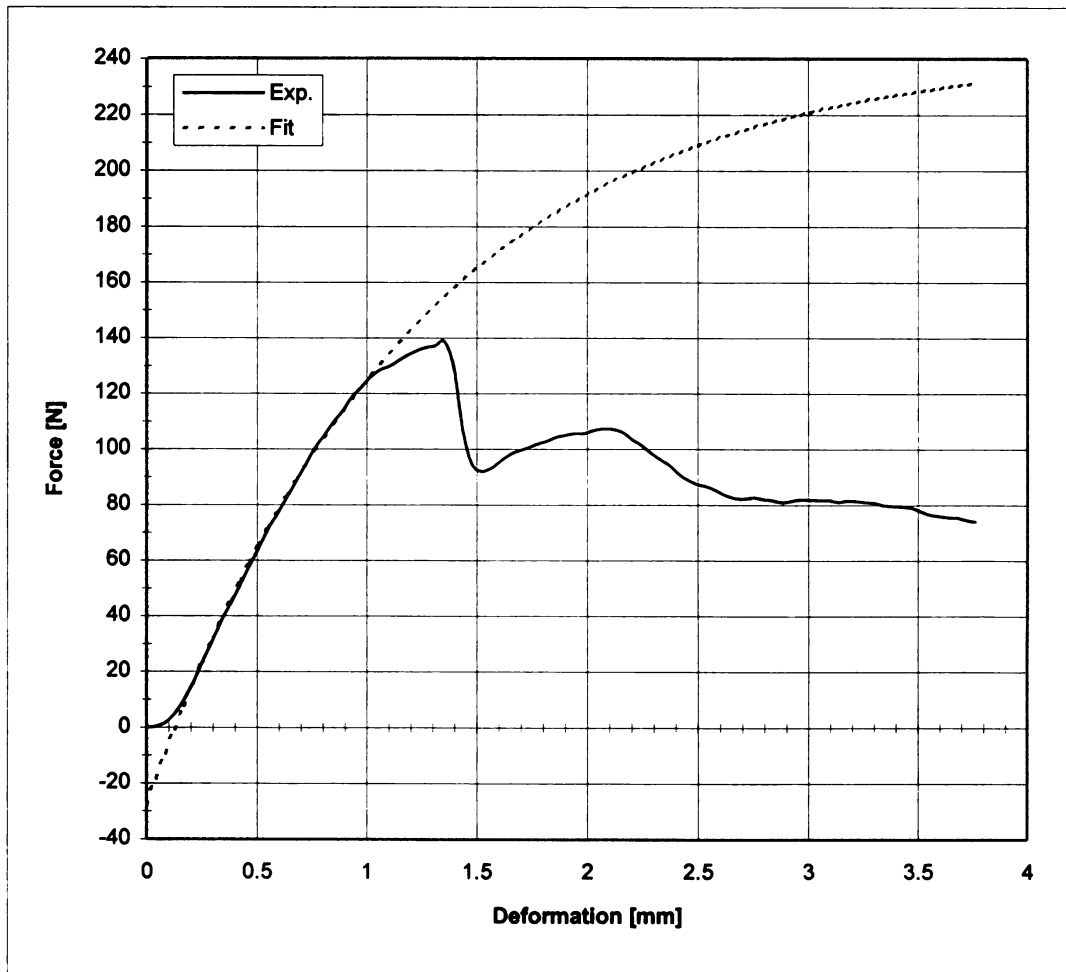


FIGURE C2 - Compression test and curve fit for Y02_03

**COMPRESSION TEST   :Maxwell Model**

| | | |
|---|---|---|
| **Elasticity** | **7.00E+08** | [Pa] |
| **Viscosity** | **2.42E+08** | [Pa*s] |
| **Yield stress** | **443736** | [Pa] |
| Velocity | 0.00423 | [m/s] |
| Contact area | 0.000314 | [m^2] |



FIGURE C3 - Compression test and curve fit for Y03_03

## COMPRESSION TEST  :Maxwell Model

| | | |
|---|---|---|
| **Elasticity** | **5.53E+08** | [Pa] |
| **Viscosity** | **1.61E+08** | [Pa*s] |
| **Yield stress** | **335967** | [Pa] |
| Velocity | 0.00423 | [m/s] |
| Contact area | 0.000314 | [m^2] |



FIGURE C4 - Compression test and curve fit for Y04_03

## COMPRESSION TEST   :Maxwell Model

| | | |
|---|---|---|
| **Elasticity** | **6.65E+08** | [Pa] |
| **Viscosity** | **2.70E+08** | [Pa*s] |
| **Yield stress** | **428455** | [Pa] |
| | | |
| Velocity | 0.00423 | [m/s] |
| Contact area | 0.000314 | [m^2] |



FIGURE C5 - Compression test and curve fit for Y05_03

## COMPRESSION TEST   :Maxwell Model

| | | |
|---|---|---|
| **Elasticity** | **7.25E+08** | [Pa] |
| **Viscosity** | **3.07E+08** | [Pa*s] |
| **Yield stress** | **446245** | [Pa] |
| **Velocity** | 0.00423 | [m/s] |
| **Contact area** | 0.000314 | [m^2] |
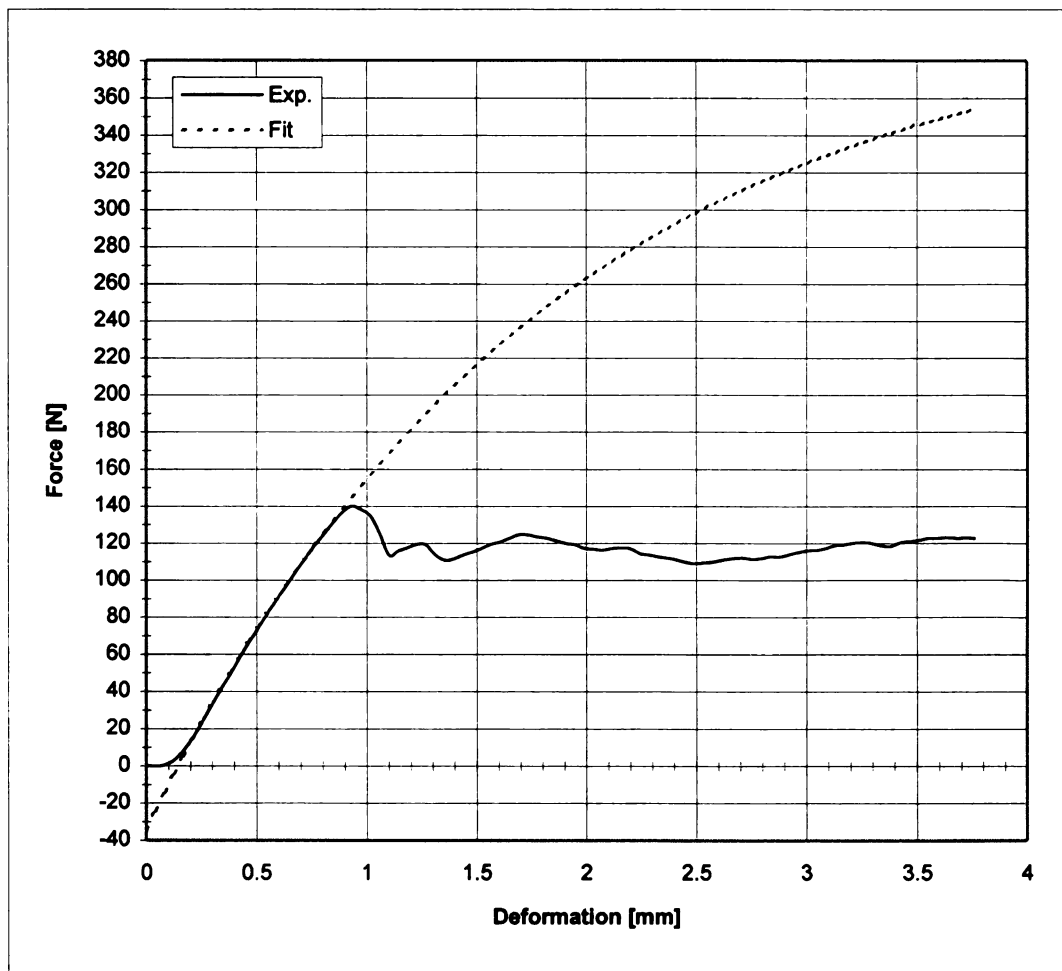


FIGURE C6 - Compression test and curve fit for Y06_03

# COMPRESSION TEST  :Maxwell Model

| | | |
|---|---|---|
| **Elasticity** | **7.25E+08** | [Pa] |
| **Viscosity** | **3.22E+08** | [Pa*s] |
| **Yield stress** | **473311** | [Pa] |
| | | |
| **Velocity** | 0.00423 | [m/s] |
| **Contact area** | 0.000314 | [m^2] |
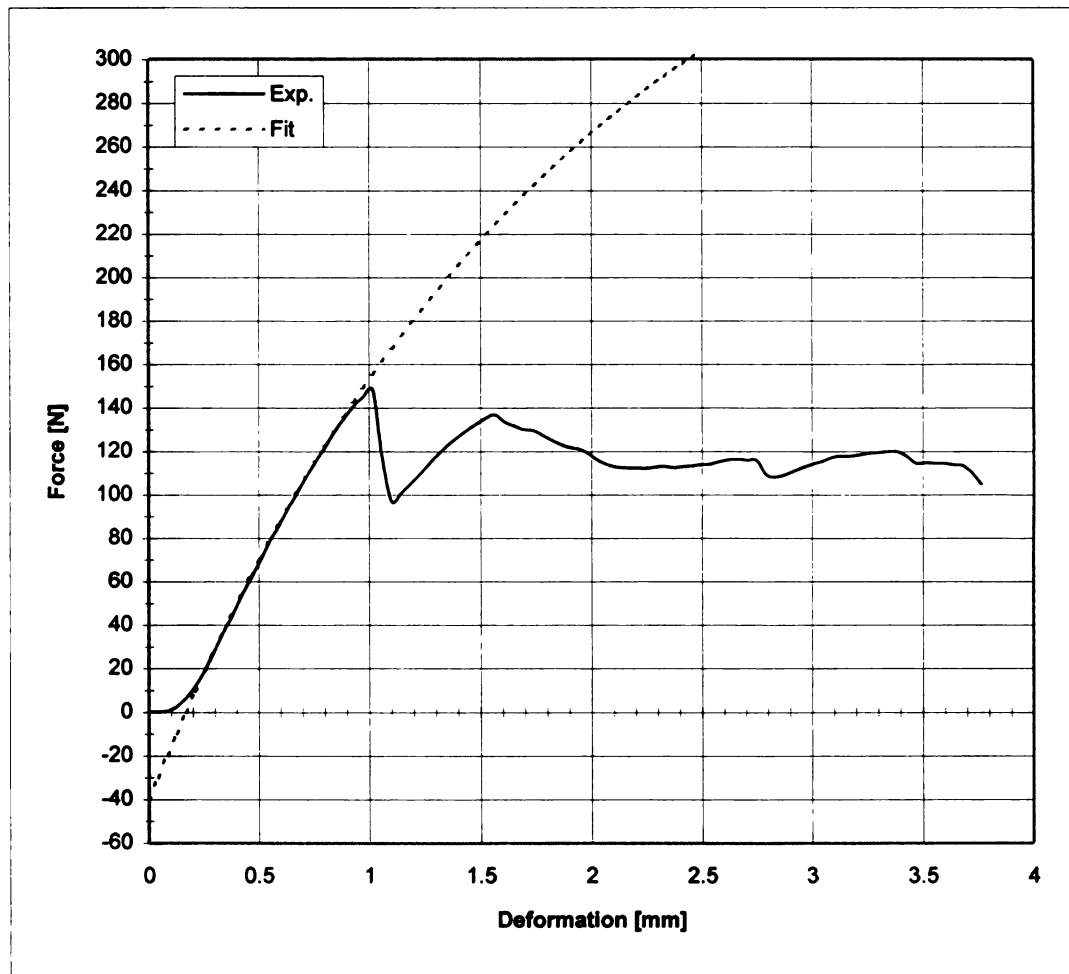


FIGURE C7 - Compression test and curve fit for Y07_03

# COMPRESSION TEST   :Maxwell Model

| | | |
|---|---|---|
| **Elasticity** | **6.52E+08** | [Pa] |
| **Viscosity** | **2.09E+08** | [Pa*s] |
| **Yield stress** | **352807** | [Pa] |
| Velocity | 0.00423 | [m/s] |
| Contact area | 0.000314 | [m^2] |
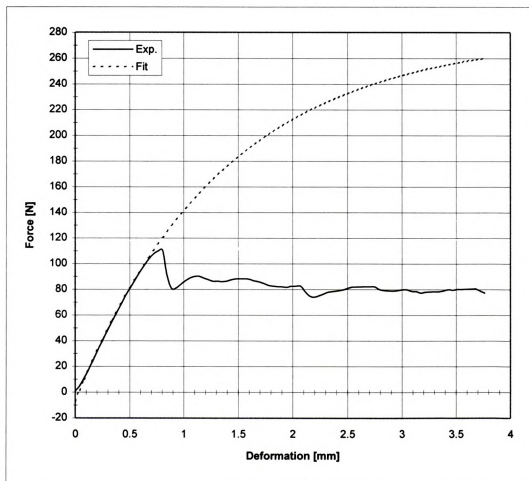


FIGURE C8 - Compression test and curve fit for Y08_03

**COMPRESSION TEST   :Maxwell Model**

| | | |
|---|---|---|
| **Elasticity** | **5.68E+08** | [Pa] |
| **Viscosity** | **2.53E+08** | [Pa*s] |
| **Yield stress** | **331709** | [Pa] |
| Velocity | 0.00423 | [m/s] |
| Contact area | 0.000314 | [m^2] |
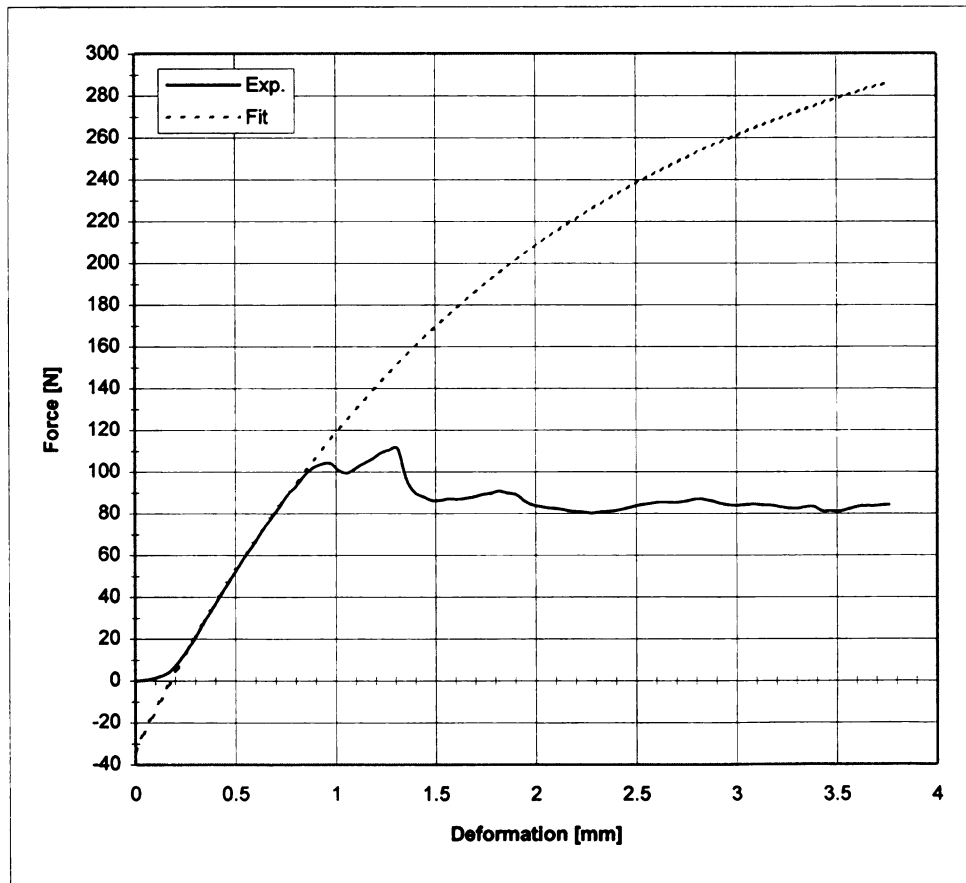


FIGURE C9 - Compression test and curve fit for Y09_03

**COMPRESSION TEST   :Maxwell Model**

| | | |
|---|---|---|
| **Elasticity** | **5.82E+08** | [Pa] |
| **Viscosity** | **2.61E+08** | [Pa*s] |
| **Yield stress** | **278642** | [Pa] |
| | | |
| Velocity | 0.00423 | [m/s] |
| Contact area | 0.000314 | [m^2] |
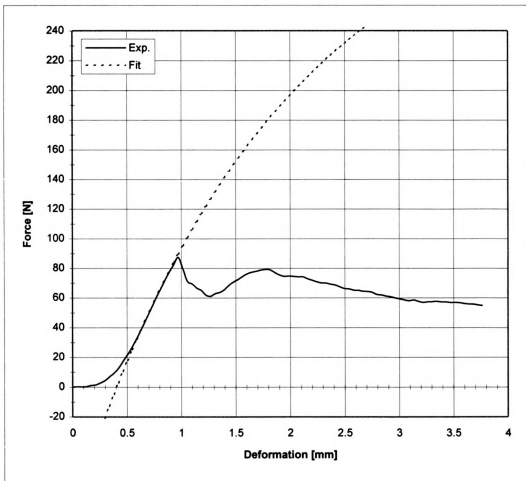


FIGURE C10 - Compression test and curve fit for Y10_03

## COMPRESSION TEST :Maxwell Model

| | | |
|---|---|---|
| Elasticity | 8.09E+08 | [Pa] |
| Viscosity | 2.75E+08 | [Pa*s] |
| Yield stress | 518319 | [Pa] |
| | | |
| Velocity | 0.00423 | [m/s] |
| Contact area | 0.000314 | [m^2] |
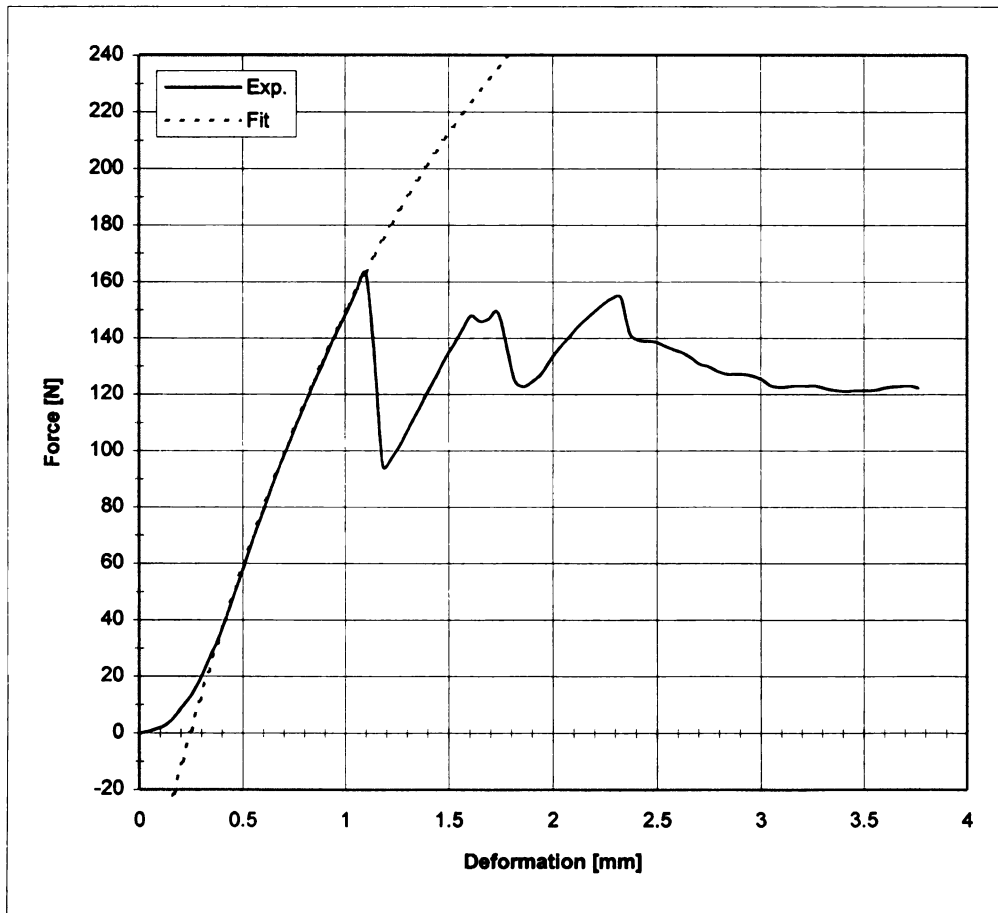


FIGURE C11 - Compression test and curve fit for Y11_03

**COMPRESSION TEST   :Maxwell Model**

| | | |
|---|---|---|
| Elasticity | **5.19E+08** | [Pa] |
| Viscosity | **4.29E+08** | [Pa*s] |
| Yield stress | **434385** | [Pa] |
| | | |
| Velocity | 0.00423 | [m/s] |
| Contact area | 0.000314 | [m^2] |
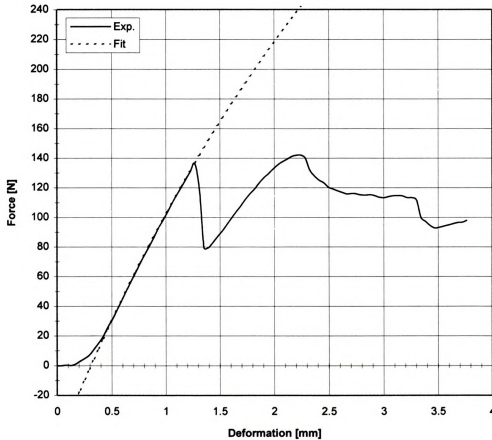


FIGURE C12 - Compression test and curve fit for Y12_03

## COMPRESSION TEST   :Maxwell Model

| | | |
|---|---|---|
| Elasticity | **6.90E+08** | [Pa] |
| Viscosity | **2.09E+08** | [Pa*s] |
| Yield stress | **476922** | [Pa] |
| | | |
| Velocity | 0.00423 | [m/s] |
| Contact area | 0.000314 | [m^2] |
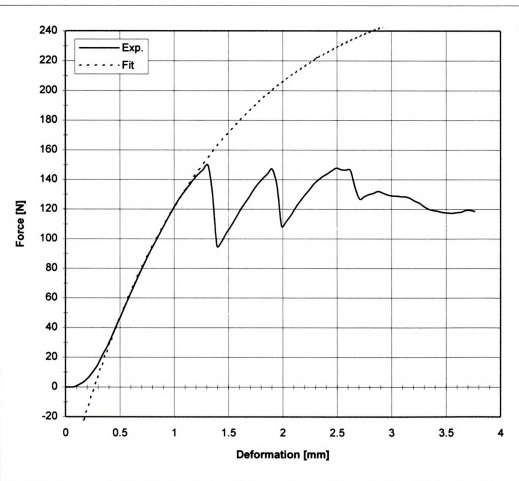


FIGURE C13 - Compression test and curve fit for Y13_03

**COMPRESSION TEST   :Maxwell Model**

| | | |
|---|---|---|
| Elasticity | **8.12E+08** | [Pa] |
| Viscosity | **2.56E+08** | [Pa*s] |
| Yield stress | **506877** | [Pa] |
| | | |
| Velocity | 0.00423 | [m/s] |
| Contact area | 0.000314 | [m^2] |
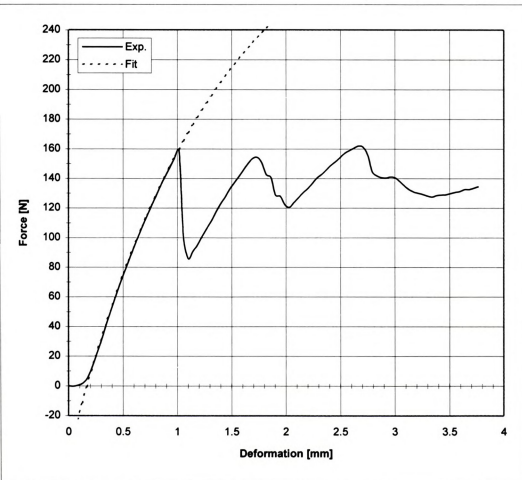


FIGURE C14 - Compression test and curve fit for Y14_03

# COMPRESSION TEST   :Maxwell Model

| | |
|---|---|
| Elasticity | **7.44E+08** [Pa] |
| Viscosity | **2.64E+08** [Pa*s] |
| Yield stress | **500491** [Pa] |
| | |
| Velocity | 0.00423 [m/s] |
| Contact area | 0.000314 [m^2] |
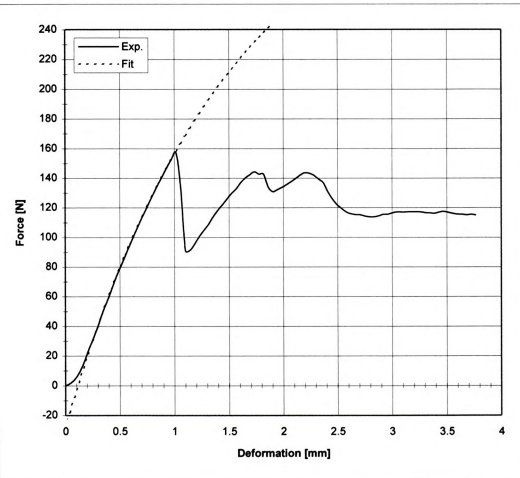


FIGURE C15 - Compression test and curve fit for Y15_03

**COMPRESSION TEST   :Maxwell Model**

| | | |
|---|---|---|
| **Elasticity** | **6.23E+08** | [Pa] |
| **Viscosity** | **5.17E+08** | [Pa*s] |
| **Yield stress** | **497526** | [Pa] |
| Velocity | 0.00423 | [m/s] |
| Contact area | 0.000314 | [m^2] |
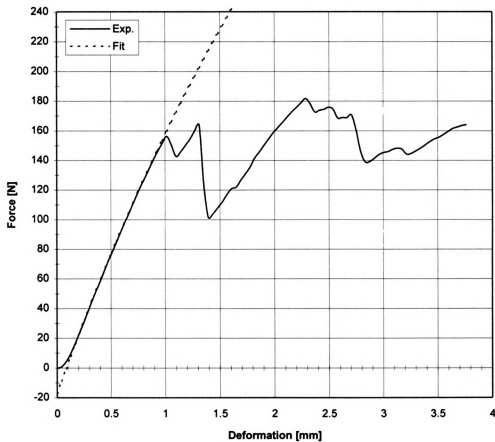


FIGURE C16 - Compression test and curve fit for Y16_03

**COMPRESSION TEST   :Maxwell Model**

| | | |
|---|---|---|
| Elasticity | **4.82E+08** | [Pa] |
| Viscosity | **2.76E+08** | [Pa*s] |
| Yield stress | **353833** | [Pa] |
| Velocity | 0.00423 | [m/s] |
| Contact area | 0.000314 | [m^2] |
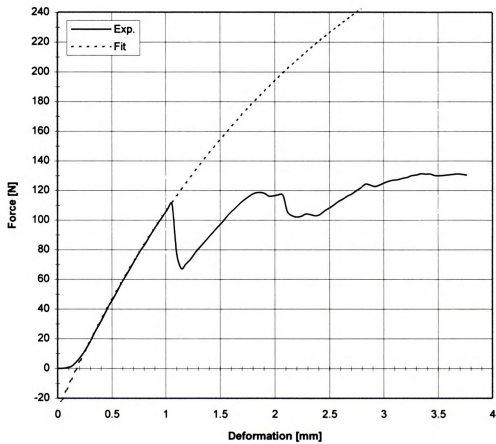


FIGURE C17 - Compression test and curve fit for Y17_03

**COMPRESSION TEST   :Maxwell Model**

| | | |
|---|---|---|
| **Elasticity** | **4.57E+08** | [Pa] |
| **Viscosity** | **4.02E+08** | [Pa*s] |
| **Yield stress** | **358053** | [Pa] |
| | | |
| **Velocity** | 0.00423 | [m/s] |
| **Contact area** | 0.000314 | [m^2] |
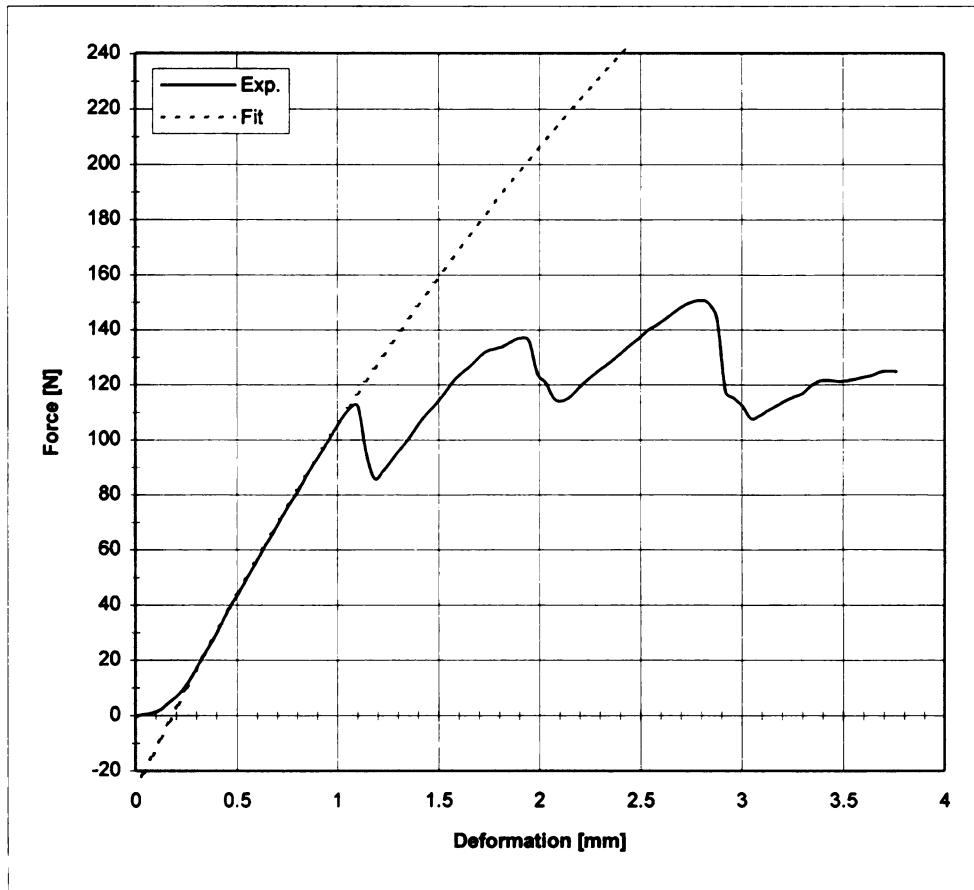


FIGURE C18 - Compression test and curve fit for Y18_03

**COMPRESSION TEST   :Maxwell Model**

| | | |
|---|---|---|
| **Elasticity** | **3.05E+08** | [Pa] |
| **Viscosity** | **1.93E+09** | [Pa*s] |
| **Yield stress** | **364249** | [Pa] |
| Velocity | 0.00423 | [m/s] |
| Contact area | 0.000314 | [m^2] |
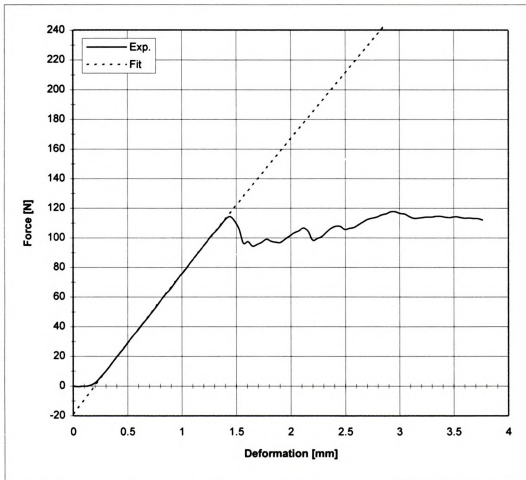


FIGURE C19 - Compression test and curve fit for Y19_03

# COMPRESSION TEST   :Maxwell Model

| | | |
|---|---|---|
| **Elasticity** | **4.84E+08** | [Pa] |
| **Viscosity** | **6.18E+08** | [Pa*s] |
| **Yield stress** | **396447** | [Pa] |
| Velocity | 0.00423 | [m/s] |
| Contact area | 0.000314 | [m^2] |
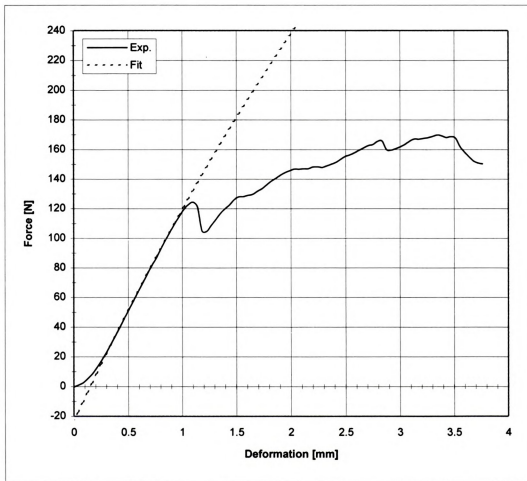


FIGURE C20 - Compression test and curve fit for Y20_03
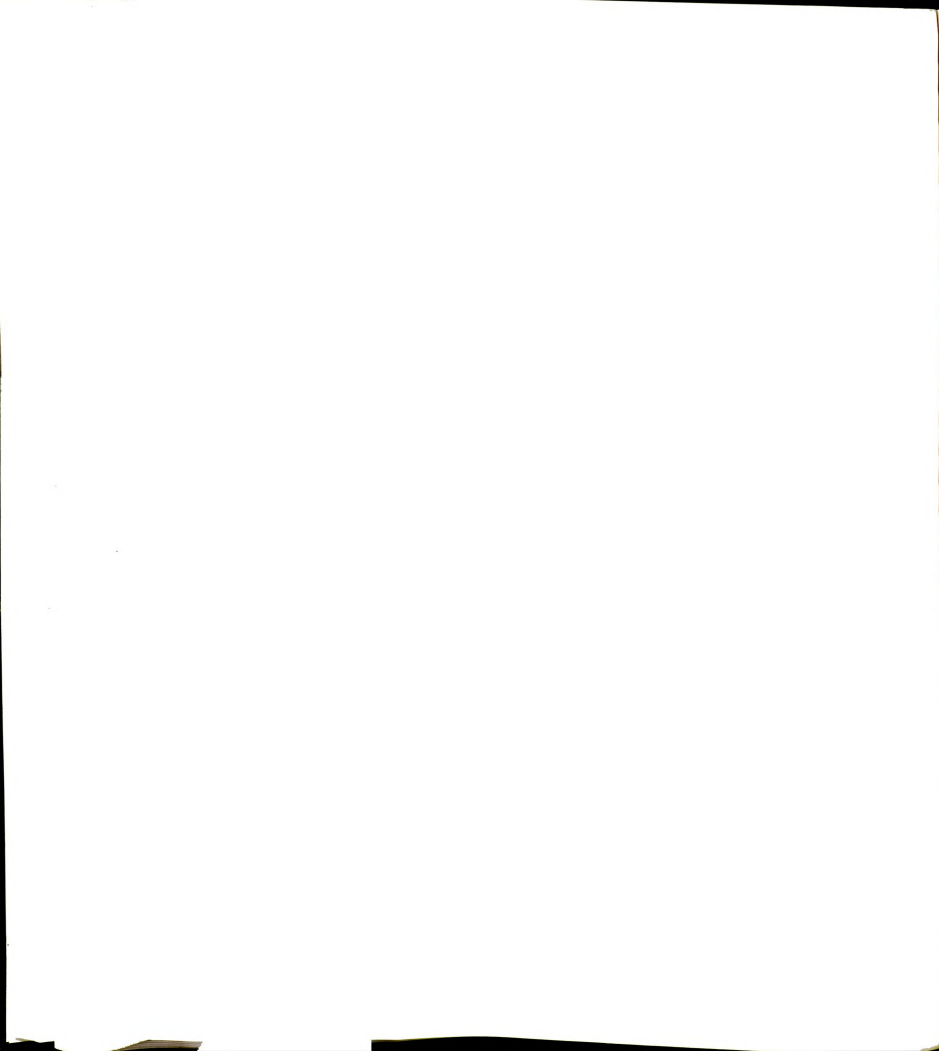
**COMPRESSION TEST   :Maxwell Model**

| | |
|---|---|
| **Elasticity** | **4.17E+08** [Pa] |
| **Viscosity** | **2.17E+08** [Pa*s] |
| **Yield stress** | **334104** [Pa] |
| Velocity | 0.00423 [m/s] |
| Contact area | 0.000314 [m^2] |
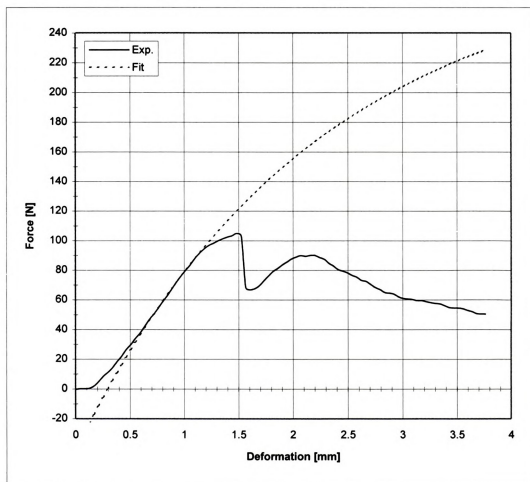


FIGURE C21 - Compression test and curve fit for Y21_03

**COMPRESSION TEST   :Maxwell Model**

| | | |
|---|---|---|
| **Elasticity** | **4.83E+08** [Pa] | |
| **Viscosity** | **2.21E+08** [Pa*s] | |
| **Yield stress** | **388122** [Pa] | |
| Velocity | 0.00423 [m/s] | |
| Contact area | 0.000314 [m^2] | |
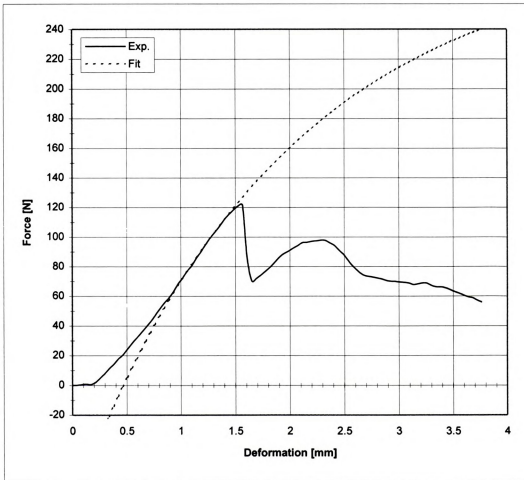


FIGURE C22 - Compression test and curve fit for Y22_03

# COMPRESSION TEST   :Maxwell Model

| | |
|---|---|
| **Elasticity** | **5.15E+08** [Pa] |
| **Viscosity** | **2.01E+08** [Pa*s] |
| **Yield stress** | **379075** [Pa] |
| Velocity | 0.00423 [m/s] |
| Contact area | 0.000314 [m^2] |
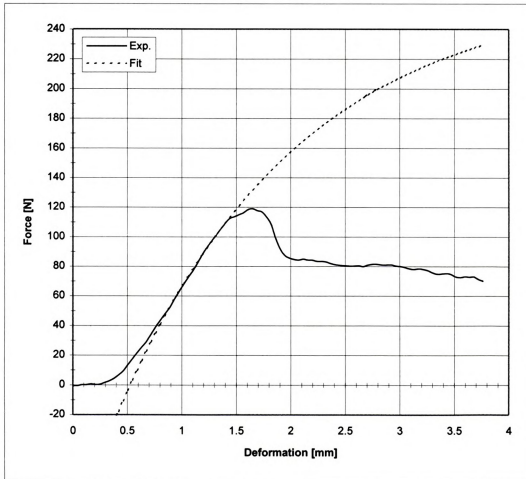


FIGURE C23 - Compression test and curve fit for Y23_03

## COMPRESSION TEST   :Maxwell Model

| | | |
|---|---|---|
| **Elasticity** | **3.30E+08** [Pa] | |
| **Viscosity** | **3.05E+08** [Pa*s] | |
| **Yield stress** | **282443** [Pa] | |
| | | |
| Velocity | 0.00423 [m/s] | |
| Contact area | 0.000314 [m^2] | |
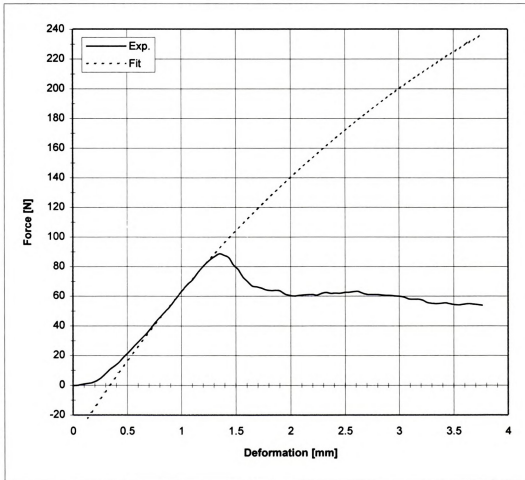


FIGURE C24 - Compression test and curve fit for Y24_03

## COMPRESSION TEST  :Maxwell Model

| | | |
|---|---|---|
| **Elasticity** | **3.36E+08** | [Pa] |
| **Viscosity** | **3.01E+08** | [Pa*s] |
| **Yield stress** | **284230** | [Pa] |
| | | |
| Velocity | 0.00423 | [m/s] |
| Contact area | 0.000314 | [m^2] |
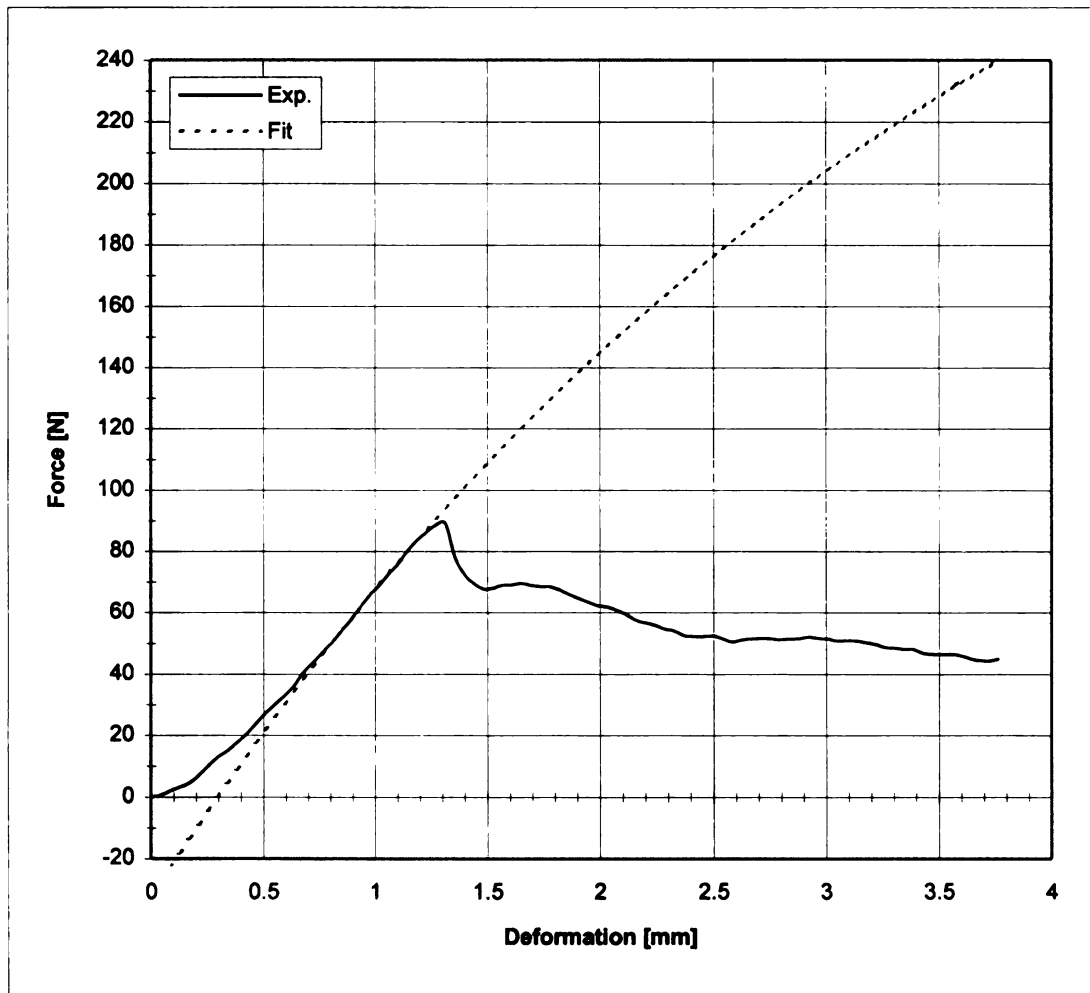


FIGURE C25 - Compression test and curve fit for Y25_03

**COMPRESSION TEST   :Maxwell Model**

| | | |
|---|---|---|
| **Elasticity** | **8.62E+08** | [Pa] |
| **Viscosity** | **1.88E+08** | [Pa*s] |
| **Yield stress** | **444801** | [Pa] |

| | | |
|---|---|---|
| Velocity | 0.00423 | [m/s] |
| Contact area | 0.000314 | [m^2] |
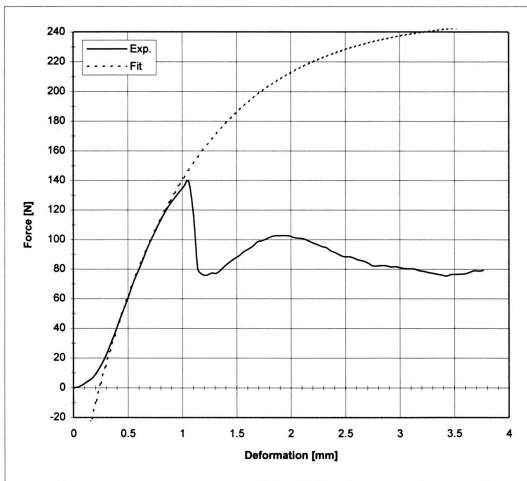


FIGURE C26 - Compression test and curve fit for Y26_03

**COMPRESSION TEST   :Maxwell Model**

| | | |
|---|---|---|
| **Elasticity** | **9.24E+08** | [Pa] |
| **Viscosity** | **3.35E+08** | [Pa*s] |
| **Yield stress** | **631107** | [Pa] |
| | | |
| Velocity | 0.00423 | [m/s] |
| Contact area | 0.000314 | [m^2] |
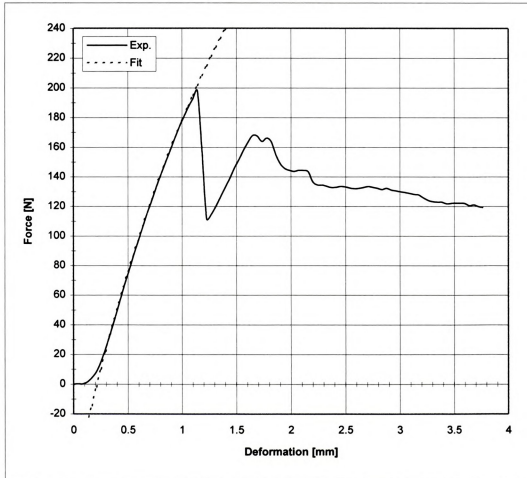


FIGURE C27 - Compression test and curve fit for Y27_03

**COMPRESSION TEST   :Maxwell Model**

| | | |
|---|---|---|
| **Elasticity** | **7.48E+08** [Pa] | |
| **Viscosity** | **3.31E+08** [Pa*s] | |
| **Yield stress** | **469624** [Pa] | |
| Velocity | 0.00423 [m/s] | |
| Contact area | 0.000314 [m^2] | |
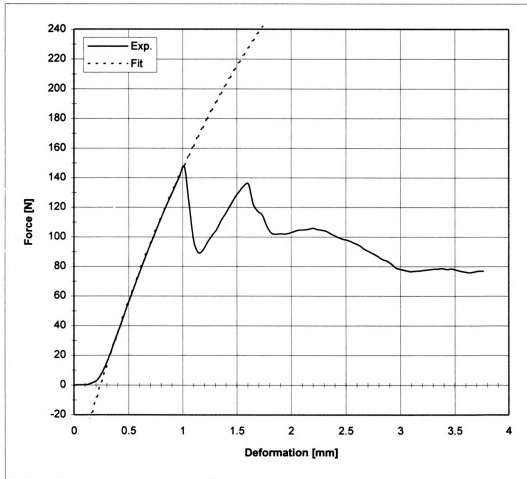


FIGURE C28 - Compression test and curve fit for Y28_03

**COMPRESSION TEST   :Maxwell Model**

| | | |
|---|---|---|
| **Elasticity** | **1.12E+09** | [Pa] |
| **Viscosity** | **3.20E+08** | [Pa*s] |
| **Yield stress** | **653307** | [Pa] |
| | | |
| Velocity | 0.00423 | [m/s] |
| Contact area | 0.000314 | [m^2] |
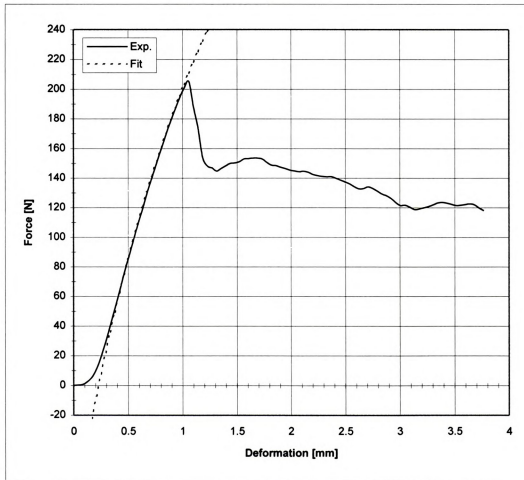


FIGURE C29 - Compression test and curve fit for Y29_03

**COMPRESSION TEST   :Maxwell Model**

| | | |
|---|---|---|
| **Elasticity** | **7.82E+08** | [Pa] |
| **Viscosity** | **4.76E+08** | [Pa*s] |
| **Yield stress** | **554547** | [Pa] |
| Velocity | 0.00423 | [m/s] |
| Contact area | 0.000314 | [m^2] |
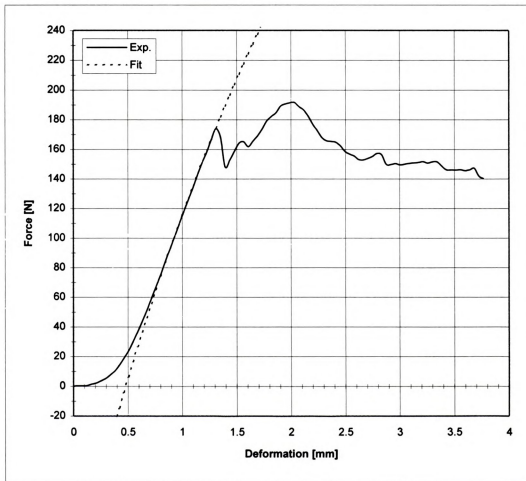


FIGURE C30 - Compression test and curve fit for Y30_03

**COMPRESSION TEST   :Maxwell Model**

| | | |
|---|---|---|
| **Elasticity** | **6.56E+08** | [Pa] |
| **Viscosity** | **1.46E+08** | [Pa*s] |
| **Yield stress** | **355620** | [Pa] |
| Velocity | 0.00423 | [m/s] |
| Contact area | 0.000314 | [m^2] |
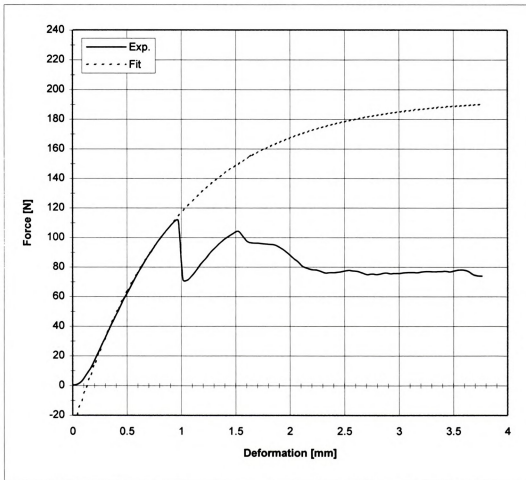


FIGURE C31 - Compression test and curve fit for Y31_03

**COMPRESSION TEST    :Maxwell Model**

| | | |
|---|---|---|
| **Elasticity** | **5.48E+08** | [Pa] |
| **Viscosity** | **2.93E+08** | [Pa*s] |
| **Yield stress** | **412565** | [Pa] |
| | | |
| Velocity | 0.00423 | [m/s] |
| Contact area | 0.000314 | [m^2] |
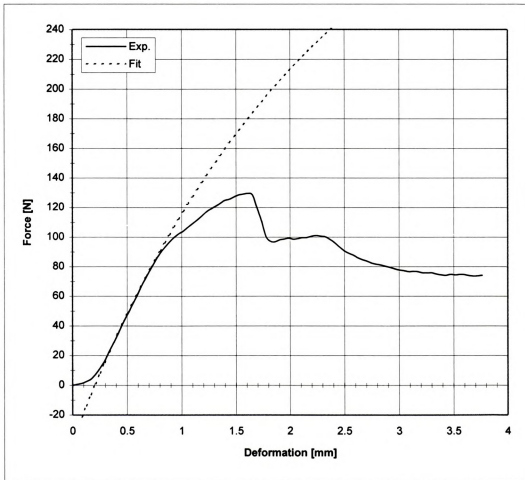


FIGURE C32 - Compression test and curve fit for Y32_03

## COMPRESSION TEST   :Maxwell Model

| | | |
|---|---|---|
| **Elasticity** | **5.94E+08** | [Pa] |
| **Viscosity** | **1.48E+08** | [Pa*s] |
| **Yield stress** | **300310** | [Pa] |
| Velocity | 0.00423 | [m/s] |
| Contact area | 0.000314 | [m^2] |
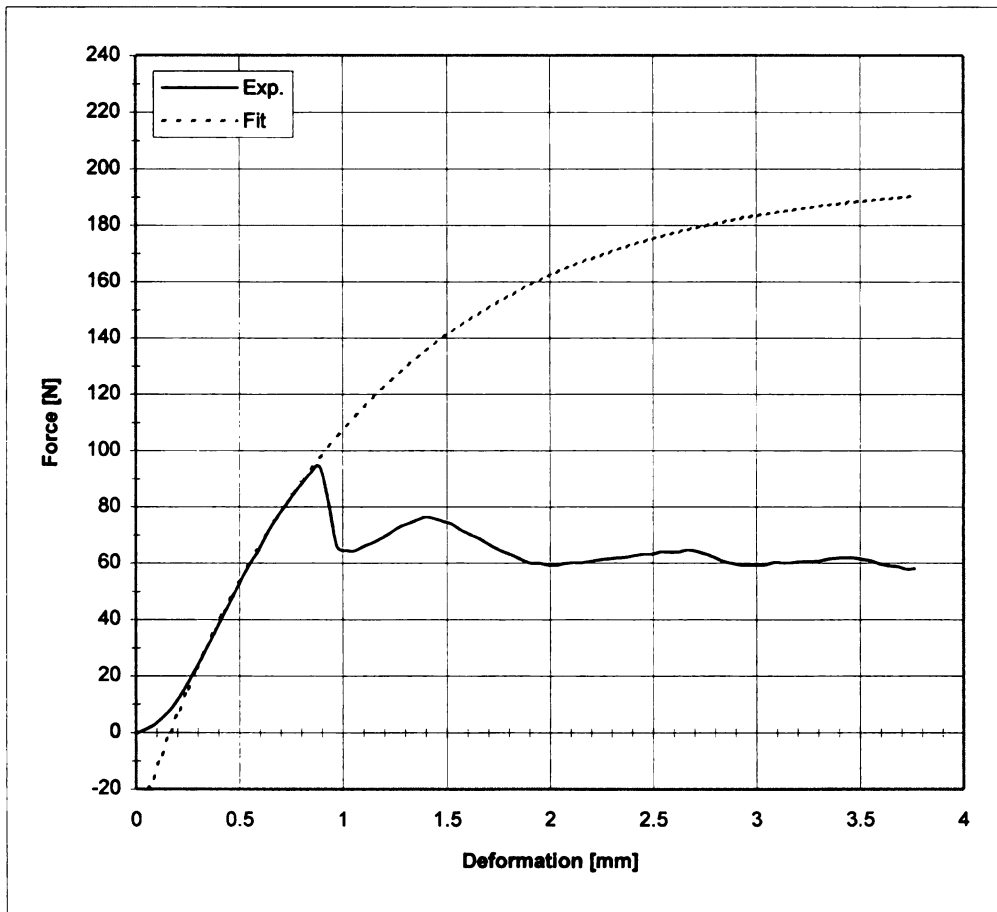


FIGURE C33 - Compression test and curve fit for Y33_03

**COMPRESSION TEST   :Maxwell Model**

| | | |
|---|---|---|
| **Elasticity** | **6.53E+08** | [Pa] |
| **Viscosity** | **1.67E+08** | [Pa*s] |
| **Yield stress** | **348930** | [Pa] |
| | | |
| Velocity | 0.00423 | [m/s] |
| Contact area | 0.000314 | [m^2] |
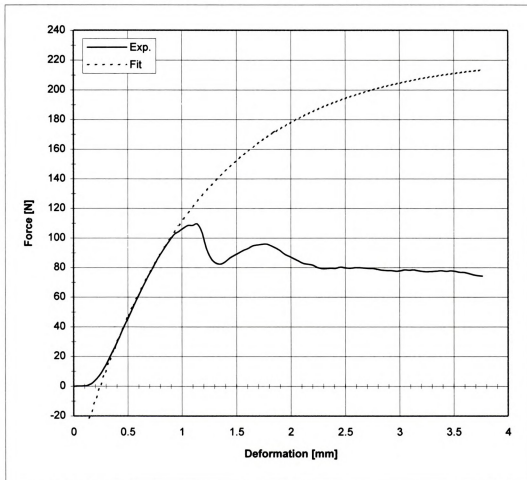


FIGURE C34 - Compression test and curve fit for Y34_03

**COMPRESSION TEST   :Maxwell Model**

| | | |
|---|---|---|
| **Elasticity** | **5.92E+08** | [Pa] |
| **Viscosity** | **1.62E+08** | [Pa*s] |
| **Yield stress** | **288335** | [Pa] |
| Velocity | 0.00423 | [m/s] |
| Contact area | 0.000314 | [m^2] |
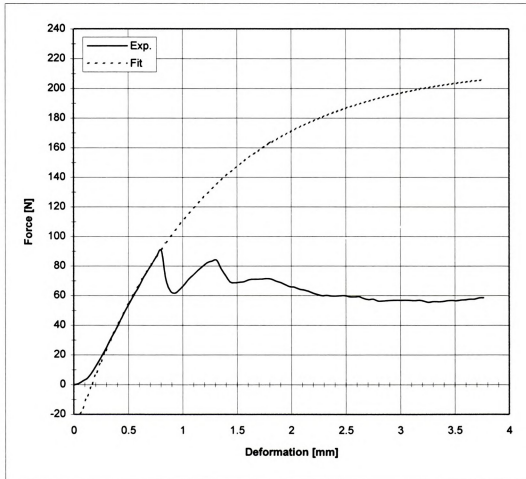


FIGURE C35 - Compression test and curve fit for Y35_03

**COMPRESSION TEST   :Maxwell Model**

| | | |
|---|---|---|
| **Elasticity** | **4.92E+08** | [Pa] |
| **Viscosity** | **7.24E+08** | [Pa*s] |
| **Yield stress** | **437958** | [Pa] |
| | | |
| Velocity | 0.00423 | [m/s] |
| Contact area | 0.000314 | [m^2] |
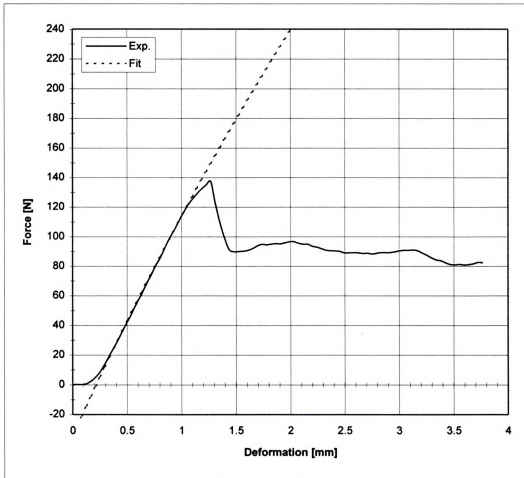


FIGURE C36 - Compression test and curve fit for Y36_03

**COMPRESSION TEST   :Maxwell Model**

| | | |
|---|---|---|
| **Elasticity** | **4.17E+08** | [Pa] |
| **Viscosity** | **6.04E+08** | [Pa*s] |
| **Yield stress** | **396105** | [Pa] |
| | | |
| Velocity | 0.00423 | [m/s] |
| Contact area | 0.000314 | [m^2] |
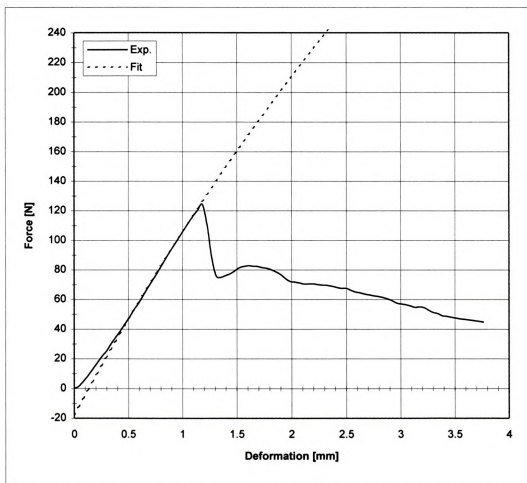


FIGURE C37 - Compression test and curve fit for Y37_03

**COMPRESSION TEST   :Maxwell Model**

| | | |
|---|---|---|
| **Elasticity** | **5.09E+08** [Pa] | |
| **Viscosity** | **4.36E+08** [Pa*s] | |
| **Yield stress** | **421764** [Pa] | |
| Velocity | 0.00423 [m/s] | |
| Contact area | 0.000314 [m^2] | |
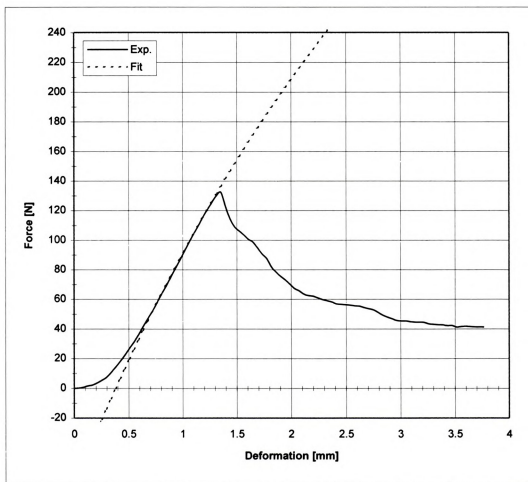


FIGURE C38 - Compression test and curve fit for Y38_03

**COMPRESSION TEST   :Maxwell Model**

| | | |
|---|---|---|
| **Elasticity** | **5.06E+08** | [Pa] |
| **Viscosity** | **2.56E+10** | [Pa*s] |
| **Yield stress** | **513378** | [Pa] |
| | | |
| Velocity | 0.00423 | [m/s] |
| Contact area | 0.000314 | [m^2] |
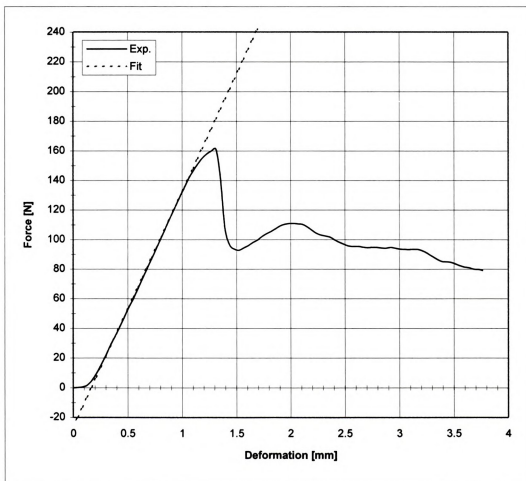


FIGURE C39 - Compression test and curve fit for Y39_03

## COMPRESSION TEST   :Maxwell Model

| | | |
|---|---|---|
| **Elasticity** | **5.56E+08** | [Pa] |
| **Viscosity** | **4.68E+08** | [Pa*s] |
| **Yield stress** | **426326** | [Pa] |
| | | |
| Velocity | 0.00423 | [m/s] |
| Contact area | 0.000314 | [m^2] |
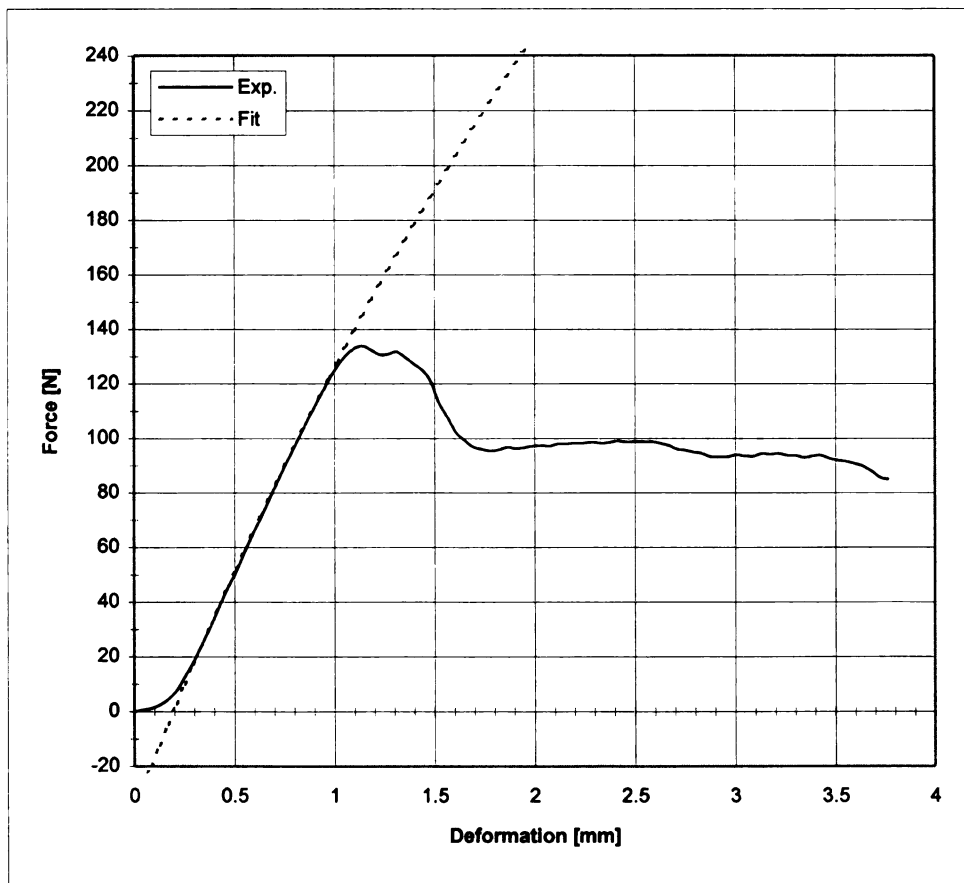


FIGURE C40 - Compression test and curve fit for Y40_03

**COMPRESSION TEST   :Maxwell Model**

| | |
|---|---|
| **Elasticity** | **3.62E+08** [Pa] |
| **Viscosity** | **4.42E+08** [Pa*s] |
| **Yield stress** | **331139** [Pa] |

| | |
|---|---|
| Velocity | 0.00423 [m/s] |
| Contact area | 0.000314 [m^2] |
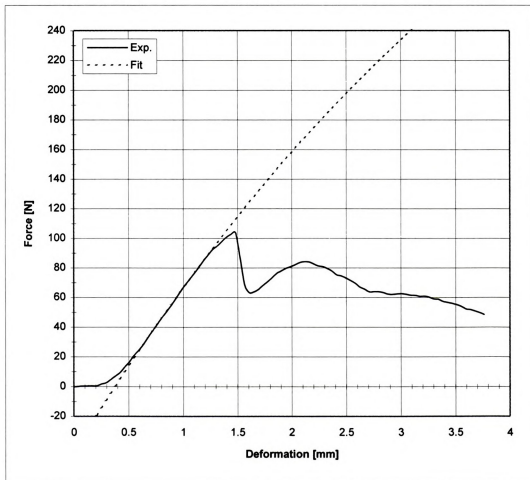


FIGURE C41 - Compression test and curve fit for Y41_03

## COMPRESSION TEST :Maxwell Model

| | | |
|---|---|---|
| **Elasticity** | **4.65E+08** | [Pa] |
| **Viscosity** | **2.38E+08** | [Pa*s] |
| **Yield stress** | **306164** | [Pa] |
| Velocity | 0.00423 | [m/s] |
| Contact area | 0.000314 | [m^2] |
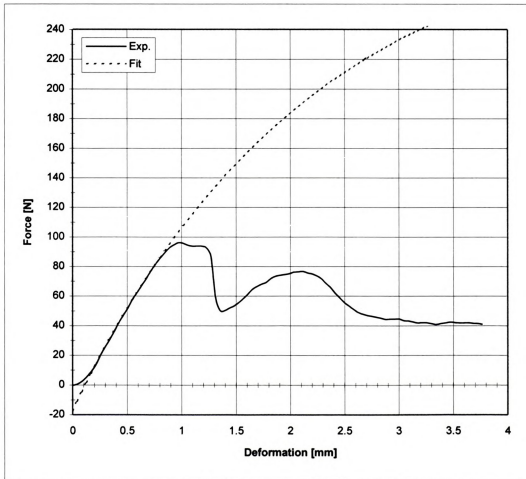


FIGURE C42 - Compression test and curve fit for Y42_03

**COMPRESSION TEST   :Maxwell Model**

| | | |
|---|---|---|
| **Elasticity** | **3.96E+08** | [Pa] |
| **Viscosity** | **2.69E+08** | [Pa*s] |
| **Yield stress** | **300994** | [Pa] |
| | | |
| Velocity | 0.00423 | [m/s] |
| Contact area | 0.000314 | [m^2] |
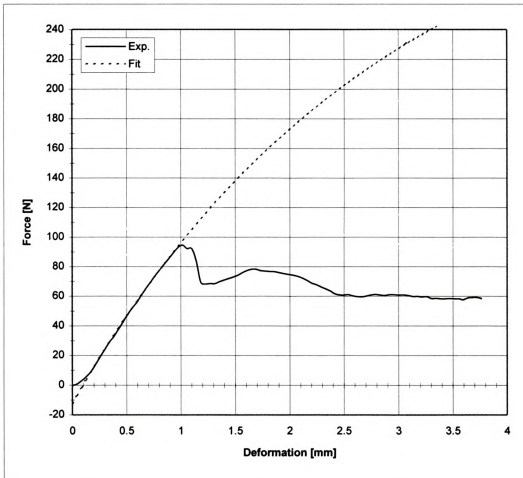


FIGURE C43 - Compression test and curve fit for Y43_03

**COMPRESSION TEST   :Maxwell Model**

| | | |
|---|---|---|
| **Elasticity** | **5.53E+08** | [Pa] |
| **Viscosity** | **1.44E+08** | [Pa*s] |
| **Yield stress** | **313349** | [Pa] |

| | | |
|---|---|---|
| Velocity | 0.00423 | [m/s] |
| Contact area | 0.000314 | [m^2] |
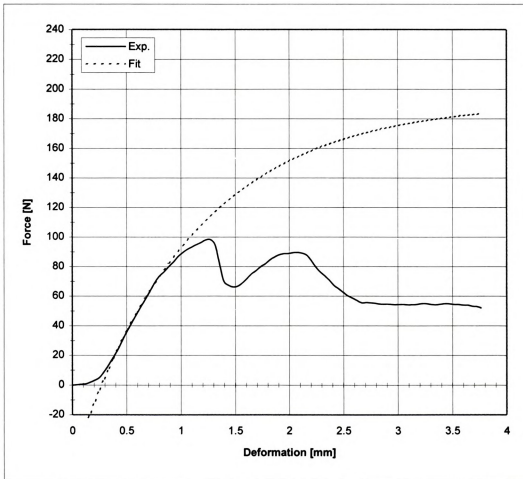


FIGURE C44 - Compression test and curve fit for Y44_03

**COMPRESSION TEST   :Maxwell Model**

| | | |
|---|---|---|
| **Elasticity** | **3.85E+08** | [Pa] |
| **Viscosity** | **2.09E+08** | [Pa*s] |
| **Yield stress** | **313121** | [Pa] |
| | | |
| Velocity | 0.00423 | [m/s] |
| Contact area | 0.000314 | [m^2] |
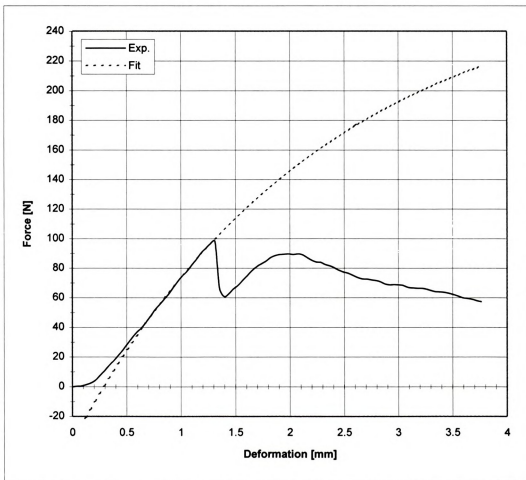


FIGURE C45 - Compression test and curve fit for Y45_03

**APPENDIX D**

# APPENDIX D

## Force-Deformation Plots of Shear Test

**SHEAR TEST**

|  |  |  |
|---|---|---|
| Thickness | 0.00218 [m] |  |
| Sample area | 0.00012 [m^2] |  |
| Velocity | 0.004233 [m/s] |  |
| *Yield stress* | 114515.0 [Pa] |  |

| MT Dia. | 0.011 [m] |
|---|---|
| MT thick | 0.0002 [m] |
| MT Area | 6.91E-06 [m^2] |

*Predicted:*

**Yield Strength**    **0.79** [N]



FIGURE D1 - Shear test result for Y01_04

**SHEAR TEST**

| | | MT Dia. | 0.011 [m] |
|---|---|---|---|
| Thickness | 0.00241 [m] | MT thick | 0.0002 [m] |
| Sample area | 0.000132 [m^2] | MT Area | 6.91E-06 [m^2] |
| Velocity | 0.004233 [m/s] | | |
| *Yield stress* | 299244 [Pa] | ***Predicted:*** | |
| | | **Yield Strength** | **2.07** [N] |
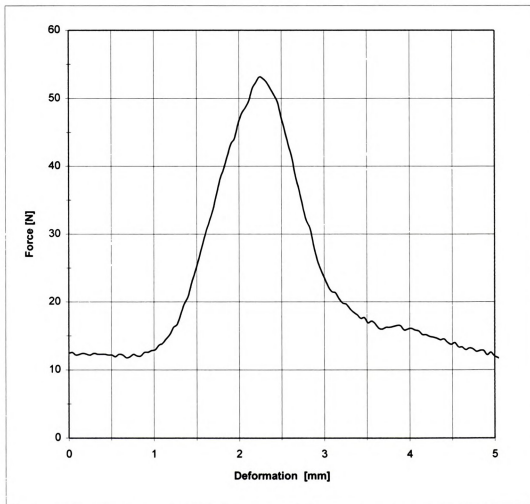


FIGURE D2 - Shear test result for Y02_04

**SHEAR TEST**

|  |  |  |  |
|---|---|---|---|
| | | MT Dia. | 0.011 [m] |
| Thickness | 0.00137 [m] | MT thick | 0.0002 [m] |
| Sample area | 7.53E-05 [m^2] | MT Area | 6.91E-06 [m^2] |
| Velocity | 0.004233 [m/s] | | |
| *Yield stress* | 185405 [Pa] | ***Predicted:*** | |
| | | **Yield Strengt** | **1.28 [N]** |



FIGURE D3 - Shear test result for Y03_04

**SHEAR TEST**

| | | | | |
|---|---|---|---|---|
| | | MT Dia. | 0.011 [m] |
| Thickness | 0.0021 [m] | MT thick | 0.0002 [m] |
| Sample area | 0.000115 [m^2] | → MT Area | 6.91E-06 [m^2] |
| Velocity | 0.004233 [m/s] | | |
| *Yield stress* | 248737 [Pa] | ***Predicted:*** | |
| | | **Yield Strength** | **1.72** [N] |



FIGURE D4 - Shear test result for Y04_04

**SHEAR TEST**

|  |  |  |
|---|---|---|
| Thickness | 0.00197 [m] | MT Dia. |
| Sample area | 0.000108 [m^2] | MT thick |
| Velocity | 0.004233 [m/s] | MT Area |
| *Yield stress* | 228580 [Pa] |  |

MT Dia.　　　0.011 [m]
MT thick　　0.0002 [m]
→ MT Area　6.91E-06 [m^2]

*Predicted:*
**Yield Strength**　**1.58** [N]



FIGURE D5 - Shear test result for Y05_04

**SHEAR TEST**

|  |  |  |  |
|---|---|---|---|
| | | MT Dia. | 0.011 [m] |
| Thickness | 0.00193 [m] | MT thick | 0.0002 [m] |
| Sample area | 0.000106 [m^2] | → MT Area | 6.91E-06 [m^2] |
| Velocity | 0.004233 [m/s] | | |
| *Yield stress* | 191686 [Pa] | *Predicted:* | |
| | | **Yield Strength** | **1.32** [N] |



FIGURE D6 - Shear test result for Y06_04

**SHEAR TEST**

| | | |
|---|---|---|
| | MT Dia. | 0.011 [m] |
| Thickness | 0.00188 [m] | MT thick | 0.0002 [m] |
| Sample area | 0.000103 [m^2] | MT Area | 6.91E-06 [m^2] |
| Velocity | 0.004233 [m/s] | | |
| *Yield stress* | 219752 [Pa] | *Predicted:* | |
| | | **Yield Strength** | **1.52 [N]** |
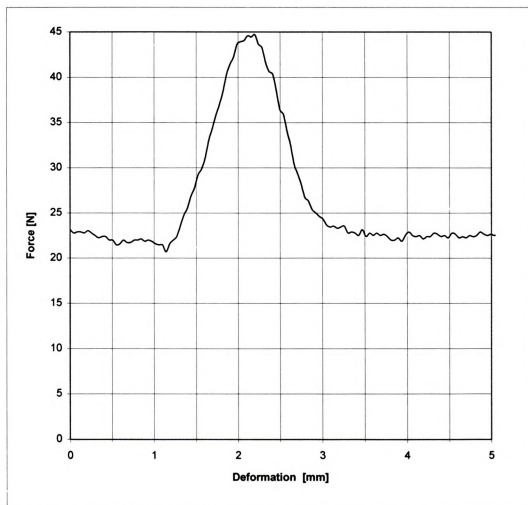


FIGURE D7 - Shear test result for Y07_04

## SHEAR TEST

| | | |
|---|---|---|
| | MT Dia. | 0.011 [m] |
| Thickness | 0.00194 [m] | MT thick | 0.0002 [m] |
| Sample area | 0.000107 [m^2] | MT Area | 6.91E-06 [m^2] |
| Velocity | 0.004233 [m/s] | | |
| *Yield stress* | 181504 [Pa] | **Predicted:** | |
| | | **Yield Strength** | **1.25** [N] |
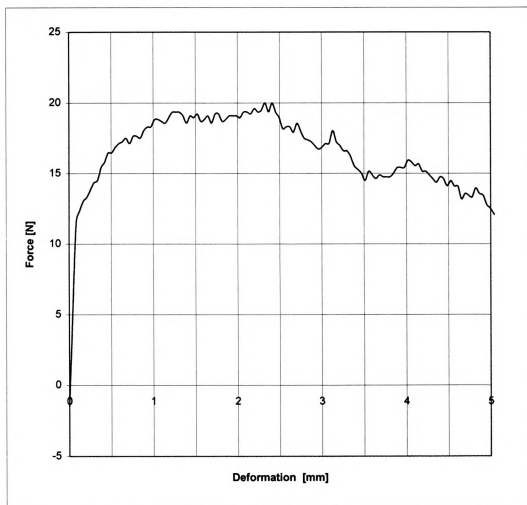


FIGURE D8 - Shear test result for Y08_04

## SHEAR TEST

| | | |
|---|---|---|
| | MT Dia. | 0.011 [m] |
| Thickness    0.00164 [m] | MT thick | 0.0002 [m] |
| Sample area  9.01E-05 [m^2] | MT Area | 6.91E-06 [m^2] |
| Velocity     0.004233 [m/s] | | |
| *Yield stress*    176118 [Pa] | *Predicted:* | |
| | **Yield Strength** | **1.22** [N] |
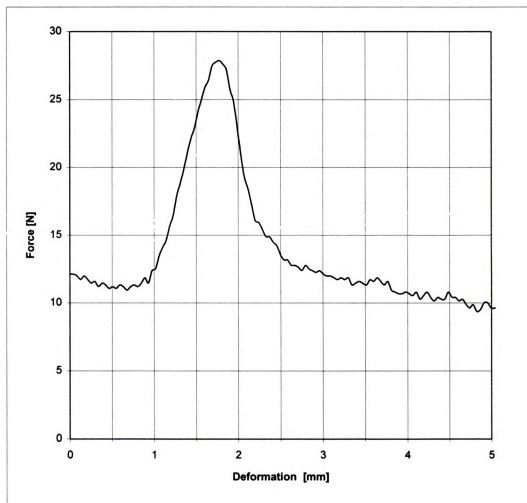


FIGURE D9 - Shear test result for Y09_04

**SHEAR TEST**

| | | |
|---|---|---|
| | MT Dia. | 0.011 [m] |
| Thickness | 0.0022 [m] | MT thick | 0.0002 [m] |
| Sample area | 0.000121 [m^2] | MT Area | 6.91E-06 [m^2] |
| Velocity | 0.004233 [m/s] | | |
| *Yield stress* | 248325 [Pa] | ***Predicted:*** | |
| | | **Yield Strength** | **1.72 [N]** |
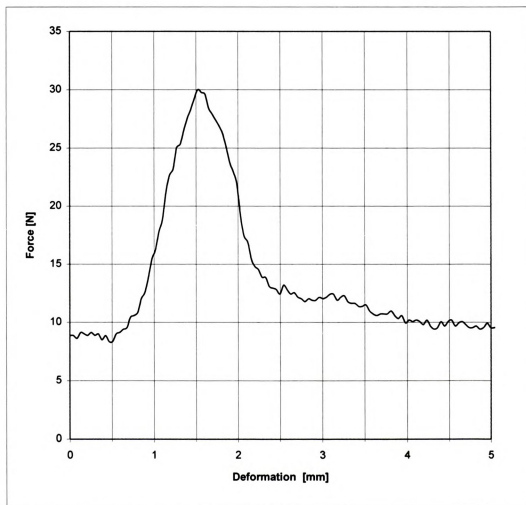


FIGURE D10 - Shear test result for Y10_04

**SHEAR TEST**

|  |  |  |  |
|---|---|---|---|
| | | MT Dia. | 0.011 [m] |
| Thickness | 0.00173 [m] | MT thick | 0.0002 [m] |
| Sample area | 9.51E-05 [m^2] | MT Area | 6.91E-06 [m^2] |
| Velocity | 0.004233 [m/s] | | |
| *Yield stress* | 312775 [Pa] | ***Predicted:*** | |
| | | **Yield Strength** | **2.16** [N] |
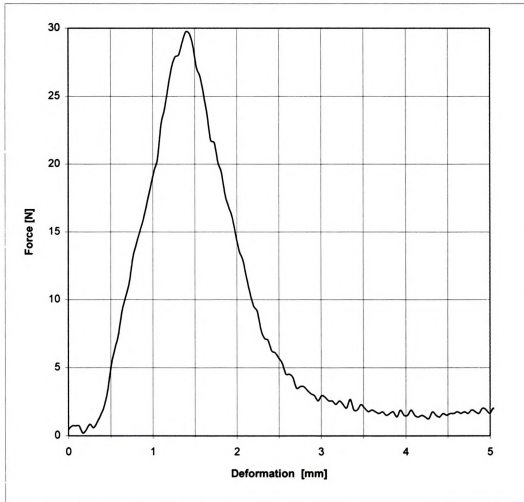


FIGURE D11 - Shear test result for Y11_04

**SHEAR TEST**

|  | | MT Dia. | 0.011 [m] |
|---|---|---|---|
| Thickness | 0.00256 [m] | MT thick | 0.0002 [m] |
| Sample area | 0.000141 [m^2] | MT Area | 6.91E-06 [m^2] |
| Velocity | 0.004233 [m/s] | | |
| *Yield stress* | 224689 [Pa] | ***Predicted:*** | |
| | | **Yield Strength** | **1.55** [N] |
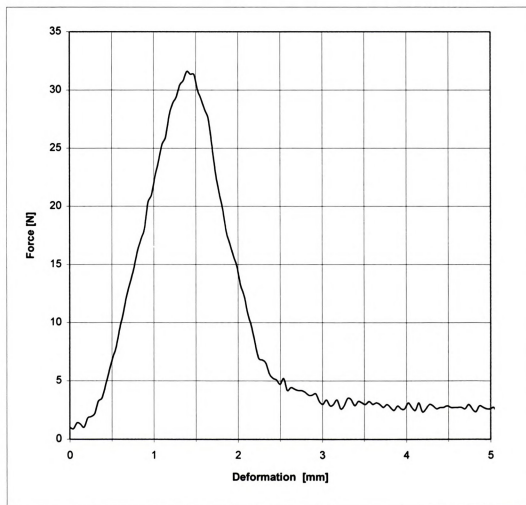


FIGURE D12 - Shear test result for Y12_04

**SHEAR TEST**

| | | | MT Dia. | 0.011 [m] |
| --- | --- | --- | --- | --- |
| Thickness | 0.00277 [m] | | MT thick | 0.0002 [m] |
| Sample area | 0.000152 [m^2] | ➤ | MT Area | 6.91E-06 [m^2] |
| Velocity | 0.004233 [m/s] | | | |
| *Yield stress* | 242944 [Pa] | | **Predicted:** | |
| | | | **Yield Strength** | **1.68** [N] |
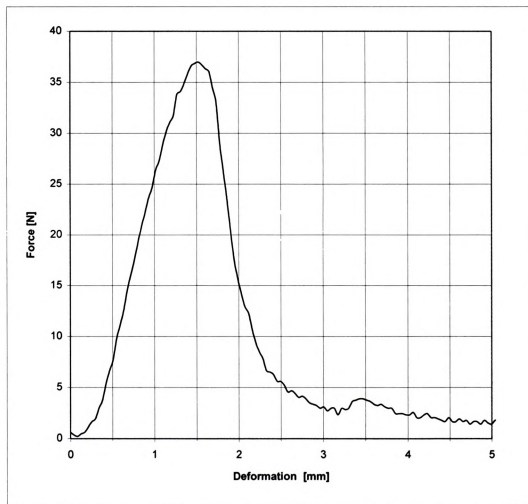


FIGURE D13 - Shear test result for Y13_04

**SHEAR TEST**

| | | MT Dia. | 0.011 [m] |
|---|---|---|---|
| Thickness | 0.0028 [m] | MT thick | 0.0002 [m] |
| Sample area | 0.000154 [m^2] | MT Area | 6.91E-06 [m^2] |
| Velocity | 0.004233 [m/s] | | |
| *Yield stress* | 201034 [Pa] | ***Predicted:*** | |
| | | **Yield Strength** | **1.39** [N] |
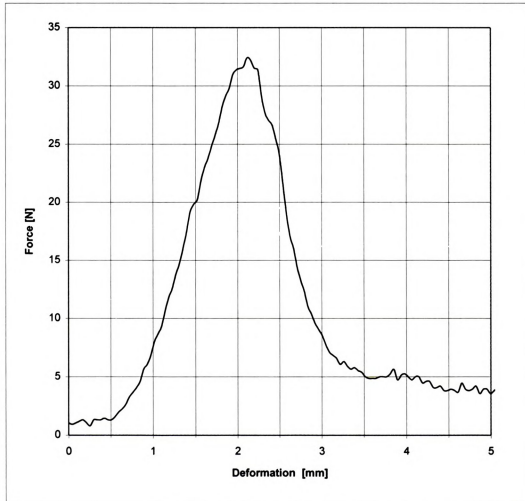


FIGURE D14 - Shear test result for Y14_04

**SHEAR TEST**

| | | | | |
|---|---|---|---|---|
| | | MT Dia. | 0.011 [m] | |
| Thickness | 0.0029 [m] | MT thick | 0.0002 [m] | |
| Sample area | 0.000159 [m^2] | MT Area | 6.91E-06 [m^2] | |
| Velocity | 0.004233 [m/s] | | | |
| *Yield stress* | 212239 [Pa] | ***Predicted:*** | | |
| | | **Yield Strength** | **1.47** [N] | |
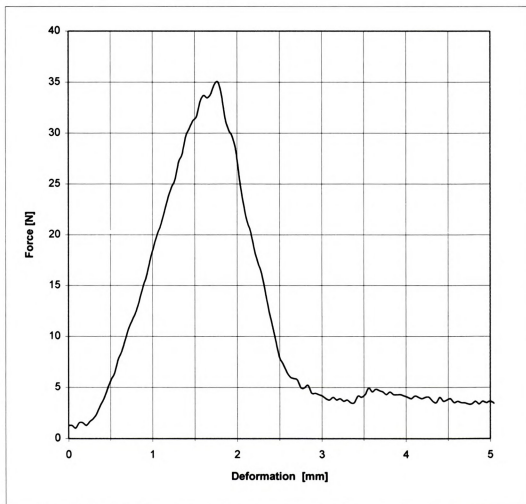


FIGURE D15 - Shear test result for Y15_04
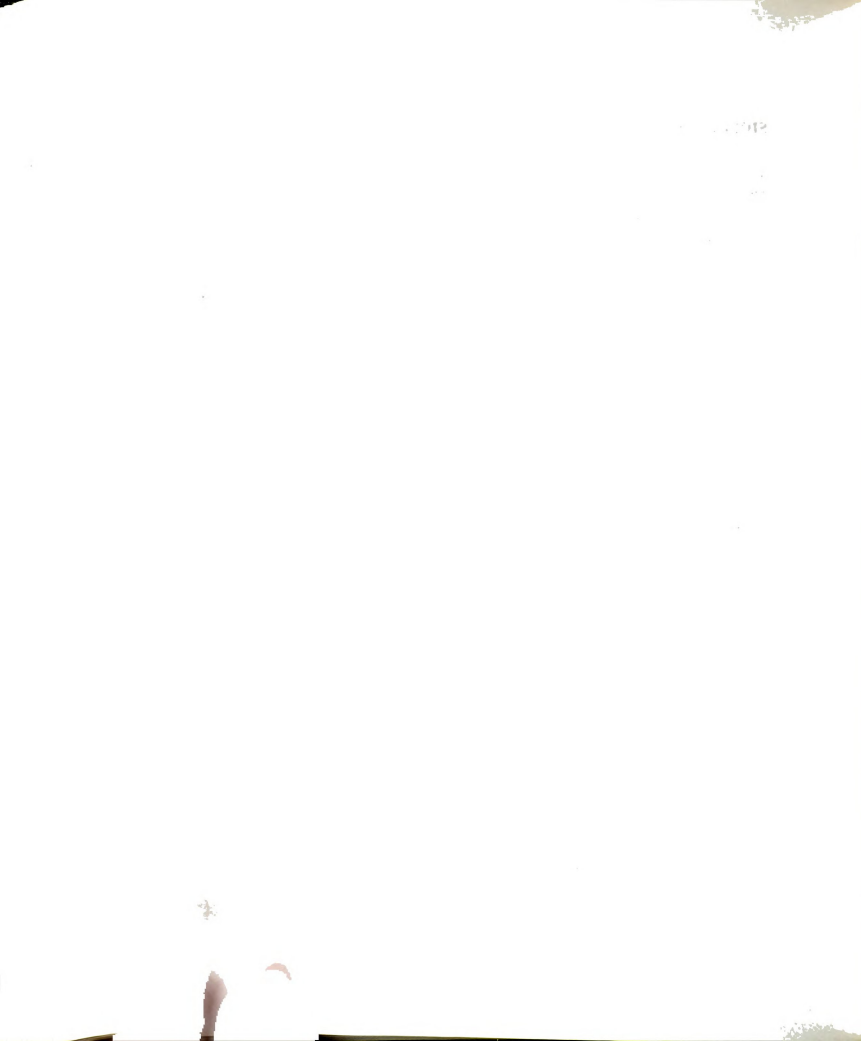
**SHEAR TEST**

| | | | | |
|---|---|---|---|---|
| | | MT Dia. | 0.011 [m] | |
| Thickness | 0.00268 [m] | MT thick | 0.0002 [m] | |
| Sample area | 0.000147 [m^2] | MT Area | 6.91E-06 [m^2] | |
| Velocity | 0.004233 [m/s] | | | |
| *Yield stress* | 300421 [Pa] | ***Predicted:*** | | |
| | | **Yield Strength** | **2.08** [N] | |
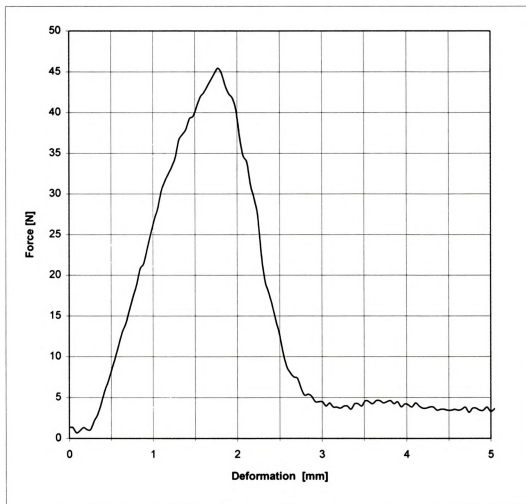


FIGURE D16 - Shear test result for Y16_04

**SHEAR TEST**

|  |  |  |  |
|---|---|---|---|
|  |  | MT Dia. | 0.011 [m] |
| Thickness | 0.0026 [m] | MT thick | 0.0002 [m] |
| Sample area | 0.000143 [m^2] | MT Area | 6.91E-06 [m^2] |
| Velocity | 0.004233 [m/s] |  |  |
| *Yield stress* | 189325 [Pa] | ***Predicted:*** |  |
|  |  | **Yield Strength** | **1.31** [N] |
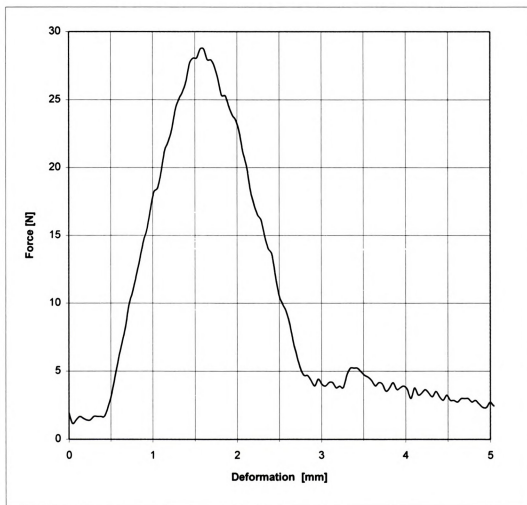


FIGURE D17 - Shear test result for Y17_04

**SHEAR TEST**

| | | MT Dia. | 0.011 [m] |
|---|---|---|---|
| Thickness | 0.00384 [m] | MT thick | 0.0002 [m] |
| Sample area | 0.000211 [m^2] | MT Area | 6.91E-06 [m^2] |
| Velocity | 0.004233 [m/s] | | |
| *Yield stress* | 235456 [Pa] | ***Predicted:*** | |
| | | **Yield Strength** | **1.63** [N] |
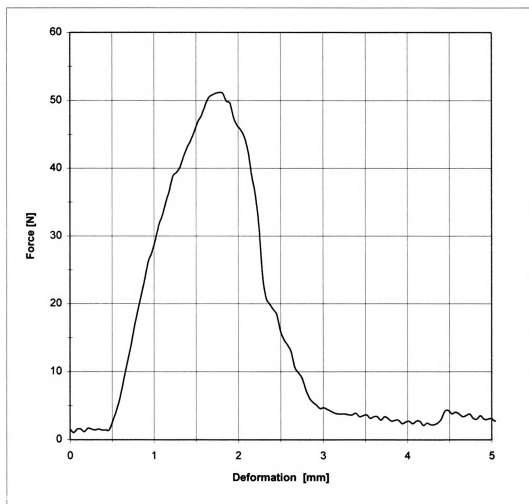


FIGURE D18 - Shear test result for Y18_04

## SHEAR TEST

| | | | | |
|---|---|---|---|---|
| | | MT Dia. | 0.011 [m] |
| Thickness | 0.003 [m] | MT thick | 0.0002 [m] |
| Sample area | 0.000165 [m^2] | MT Area | 6.91E-06 [m^2] |
| Velocity | 0.004233 [m/s] | | |
| *Yield stress* | 160527 [Pa] | **Predicted:** | |
| | | **Yield Strength** | **1.11** [N] |
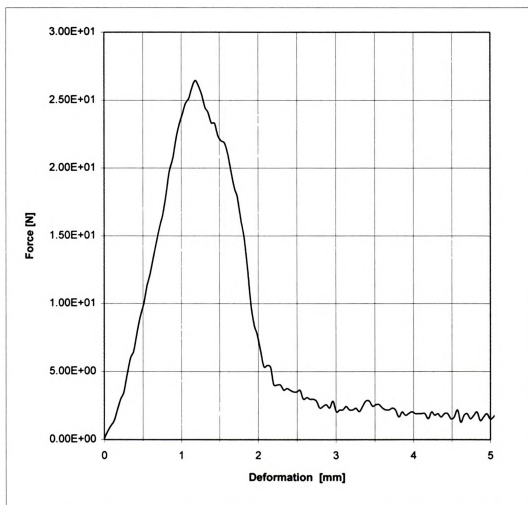


FIGURE D19 - Shear test result for Y19_04

**SHEAR TEST**

| | | MT Dia. | 0.011 [m] |
|---|---|---|---|
| Thickness | 0.00221 [m] | MT thick | 0.0002 [m] |
| Sample area | 0.000121 [m^2] | MT Area | 6.91E-06 [m^2] |
| Velocity | 0.004233 [m/s] | | |
| *Yield stress* | 288385 [Pa] | ***Predicted:*** | |
| | | **Yield Strength** | **1.99 [N]** |
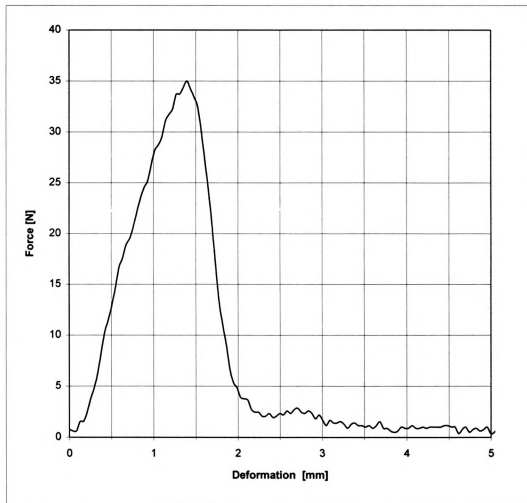


FIGURE D20 - Shear test result for Y20_04

## SHEAR TEST

| | | | |
|---|---|---|---|
| | | MT Dia. | 0.011 [m] |
| Thickness | 0.00306 [m] | MT thick | 0.0002 [m] |
| Sample area | 0.000168 [m^2] | MT Area | 6.91E-06 [m^2] |
| Velocity | 0.004233 [m/s] | | |
| *Yield stress* | 102475 [Pa] | ***Predicted:*** | |
| | | **Yield Strength** | **0.71** [N] |
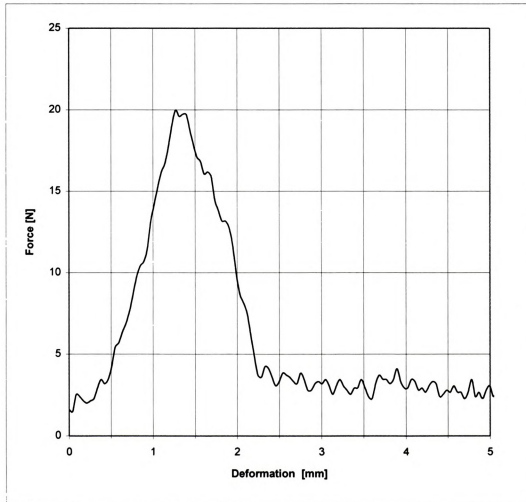


FIGURE D21 - Shear test result for Y21_04

**SHEAR TEST**

| | | | |
|---|---|---|---|
| | | MT Dia. | 0.011 [m] |
| Thickness | 0.00336 [m] | MT thick | 0.0002 [m] |
| Sample area | 0.000185 [m^2] | → MT Area | 6.91E-06 [m^2] |
| Velocity | 0.004233 [m/s] | | |
| *Yield stress* | 145849 [Pa] | ***Predicted:*** | |
| | | **Yield Strength** | **1.01** [N] |
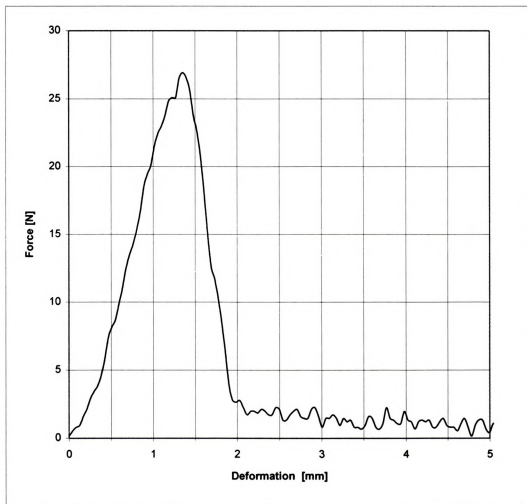


FIGURE D22 - Shear test result for Y22_04

**SHEAR TEST**

| | | | |
|---|---|---|---|
| | | MT Dia. | 0.011 [m] |
| Thickness | 0.00302 [m] | MT thick | 0.0002 [m] |
| Sample area | 0.000166 [m^2] | → MT Area | 6.91E-06 [m^2] |
| Velocity | 0.004233 [m/s] | | |
| *Yield stress* | 130190 [Pa] | ***Predicted:*** | |
| | | ***Yield Strength*** | **0.90** [N] |
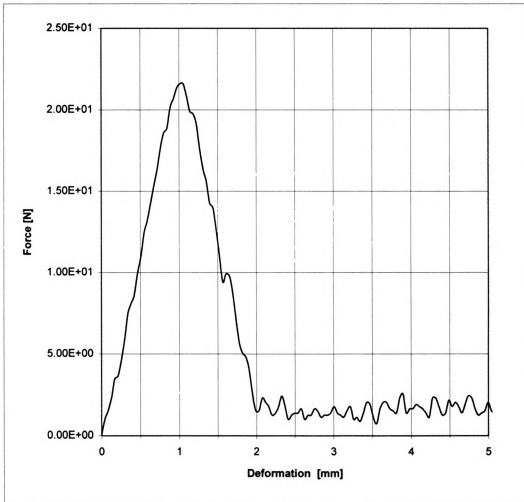


FIGURE D23 - Shear test result for Y23_04

## SHEAR TEST

| | | | | |
|---|---|---|---|---|
| | | MT Dia. | 0.011 [m] | |
| Thickness | 0.00292 [m] | MT thick | 0.0002 [m] | |
| Sample area | 0.00016 [m^2] | ➤ MT Area | 6.91E-06 [m^2] | |
| Velocity | 0.004233 [m/s] | | | |
| *Yield stress* | 89790 [Pa] | ***Predicted:*** | | |
| | | **Yield Strength** | **0.62 [N]** | |
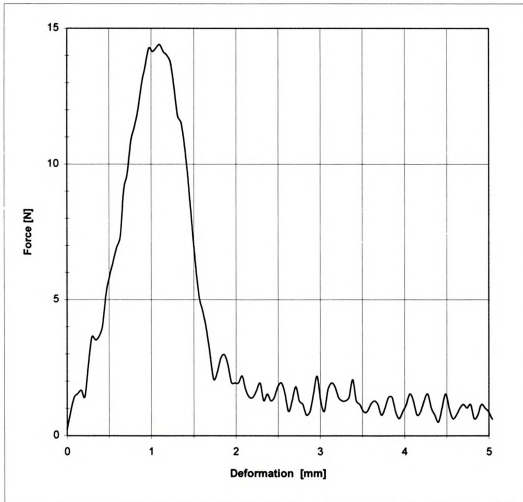


FIGURE D24 - Shear test result for Y24_04

**SHEAR TEST**

| | | | | |
|---|---|---|---|---|
| | | MT Dia. | 0.011 [m] | |
| Thickness | 0.00376 [m] | MT thick | 0.0002 [m] | |
| Sample area | 0.000207 [m^2] | MT Area | 6.91E-06 [m^2] | |
| Velocity | 0.004233 [m/s] | | | |
| *Yield stress* | 112771 [Pa] | ***Predicted:*** | | |
| | | **Yield Strength** | **0.78** [N] | |
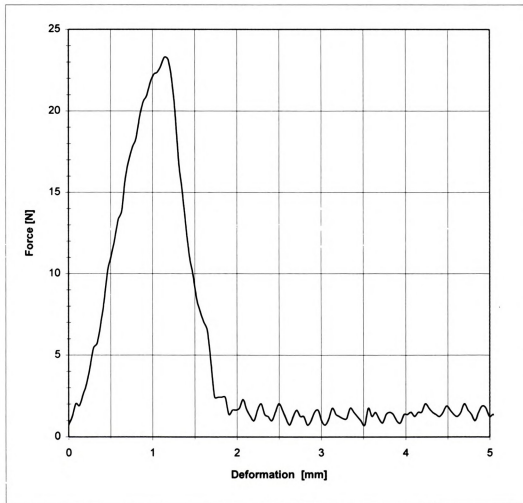


FIGURE D25 - Shear test result for Y25_04

**SHEAR TEST**

| | | MT Dia. | 0.011 [m] |
|---|---|---|---|
| Thickness | 0.00248 [m] | MT thick | 0.0002 [m] |
| Sample area | 0.000136 [m^2] | MT Area | 6.91E-06 [m^2] |
| Velocity | 0.004233 [m/s] | | |
| *Yield stress* | 211617 [Pa] | ***Predicted:*** | |
| | | **Yield Strength** | **1.46** [N] |
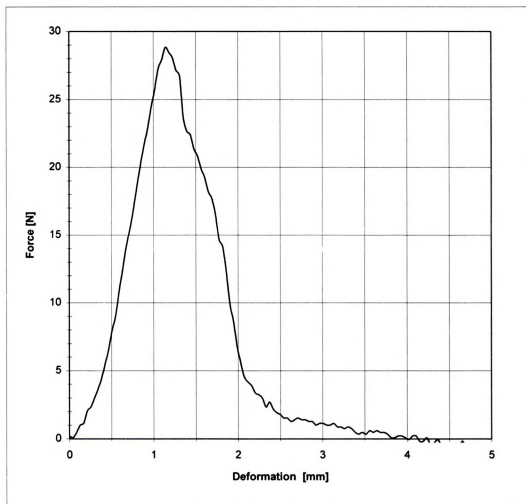


FIGURE D26 - Shear test result for Y26_04

**SHEAR TEST**

| | | MT Dia. | 0.011 [m] |
|---|---|---|---|
| Thickness | 0.00263 [m] | MT thick | 0.0002 [m] |
| Sample area | 0.000145 [m^2] | MT Area | 6.91E-06 [m^2] |
| Velocity | 0.004233 [m/s] | | |
| *Yield stress* | 293539 [Pa] | **Predicted:** | |
| | | **Yield Strength** | **2.03** [N] |
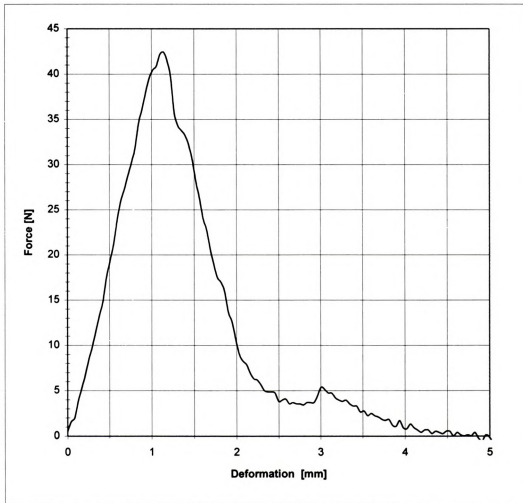


FIGURE D27 - Shear test result for Y27_04

## SHEAR TEST

| | | | | |
|---|---|---|---|---|
| | | MT Dia. | 0.011 [m] | |
| Thickness | 0.00263 [m] | MT thick | 0.0002 [m] | |
| Sample area | 0.000145 [m^2] | ➤ MT Area | 6.91E-06 [m^2] | |
| Velocity | 0.004233 [m/s] | | | |
| *Yield stress* | 200621 [Pa] | **Predicted:** | | |
| | | **Yield Strength** | **1.39** [N] | |
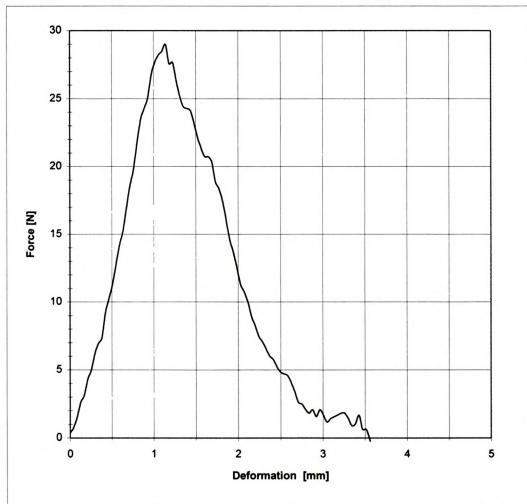


FIGURE D28 - Shear test result for Y28_04

## SHEAR TEST

| | | | | |
|---|---|---|---|---|
| | | MT Dia. | 0.011 [m] | |
| Thickness | 0.00251 [m] | MT thick | 0.0002 [m] | |
| Sample area | 0.000138 [m^2] | MT Area | 6.91E-06 [m^2] | |
| Velocity | 0.004233 [m/s] | | | |
| *Yield stress* | 318823 [Pa] | **Predicted:** | | |
| | | **Yield Strength** | **2.20** [N] | |
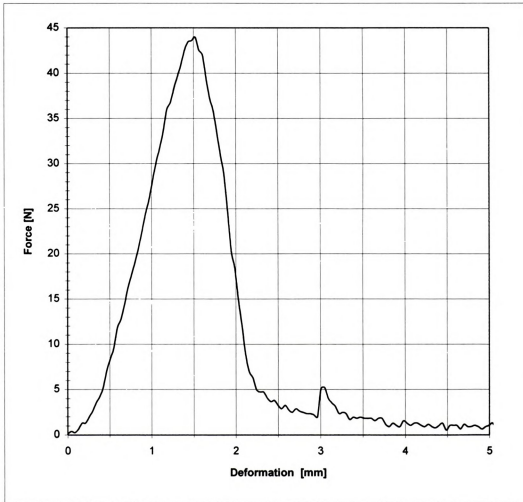


FIGURE D29 - Shear test result for Y29_04

**SHEAR TEST**

| | | MT Dia. | 0.011 [m] |
|---|---|---|---|
| Thickness | 0.0024 [m] | MT thick | 0.0002 [m] |
| Sample area | 0.000132 [m^2] | MT Area | 6.91E-06 [m^2] |
| Velocity | 0.004233 [m/s] | | |
| *Yield stress* | 293341 [Pa] | *Predicted:* | |
| | | **Yield Strength** | **2.03** [N] |
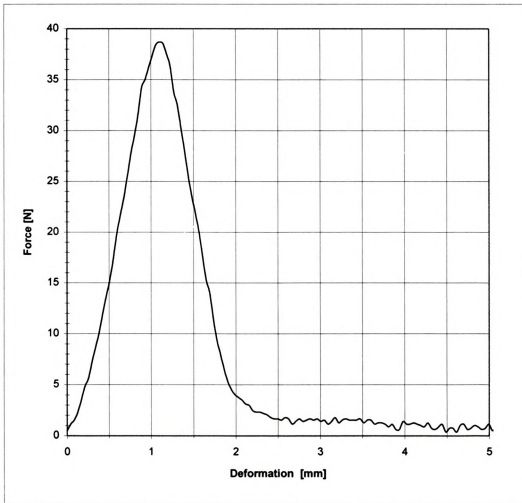


FIGURE D30 - Shear test result for Y30_04
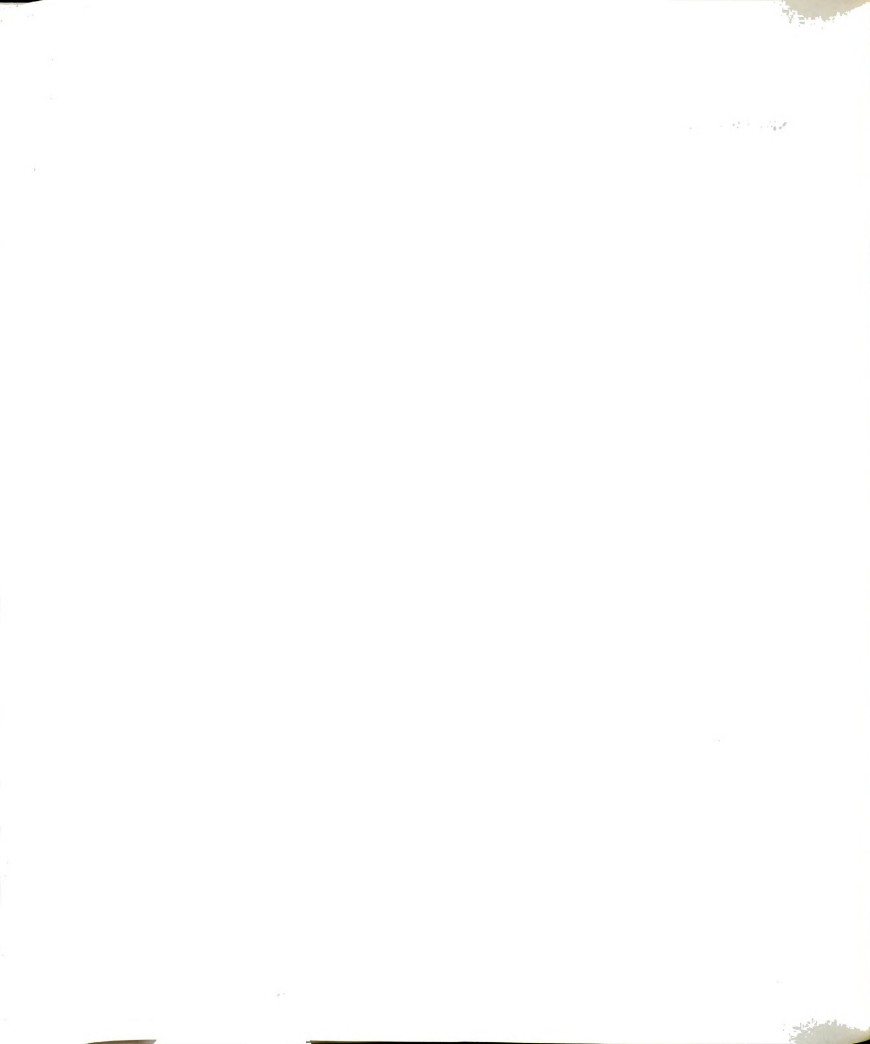
**SHEAR TEST**

| | | | |
|---|---|---|---|
| | | MT Dia. | 0.011 [m] |
| Thickness | 0.00316 [m] | MT thick | 0.0002 [m] |
| Sample area | 0.000174 [m^2] | MT Area | 6.91E-06 [m^2] |
| Velocity | 0.004233 [m/s] | | |
| *Yield stress* | 177696 [Pa] | *Predicted:* | |
| | | **Yield Strength** | **1.23** [N] |
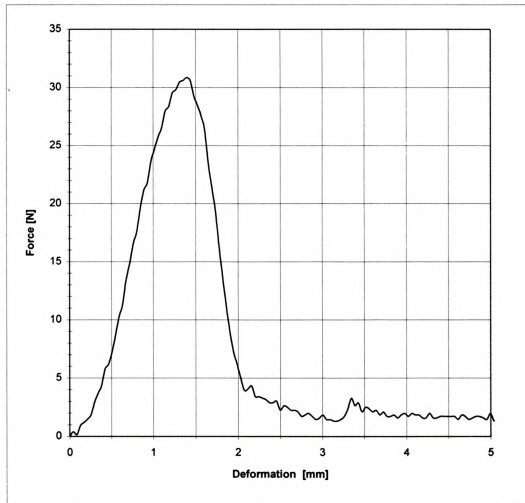


FIGURE D31 - Shear test result for Y31_04

**SHEAR TEST**

|  |  |  |  |
|---|---|---|---|
| Thickness | 0.00318 [m] | MT Dia. | 0.011 [m] |
|  |  | MT thick | 0.0002 [m] |
| Sample area | 0.000175 [m^2] | → MT Area | 6.91E-06 [m^2] |
| Velocity | 0.004233 [m/s] |  |  |
| *Yield stress* | 120155 [Pa] | ***Predicted:*** |  |
|  |  | **Yield Strength** | **0.83** [N] |
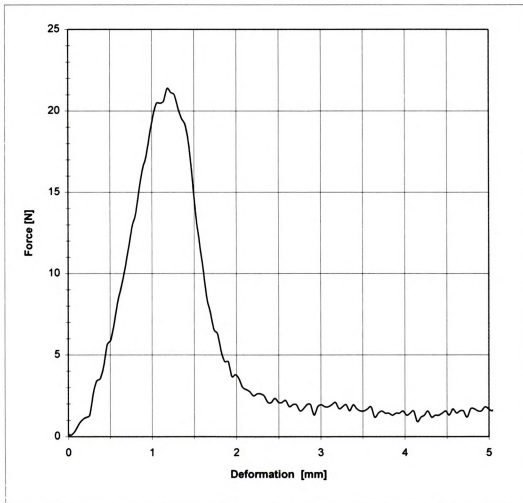


FIGURE D32 - Shear test result for Y32_04

## SHEAR TEST

| | | | | |
|---|---|---|---|---|
| Thickness | 0.00285 [m] | | MT Dia. | 0.011 [m] |
| Sample area | 0.000157 [m^2] | → | MT thick | 0.0002 [m] |
| Velocity | 0.004233 [m/s] | | MT Area | 6.91E-06 [m^2] |
| *Yield stress* | 129266 [Pa] | | *Predicted:* | |
| | | | **Yield Strength** | **0.89** [N] |
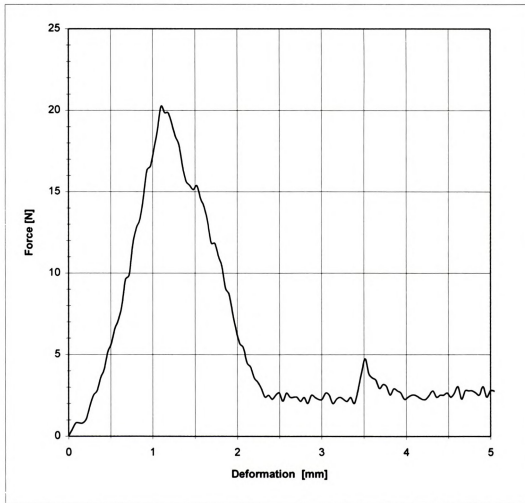


FIGURE D33 - Shear test result for Y33_04

**SHEAR TEST**
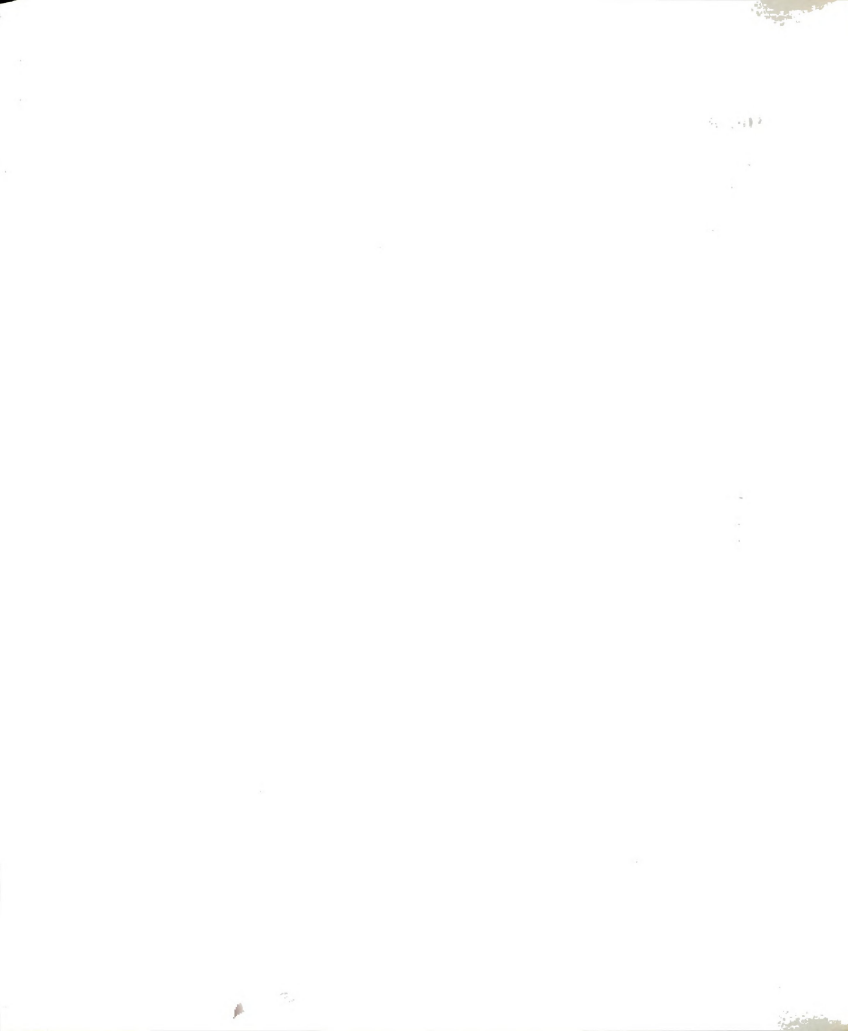
|  |  |  |  |
|---|---|---|---|
| | | MT Dia. | 0.011 [m] |
| Thickness | 0.00229 [m] | MT thick | 0.0002 [m] |
| Sample area | 0.000126 [m^2] | MT Area | 6.91E-06 [m^2] |
| Velocity | 0.004233 [m/s] | | |
| *Yield stress* | 111836 [Pa] | ***Predicted:*** | |
| | | **Yield Strength** | **0.77** [N] |
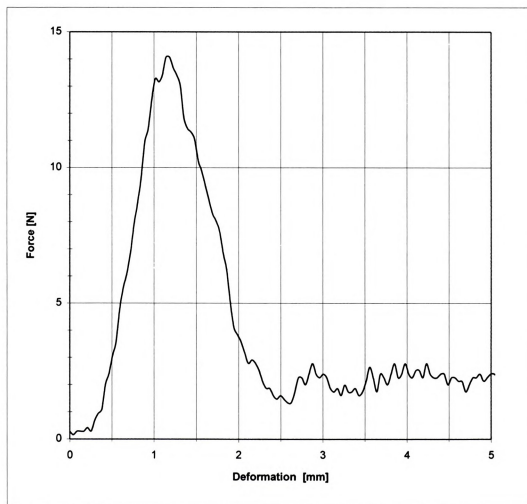


FIGURE D34 - Shear test result for Y34_04

**SHEAR TEST**

|  |  |  |  |
|---|---|---|---|
| | | MT Dia. | 0.011 [m] |
| Thickness | 0.00202 [m] | MT thick | 0.0002 [m] |
| Sample area | 0.000111 [m^2] | MT Area | 6.91E-06 [m^2] |
| Velocity | 0.004233 [m/s] | | |
| *Yield stress* | 132484 [Pa] | ***Predicted:*** | |
| | | **Yield Strength** | **0.92 [N]** |
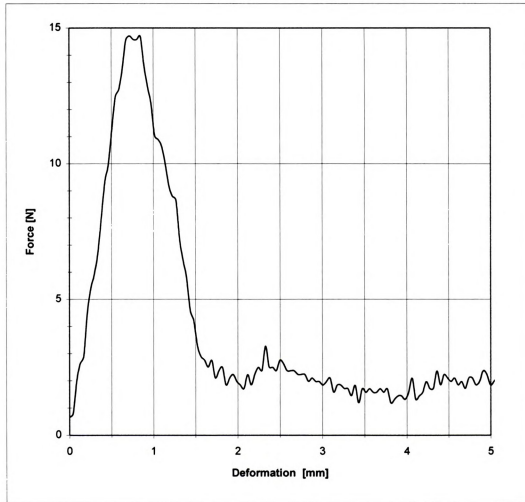


FIGURE D35 - Shear test result for Y35_04

**SHEAR TEST**

| | | |
|---|---|---|
| | | MT Dia. | 0.011 [m] |
| Thickness | 0.0024 [m] | MT thick | 0.0002 [m] |
| Sample area | 0.000132 [m^2] | ➤ MT Area | 6.91E-06 [m^2] |
| Velocity | 0.004233 [m/s] | | |
| *Yield stress* | 155948 [Pa] | ***Predicted:*** | |
| | | **Yield Strength** | **1.08** [N] |
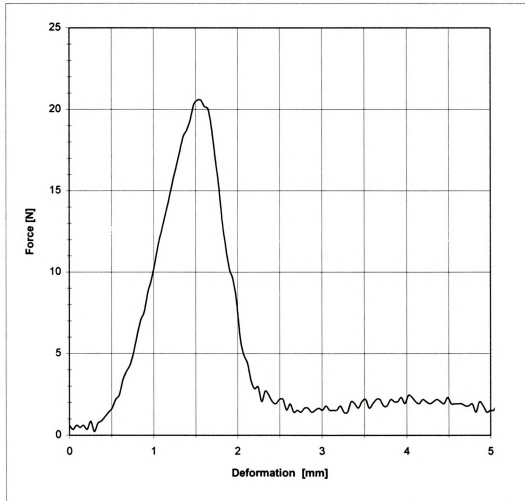


FIGURE D36 - Shear test result for Y36_04

**SHEAR TEST**

| | | | |
|---|---|---|---|
| | | MT Dia. | 0.011 [m] |
| Thickness | 0.0024 [m] | MT thick | 0.0002 [m] |
| Sample area | 0.000132 [m^2] | MT Area | 6.91E-06 [m^2] |
| Velocity | 0.004233 [m/s] | | |
| *Yield stress* | 159658 [Pa] | ***Predicted:*** | |
| | | **Yield Strength** | **1.10** [N] |
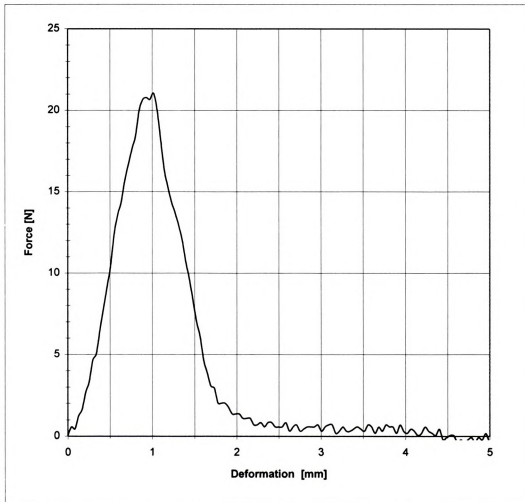


FIGURE D37 - Shear test result for Y37_04

**SHEAR TEST**

|  |  |
|---|---|
| Thickness | 0.00223 [m] |
| Sample area | 0.000123 [m^2] |
| Velocity | 0.004233 [m/s] |
| *Yield stress* | 146990 [Pa] |

|  |  |
|---|---|
| MT Dia. | 0.011 [m] |
| MT thick | 0.0002 [m] |
| MT Area | 6.91E-06 [m^2] |

***Predicted:***
**Yield Strength**   **1.02** [N]
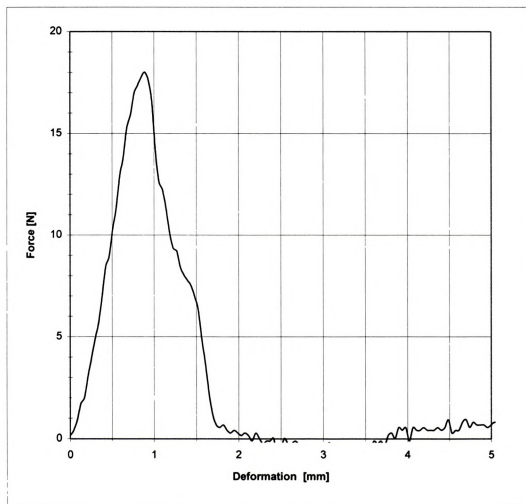


FIGURE D38 - Shear test result for Y38_04

**SHEAR TEST**

| | | | | |
|---|---|---|---|---|
| | | MT Dia. | 0.011 [m] | |
| Thickness | 0.0021 [m] | MT thick | 0.0002 [m] | |
| Sample area | 0.000115 [m^2] | MT Area | 6.91E-06 [m^2] | |
| Velocity | 0.004233 [m/s] | | | |
| *Yield stress* | 165813 [Pa] | *Predicted:* | | |
| | | **Yield Strength** | **1.15** [N] | |
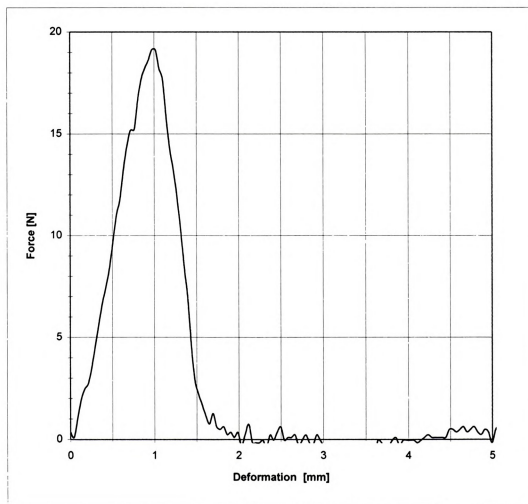


FIGURE D39 - Shear test result for Y39_04

204

**SHEER TEST**

|  | MT Dia. | 0.011 [m] |
|---|---|---|
| Thickness 0.00154 [m] | MT thick | 0.0002 [m] |
| Sample area 8.46E-05 [m^2] | MT Area | 6.91E-06 [m^2] |
| Velocity 0.004233 [m/s] | | |
| *Yield stress* 168136 [Pa] | ***Predicted:*** | |
| | **Yield Strength** | **1.16** [N] |
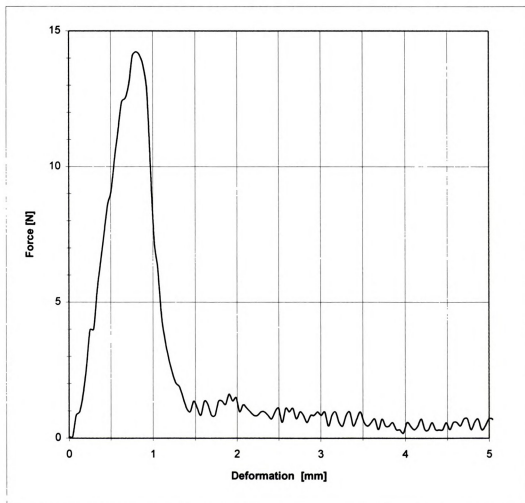


FIGURE D40 - Shear test result for Y40_04

**SHEAR TEST**

|  |  |  |  |
|---|---|---|---|
| | | MT Dia. | 0.011 [m] |
| Thickness | 0.00214 [m] | MT thick | 0.0002 [m] |
| Sample area | 0.000118 [m^2] | MT Area | 6.91E-06 [m^2] |
| Velocity | 0.004233 [m/s] | | |
| *Yield stress* | 146777 [Pa] | *Predicted:* | |
| | | **Yield Strength** | **1.01** [N] |
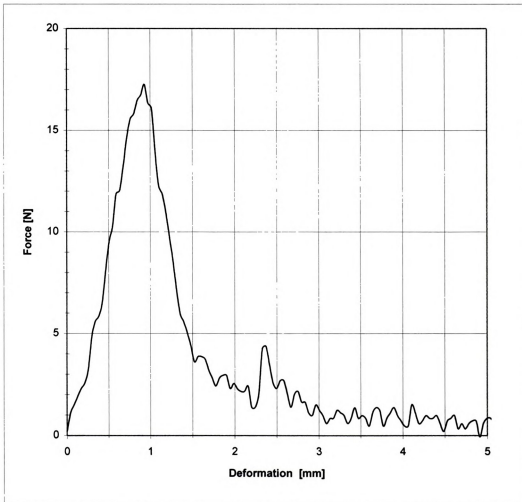


FIGURE D41 - Shear test result for Y41_04
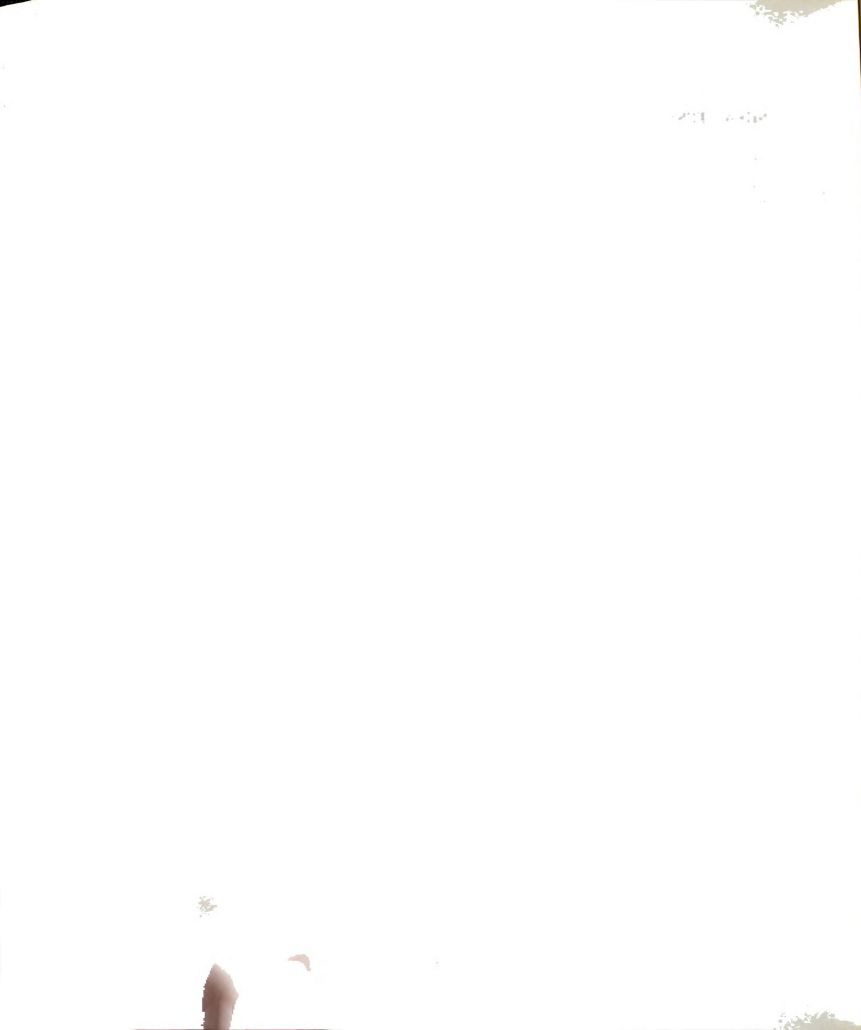
**SHEAR TEST**

| | | MT Dia. | 0.011 [m] |
|---|---|---|---|
| Thickness | 0.00237 [m] | MT thick | 0.0002 [m] |
| Sample area | 0.00013 [m^2] | → MT Area | 6.91E-06 [m^2] |
| Velocity | 0.004233 [m/s] | | |
| *Yield stress* | 116952 [Pa] | ***Predicted:*** | |
| | | **Yield Strength** | **0.81** [N] |
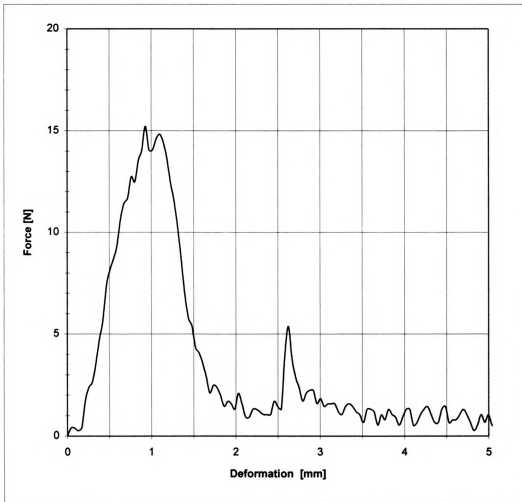


FIGURE D42 - Shear test result for Y42_04

## SHEAR TEST

| | | |
|---|---|---|
| | MT Dia. | 0.011 [m] |
| Thickness | 0.00262 [m] | MT thick | 0.0002 [m] |
| Sample area | 0.000144 [m^2] | MT Area | 6.91E-06 [m^2] |
| Velocity | 0.004233 [m/s] | | |
| *Yield stress* | 134993 [Pa] | ***Predicted:*** | |
| | | **Yield Strength** | **0.93** [N] |
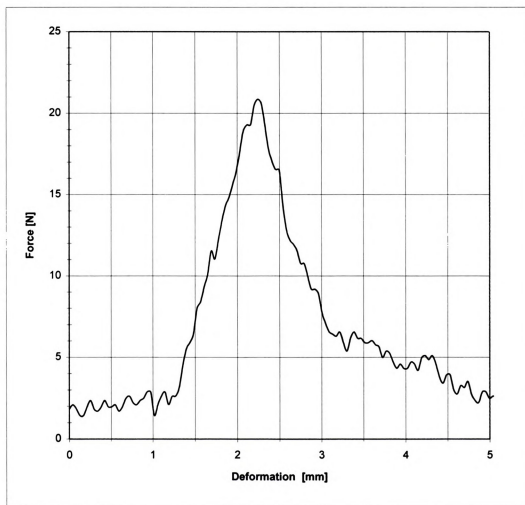


FIGURE D43 - Shear test result for Y43_04

**SHEAR TEST**

| | | | | | |
|---|---|---|---|---|---|
| | | | MT Dia. | 0.011 [m] | |
| Thickness | 0.00256 [m] | | MT thick | 0.0002 [m] | |
| Sample area | 0.000141 [m^2] | | MT Area | 6.91E-06 [m^2] | |
| Velocity | 0.004233 [m/s] | | | | |
| *Yield stress* | 123545 [Pa] | | *Predicted:* | | |
| | | | **Yield Strength** | **0.85** [N] | |
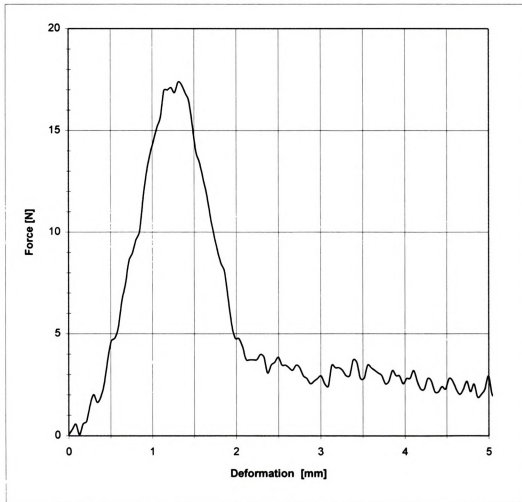


FIGURE D44 - Shear test result for Y44_04

**SHEAR TEST**

|  |  | MT Dia. | 0.011 [m] |
|---|---|---|---|
| Thickness | 0.00229 [m] | MT thick | 0.0002 [m] |
| Sample area | 0.000126 [m^2] | MT Area | 6.91E-06 [m^2] |
| Velocity | 0.004233 [m/s] | | |
| *Yield stress* | 130808 [Pa] | ***Predicted:*** | |
| | | **Yield Strength** | **0.90** [N] |
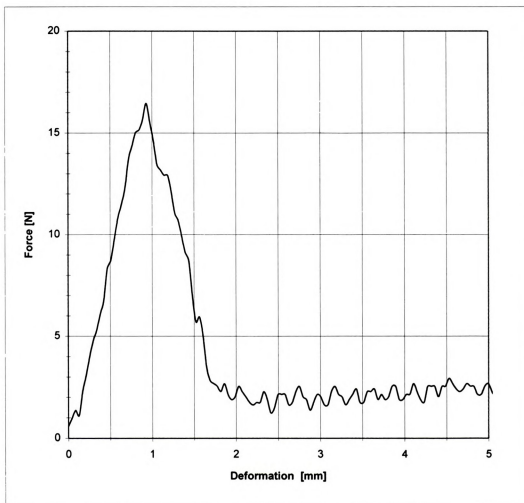


FIGURE D45 - Shear test result for Y45_04

**APPENDIX E**

# APPENDIX E

## Stress-Strain Plots of Tensile Test

211

**TENSILE TEST**

Sample   Thickness   0.00206 [m]          **Elasticity  2219400 [Pa]**
         Width       0.009 [m]
         Area        1.9E-05 [m^2]
         Length      0.02 [m]
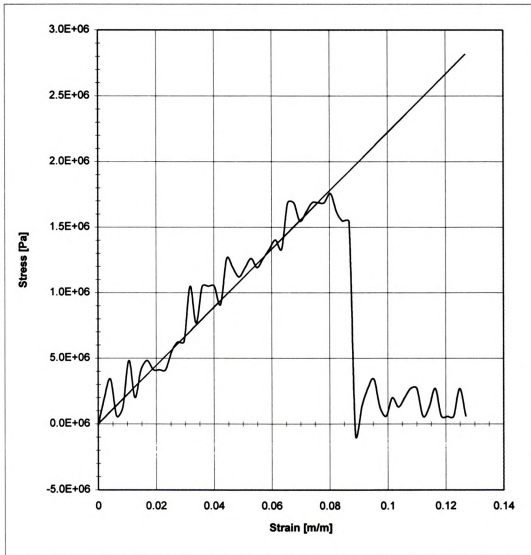


FIGURE E1 - Tensile test result for Y01_05

## TENSILE TEST

Sample    Thickness    0.00208 [m]        **Elasticity   2893126 [Pa]**
           Width           0.009 [m]
           Area          1.9E-05 [m^2]
           Length         0.02 [m]
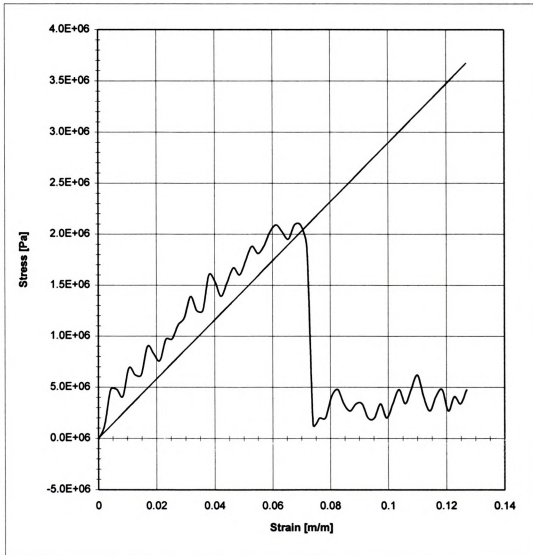


FIGURE E2 - Tensile test result for Y02_05

# TENSILE TEST

| Sample | Thickness | 0.00191 [m] | | Elasticity 2661102 [Pa] |
|--------|-----------|-------------|---|-------------------------|
| | Width | 0.009 [m] | | |
| | Area | 1.7E-05 [m^2] | | |
| | Length | 0.02 [m] | | |
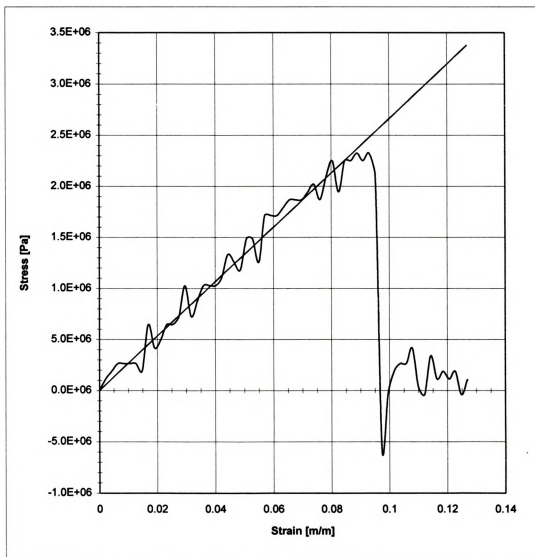


FIGURE E3 - Tensile test result for Y03_05

# TENSILE TEST

Sample    Thickness    0.00261 [m]        **Elasticity  2019565 [Pa]**
         Width          0.009 [m]
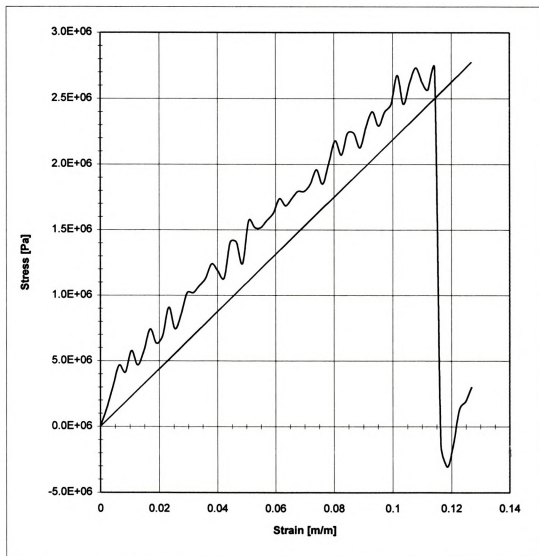         Area          2.3E-05 [m^2]
         Length        0.02 [m]
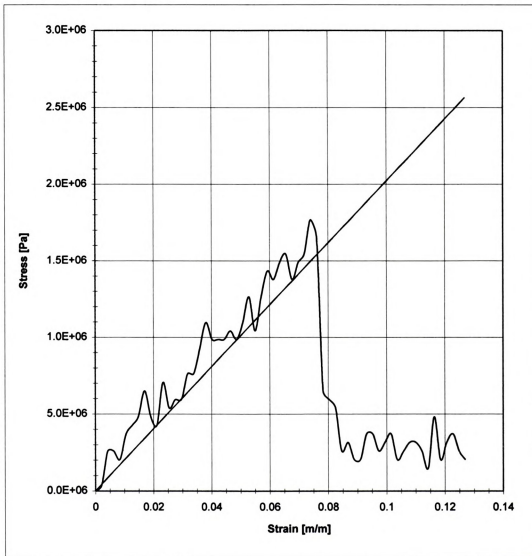


FIGURE E4 - Tensile test result for Y04_05

## TENSILE TEST

Sample  Thickness  0.00178 [m]                    **Elasticity  2603817 [Pa]**
        Width         0.009 [m]
        Area        1.6E-05 [m^2]
        Length        0.02 [m]
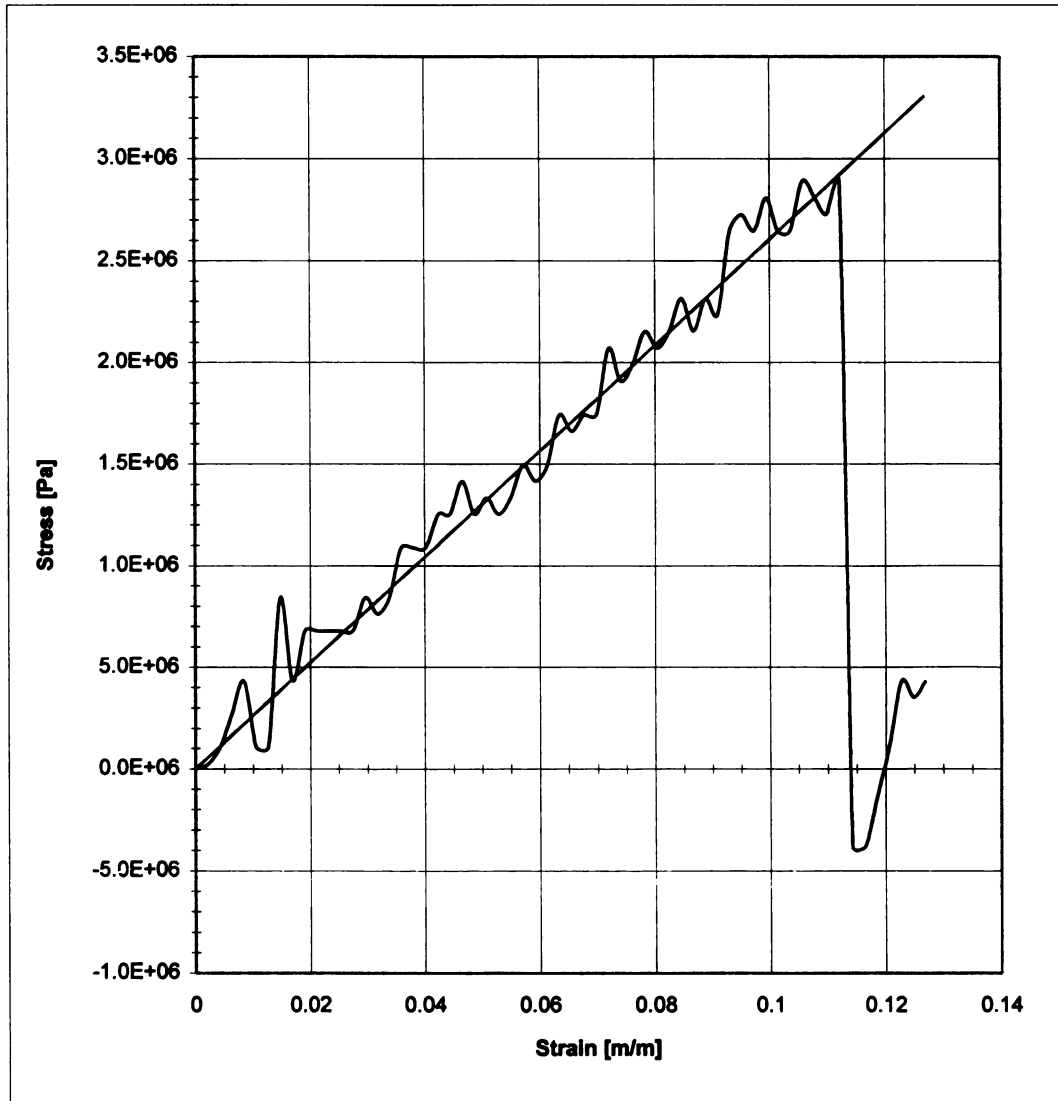


FIGURE E5 - Tensile test result for Y05_05

**TENSILE TEST**

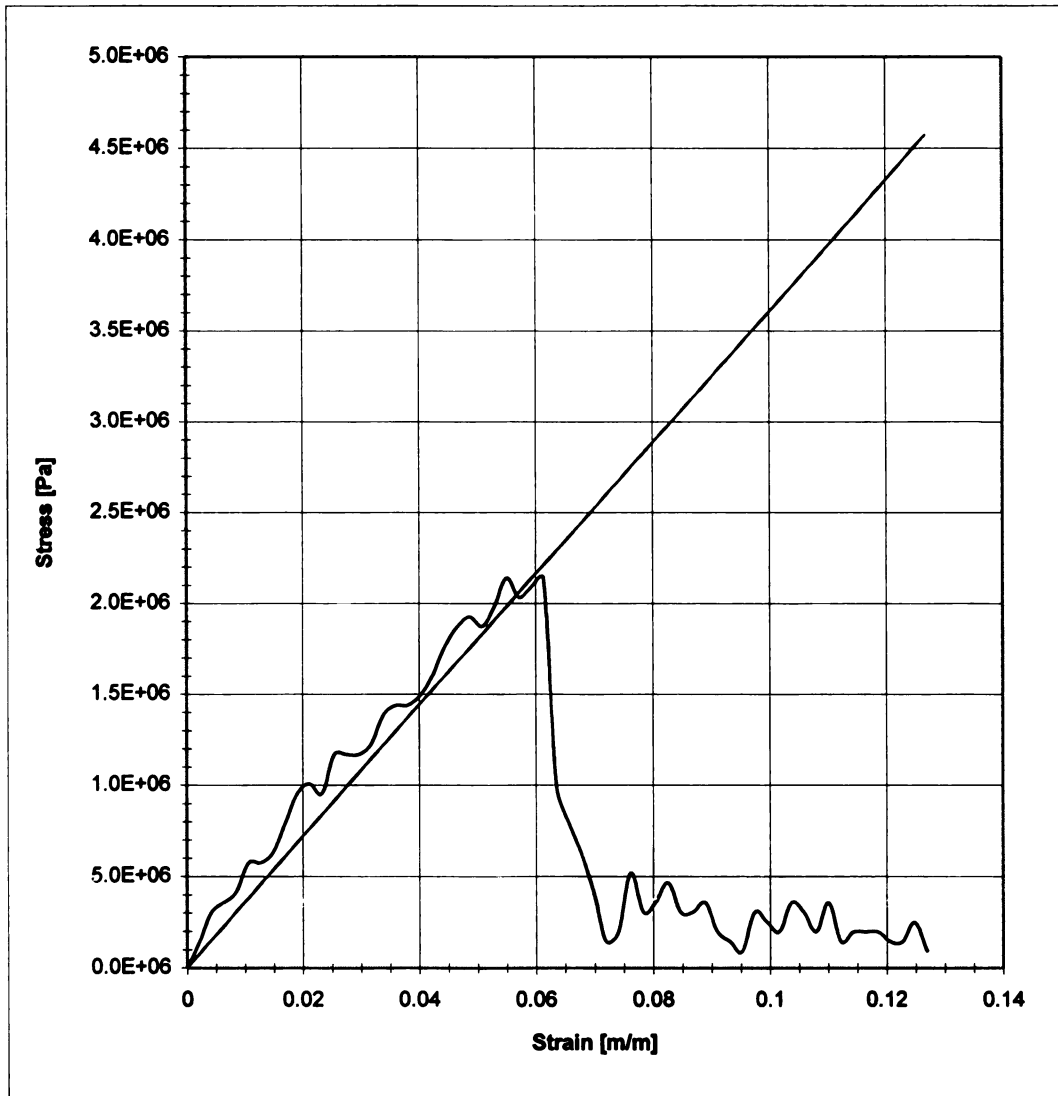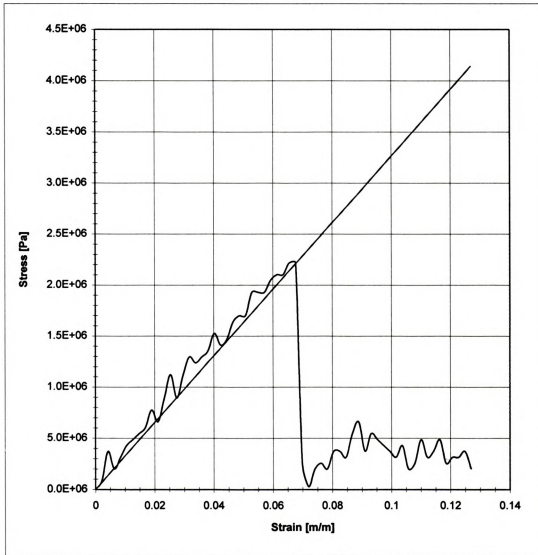| Sample | Thickness | 0.00264 [m] | **Elasticity  2186119 [Pa]** |
|--------|-----------|-------------|------------------------------|
|        | Width     | 0.009 [m]   |                              |
|        | Area      | 2.38E-05 [m^2] |                           |
|        | Length    | 0.02 [m]    |                              |



FIGURE E6 - Tensile test result for Y06_05

**TENSILE TEST**

| | | | | | |
|---|---|---|---|---|---|
| Sample | Thickness | 0.00273 [m] | | **Elasticity** | **2644603** [Pa] |
| | Width | 0.009 [m] | | | |
| | Area | 2.46E-05 [m^2] | | | |
| | Length | 0.02 [m] | | | |
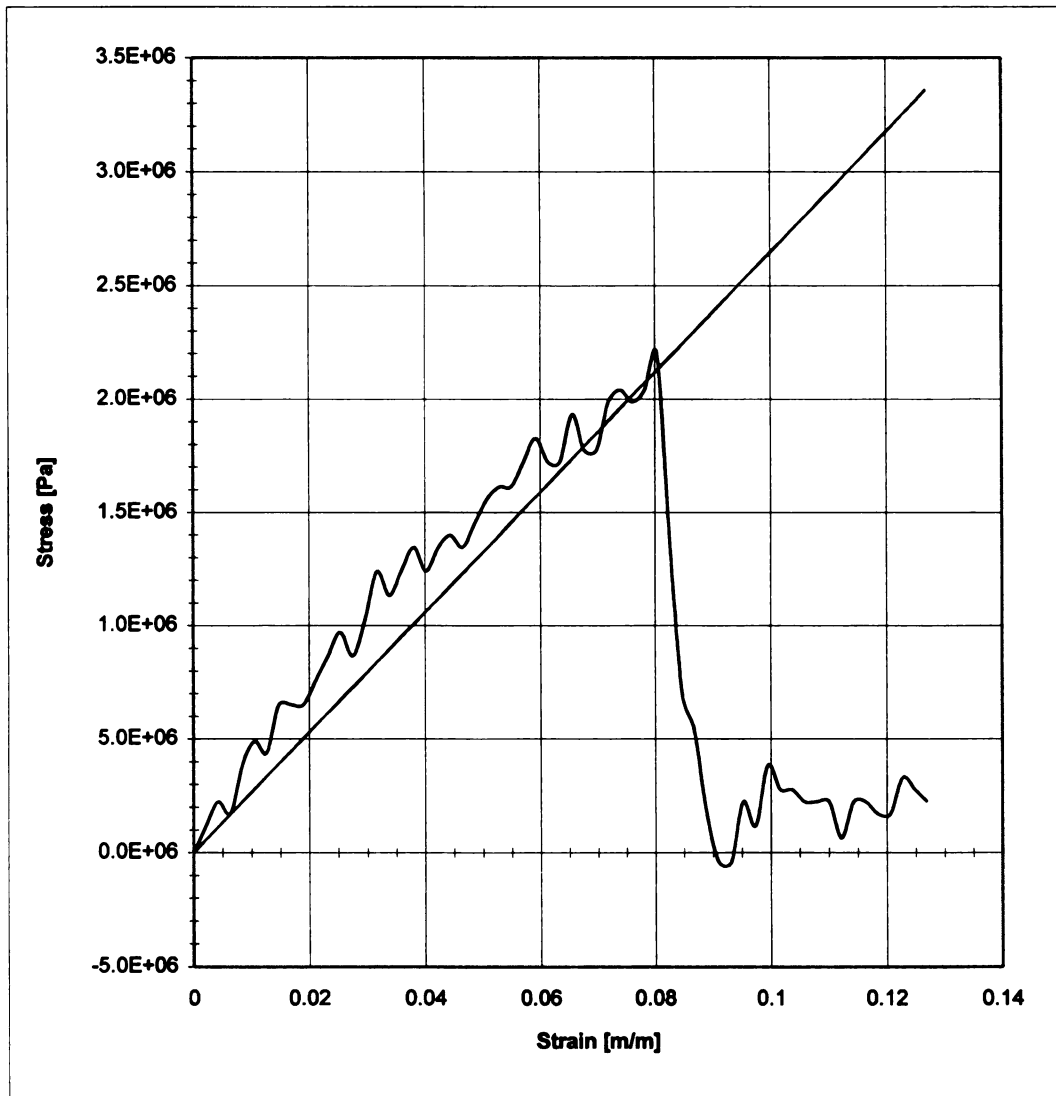


FIGURE E7 - Tensile test result for Y07_05

# TENSILE TEST

| | | | | |
|---|---|---|---|---|
| Sample | Thickness | 0.0027 [m] | **Elasticity** | **3603414 [Pa]** |
| | Width | 0.009 [m] | | |
| | Area | 2.43E-05 [m^2] | | |
| | Length | 0.02 [m] | | |



FIGURE E8 - Tensile test result for Y08_05

**TENSILE TEST**

| Sample | Thickness | 0.00253 [m] | **Elasticity  3262707 [Pa]** |
|--------|-----------|-------------|------------------------------|
|        | Width     | 0.009 [m]   |                              |
|        | Area      | 2.28E-05 [m^2] |                           |
|        | Length    | 0.02 [m]    |                              |



FIGURE E9 - Tensile test result for Y09_05

**TENSILE TEST**

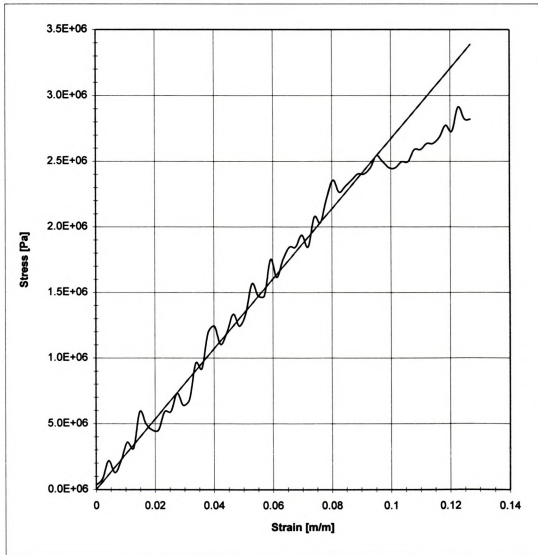| Sample | Thickness | 0.00272 [m] | **Elasticity** | **2382488** [Pa] |
|--------|-----------|-------------|------------------|-------------------|
|        | Width     | 0.009 [m]   |                  |                   |
|        | Area      | 2.45E-05 [m^2] |               |                   |
|        | Length    | 0.02 [m]    |                  |                   |
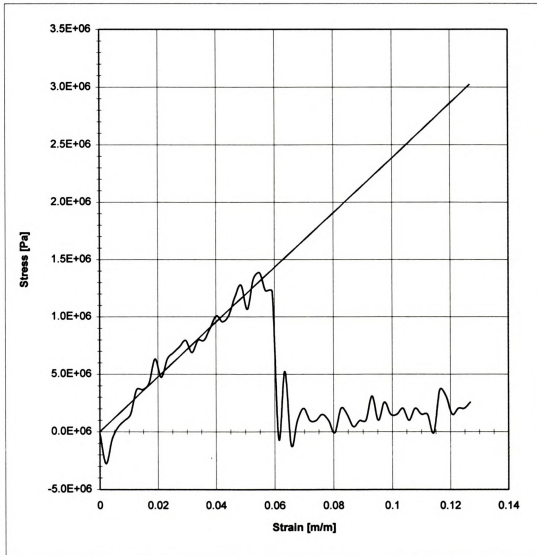


FIGURE E10 - Tensile test result for Y10_05

**TENSILE TEST**

| Sample | Thickness | 0.00207 [m] | | **Elasticity 3038228 [Pa]** |
|--------|-----------|-------------|---|---|
| | Width | 0.009 [m] | | |
| | Area | 1.86E-05 [m^2] | | |
| | Length | 0.02 [m] | | |
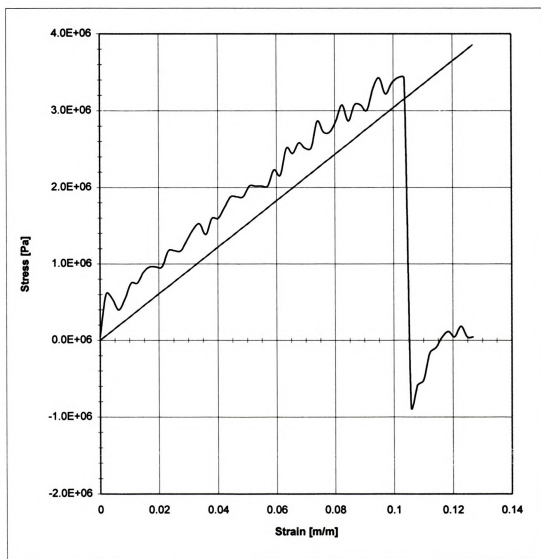


FIGURE E11 - Tensile test result for Y11_05

**TENSILE TEST**

Sample   Thickness   0.00276 [m]           **Elasticity  2365463 [Pa]**
          Width         0.009 [m]
          Area        2.48E-05 [m^2]
          Length       0.02 [m]
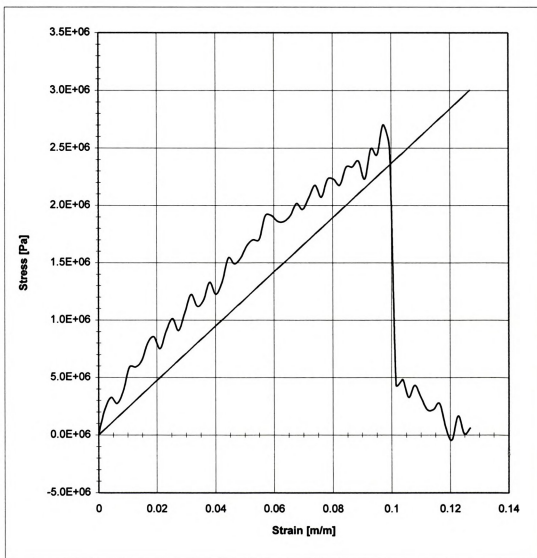


FIGURE E12 - Tensile test result for Y12_05

**TENSILE TEST**

Sample    Thickness    0.00314 [m]        **Elasticity   2669880 [Pa]**
         Width        0.009 [m]
         Area       2.83E-05 [m^2]
         Length       0.02 [m]



FIGURE E13 - Tensile test result for Y13_05

**TENSILE TEST**

Sample   Thickness   0.00261 [m]      **Elasticity   3140829 [Pa]**
        Width       0.009 [m]
        Area       2.35E-05 [m^2]
        Length      0.02 [m]
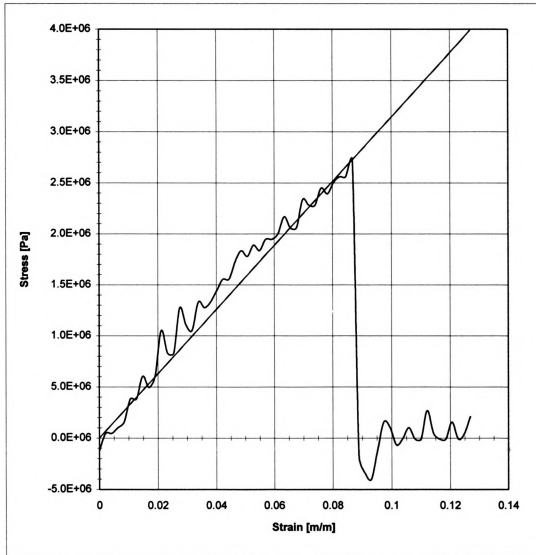


FIGURE E14 - Tensile test result for Y14_05

**TENSILE TEST**

Sample  Thickness  0.00288 [m]                    **Elasticity  3262553 [Pa]**
        Width          0.009 [m]
        Area      2.59E-05 [m^2]
        Length        0.02 [m]
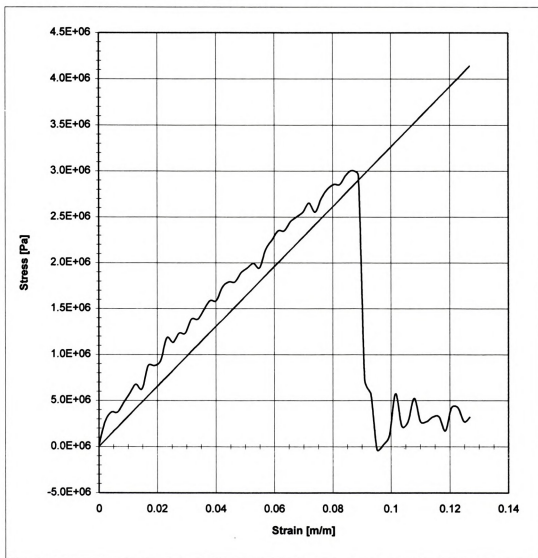


FIGURE E15 - Tensile test result for Y15_05

**TENSILE TEST**

Sample    Thickness    0.0024 [m]          **Elasticity   3204485** [Pa]
           Width         0.009 [m]
           Area          2.16E-05 [m^2]
           Length       0.02 [m]
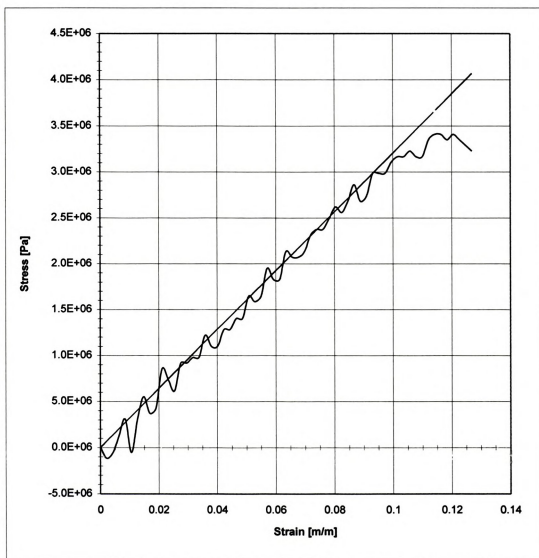


FIGURE E16 - Tensile test result for Y16_05

**TENSILE TEST**

Sample    Thickness    0.00153 [m]                    **Elasticity  2495790 [Pa]**
          Width             0.009 [m]
          Area         1.38E-05 [m^2]
          Length            0.02 [m]
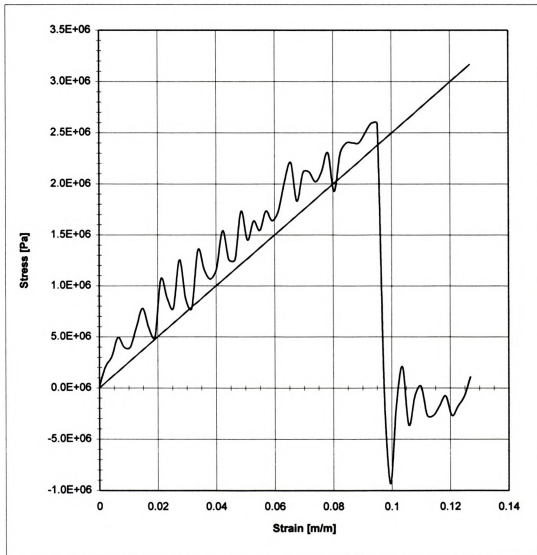


FIGURE E17 - Tensile test result for Y17_05

**TENSILE TEST**

| Sample | Thickness | 0.00193 [m] | **Elasticity 2556493 [Pa]** |
|--------|-----------|-------------|------------------------------|
|        | Width     | 0.009 [m]   |                              |
|        | Area      | 1.74E-05 [m^2] |                           |
|        | Length    | 0.02 [m]    |                              |
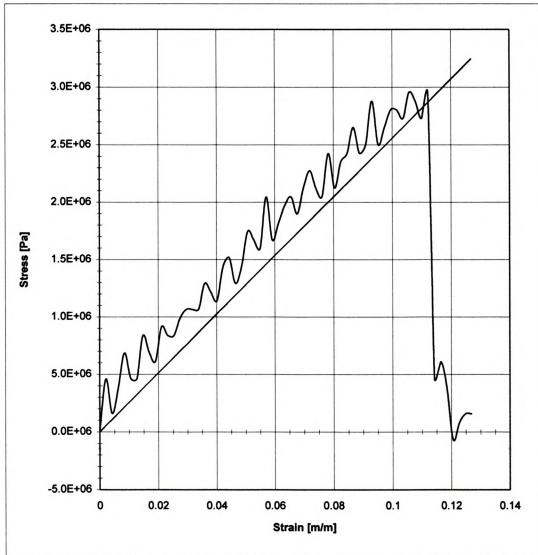


FIGURE E18 - Tensile test result for Y18_05

**TENSILE TEST**

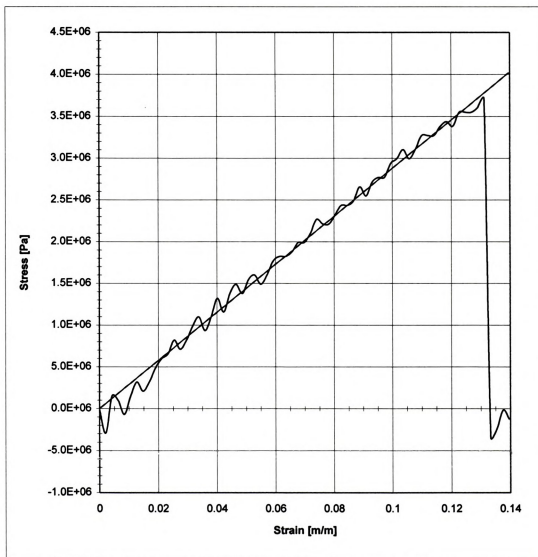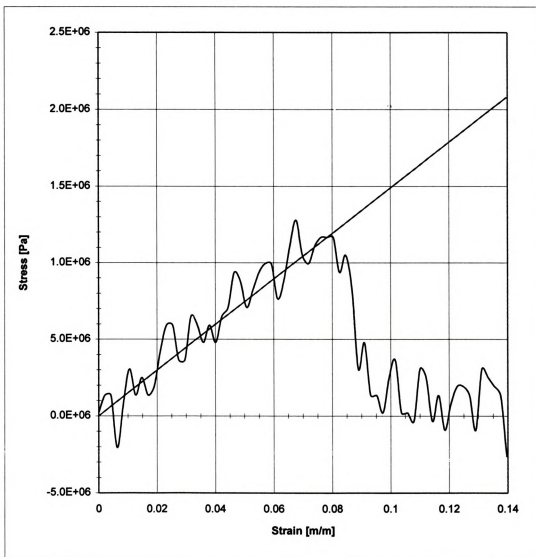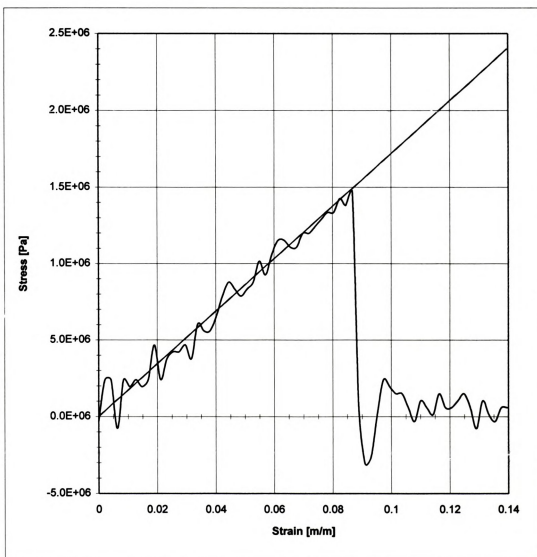| Sample | Thickness | 0.00307 [m] | **Elasticity 2106323 [Pa]** |
|--------|-----------|-------------|------------------------------|
|        | Width     | 0.009 [m]   |                              |
|        | Area      | 2.76E-05 [m^2] |                           |
|        | Length    | 0.02 [m]    |                              |
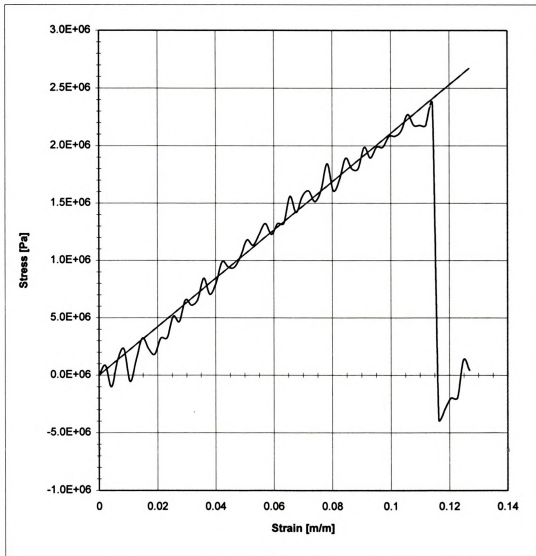


FIGURE E19 - Tensile test result for Y19_05

**TENSILE TEST**

Sample   Thickness   0.00262 [m]          **Elasticity  2878381 [Pa]**
         Width         0.009 [m]
         Area       2.36E-05 [m^2]
         Length        0.02 [m]



FIGURE E20 - Tensile test result for Y20_05

**TENSILE TEST**

| Sample | Thickness | 0.00255 [m] | **Elasticity 1488604 [Pa]** |
|--------|-----------|-------------|------------------------------|
| | Width | 0.009 [m] | |
| | Area | 2.3E-05 [m^2] | |
| | Length | 0.02 [m] | |



FIGURE E21 - Tensile test result for Y21_05

**TENSILE TEST**

| Sample | Thickness | 0.0032 [m] | | **Elasticity  1718797 [Pa]** |
|---|---|---|---|---|
| | Width | 0.009 [m] | | |
| | Area | 2.88E-05 [m^2] | | |
| | Length | 0.02 [m] | | |



FIGURE E22 - Tensile test result for Y22_05

**TENSILE TEST**

| Sample | Thickness | 0.0028 [m] | | **Elasticity  1910229 [Pa]** |
|---|---|---|---|---|
| | Width | 0.009 [m] | | |
| | Area | 2.52E-05 [m^2] | | |
| | Length | 0.02 [m] | | |



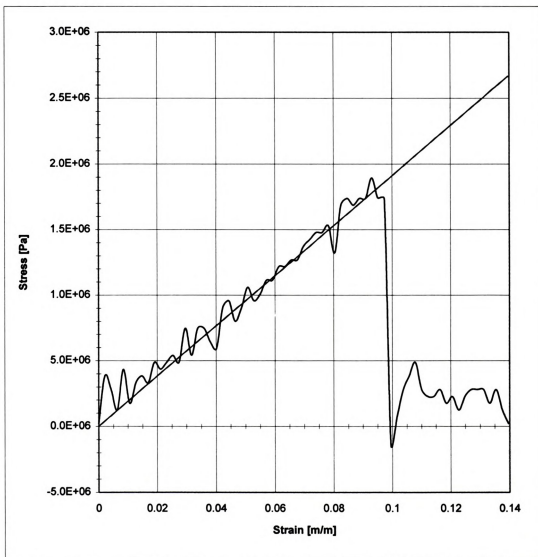FIGURE E23 - Tensile test result for Y23_05

**TENSILE TEST**

Sample    Thickness    0.00324 [m]           **Elasticity  1113635** [Pa]
              Width          0.009 [m]
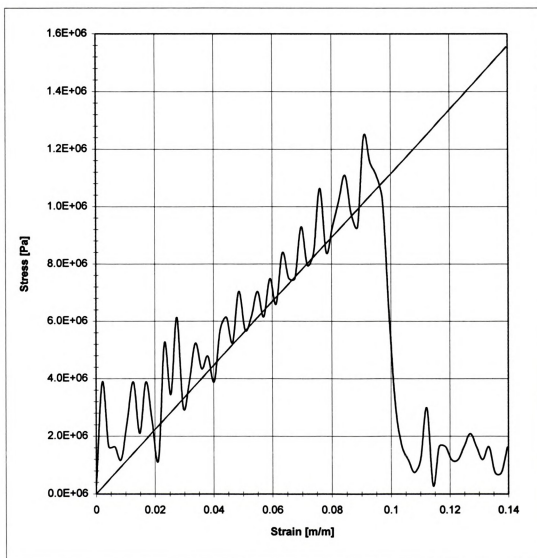              Area        2.92E-05 [m^2]
              Length       0.02 [m]



FIGURE E24 - Tensile test result for Y24_05

**TENSILE TEST**

| Sample | Thickness | 0.00292 [m] | **Elasticity 1423046 [Pa]** |
|--------|-----------|-------------|------------------------------|
| | Width | 0.009 [m] | |
| | Area | 2.63E-05 [m^2] | |
| | Length | 0.02 [m] | |
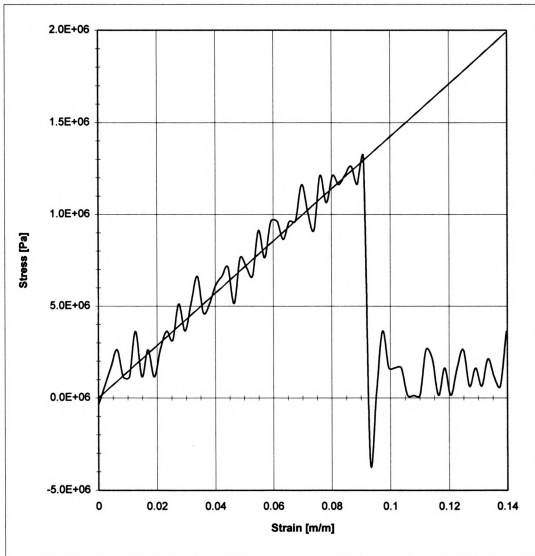


FIGURE E25 - Tensile test result for Y25_05
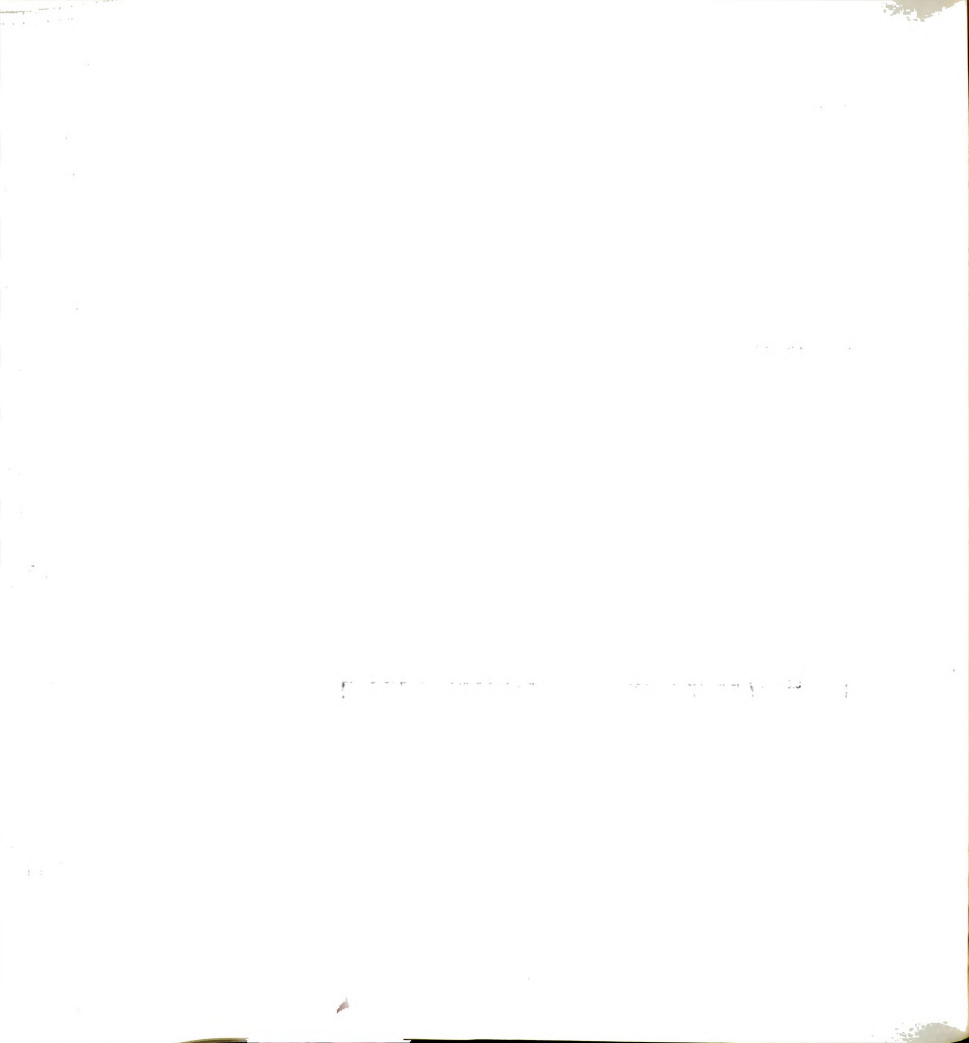
**TENSILE TEST**

Sample   Thickness   0.00248 [m]         **Elasticity  3227850** [Pa]
            Width         0.009 [m]
            Area        2.23E-05 [m^2]
            Length      0.02 [m]
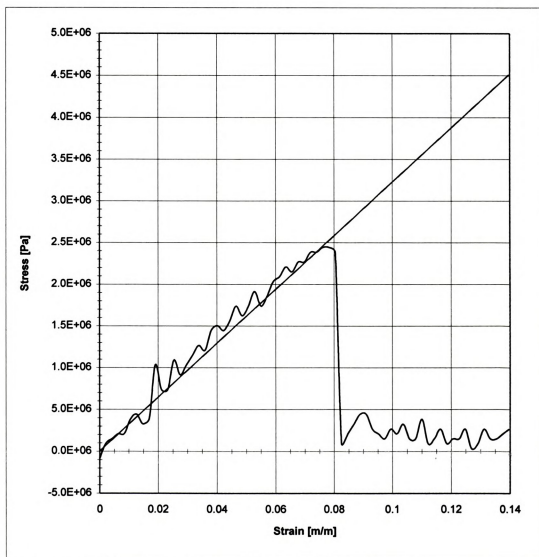


FIGURE E26 - Tensile test result for Y26_05

**TENSILE TEST**

| Sample | Thickness | 0.00274 [m] | | Elasticity 3545828 [Pa] |
| --- | --- | --- | --- | --- |
| | Width | 0.009 [m] | | |
| | Area | 2.47E-05 [m^2] | | |
| | Length | 0.02 [m] | | |
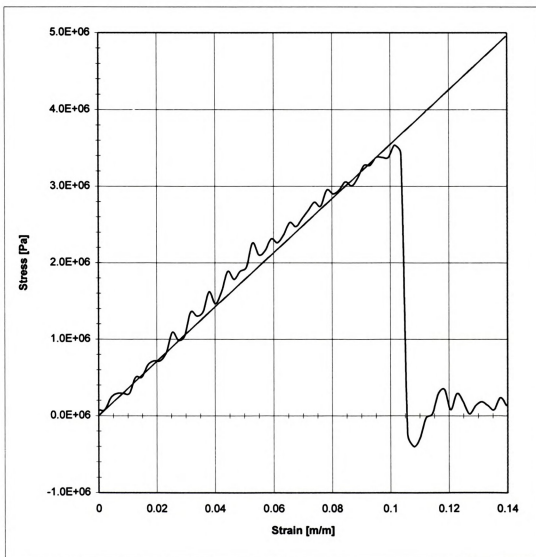


FIGURE E27 - Tensile test result for Y27_05
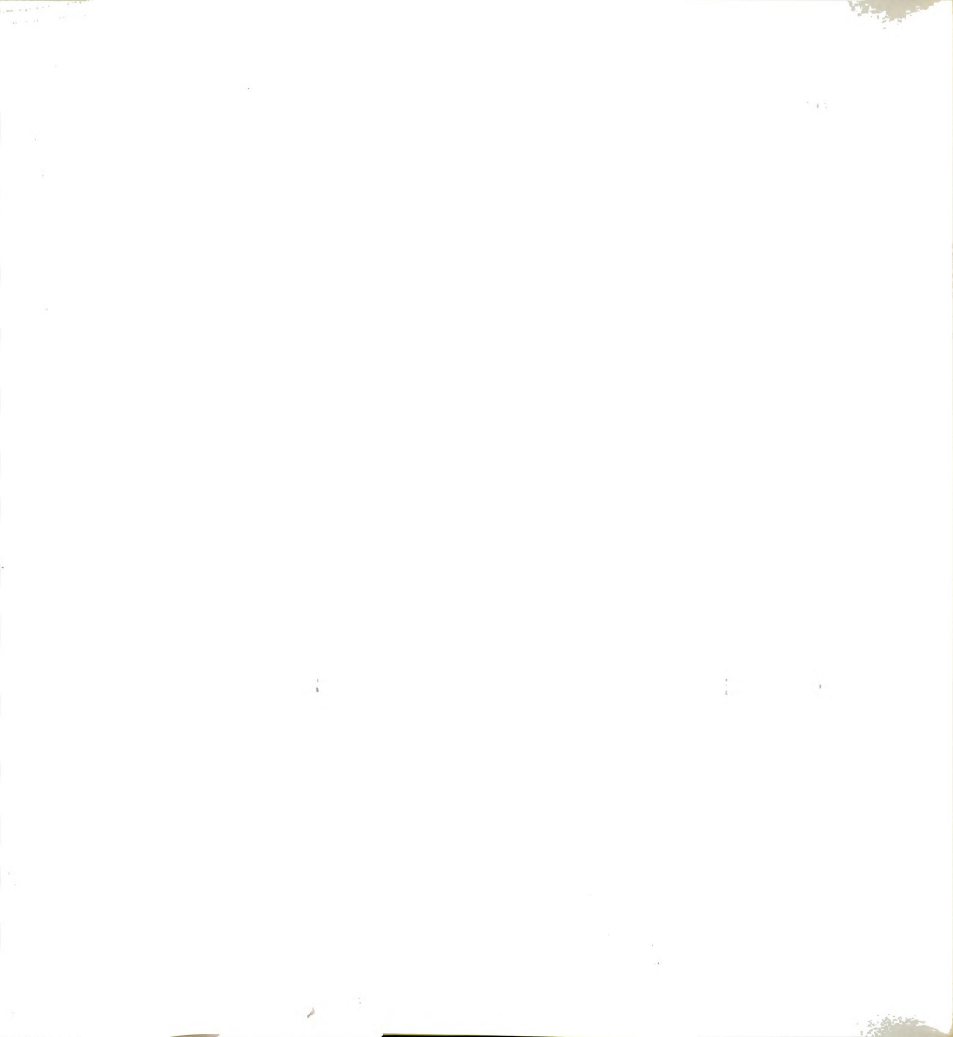
**TENSILE TEST**

| Sample | Thickness | 0.00259 [m] | **Elasticity 3437427 [Pa]** |
|--------|-----------|-------------|------------------------------|
| | Width | 0.009 [m] | |
| | Area | 2.33E-05 [m^2] | |
| | Length | 0.02 [m] | |
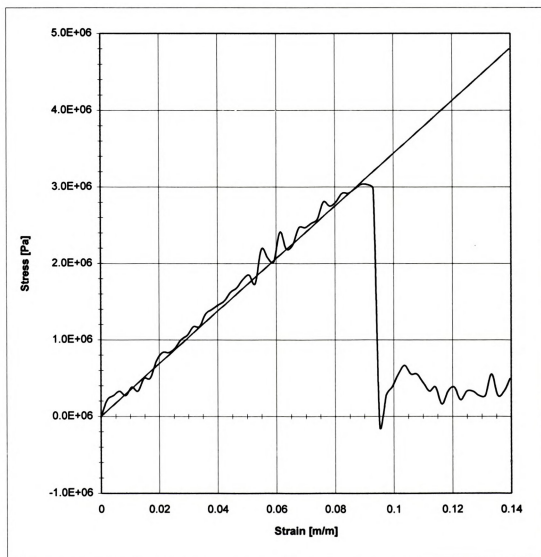


FIGURE E28 - Tensile test result for Y28_05

**TENSILE TEST**

Sample  Thickness    0.0024 [m]              **Elasticity  3034021** [Pa]
       Width        0.009 [m]
       Area         2.16E-05 [m^2]
       Length       0.02 [m]



FIGURE E29 - Tensile test result for Y29_05

**TENSILE TEST**

Sample   Thickness   0.00202 [m]               **Elasticity  3415703 [Pa]**
             Width        0.009 [m]
             Area      1.82E-05 [m^2]
             Length     0.02 [m]
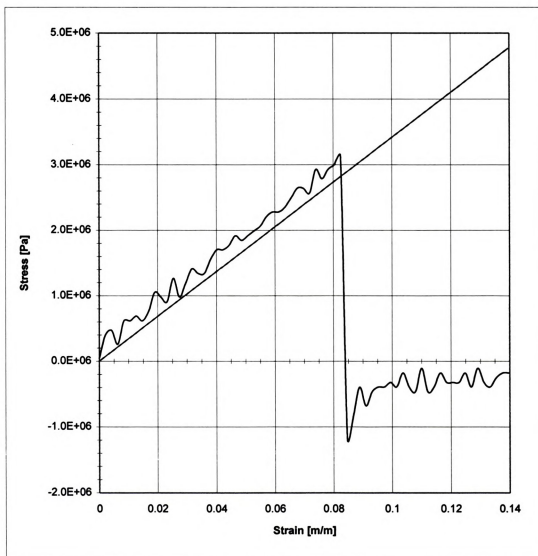


FIGURE E30 - Tensile test result for Y30_05

**TENSILE TEST**

Sample    Thickness    0.0019 [m]        **Elasticity   3085208** [Pa]
          Width          0.009 [m]
          Area         1.71E-05 [m^2]
          Length       0.02 [m]



FIGURE E31 - Tensile test result for Y31_05

# TENSILE TEST

Sample  Thickness  0.00305 [m]          **Elasticity  1748530 [Pa]**
        Width          0.009 [m]
        Area       2.75E-05 [m^2]
        Length        0.02 [m]
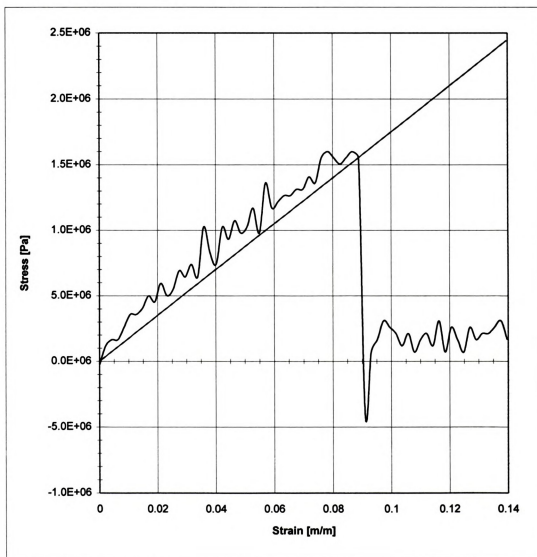


FIGURE E32 - Tensile test result for Y32_05

**TENSILE TEST**

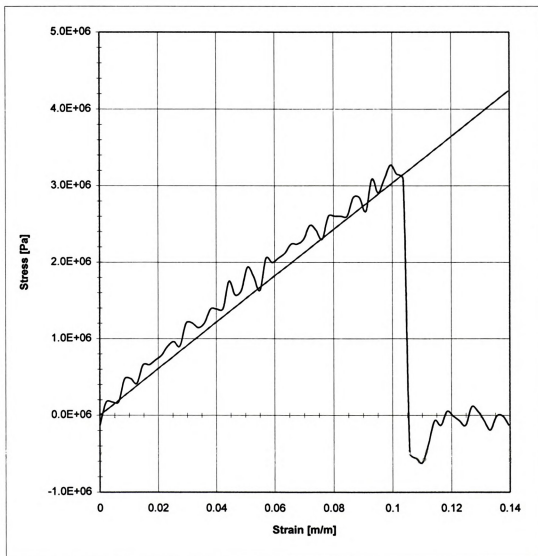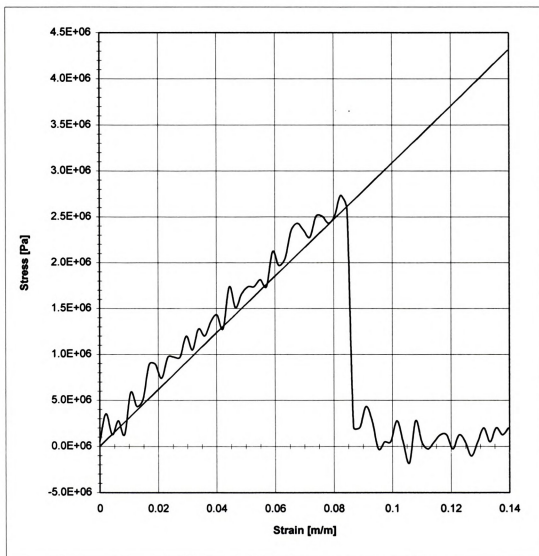| Sample | Thickness | 0.00228 [m] | **Elasticity  2268548 [Pa]** |
| | Width | 0.009 [m] | |
| | Area | 2.05E-05 [m^2] | |
| | Length | 0.02 [m] | |
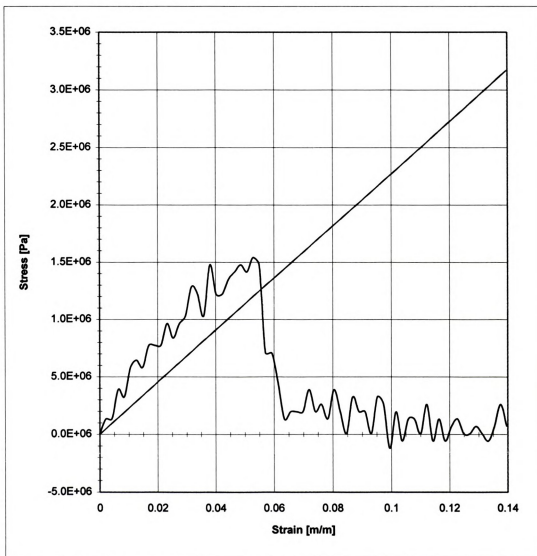


FIGURE E33 - Tensile test result for Y33_05

# TENSILE TEST

Sample Thickness  0.00267 [m]         **Elasticity  3514630 [Pa]**
       Width          0.009 [m]
       Area       2.4E-05 [m^2]
       Length         0.02 [m]
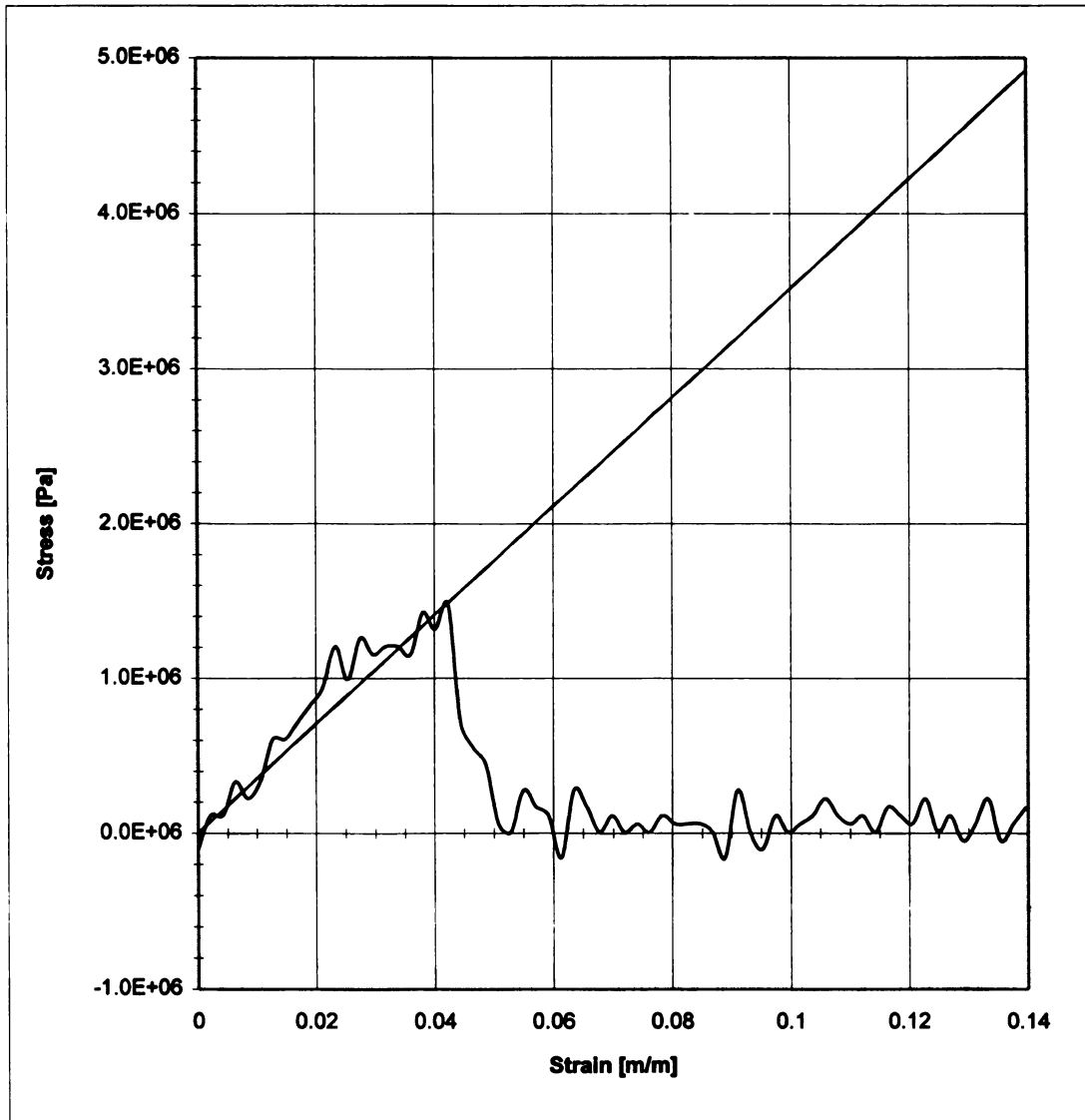


FIGURE E34 - Tensile test result for Y34_05

## TENSILE TEST

Sample  Thickness  0.00272 [m]          **Elasticity  2438245 [Pa]**
        Width          0.009 [m]
        Area      2.45E-05 [m^2]
        Length        0.02 [m]
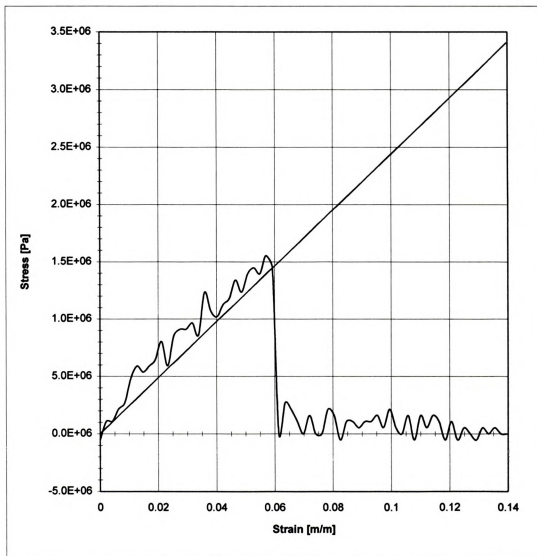


FIGURE E35 - Tensile test result for Y35_05

## TENSILE TEST

Sample   Thickness   0.00209 [m]                 **Elasticity   1687081 [Pa]**
            Width          0.009 [m]
            Area           1.88E-05 [m^2]
            Length         0.02 [m]
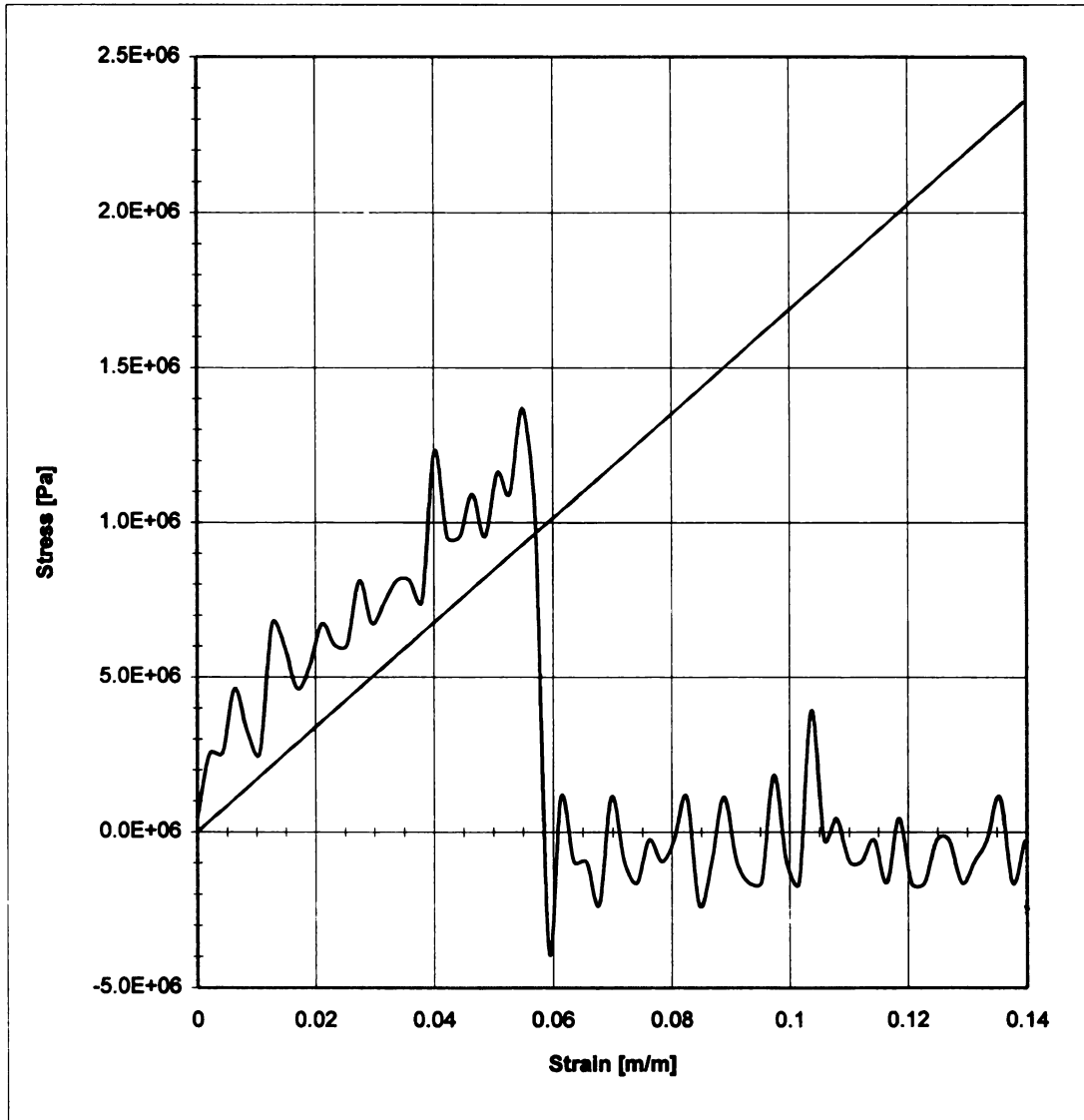


FIGURE E36 - Tensile test result for Y36_05

**TENSILE TEST**

| Sample | Thickness | 0.00273 [m] | | **Elasticity** | **1794603 [Pa]** |
|--------|-----------|-------------|---|---|---|
| | Width | 0.009 [m] | | | |
| | Area | 2.46E-05 [m^2] | | | |
| | Length | 0.02 [m] | | | |
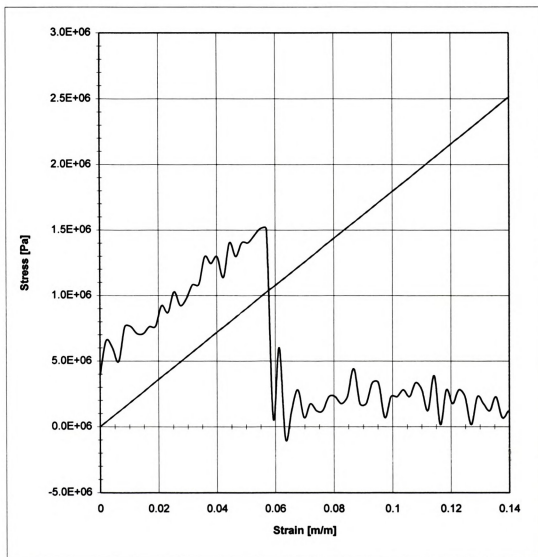


FIGURE E37 - Tensile test result for Y37_05

## TENSILE TEST

| Sample | Thickness | 0.00282 [m] | | Elasticity 2176547 [Pa] |
|--------|-----------|-------------|--|-------------------------|
| | Width | 0.009 [m] | | |
| | Area | 2.54E-05 [m^2] | | |
| | Length | 0.02 [m] | | |



FIGURE E38 - Tensile test result for Y38_05

**TENSILE TEST**

| Sample | Thickness | 0.00272 [m] | | **Elasticity** | **1578980 [Pa]** |
|--------|-----------|-------------|--|----------------|-------------------|
| | Width | 0.009 [m] | | | |
| | Area | 2.45E-05 [m^2] | | | |
| | Length | 0.02 [m] | | | |



FIGURE E39 - Tensile test result for Y39_05

## TENSILE TEST

Sample    Thickness    0.00225 [m]                **Elasticity  2231997 [Pa]**
          Width          0.009 [m]
          Area       2.03E-05 [m^2]
          Length        0.02 [m]



FIGURE E40 - Tensile test result for Y40_05

**TENSILE TEST**

Sample    Thickness    0.00234 [m]        **Elasticity   1916969 [Pa]**
           Width          0.009 [m]
           Area         2.11E-05 [m^2]
           Length       0.02 [m]
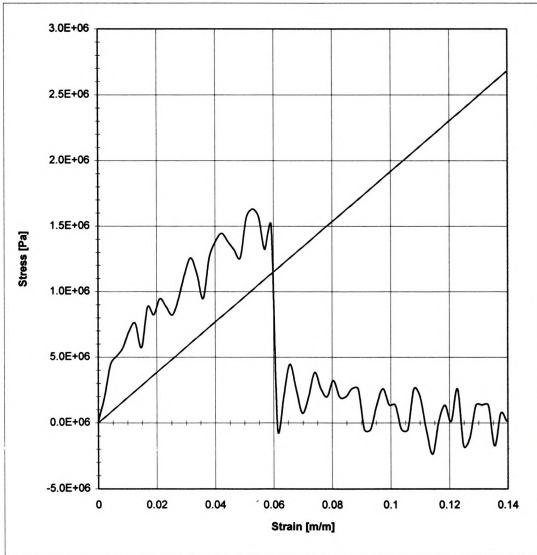


FIGURE E41 - Tensile test result for Y41_05

**TENSILE TEST**

Sample  Thickness  0.00241 [m]  **Elasticity  2252100 [Pa]**
        Width  0.009 [m]
        Area  2.17E-05 [m^2]
        Length  0.02 [m]



FIGURE E42 - Tensile test result for Y42_05

**TENSILE TEST**

Sample | Thickness | 0.00289 [m] | **Elasticity 2116101 [Pa]**
| Width | 0.009 [m] |
| Area | 2.6E-05 [m^2] |
| Length | 0.02 [m] |
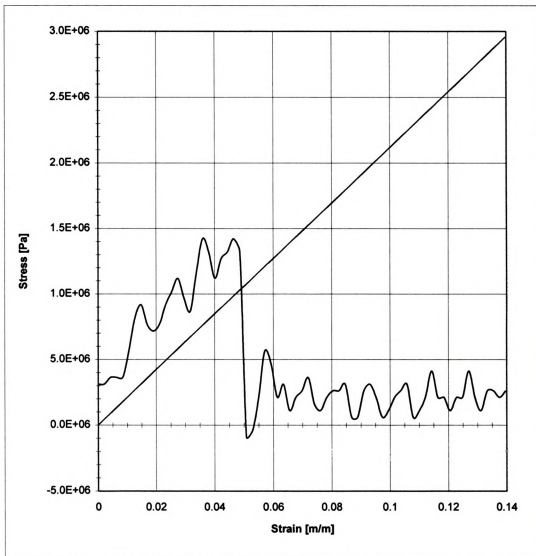


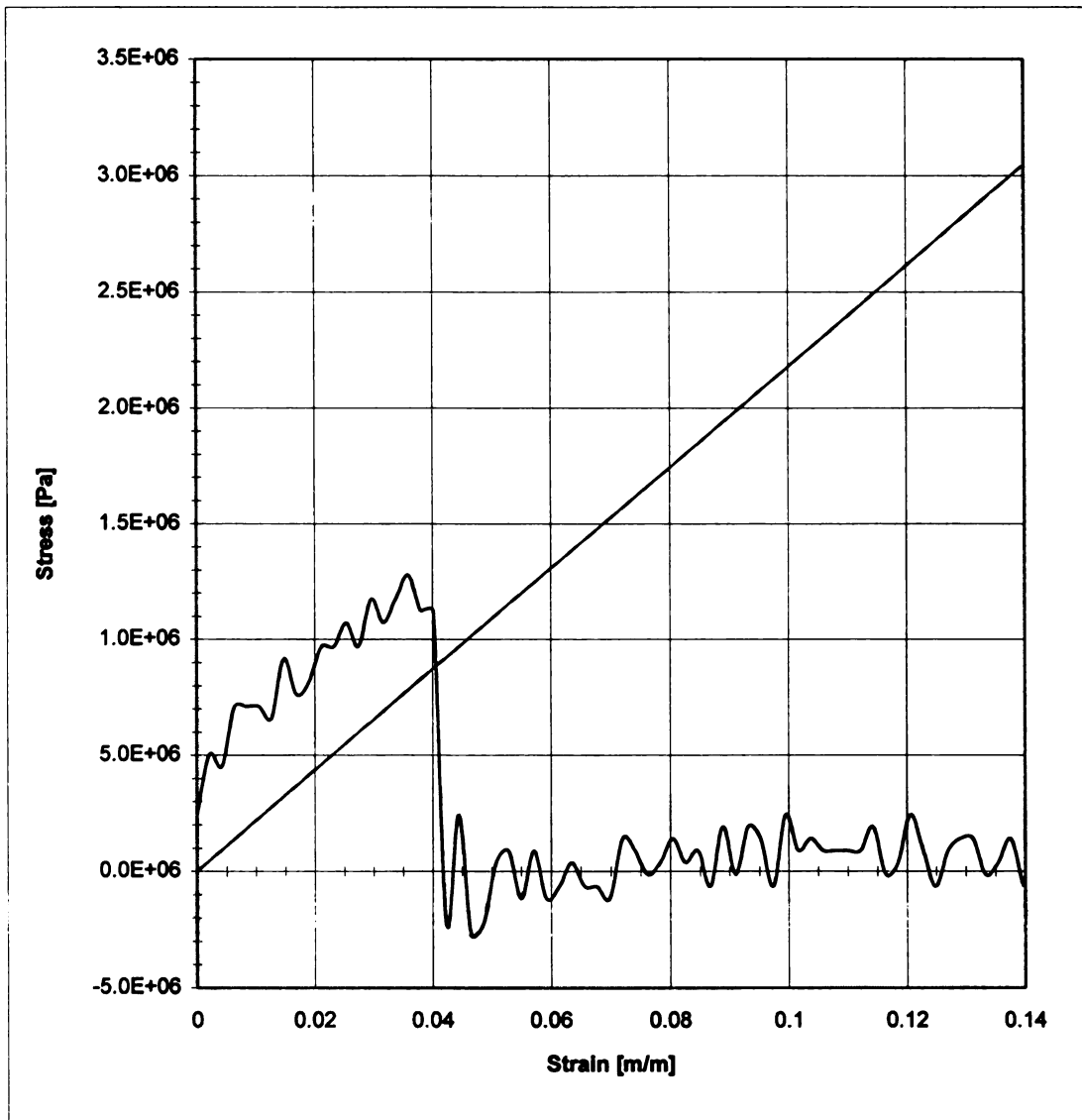FIGURE E43 - Tensile test result for Y43_05

**TENSILE TEST**

Sample   Thickness   0.00289 [m]        **Elasticity  2116101** [Pa]
         Width          0.009 [m]
         Area       2.6E-05 [m^2]
         Length        0.02 [m]



FIGURE E43 - Tensile test result for Y43_05

**TENSILE TEST**

Sample    Thickness    0.00269 [m]          **Elasticity  1938822 [Pa]**
          Width            0.009 [m]
          Area        2.42E-05 [m^2]
          Length           0.02 [m]
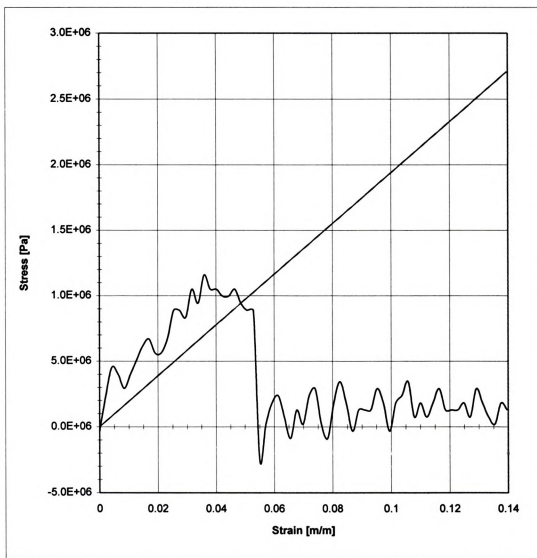


FIGURE E44 - Tensile test result for Y44_05

**TENSILE TEST**

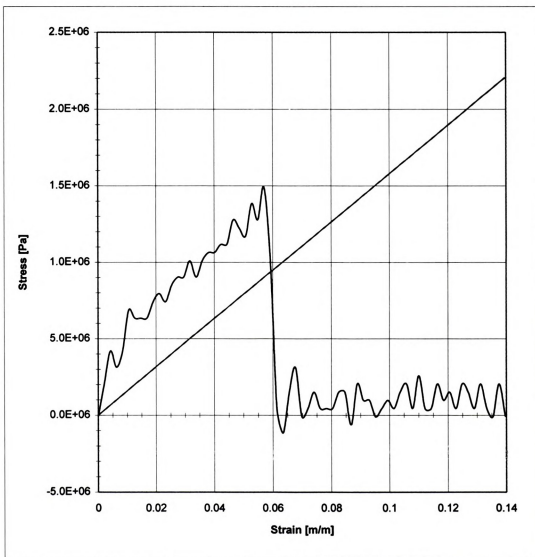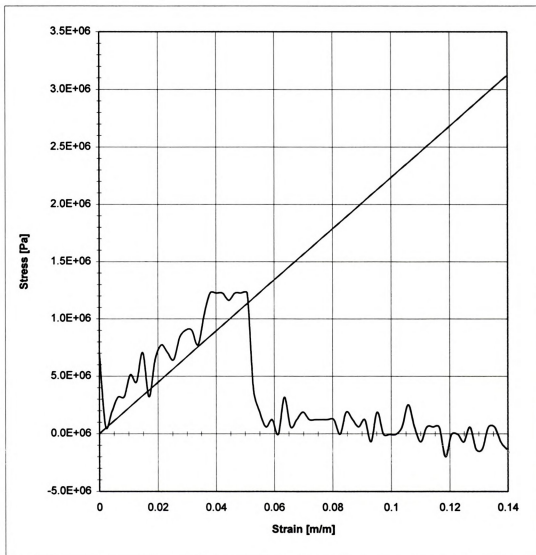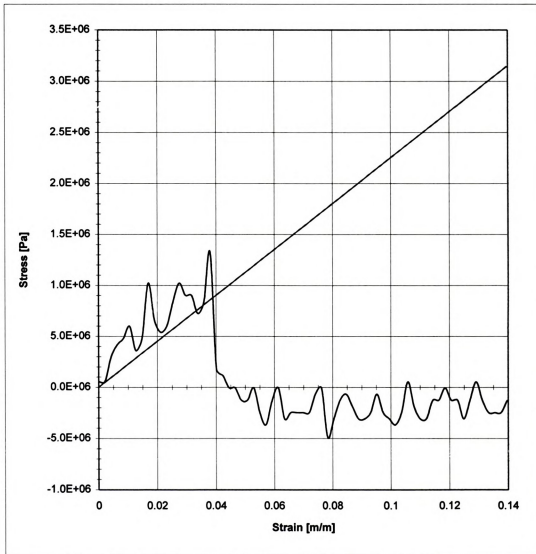| Sample | Thickness | 0.00266 [m] | **Elasticity 2625809 [Pa]** |
| | Width | 0.009 [m] | |
| | Area | 2.39E-05 [m^2] | |
| | Length | 0.02 [m] | |
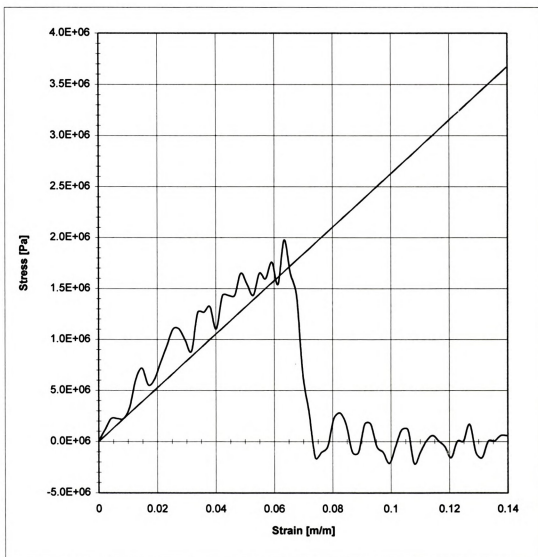


FIGURE E45 - Tensile test result for Y45_05

**APPENDIX F**

## APPENDIX F

### Computer Simulation Program

```
#include <stdio.h>
#include <stdlib.h>
#include <math.h>

#define V1          1        /* 1 in/min */
#define V10         10       /* 10 in/min */

#define r           0.997
#define N           100.0

        /* # of layers for grand simulation  */

#define lambda      1
#define alpha       3.0
#define freq        100.0    /* sampling rate [Hz]*/

#define Th          0.0002   /* Thickness of unit layer */
#define Area        3.14*pow(0.011,2)/4   /* Area of the
plunger */

#define Area2       3.14*0.011*Th


double   Vch1, Vch10;
float    F[500],
iFC[500],iFS[500],FC[500],pFC[500],FS[500],U[500],iF[500],Fc
omp[500],Fshear[500];
float    dtot[500], Frac;
float    D_max;
double   d_max, f_max;
double   kf_s, kd_s,pc,mo;
float    Fvisco=9;
int      m, mt;
  float  ip[45][6]={  {2.36, 1.59, 338438, 0.79, 2219400,
0.42},
        {3.85, 1.10, 441721, 2.07, 2893126, 0.33},
        {4.20, 1.45, 443736, 1.28, 2661103, 0.40},
```
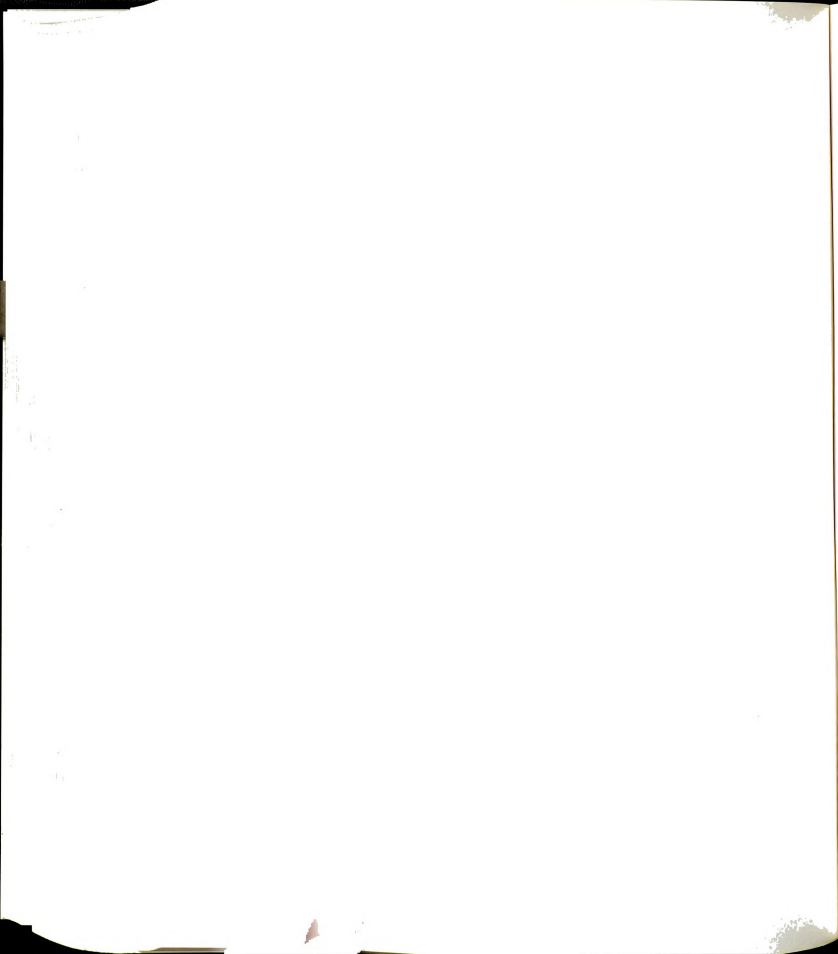
```
{3.32, 0.97, 335967, 1.72, 2019565, 0.41},
{3.99, 1.62, 428455, 1.58, 2603817, 0.39},
{4.35, 1.84, 446245, 1.32, 2186119, 0.41},
{4.35, 1.93, 473311, 1.52, 2644603, 0.37},
{3.91, 1.25, 352807, 1.25, 3603414, 0.37},
{3.41, 1.52, 331709, 1.22, 3262707, 0.35},
{3.49, 1.57, 278642, 1.72, 2382488, 0.26},
{4.85, 1.65, 518319, 2.16, 3038228, 0.27},
{3.11, 2.57, 434385, 1.55, 2365463, 0.38},
{4.14, 1.25, 476922, 1.68, 2669880, 0.44},
{4.87, 1.54, 506877, 1.39, 3140829, 0.28},
{4.46, 1.58, 500491, 1.47, 3262553, 0.55},
{3.74, 3.10, 497526, 2.08, 3204485, 0.41},
{2.89, 1.66, 353833, 1.31, 2495790, 0.35},
{2.74, 2.41, 358053, 1.63, 2556493, 0.41},
{1.83, 11.6, 364249, 1.11, 2106323, 0.42},
{2.90, 3.71, 396447, 2.00, 2878381, 0.38},
{2.50, 1.30, 334104, 0.71, 1488604, 0.41},
{2.90, 1.33, 388122, 1.01, 1718797, 0.43},
{3.09, 1.21, 379075, 0.90, 1910229, 0.44},
{1.98, 1.83, 282443, 0.62, 1113635, 0.48},
{2.02, 1.81, 284230, 0.78, 1423046, 0.35},
{5.17, 1.13, 444801, 1.46, 3227850, 0.38},
{5.54, 2.01, 631107, 2.03, 3545828, 0.43},
{4.49, 1.99, 469624, 1.39, 3437427, 0.30},
{6.72, 1.92, 653307, 2.20, 3034021, 0.45},
{4.69, 2.86, 554547, 2.03, 3415703, 0.40},
{3.94, 0.88, 355620, 1.23, 3085208, 0.29},
{3.29, 1.76, 412565, 0.83, 1748530, 0.30},
{3.56, 0.89, 300310, 0.89, 2268548, 0.34},
{3.92, 1.00, 348930, 0.77, 3514630, 0.33},
{3.55, 0.97, 288335, 0.92, 2438245, 0.27},
{2.95, 4.34, 437958, 1.08, 1687081, 0.51},
{2.50, 3.62, 396105, 1.10, 1794609, 0.55},
{3.05, 2.62, 421764, 1.02, 2176547, 0.44},
{3.04, 154 , 513378, 1.15, 1578980, 0.42},
{3.34, 2.81, 426326, 1.16, 2231997, 0.38},
{2.17, 2.65, 331139, 1.01, 1916969, 0.31},
{2.79, 1.43, 306164, 0.81, 2252100, 0.33},
{2.38, 1.61, 300994, 0.93, 2116101, 0.33},
{3.32, 0.86, 313349, 0.85, 1938822, 0.32},
{2.31, 1.25, 313121, 0.90, 2625809, 0.43} ,


                    };
```

```c
void main(void)
{
    int    x, i, j, k, c, h,z,q,qc,y[30],s[3],minj;
    float  pd[150],pt,A,tt,sFC,sFS,ppt,max,min,Fv;

    float a[150], as[150], t, dl, d[150];
    float ds[150],dss,dds,dx,temp,pop,force,pc;
    float Eu,Nu,SIGMAc,F_max,Es1,ct;
    char
*fn[45]={"m:\\m01","m:\\m02","m:\\m03","m:\\m04","m:\\m05",
         "m:\\m06","m:\\m07","m:\\m08","m:\\m09","m:\\m10",
"m:\\m11","m:\\m12","m:\\m13","m:\\m14","m:\\m15","m:\\m16",
"m:\\m17","m:\\m18","m:\\m19","m:\\m20","m:\\m21","m:\\m22",
"m:\\m23","m:\\m24","m:\\m25","m:\\m26","m:\\m27","m:\\m28",
"m:\\m29","m:\\m30","m:\\m31","m:\\m32","m:\\m33","m:\\m34",
"m:\\m35","m:\\m36","m:\\m37","m:\\m38","m:\\m39","m:\\m40",
"m:\\m41","m:\\m42","m:\\m43","m:\\m44","m:\\m45"};
    FILE   *destin, *M_T;



    Vch1=V1*0.0254/60;
    Vch10=V10*0.0254/60;

    M_T=fopen("m:\\MagT","wt");

for(x=0;x<=44;x++) {


  Eu=ip[x][0]*pow(10,10);
  Nu=ip[x][1]*pow(10,10);
    SIGMAc=ip[x][2];
      F_max=ip[x][3];
        Es1=ip[x][4];
          ct=ip[x][5];



  destin=fopen(fn[x],"wt");

  q=1;
  Fv=0;
a[1]=(1-r)*Vch10/(1-powl(r,N));

    for(i=0;i<=149;i++) {
```

```
        ds[i]=0.0;
              }

    Frac=SIGMAc*Area;
    dx=Vch10*(1/freq);

      ppt=0;
       pt=0;
         c=1;
         A=0;
       pc=c;
       qc=0;

    for(i=0;i<=499;i++) {
      iFC[i]=0;
      iFS[i]=0;
        U[i]=0;
      pFC[i]=0;
              }


    for(i=0;i<=N;i++) {
      pd[i]=0;
            }


      as[1]=a[1];
      for(j=2;j<=N;j++) {
        a[j]=a[j-1]*r;
        as[j]=a[j];
              }

    for(i=0;i<=499;i++) {
      t=i*(1/freq);    /* time */
      dtot[i]=t*Vch10;

    for(j=1;j<=N;j++) {
        d[j]=pd[j]+a[j]*(t-pt);
                }
for(j=c;j<=N;j++) {
   /* tt=(dtot[i]-A*(c-1))/Vch10;*/

        FC[j]=Area*a[j]*Nu*(1-1/exp(Eu*((t-pt)+0.6*ppt)/Nu));
        if(j==c) FC[j]=Area*a[j]*(Nu*(1-0.06*c))*(1-
1/exp(Eu*((t-pt)+0.6*ppt)/(Nu*(1-0.06*c))));
```

```
      if(c==1)   FC[j]=Area*a[j]*Nu*(1-1/exp(Eu*t/Nu));
   if(FC[j]>=(Frac*(1+0.03*(c-1)))) {
            y[c]=i;
     for(k=c+1;k<=N;k++) {
     pFC[k]=FC[k];
                                    }
   pt=t;

         if(c==1) ppt=t;
   c+=1;
   FC[j]=0;

   d[j]=Th;
   A=Th;
   pd[j]=A;

   if((N-c+1)==0) goto SSS;
    a[c]=(1-r)*Vch10*(1-0.09*c)/(1-powl(r,(N-c+1)));
           for(k=(c+1);k<=N;k++) {
           a[k]=a[k-1]*r;
                 }
     for(k=c;k<=N;k++) {
        pd[k]=a[k]*(dtot[i]-A*(c-1))/Vch10;
        d[k]=pd[k];
                }
   goto FFF;
            }
        }
FFF:
;


    sFC=0;
  for(j=1;j<=N;j++) {
     sFC=sFC+FC[j]*(a[j]*(1/freq));
         }

       iFC[i]=iFC[i-1]+sFC;
     if(i==0) iFC[i]=sFC;

      a[0]=Vch10;
      as[0]=a[0];
      sFS=0;
      z=1;
      for(j=q;j<=N;j++) {
```

```
      dss=0;
          dds=0;
  for(k=j;k<=N;k++)  {
          if(i==0)  z=0;
    dss+=a[k]*(1/freq)*z;
    dds+=a[k]*(1/freq)*z;
          }
  if(qc!=q)  {  mo=0.6;    }
  else  {  mo=1;}
        ds[j]=ds[j]*mo+dds;

force=(Es1*(ds[j]*0.7)/0.025)*Area2;
        if(force>F_max)  q+=1;
        sFS=sFS+dss*force;
              }
pc=c;
iFS[0]=0;
if(i>0)    iFS[i]=iFS[i-1]+sFS;


    U[i]=iFC[i]+iFS[i];


      }
  SSS:
  ;

    F[0]=0;
h=0;

    min=200;
  for(j=y[1];j<=y[2];j++)  {
    if(F[j]<min)  {
  minj=j;
  min=F[j];
                }
          }
  for(i=1;i<=498;i++)  {
    Fcomp[i]=(iFC[i+1]-iFC[i-1])/(2*dx);
    Fshear[i]=(iFS[i+1]-iFS[i-1])/(2*dx);
   if(i>=minj)  {
     h=1;
     Fv=h*(i-minj)*(1/freq)*Fvisco/(minj*0.01);
      if(Fv>=Fvisco)  Fv=Fvisco;
                      }
```

```
        F[i]=(U[i+1]-U[i-1])/(2*dx)+Fv;
fprintf(destin,"%f %f %f %f
%f\n",i*(1/freq),iFC[i],iFS[i],U[i],F[i]);
            }


  for(i=1;i<=2;i++) {
      max=0;
    for(j=(y[i]-10);j<=(y[i]+10);j++) {
      if(F[j]>max) {
   max=F[j];
   s[i]=j;
                    }
                        }
          }
      max=0;
  for(i=1;i<=189;i++) {        /* 189: Depth of MT [8 mm]*/
      if(F[i]>max) {
   max=F[i];
   mt=i;
         }
                    }


  fprintf(M_T,"%d %g %g %g %d
%g\n",x+1,F[s[1]],F[s[2]],F[s[1]]/(s[1]*0.01*Vch10),mt,F[mt]
);

fclose(destin);
  printf("%2d\n",x+1);
      }
fclose(M_T);

}
```

---

* This program was written by using C language.

# LIST OF REFERENCES

# LIST OF REFERENCES

Armstrong, P.R. 1989. Measurement of apple firmness using the acoustic impulse response. Ph. D. Dissertation. Michigan State University, East Lansing, MI.

Armstrong, P.R. and G.K. Brown. 1992. Non-destructive firmness measurement of apple. ASAE Paper No. 936023. St. Joseph, Mich.:ASAE.

Bourne, M.C. 1982. Considerations of a general rheological model for the mechanical behavior of viscoelastic solid food materials. *J. of Texture Studies* 7:243-255.

Chen, Y. and J. Rosenberg. 1977. Nonlinear viscoelastic model containing a yield element for modeling a food material. *J. of Texture Studies* 8:477-485.

Crandall, S.H., N.C. Dahl, and T.J. Lardner. 1978. *An Introduction to the Mechanics of Solids.* New York: McGraw-Hill Book Co.

Dickinson, E. and I.C. Goulding. 1980. Yield behavior of crumbly English cheeses in compression. *J. of Texture Studies* 11:51-63.

Drake, B. 1971. A quasi-rheological model element for fracture. *J. of Texture Studies* 2:365-372.

Johnson, E.A., M. Peleg, R.A. Segars, and J.G. Kapsalis. 1981. A generalized phenomenological rheological model for fish flesh. *J. of Texture Studies* 12:413-425.

Khan, A.A. and J.F.V. Vincent. 1990. Anisotropy of apple parenchyma. *J. Sci. Food and Agric.* 52:455-466.

Khan, A.A. and J.F.V. Vincent. 1993. Compressive stiffness and fracture properties of apple and potato parenchyma. *J. of Texture Studies* 24:423-435.


Lin, T. and R.E. Pitt. 1986. Rheology of apple and potato tissue as affected by cell turgor pressure. *J. of Texture Studies* 17:291-313.


McLaughlin, N.B. 1987. Statistical models for failure of apple tissue under constant-strain-rate loading. *J. of Texture Studies* 18:173-186.


Mohsenin, N.N. 1977. Characterization and failure in solid foods with particular reference to fruits and vegetables. *J. of Texture Studies* 8:169-193.


Mohsenin, N.N. and H. Gohlich. 1962. Techniques for determination of mechanical properties of fruits and vegetables as related to design and development of harvesting and processing machinery. *J. of Agricultural Engineering Research* 7:300-315.


Mohsenin, N.N. 1986. *Physical Properties of Plant and Animal Materials*. New York: Gordon and Breach Science Publishers.

Peleg, M. 1976. Consideration of general rheological model for the mechanical behavior of viscoelastic solid food materials. *J. of Texture Studies* 7:243-255.


Peleg, M. 1976. Compressive failure patterns of some juicy fruits. *J. of Food Sci.* 41:1320-1324.


Pitt, R.E. 1982. Models for the rheology and statistical strength of uniformly stressed vegetative tissue. *Transaction of ASAE* 1776-1784.


Shigley, J.E. and C.R. Mischke. 1984. *Mechanical Engineering Design*. New York: McGraw-Hill Book Co.


White, F.M. 1986. *Fluid Mechanics*. New York: McGraw-Hill Book Co.